

Electronic Thesis and Dissertation Repository

---

6-21-2011 12:00 AM

## Measurement of Dynamic Temperatures and Pressures in Nuclear Power Plants

Hashem M. Hashemian, *The University of Western Ontario*

Supervisor: Dr. Jin Jiang, *The University of Western Ontario*

A thesis submitted in partial fulfillment of the requirements for the Doctor of Philosophy degree in Electrical and Computer Engineering

© Hashem M. Hashemian 2011

Follow this and additional works at: <https://ir.lib.uwo.ca/etd>



Part of the [Power and Energy Commons](#)

---

### Recommended Citation

Hashemian, Hashem M., "Measurement of Dynamic Temperatures and Pressures in Nuclear Power Plants" (2011). *Electronic Thesis and Dissertation Repository*. 189.

<https://ir.lib.uwo.ca/etd/189>

This Dissertation/Thesis is brought to you for free and open access by Scholarship@Western. It has been accepted for inclusion in Electronic Thesis and Dissertation Repository by an authorized administrator of Scholarship@Western. For more information, please contact [wlsadmin@uwo.ca](mailto:wlsadmin@uwo.ca).

MEASUREMENT OF DYNAMIC TEMPERATURES AND PRESSURES IN  
NUCLEAR POWER PLANTS

(Dissertation Format: Monograph)

(Spine Title: Measurement of Dynamic Temperatures and Pressures in NPPs)

by

Hashem Mehrdad Hashemian

Graduate Program in Engineering Science  
Department of Electrical and Computer Engineering

A dissertation submitted in partial fulfillment of the  
requirements for the degree of Doctor of Philosophy

School of Graduate and Postdoctoral Studies  
The University of Western Ontario  
London, Ontario, Canada

© H.M. Hashemian 2011

THE UNIVERSITY OF WESTERN ONTARIO  
SCHOOL OF GRADUATE AND POSTDOCTORAL STUDIES

**CERTIFICATE OF EXAMINATION**

Supervisor

\_\_\_\_\_  
Dr. Jin Jiang

Examining Board

\_\_\_\_\_  
Dr. Belle R. Upadhyaya

\_\_\_\_\_  
Dr. Rajiv K. Varma

\_\_\_\_\_  
Dr. Amirnaser Yazdani

\_\_\_\_\_  
Dr. Sohrab Rohani

The dissertation by

**HASHEM MEHRDAD HASHEMIAN**

entitled:

**MEASUREMENT OF DYNAMIC TEMPERATURES AND PRESSURES IN  
NUCLEAR POWER PLANTS**

is accepted in partial fulfillment of the

requirements for the degree of

Doctor of Philosophy

Date \_\_\_\_\_

\_\_\_\_\_  
Chair of the Dissertation Examination Board

## ABSTRACT

---

The dynamic response of the process sensors that supply real-time data to the safety systems in nuclear power plants (NPP) plays a vital role in preventing plant accidents. If a critical process temperature, pressure, level, or flow experiences a step change, for example, the sensors that measure the process variable must act quickly to actuate the safety systems that will mitigate the consequence of an undesirable process excursion. The research conducted for this dissertation has been performed to ensure the prompt response of critical sensors by advancing, refining, validating, and implementing new methods for measuring the response time of temperature, pressure, level, and flow sensors in NPP safety systems. The essential significance of the new methods is that they can be performed remotely on installed sensors at operating conditions, thereby providing the actual in-service response time as opposed to the unrealistic response time provided by the manufacturer or by offline testing.

The in-situ response time testing technique for temperature sensors is referred to as the Loop Current Step Response (LCSR) test. This technique is based on heating the sensor internally by applying a step change in the DC current to the sensor extension leads in the plant control room. The DC current heats the sensing element of the sensor, resulting in a temperature transient that is then analyzed to provide a true sensor response time, which accounts for all process conditions as well as for the effects of installation and aging. This dissertation presents the theoretical foundation of the LCSR, the details of the author's extensive experimental research to validate and refine its use in multiple nuclear plant safety applications, and the assumptions that support the validity of the author's research and experimental results.



The in-situ response time testing technique for pressure, level, and flow transmitters is the so-called noise analysis method. This method is based on recording and analyzing the inherent process fluctuations present at the output of transmitters while the plant is operating. These fluctuations (noise) arise from random flux, turbulent flow, random heat transfer, process control action, and vibration. They are separated from the output of the transmitter by signal conditioning, recorded for about an hour, and analyzed in frequency and/or time domain to yield the response time of the pressure sensing system. This dissertation describes the theoretical foundation of the noise analysis technique, the details of the experimental research that the author has conducted for this dissertation to validate and expand the scope of this technique in actual plant applications, and the assumptions informing the author's confidence that the research in this dissertation validates the noise analysis technique. The significance of the noise analysis technique is that it not only measures the in-service response time of the transmitter but also of its sensing lines. In contrast to other methods, it can thereby account for the effect of sensing-line length, blockages, and voids on sensor response time.

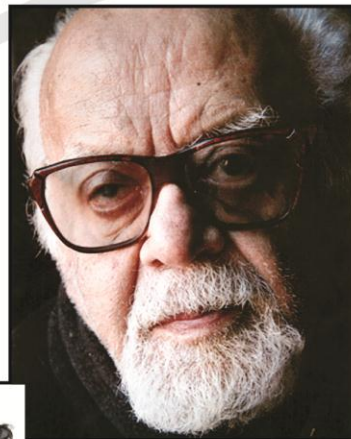
As part of this research, both the LCSR and noise analysis techniques were validated through extensive laboratory measurements performed on temperature and pressure sensors of the types used in nuclear power plants. The author has used these results to indicate where these methods are most effective but also where they may pose significant uncertainties or may fail. In general, this research has concluded that the LCSR method can identify the response time of RTDs with better than 90 percent accuracy and that the noise analysis technique provides response time results for pressure transmitters to better than 80 percent accuracy. This is provided that the RTDs and pressure transmitters tested meet the assumptions that must be satisfied in the design of the sensors and the conditions of the tests.

KEYWORDS:

Process Instrumentation, Dynamic Measurements, Temperature Sensors, Pressure Transmitters, Sensing Lines, Nuclear Power Plants, In-Situ Testing, Response Time Degradation

---

DR.  
ALI  
HASHEMIAN



*My Dad - 2005*



*My Dad and Me - 1953*

This thesis is dedicated to my late father, Dr. Ali Hashemian, who passed away in Knoxville, Tennessee, USA, on April 25, 2009, at the age of 90. He was a prominent attorney, a brave man, a great husband, and a wonderful father. My dad was my mentor, best friend, and a source of joy, laughter, and fun for the whole family.

I love my dad very much and cherish his memory.

## ACKNOWLEDGMENTS

---

I am indebted to Professor Jin Jiang, who provided me with the opportunity to pursue my Ph.D. at the University of Western Ontario (UWO) and directed me in my research and the writing of this dissertation. I have learned a great deal from Dr. Jiang and am grateful to him for his generous support of my work.

My good friend Dr. Abdullah Kadri, who received his Ph.D. in 2009 from the Department of Electrical and Computer Engineering at UWO, is also gratefully acknowledged. Abdullah gave me my first tour of UWO, helped me with my first registration, and answered the many questions that I posed to him in person and by phone regarding my UWO courses, Ph.D. proposal, research work, dissertation, and exams.

Most importantly, I must thank Debbie Ashton, who typed my dissertation and worked many nights, weekends, and holidays to help me meet my deadlines. I am absolutely indebted to her for the great job that she has done in typing and proofing this work, coordinating the production of the figures, tables, and photographs, and always smiling throughout the years that we worked together in my pursuit of this degree. I started my work on this Ph.D. in January 2008 and finished it at the end of summer 2011. Debbie supported me with her strong administrative skills throughout this whole period.

I am also grateful to Kevin Lynn and Chris Key for drawing the figures for this dissertation, and Darrell Mitchell and Edwin Riggsbee for helping me produce some of the derivations and data that are included in this dissertation.

## CONTENTS

---

CERTIFICATE OF EXAMINATION .....	ii
ABSTRACT.....	iii
DEDICATION.....	v
ACKNOWLEDGEMENT .....	vi
TABLE OF CONTENTS.....	vii
LIST OF TABLES .....	x
LIST OF FIGURES .....	xii
LIST OF APPENDICES.....	xvii
LIST OF ABBREVIATIONS.....	xviii
LIST OF SI UNITS AND MATHEMATICAL SYMBOLS.....	xx
<b>1 INTRODUCTION.....</b>	<b>1</b>
1.1 Motivation.....	3
1.2 Current Solutions .....	5
1.3 Solutions Demonstrated by This Research .....	8
1.3.1 Method for Measuring the Response Time of RTDs.....	10
1.3.2 Method for Measuring the Response Time of Pressure Transmitters .....	11
1.4 Goal and Objectives of This Research.....	13
1.5 Contributions of This Dissertation.....	15
1.6 Organization of This Dissertation.....	16
<b>2 SCIENCE OF MEASURING PROCESS VARIABLES .....</b>	<b>18</b>
2.1 Resistance Temperature Detectors (RTDs) .....	18
2.2 Pressure Transmitters.....	26

2.3	Sensing Lines .....	31
2.4	Science of Sensor Response Time Testing .....	36
2.5	Sensing Line Effects on Dynamics of Pressure Transmitters .....	38
<b>3</b>	<b>BACKGROUND AND LITERATURE REVIEW .....</b>	<b>49</b>
3.1	Conventional Method for Testing RTD Response Time .....	49
3.2	Conventional Method for Testing Response Time of Pressure Transmitter .....	55
3.3	Prior Work .....	65
3.4	History of Sensor Response Time Testing in Nuclear Power Plants .....	68
<b>4</b>	<b>FACTORS INFLUENCING SENSOR PERFORMANCE .....</b>	<b>71</b>
4.1	Effects on RTDs .....	71
4.2	Effects on Pressure Transmitters .....	77
4.3	Aging Effects .....	84
	4.3.1 Aging of RTDs .....	84
	4.3.2 Aging of Pressure Transmitters .....	87
<b>5</b>	<b>SOLUTIONS DEVELOPED FROM THIS RESEARCH .....</b>	<b>93</b>
5.1	LCSR Test Principle .....	93
5.2	LCSR Test Theory .....	104
5.3	LCSR Test Procedure .....	114
5.4	Noise Analysis Technique .....	120
	5.4.1 Noise Data Acquisition .....	120
	5.4.2 Test Assumptions .....	122
	5.4.3 Data Processing for Response Time Measurements .....	122
	5.4.4 Effect of Process Bandwidth on Noise Analysis Results .....	123
	5.4.5 Theory of Noise Analysis Technique .....	127
<b>6</b>	<b>VALIDATION OF RESEARCH TECHNIQUES .....</b>	<b>133</b>
6.1	Validation of the LCSR Technique .....	133
6.2	Validation of Noise Analysis Technique .....	141

6.3	Validation of the Noise Analysis Technique to Account for Sensing Lines .....	146
6.4	In-Plant Experience with Detection of Sensing Line Problems.....	152
6.5	In-Plant Experience with Response Time Testing Using Noise Analysis.....	152
6.6	When the Methods Fail.....	159
7	<b>APPLICATIONS OF RESEARCHED TECHNIQUES IN AND BEYOND THE NUCLEAR INDUSTRY</b> .....	170
8	<b>CONCLUSIONS</b> .....	173
8.1	Conclusions From This Research .....	173
8.2	Recommendations for Future Research .....	174
9	<b>REFERENCES</b> .....	182
	CURRICULUM VITAE.....	189
	APPENDICES .....	192

## LIST OF TABLES

---

2-1	Typical Characteristics of RTDs in Nuclear Power Plants .....	22
2-2	Typical Characteristics of Nuclear Plant Pressure Transmitters.....	33
2-3	Compliance Values of Pressure Transmitters Used in This Study .....	41
2-4	Theoretical Effect of Sensing Line Length on Response Time .....	43
2-5	Theoretical Effect of Diameter (Simulating Blockage) on Transmitter Response Time .....	44
2-6	Theoretical Effect of Void on Response Time .....	45
3-1	Plunge Test Results for Representative RTDs Used in this Research.....	53
3-2	Results of Laboratory Testing of Response Time of Representative Nuclear-Grade Pressure Transmitters.....	61
3-3	Ramp Test Results to Demonstrate Transmitter Linearity .....	63
4-1	Research Results on Study of Dimensional Tolerances on RTD Response Time .....	74
4-2	Laboratory Data on Influence of Process Media on RTD Response Time .....	75
4-3	Experimental Research Data on the Effect of Length and Blockage on Response Time .....	79
4-4	Theoretical and Experimental Estimations of Response Time of Sensing Line Alone.....	80
4-5	Experimental Results on the Effect of Sensing Line Length on Transmitter Response Time .....	81

4-6	Response Time of a Barton Pressure Transmitter with a Long Sensing Line (30 meters) and a Simulated Blockage (75% of Sensing Line Diameter Blocked).....	82
4-7	Response Time of a Foxboro Transmitter as a Function of Air in Sensing Line.....	83
4-8	Examples of Potential Causes of RTD Degradation.....	85
4-9	Examples of Potential Causes of Performance Degradation in Nuclear Plant Pressure Transmitters .....	86
4-10	Examples of RTD Response Time Degradation in Nuclear Power Plants.....	88
4-11	Aging Effects on RTD Response Time .....	90
5-1	Summary of Problems with Conventional Plunge Test Method for RTD Response Time Testing and Solutions Offered by the LCSR Technique.....	94
5-2	Summary of Problems with Conventional Ramp Test Method for Response Time Testing of Pressure Transmitters and Solutions Offered by the Noise Analysis Technique.....	95
5-3	Typical Services for Which Transmitter Response Time Testing Is Performed in Nuclear Power Plants .....	132
6-1	LCSR Results for RTD Installation Tests .....	141
6-2	Summary from Transmitter Database .....	149
6-3	Laboratory Test to Demonstrate Effectiveness of Noise Analysis Method in Identifying Sensing Line Effects .....	150
6-4	Response Time Problems Detected by Noise Analysis Method .....	158
6-5	Results of Laboratory Testing of Sizewell RTDs .....	163
6-6	Noise Analysis Results for Sizewell RTDs .....	164
8-1	Results of Validation of Noise Analysis Technique for In-Situ Response Time Testing of RTDs.....	179



## LIST OF FIGURES

---

1-1	Example of a Typical Process Instrumentation Channel .....	4
1-2	Illustration of Ramp and Step Test Setups to Measure the Response Time of a Pressure Transmitter and an RTD.....	6
1-3	A Step Change in Temperature in the Core of a Nuclear Reactor and the Resulting Response of an RTD Sensor at the Output of the Reactor .....	7
1-4	Example of an RTD Installation in a Nuclear Power Plant .....	9
1-5	Typical Pressure Transmitter Installation in a Nuclear Power Plant .....	12
1-6	Raw Noise Data from a Nuclear Plant Pressure Transmitter.....	14
2-1	RTD Sensing Element.....	19
2-2	Typical RTD Assembly .....	21
2-3	Installation of Direct-Immersion and Thermowell-Mounted RTDs.....	23
2-4	Direct-Immersion RTDs in Bypass Loops of a PWR Plant.....	24
2-5	Thermowell-Mounted RTDs Installed Directly in the Primary Coolant Loops of a PWR Plant .....	25
2-6	Wheatstone Bridge Configurations for Measuring RTD Resistance.....	27
2-7	RTD Wire Configurations.....	28
2-8	A Four-Wire RTD Measurement Circuit .....	28
2-9	Typical Transmitter Configurations and Sensing Element Varieties to Measure Gauge, Absolute, and Differential Pressures.....	30
2-10	Various Ways to Display the Output of a Pressure Transmitter .....	32
2-11	Example of Pressure Transmitter and Sensing Line Installation .....	34

2-12	Step, Ramp, and Frequency Response for a First-Order Dynamic Model.....	37
2-13	Steps in Testing Response Time of a Temperature or Pressure Sensor .....	39
2-14	Output of an Underdamped System for a Step Input and Calculation of Sensor Response Time .....	46
2-15	Frequency Responses of Representative Pressure Transmitters from Four Sensing Line Configurations.....	47
3-1	Plunge Test Procedure.....	50
3-2	Plunge Test Transient for an RTD and Calculation of Response Time .....	52
3-3	Hydraulic Ramp Generator and Test Results from Laboratory/Bench Testing of Response Time of a Pressure Transmitter .....	56
3-4	Response Time Testing of an Installed Transmitter Using the Ramp or Noise Methods .....	57
3-5	Oscillatory Output of a Pressure Transmitter During a Ramp Test.....	58
3-6	Example of Ramp Test Results Produced During this Research.....	59
3-7	Summary of Results of Baseline Response Time Measurements Performed in This Study .....	62
3-8	Ramp Test Results for a Transmitter with Minor Nonlinearity.....	64
4-1	Laboratory Research to Study the Effect of Installation on an RTD Response Time.....	72
4-2	Results of Laboratory Testing to Demonstrate the Effect of Process Media on Dynamic Response of an RTD (from LCSR Test) .....	76
4-3	Distribution of Response Time Results, Indicating an Increase over the Period of Observation.....	89
4-4	Response Time Trends from In-plant Testing of Pressure Transmitters in Four Different Services in a PWR Plant .....	91
5-1	Heat Transfer Process in Plunge and LCSR Methods .....	96
5-2	LCSR and Plunge Test Transients.....	97

5-3	Direction of Heat/Cooling through the RTD Material during an LCSR or a Plunge Test .....	99
5-4	RTD Designs Which Satisfy LCSR Assumptions .....	100
5-5	Radial Heat Transfer to and from an RTD .....	101
5-6	LCSR Transient from Laboratory Testing of an RTD (in Room-Temperature Water Flowing at 1m/sec) .....	102
5-7	Lump Variable Representations for LCSR Analysis .....	105
5-8	Conversion of LCSR Data to Equivalent Plunge Test Data .....	116
5-9	LCSR Correction Factor .....	118
5-10	LCSR Test and Analysis Procedure .....	119
5-11	Principle of Noise Analysis Technique (a, b) and Actual Noise Record from a Nuclear Plant Pressure Transmitter (c) .....	121
5-12	Response of Four Different Pressure Transmitters to the Same Input .....	124
5-13	Pressure Transmitter PSD and Determination of Response Time .....	125
5-14	Potential Results of Noise Analysis in Relation to the Bandwidth of the Input Noise .....	126
5-15	Input and Output Noise through a Sensor .....	128
5-16	Two APDs for a Nuclear Plant Pressure Transmitter .....	130
5-17	Noise Analysis Procedure to Measure the In-Situ Response Time of a Pressure Transmitter .....	131
6-1	Single (a) and Average (b, c) LCSR Transients Obtained by Testing an RTD in an Operating Nuclear Power Plant .....	135
6-2	Output of Software Program That Automatically Reads and Averages Multiple LCSR Transients .....	136

6-3	Results of Laboratory Tests of One Population of RTDs Involved in this Research.....	137
6-4	Summary of Research Results on LCSR Validation .....	139
6-5	Summary of Research Results to Quantify the Accuracy of LCSR Method .....	140
6-6	Example of an RTD Installation Mishap in a Nuclear Power Plant (a) and Resulting LCSR Data (b) .....	143
6-7	Raw LCSR Data from Redundant RTDs Tested at Cold Shutdown to Identify Installation Problems.....	144
6-8	Summary of Research Results on Validation of Noise Analysis Technique .....	145
6-9	Summary of Research Results to Quantify the Accuracy of Noise Analysis Technique .....	147
6-10	Response Time of Pressure Transmitters in Nuclear Power Plants.....	148
6-11	Summary of Research Results on Validation of Noise Analysis Technique for Detecting Sensing Line Effects.....	151
6-12	Results of Noise Analysis Test of Pressure Transmitters Before and After Flushing the Sensing Line to Clear Blockages.....	153
6-13	Online Monitoring Data for Four Transmitters during a Plant Transient.....	154
6-14	APD (a) and PSD (b) Results from In-Plant Test of Four Pressure Transmitters .....	155
6-15	Tracking PSDs of a Nuclear Plant Pressure Transmitter .....	156
6-16	Plant Computer Data for the Transmitter Degradation Observed in November 2010 .....	157
6-17	Results of In-Plant Validation of Noise Analysis Technique with Correction of Ramp Results for Sonic and Hydraulic Delays .....	160
6-18	Spread of Response Time Data from Ramp and Noise Tests.....	161
6-19	Response Time and APD Results for Three Pressure Transmitters .....	165
6-20	Shared Sensing Line in a Nuclear Power Plant.....	167

6-21	Example of Shared Sensing Line Arrangement in a Nuclear Power Plant .....	168
6-22	PSDs of Four Steam Generator Level Transmitters with Shared Sensing Lines .....	169
7-1	Temperature Data from Jet Engine under Test Firing .....	172
7-2	True Temperature Curve Constructed by Correcting the Output of Thermocouple for Response Time .....	172
8-1	Principle of LCSR Test for Thermocouples .....	175
8-2	LCSR Validation Performed at EdF Test Loop .....	181

## LIST OF APPENDICES

---

<b>APPENDIX A:</b>	Sensor Response Time Testing Theory .....	189
<b>APPENDIX B:</b>	Pressure Sensors and Sensing Line Dynamics.....	204
<b>APPENDIX C:</b>	Correlations Between Response Time and Process Conditions ....	215
<b>APPENDIX D:</b>	Self-Heating Index and Its Correlation with RTD Response Time .....	228

## LIST OF ABBREVIATIONS

---

A/D	analog to digital
AGR	advanced gas reactor
AMS	Analysis and Measurement Services Corporation
ANO	Arkansas Nuclear One
ANS	American Nuclear Society
APD	amplitude probability density
AR	autoregressive
ASTM	American Society for Testing and Material
BWR	boiling water reactor
CANDU	Canadian deuterium uranium reactor
CEA	Commissariat à l'énergie atomique
CF	correction factor
cm	centimeter
CRBR	Clinch River Breeder Reactor
CV	curriculum vitae
DB	decade box
DC	direct current
EdF	Électricité de France
ENS	European Nuclear Society
EPRI	Electric Power Research Institute
FFT	fast Fourier transform
Gen IV	Generation Four
Hz	Hertz

I&C	instrumentation and control
IAEA	International Atomic Energy Agency
ID	inside diameter
IEC	International Electrotechnical Commission
IEEE	Institute of Electrical and Electronics Engineers
IR	insulation resistance
ISA	International Society of Automation
LCSR	loop current step response
LMFBR	liquid metal fast breeder reactor
mA	milliamperere
mm	millimeter
m/s	meter per second
MWe	megawatt electrical
NASA	National Aeronautics and Space Administration
NBS	National Bureau of Standards
NPIC&HMIT	nuclear plant instrumentation, control and human-machine interface technologies
NPP	nuclear power plant
NRC	Nuclear Regulatory Commission
N/A	Not Applicable
OD	outside diameter
ORNL	Oak Ridge National Laboratory
PSD	power spectral density
PWR	pressurized water reactor
R&D	research & development
RTD	resistance temperature detector
SD	sonic delay
TDR	time domain reflectometry
UWO	University of Western Ontario
VVER	Russian pressurized water reactor



## LIST OF SI UNITS AND MATHEMATICAL SYMBOLS

<b><u>Term</u></b>	<b><u>Unit</u></b>	<b><u>Definition</u></b>	<b><u>Equation(s)</u></b>
$\alpha$	N/sec·m	damping coefficient N:Newton, m:meter	2.3, 2.4, B.21, B.22
$A$	cm <sup>2</sup>	heat-transfer surface area	4.1, A.1, B.18, C.1, C.2, C.6, D.1-D.6
$B$	<i>bar</i>	bulk modulus for the fluid	B.15 – B.20
$c$	J/Kg·°C	specific heat capacity J: Joules, Kg: kilogram, C: Celsius	4.1, 5.4, 5.6, A.1, C.1, C.6, D.5
$C_b$	cm <sup>3</sup> /bar	bubble compliance	B.14, B.15
$C_{FS}$	cm <sup>3</sup> /bar	compliance of fluid in the sensing line	B.14, B.15
$C_{FT}$	cm <sup>3</sup> /bar	compliance of the fluid in the transmitter	B.14, B.15
$C_s$	cm <sup>3</sup> /bar	compliance of the total system	B.14, B.16, B.17
$C_t$	cm <sup>3</sup> /bar	compliance of the transmitter	B.1, B.3, B.8 – B.12, B.14, B.20
$D$	<i>cm</i>	sensor diameter	C.10
$d_p$	<i>cm</i>	diameter of piston in pressure transmitter	B.3, B.5
$d_s$	<i>cm</i>	inside diameter of the sensing line	B.4, B.5, B.8, B.9, B.10 – B.13
$E$	<i>Volts</i>	bridge voltage	5.1
$F_b$	<i>Hz</i>	break frequency (also known as corner frequency)	Figure 5.13
$G$	<i>N/A</i>	transfer function	5.13, 5.20, 5.26 - 5.28, A.2, A.4, A.11, A.12
$h$	W/m <sup>2</sup> K	convection heat transfer coefficient W:watts, m:meter, K:Kelvin	4.1, A.1, C.4 – C.7, C.13, C.16, C.17
$k$	W/mK	thermal conductivity W:watts, m:meter, K:Kelvin	C.3, C.5, C.6, C.10

$k$	$bar/sec$	ramp rate	A.19, A.21, A.22
$k$	$N/m$	spring constant N:Newton, m:meter	B.2, B.3, B.6
$K$	$N/A$	system gain	B.21, C.17
$L$	$cm$	length	B.4, B.5, B.8, B.11, B.12, B.18, B.20, C.3, C.4, Eq pg 84
$m$	gram	mass	4.1, 5.4, 5.6, A.1, B.2, B.6, C.1, C.6, D.5
$M_e$	gram	rigid mass	B.5, B.6, B.7
$P$	$W$	Power W:watt	D.3
$p$	$N/A$	pole of a system transfer function	5.13, 5.14, 5.15, A.4, A.5, A.12
$P_b$	bar	pressure applied to gas bubble	B.15, B.20
$P_s$	bar	pressure in sensing system	B.1, B.3, B.16, B.17
$Pr$	$N/A$	Prandtl number	C.10, C.11, C.12
$Q$	$J$	joule heating generated in the RTD by applying $I^2R$ heating	D.1 – D.5, D.7
$R$	$\Omega (ohm)$	resistance	D.4
$r$	$bar/sec$	ramp rate	B.22
$R_L, R_d, R_{RTD}$	$\Omega (ohm)$	electrical resistances	5.1, 5.2, D.4, D.7
$Re$	$N/A$	Reynolds number	C.10, C.11, C.12
$r_i$	$cm$	radius at which the sensing tip is located	C.3, C.5, C.6, C.9
$R_{int}$	$^{\circ}C/W$	internal heat-transfer resistance C:Celsius, W:watt	C.2
$r_o$	$cm$	outside radius of sensor	C.3 – C.6, C.8, C.9
$R_{surf}$	$^{\circ}C/W$	surface heat-transfer resistance C:Celsius, W:watt	C.2
$R_{tot}$	$^{\circ}C/W$	total heat-transfer resistance C:Celsius, W:watt	C.2
$S_n$	$N/A$	Stokes number	B.10 – B.13
$T$	$^{\circ}C$	RTD temperature	C.17, D.1 – D.5
$T_F$	$^{\circ}C$	fluid temperature from its initial value	5.7, 5.8, 5.10, 5.12
$T_i$	$^{\circ}C$	temperature of the $i^{th}$ node	5.4, 5.5, 5.7
$U$	$W/m^2K$	overall heat-transfer coefficient W:watts, m:meter, K:Kelvin	C.1, C.2, C.5, C.6, D.1 – D.6

$u$	m/sec	flow rate m: meter	C.13 – C.15
$U_a$	m/sec	acoustic velocity of fluid in the sensing line m: meter	B.19, B.20
$\nu$	<i>bar·sec</i>	kinematic viscosity of fluid	B.10, B.13
$V$	<i>volts</i>	voltage	5.1
$V_b$	cm <sup>3</sup>	volume of the bubble	B.15, B.20
$V_{FS}$	cm <sup>3</sup>	volume of fluid in the sensing line	B.15, B.18, B.20
$V_s$	m/sec	average velocity of fluid in the sensing line m: meter	B.4
$V_t$	cm <sup>3</sup>	volume change	B.1, B.15 – B.17, B.20
$\Delta P_s$	bar	change in input pressure	B.1
$\Delta V_t$	cm <sup>3</sup>	volume change in the transmitter cavity	B.1
$\gamma$	N/A	ratio of specific heat capacities of gas bubble at constant pressure	B.15, B.20
$\theta$	°C	temperature of fluid in which the RTD is installed	D.1
$\mu$	<i>bar·sec</i>	viscosity of process fluid	B.9, B.11, B.12, C.10, C.17
$\rho$	gram/cm <sup>3</sup>	density	Pg 84, B.4, B.5, B.8, B.9, B.11, B.12, B.18, B.19, C.6, C.8, C.9, C.10, C.17
$\tau$	<i>sec</i>	response time	2.1, 4.1, 5.23 - 5.26, A.6, A.8, A.9 - A.11, A.14, A.15, A.23, C.1, C.6, C.14, C.15, D.5 – D.7
$\tau_1, \tau_2, \dots$	<i>sec</i>	modal time constants	2.1, 5.25 – 5.28
$\omega_d$	<i>rad/s</i>	damped natural frequency	2.3, 2.4, B.21, B.22
$\omega_n$	<i>rad/s</i>	undamped natural frequency	2.3, 2.4, B.2, B.10, B.13, B.21, B.22
$z$	N/A	zero of a system transfer function	5.13-5.15, 5.19, 5.20

# 1

## INTRODUCTION

---

To measure the true value of a process variable it is essential that the sensors chosen fit the application and provide very accurate and stable calibration for steady-state measurements and fast dynamic response for transient measurements. A second requirement is the appropriate process-to-sensor interface. For example, fluid temperatures in industrial plants are typically measured with sensors that are installed in thermowells secured to the process piping. The thermowell serves as the process-to-sensor interface and must be designed and installed in the process with the correct insertion depth, exact dimensional tolerances, and proper support to protect the temperature sensor, allow for its easy insertion and removal, and optimize dynamic response. At first glance, these provisions would seem to be easy to accommodate, and frequently they are. However, even a slight deviation can significantly affect critical process measurements, especially when temperatures, pressures, and flow rates are high. For example, tolerance issues involving the length or diameter of sensors or thermowells can cause temperature data to lag far behind the true process temperature, causing control issues and safety concerns.

The process-to-sensor interface for pressure transmitters (including liquid level and fluid flow sensors) are the sensing lines that connect the transmitter to the process. Fluid sensing lines are typically made of small-diameter tubing or piping consisting of root, isolation, and check valves; condensation pots; and other components. All these components must function properly to yield accurate and timely data to the plant control and safety systems. Naturally, operational stresses, aging, and installation issues can cause anomalies in sensing lines and contribute to measurement errors as well as dynamic response problems. For example, blockages can develop in sensing lines as a result of deposits of residues in the process fluid. Depending on its magnitude and the

compliance of the pressure transmitter, a blockage can reduce the dynamic performance of a pressure sensing system by as much as an order of magnitude. Also, valves in the sensing lines can fail partially closed, causing sluggish pressure transmitter response time.

This dissertation presents state-of-the-art testing techniques for identifying problems in the dynamic performance of industrial temperature, pressure, level, and flow sensors, including their critical process-to-sensor interfaces in-situ. These techniques are particularly useful for the most common type of nuclear power plant, the pressurized water reactor (PWR), an application for which testing accuracy and responsiveness is mission-critical. More specifically, in PWRs, the plant power level is set based on the performance of process instrumentation, among other factors. The better the performance of the process instrumentation in terms of measurement certainty, the more power the plant is allowed to produce and the larger the operating margin the plant is afforded (and vice versa). As an example, one U.S. PWR plant, which was suspected of having sluggish temperature sensors, was informed by regulators that it could operate at 100% power only if it could demonstrate that the response time of its safety system temperature instrumentation was 6.0 seconds or less. Conversely, if the response time of its temperature instrumentation degraded to above 6.0 seconds, this plant was ordered to reduce its power production level by an amount proportional to the increased response time.<sup>[1]</sup> At an operating revenue of over US\$1 million per day for a 1000 MWe plant, even a 1 percent loss in power generation level can amount to millions of dollars in lost revenue. To cite another example, a recent regulatory pronouncement has authorized nuclear power plants in the U.S. to increase their power output by as much as 1.6 percent provided they demonstrate to the satisfaction of regulators that they can measure feedwater flow rate with better accuracies than were assumed when the plants were originally licensed. Today, over 50 percent of the U.S. fleet of 104 reactors has taken advantage of this provision. This process is referred to as “measurement uncertainty recapture” or “power uprate through more accurate process measurements.”<sup>[2]</sup> These examples testify that the performance of process instrumentation is critical to plant safety and economy.

## 1.1 Motivation

Instrumentation and control (I&C) equipment, including the sensors and process-to-sensor interface, essentially constitutes the central nervous system of a nuclear power plant. I&C equipment measures thousands of variables and processes data to activate pumps, valves, motors, and other electromechanical equipment that control the plant. It also displays the plant conditions and keeps the process variables within the design limits to maintain safety, efficiency, and availability. As such, the performance of I&C equipment is vital to the operation of the plant and the protection of the public from radiation releases. In particular, nuclear plant I&C systems must be *accurate* to properly sense and communicate the process variables and have a short response time to provide timely regulations, display, and protection against upsets in both the main plant and its ancillary systems. For example, temperature sensors such as resistance temperature detectors (RTDs), which feed the nuclear plant's safety system instrumentation, may be expected to provide accuracy to within 0.1 percent and respond to a step change in temperature in less than 4.0 seconds. Although the accuracy requirement is not always as tight for pressure transmitters, they may be expected to have an accuracy of 0.25 percent but a response time of less than 0.5 seconds, especially if they are a part of the plant's protection instrumentation.<sup>[3]</sup>

*To ensure good accuracy and short response time, nuclear power plants must perform calibration and response time tests on their important I&C systems.*<sup>[4]</sup> The frequency of these calibration and response time tests is typically specified in the plant's technical specifications, regulatory requirements, or industry standards.<sup>[5,6]</sup> Generally, the frequency is tied to the length of the operating cycle of the plant, which varies between 12 and 24 months.

Figure 1-1 shows a typical process instrumentation channel in a PWR plant. The sensors and process-to-sensor interfaces are in the reactor containment or elsewhere in the field and are therefore subject to harsh environments. The rest of the instrument channel, except for the actuation systems, consists of electronics that are housed in the

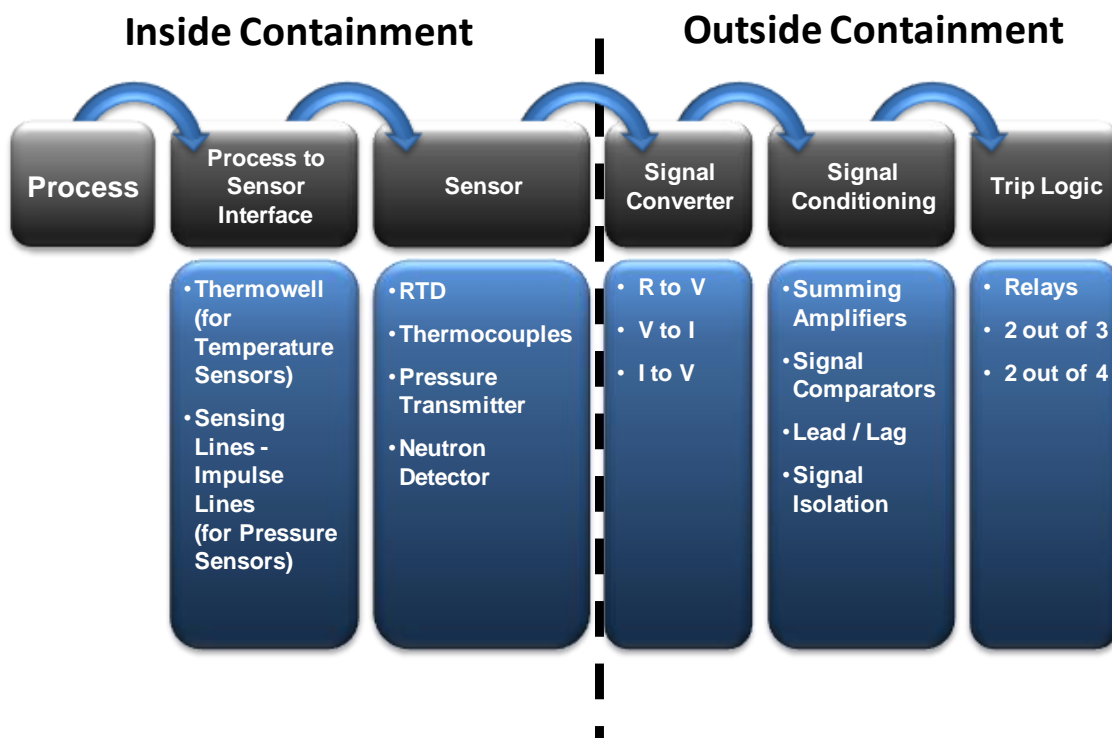


**Figure 1-1 Example of a Typical Process Instrumentation Channel**

process instrumentation cabinets in air-conditioned rooms located remotely from the reactor containment or the field. Furthermore, the sensors and process-to-sensor interfaces are not readily accessible during plant operation. Therefore, performing calibration, response time testing, or maintenance on field sensors is not practical during plant operation. The methods presented in this dissertation help resolve this issue.

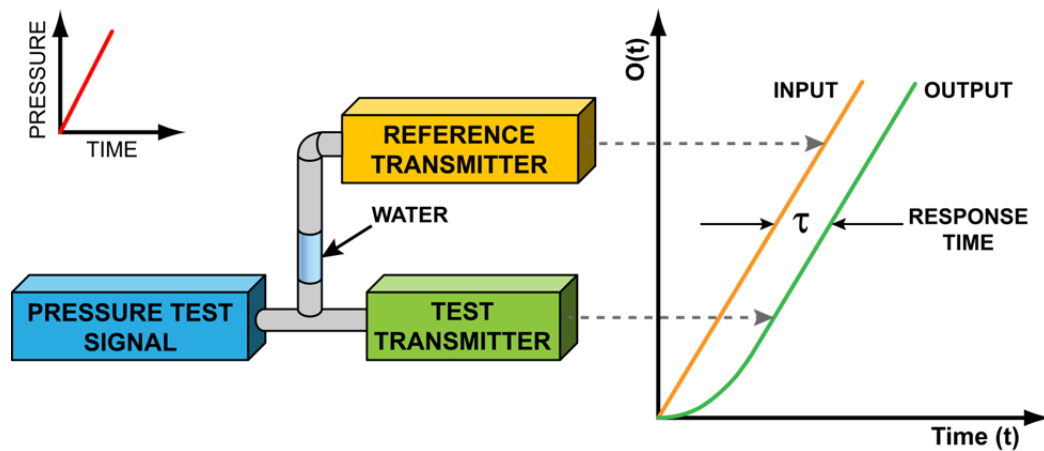
## 1.2 Current Solutions

Current solutions for sensor response time testing in nuclear power plants include the plunge test for temperature sensors and the ramp test for pressure transmitters. These methods are described in detail in Chapter 3. For now, it is sufficient to say that the current methods depend on a step or a ramp change in temperature or pressure to test the sensor. For temperature sensors, a step change in temperature is imposed in a laboratory environment by suddenly drawing the sensor from one medium at a given temperature and immersing it into another medium, usually water flowing at 1 meter per second, at a different temperature. This procedure is referred to as the “plunge” test.<sup>[7]</sup>

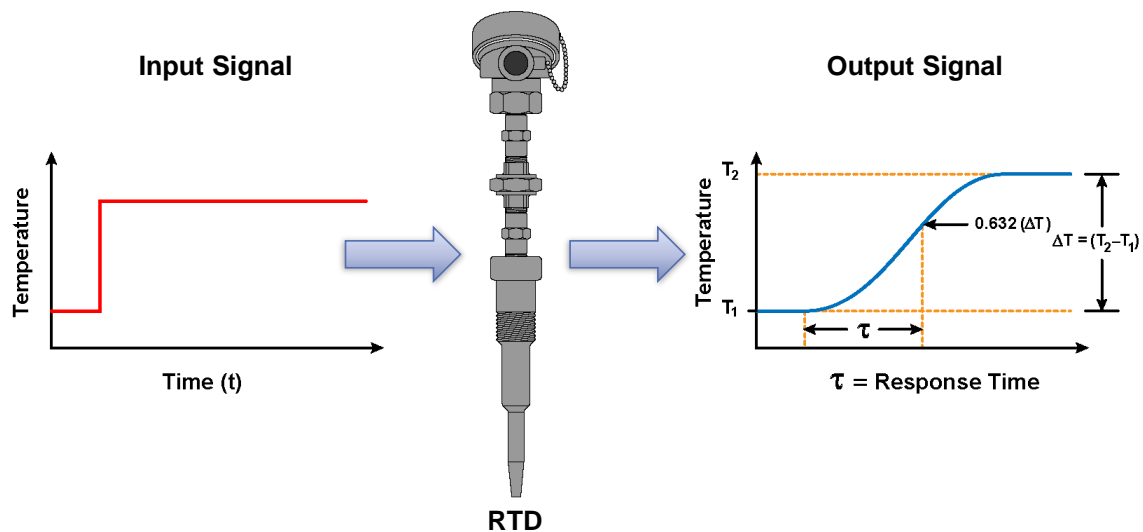
For pressure sensors, a hydraulic signal generator is employed to produce a ramp pressure signal for the response time measurement. The ramp signal is fed to the pressure sensor under test and simultaneously to an ultrafast reference sensor. The output of the two sensors is then recorded. From this output, the response time is identified by measuring the asymptomatic delay between the output of the sensor under test and that of the reference sensor (Figure 1-2). Temperature sensors are tested with a step input whereas pressure sensors are tested with a ramp input because the safety analysis of nuclear power plants involves testing for potential “design basis” accidents. These accidents are assumed to result in a step change in temperature and/or a ramp change in pressure. Figure 1-2 illustrates the procedures for response time testing of RTDs and pressure transmitters. The figure also includes the equations which describe the step and ramp responses of the sensors assuming that they are first order systems.

Figure 1-3 is a simplified schematic of the core of a nuclear plant, showing a step change in temperature in the reactor. The figure also shows an RTD sensor at the





The ramp response of a pressure sensor is given by  $O(t) = K(t - \tau + e^{-t/\tau})$  where  $t$  is time,  $K$  is a constant, and  $\tau$  is the time constant of the sensor. The response time obtained as shown above is also referred to as ramp time delay.



The step response of an RTD is given by  $O(t) = A(1 - e^{-t/\tau})$  where  $t$  is time,  $A$  is a constant, and  $\tau$  is the RTD time constant. The time constant is defined by substituting  $t = \tau$  in this equation to arrive at  $O(t) = 0.632A$ .

**Figure 1-2 Illustration of Ramp and Step Test Setups to Measure the Response Time of a Pressure Transmitter and an RTD**

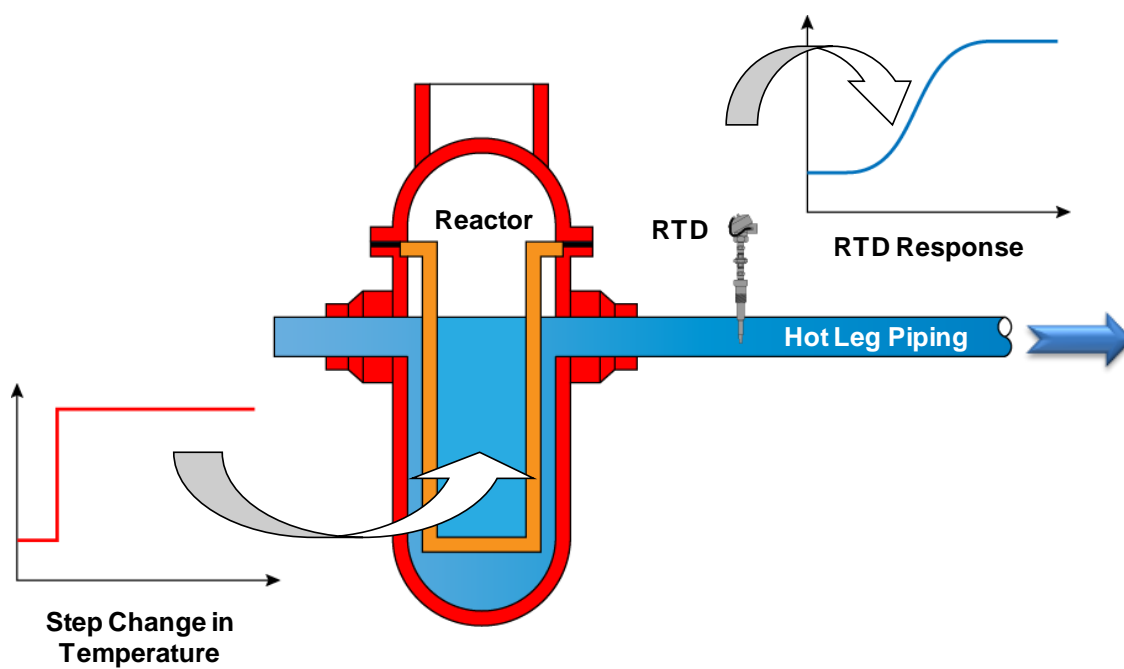


**Figure 1-3** A Step Change in Temperature in the Core of a Nuclear Reactor and the Resulting Response of an RTD Sensor at the Output of the Reactor

output of the reactor that is undergoing a transient response to the step change in temperature. Typically, the RTD in this situation must respond quickly (e.g., in less than 4.0 seconds) in order to initiate timely actuation of safety systems so as to mitigate any adverse consequences from the step change.

### **1.3 Solutions Demonstrated by This Research**

Most regulations, standards, and guidelines for the performance of nuclear plant I&C systems specify that the response time of the field sensors that feed the safety systems of the plant must be verified periodically. In particular, the “in-service” response time of these sensors must be measured and compared with the acceptance criteria in the plant’s technical specification document to ensure compliance. The challenge is in measuring the *actual* “in-service” response time of the sensors under plant operating conditions. It is not difficult to measure the response time of a sensor in a laboratory, and such measurements are typically performed on most safety system sensors before they are installed in a plant. However, unless the response time measurements are performed under plant operating conditions, there is no way to determine the actual in-service response time of the sensor or transmitter. This is due to the effect of both process conditions and sensor installation on response time (see Chapter 4). For example, temperature sensors such as RTDs are used in PWR plants to measure the primary coolant temperature. Typically, these RTDs are installed in thermowells that are welded to the primary coolant piping (Figure 1-4). If an RTD is response time tested in a test thermowell in a laboratory and then installed in the plant thermowell, its response time can change by as much as a factor of two or more. Therefore, the response time must be measured while the RTD is installed in its plant thermowell and under normal operating temperature, pressure, and flow. In particular, the process flow rate has an effect on RTD response time that is predictable; however, the effect of temperature is not predictable. More specifically, the response time of RTDs decreases as flow rate is increased, but temperature may cause either an increase or a decrease in response time. Therefore, in-situ response time testing is the only way to measure the

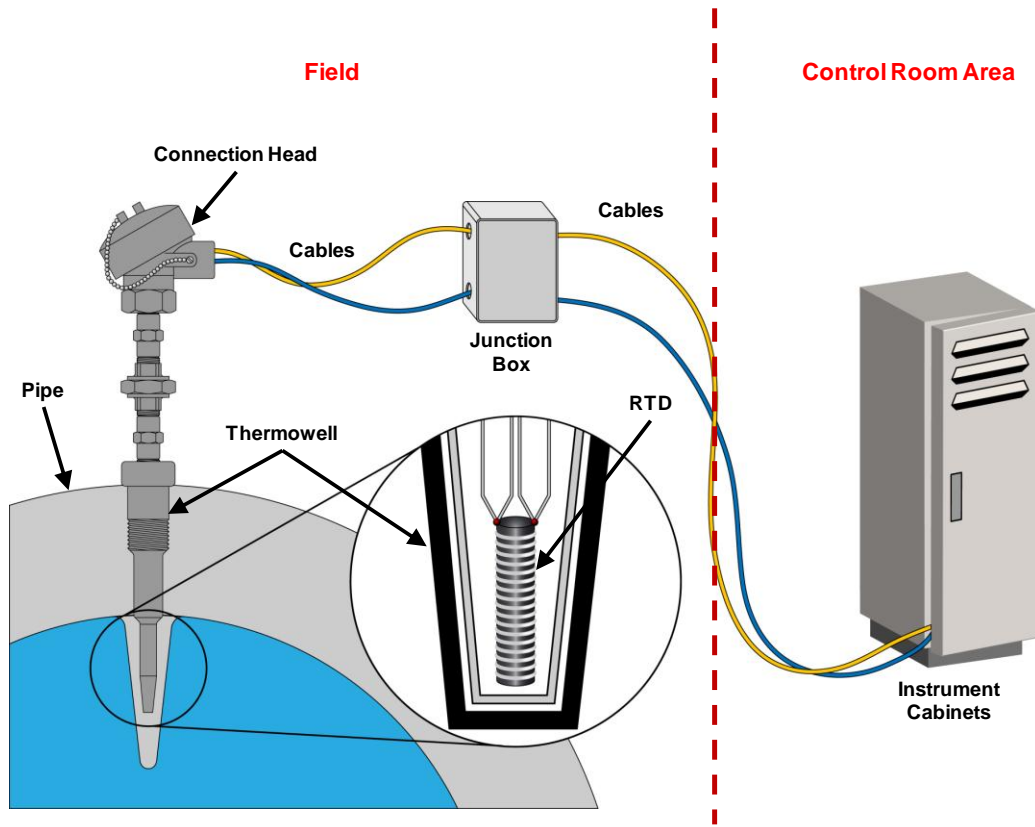


**Figure 1-4 Example of an RTD Installation in a Nuclear Power Plant**

“in-service” response time of nuclear plant RTDs. Another reason why the “in-service” response time of pressure transmitters can only be measured by in-situ testing is that this is the only method that accounts for the effect of sensing line problems (e.g., blockages and voids) on the response time. Summaries of state-of-the-art testing techniques that can provide “in-service” response times for nuclear plant RTDs and pressure transmitters are presented in the following two subsections. The application and refinement of these techniques constitute the focus of the research conducted for this dissertation. The details, methods, and validation are presented in the body of this dissertation (Chapters 2 through 5).

In the remainder of this dissertation, the term *pressure transmitter* refers to sensors that measure pressure and differential pressure to yield pressure, level, and flow data. It should also be noted that the terms *pressure sensor* and *pressure transmitter* are synonymous.

### **1.3.1 Method for Measuring the Response Time of RTDs**

The “Loop Current Step Response” test or LCSR provides the “in-service” or in situ response time of RTDs as they are installed in an operating plant. To perform the test in a nuclear power plant, the LCSR equipment is set up in the control room area, the point at which the RTD field wires reach their signal converters in the instrument cabinets. Each RTD is connected to this equipment. A step change in electrical current is sent to the RTD using a Wheatstone bridge. A current of between 30 to 60 mA is adequate depending on the RTD and the conditions in the plant. This current causes the RTD sensing element to heat up by several degrees (e.g., 5 to 10°C) above the process temperature. As the heat increases, the resistance of the RTD gradually increases and produces an exponential transient at the output of the Wheatstone bridge. The exponential transient is referred to as the LCSR signal. Chapters 5 and 6 demonstrate that the LCSR signal can be analyzed to yield the response time of the RTD under the installation and process conditions tested. This is provided that the RTD design characteristics and the process conditions meet the assumptions that are required for the validity of the LCSR test. These assumptions are identified in Chapter 5.

### 1.3.2 Method for Measuring the Response Time of Pressure Transmitters

Unlike RTDs, the response time of pressure transmitters is not affected by process conditions. Therefore, the response time that is measured in a laboratory or on the bench does not normally change when the transmitter is installed in the plant. RTDs are thermal devices, and their dynamic characteristics are sensitive to process conditions. However, pressure transmitters are electromechanical devices made of components that respond at essentially the same rate whether they are at ambient temperature or at the process operating temperature. Also, static pressure and fluid flow rate have little or no effect on the dynamic response of pressure transmitters. The problem posed by measuring pressure transmitters in situ lies in the sensing lines that connect the transmitters to the process (Figure 1-5). Sensing lines are typically made of small-diameter (e.g., 20 mm O.D.) piping or tubing that ranges in length from 20 to 200 meters, depending on the transmitter's service and location in the plant. The sensing lines add a sonic delay to the response time of pressure transmitters that is on the order of a few milliseconds and thus negligible. However, they also add a hydraulic delay that can add hundreds of milliseconds to the response time of a pressure sensing system and cannot therefore be ignored. In fact, hydraulic delays can be very significant, especially if blockages or voids are present in the sensing lines. (Note: Sensing lines are also referred to as "impulse lines.")

To ensure that sensing lines are not fouled or blocked, nuclear power plants periodically purge them with nitrogen gas. However, this procedure does not guarantee that the blockage is cleared. Moreover, it is very time consuming and radiation intensive for the plant maintenance crew. These considerations stimulated the development of the noise analysis technique for response time testing of pressure transmitters. This technique is based on monitoring the natural fluctuations arising from turbulence, random flux, random heat transfer, controller action, and vibration that exist in the output of transmitters while the process is operating. Because these fluctuations are referred to as "noise," the method is therefore called "noise analysis." In fact, the term "noise," which implies high-frequency effects and undesirable interferences, is a misnomer because it is only low-frequency fluctuations (1 to 10 Hz) that are relevant to response

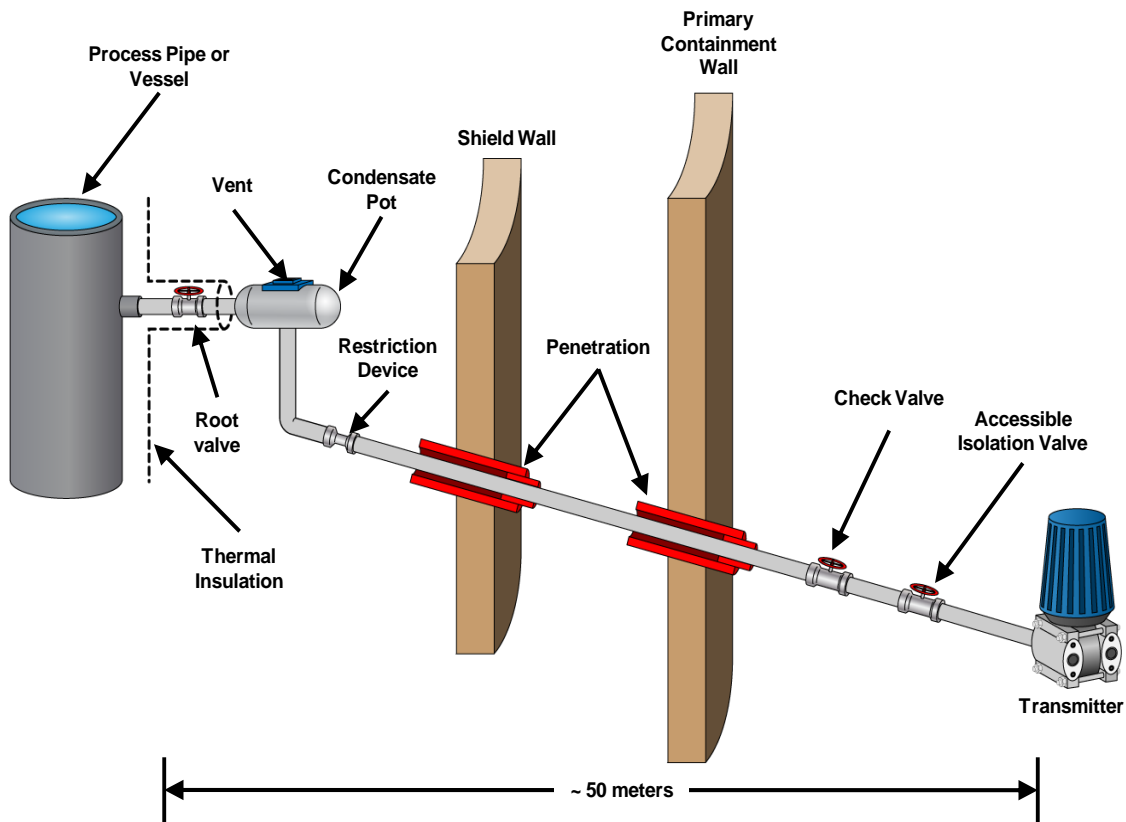


**Figure 1-5 Typical Pressure Transmitter Installation in a Nuclear Power Plant**

time testing. However, “noise analysis” has become the accepted term among signal processing experts for this application.

The process noise can be separated from the transmitter output by signal conditioning and analyzed to yield the response time of the transmitter. This is provided that the dynamics of the transmitter are linear, the process fluctuations that drive the transmitter are broadband with adequate amplitude, the statistical distribution of the noise signal at the output of the transmitter is Gaussian (normal), and that there are no resonances in the process that can cause the transmitter’s frequency response to shift to higher frequencies. Based on experience using the noise analysis technique in nuclear power plants, the author has discovered that these assumptions are often met and that noise analysis is therefore effective for in-situ response time testing of nuclear plant pressure transmitters.

Figure 1-6 shows a noise data record obtained for this research from testing of a transmitter in an operating nuclear power plant. To illustrate the features of the data only 5 seconds is shown, although about an hour of such data is normally collected and analyzed to determine the response time of a pressure sensor.

#### **1.4 Goal and Objectives of This Research**

The goal of the work described in this dissertation was to provide validated techniques for measuring the response time of temperature, pressure, level, and flow sensors as installed in nuclear power plants. This goal has been attained through successful execution of the following research objectives.

1. Introduce methods that allow the remote testing of nuclear plant temperature and pressure sensors. The methods must provide remote in-situ testing capabilities during plant operation without disturbing the plant or its crew, must not harm the sensors, and must be accurate, repeatable, and amenable to regulatory approval. Furthermore, the methods must provide the response time of both the sensor and the process-to-sensor interface (e.g., thermowell in the case of RTDs and sensing lines in the case of pressure transmitters).
2. Establish the theoretical foundation for the sensor response time testing methods and show the derivations that correlate the test data to the sensor response time



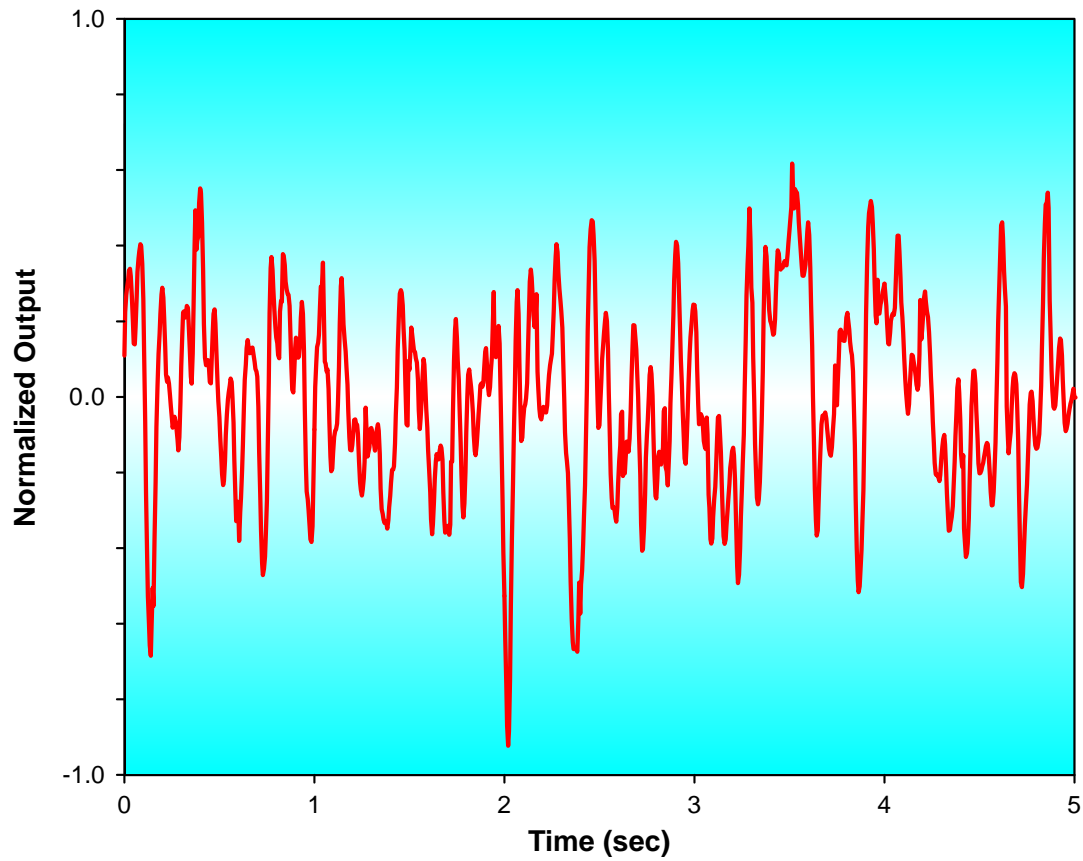


**Figure 1-6 Raw Noise Data from a Nuclear Plant Pressure Transmitter**

results. Any assumptions that are involved in arriving at these correlations must be stated and justified.

3. Demonstrate the validity of the in-situ response time testing methods through simulation, laboratory testing, in-plant data, or a combination of these approaches. The new methods must provide essentially the same results (within the accuracy limitations of the tests) as the conventional techniques for sensor response time testing. That is, the equivalence between the results of the in-situ testing techniques and sensor response time results from classical methods must be substantiated.

### **1.5 Contributions of This Dissertation**

The contribution of this dissertation derives from the broad applicability and significant ramifications of the two new methods—LCSR and noise analysis—that the author has refined, implemented, and validated through his research. Through it, the author has evolved LCSR as a method by testing and adapting it to multiple practical applications, demonstrated the effect of sensing line blockages and voids on response time, and verified that the noise analysis technique can identify these effects. More specifically, this dissertation identifies the effect of compliance on the total response time of a pressure sensing system and quantifies this effect through laboratory measurements using multiple pressure transmitters. Using nuclear-grade pressure transmitters, the author demonstrates that the response time of a pressure sensing system can be dominated by the sensing line to an extent governed by the transmitter's compliance value. He also demonstrates that the noise analysis technique can yield the response time of a pressure sensor and its sensing line in a single test.

The ramifications of these findings are substantial. Because conventional response time test procedures—the plunge test and ramp test--do not account for the influence of process conditions and installation on response time, they open an important gap in the industry's ability to meet a key safety requirement. The work of this dissertation closes this gap by demonstrating, first, that that the LCSR method as advanced by the author can be performed remotely on installed RTDs at operating conditions, thereby providing the actual in-situ response time rather than the manufacturer's unrealistic response time or the time produced by costly offline testing. Second, this dissertation also closes the industry safety gap by demonstrating that the

noise analysis technique not only measures the pressure transmitter's in-situ response time but also that of its sensing lines, accounting for sensing-line length, blockages, and voids. By subjecting the LCSR and noise analysis technique to extensive real-world tests in multiple operating environments, the author has demonstrated their utility not only in terms of test accuracy, repeatability, and regulatory compliance, but as robust and reliable tools for improving plants' cost efficiency and employee safety.

Finally, the contribution of this dissertation lies in pointing the way forward to new applications of the LCSR and noise analysis methods, not only across the spectrum of nuclear reactor types but in unexplored sensor applications such as thermocouples and neutron detectors.

## **1.6 Organization of This Dissertation**

In this introductory chapter, the author has described his motivation for conducting the research described in this dissertation. Chapter 1 has also briefly presented the current solutions for measuring the response time of RTDs and pressure transmitters, namely, the plunge test and the ramp test, and the new solutions demonstrated by this research and described in this dissertation—the LCSR and noise analysis methods.

Chapter 2 presents an overview of nuclear plant RTDs and pressure transmitters, describes pressure sensing lines and their effect on the dynamics of pressure sensing systems, and briefly presents the science behind sensor response time testing. Chapter 3 examines the conventional plunge and ramp test methods for measuring the response time of temperature and pressure sensors and reviews the history of and literature on sensor response time testing in the nuclear power industry. Chapter 4 describes the experiments the author conducted to demonstrate the influence of installation, process conditions, and aging on sensor response time.

Chapter 5 describes the two techniques—LCSR and noise analysis—developed to address the inadequacies of the plunge test and the ramp test. Chapter 6 describes the results of the validation experiments the author performed to determine the equivalence and reliability of the LCSR and noise analysis techniques as substitutes for conventional

response-time testing methods. Chapter 7 considers the broader applications of these two new techniques beyond the nuclear power industry, in the process, power, aerospace, manufacturing, and other industries.

Chapter 8 of this dissertation summarizes the conclusions that can be drawn from the author's research and offers recommendations for future research into the wider application of the LCSR and noise analysis techniques.

# 2

## SCIENCE OF MEASURING PROCESS VARIABLES

---

This chapter provides a basic overview of nuclear plant RTDs and pressure transmitters to set the stage for a full description of the new techniques for measuring the dynamic performance of these sensors in subsequent chapters. Also presented is a description of pressure sensing lines, a brief review of the science of sensor response time testing, and a discussion of effect of sensing lines on the dynamics of pressure sensing systems.

### 2.1 Resistance Temperature Detectors (RTDs)

RTDs are thermal devices containing a resistance element that is referred to as the sensing element. The resistance of the sensing element changes with temperature, and by measuring the resistance, one can therefore indirectly determine the temperature. Today, the sensing element of almost all RTDs is made of fine platinum wire, which is often coiled around a support structure referred to as a mandrel (see Figure 2-1). Figure 2-1 also shows a microscopic-scale photograph of an actual platinum element of a nuclear plant RTD. As shown in the figure, four wires, known as the RTD extension leads, are connected to the two ends of the platinum element. In RTDs that have four extension leads (referred to as a four-wire RTD), the two extra wires make it possible to measure the resistance of the lead wires and subtract that resistance from the loop resistance to yield the resistance of the platinum element alone. In most four-wire RTDs, two of the four leads are used to apply a constant current to the RTD, and the other two leads are used to measure the voltage drop in the platinum element, from which the RTD resistance is deduced.

The typical resistance of industrial RTDs (known as 100-ohm or 200-ohm sensors) is either 100-ohm or 200-ohm at ice point (0°C). When the sensing elements are manufactured, the resistance of the platinum wire is measured in an ice bath, and its

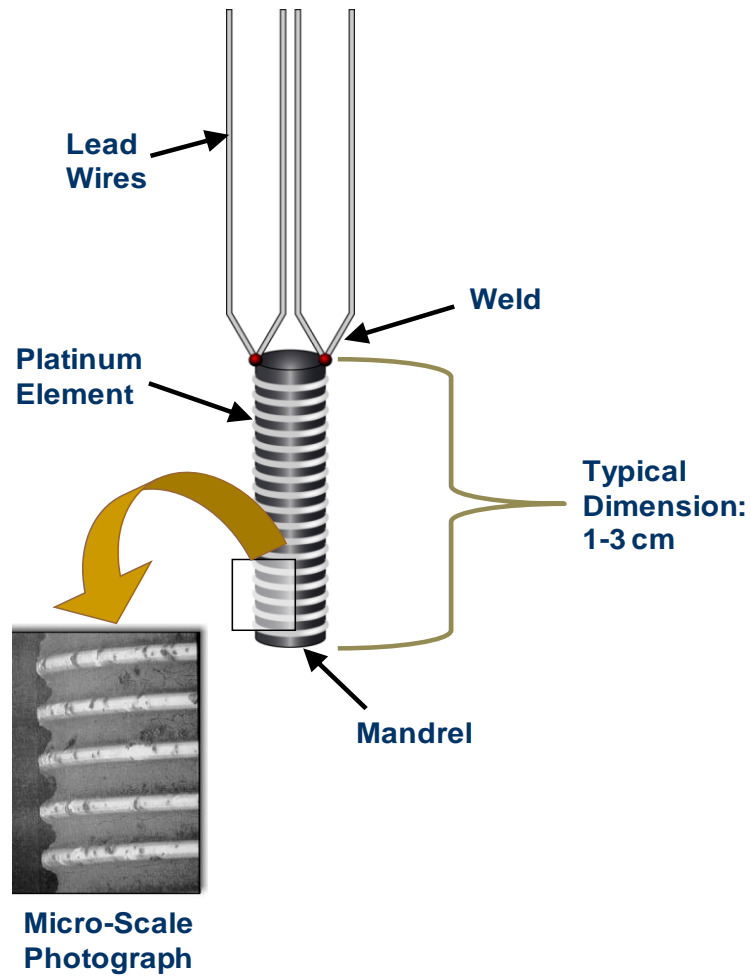


**Figure 2-1 RTD Sensing Element**

length is adjusted as necessary to yield an ice point resistance ( $R_0$ ) of 100-ohm, 200-ohm (or whatever is desired).

The construction of an industrial RTD is completed by inserting the sensing element into a tube, usually made of stainless steel, known as the sheath (Figure 2-2). Next, the sheath is packed with insulation material (to hold the sensing element and the extension wires in place and insulate them from the sheath) and then sealed. The property of the insulation material is important in providing both proper electrical insulation and reasonable thermal conductivity. In general-purpose RTDs, aluminum oxide ( $\text{Al}_2\text{O}_3$ ) or magnesium oxide ( $\text{MgO}$ ) may be used for insulation material.

RTDs are supplied in several configurations, varying in terms of length, diameter, and other characteristics. Table 2-1 lists typical characteristics of RTDs for nuclear power plant applications. The number of RTDs in a nuclear power plant varies depending on the plant design and its thermal hydraulic requirements. For example, PWR plants have up to 60 RTDs that are important to plant operation and safety, while heavy water reactors such as CANDU plants have several hundred key RTDs.<sup>[8,9]</sup>

Two groups of RTDs are typically used in nuclear power plants: direct immersion (or wet-type) and thermowell mounted (or well-type) (see Figure 2-3). The advantage of direct-immersion RTDs is better response time, while the disadvantage is the difficulty of replacing them. The advantage of well-type RTDs is ease of replacement; their disadvantages are a longer response time than direct-immersion RTDs and susceptibility to response time degradation caused by changes in the RTD/ thermowell interface. Direct immersion RTDs are usually used in by-pass loops in PWR plants (see Figure 2-4) and must therefore be fast so as to overcome the transport time delay. This is the time required for a signal to travel through the bypass piping and reach the RTD manifolds shown in Figure 2-4. As for thermowell-mounted RTDs, they are typically installed in the primary coolant loops as shown in Figure 2-5.

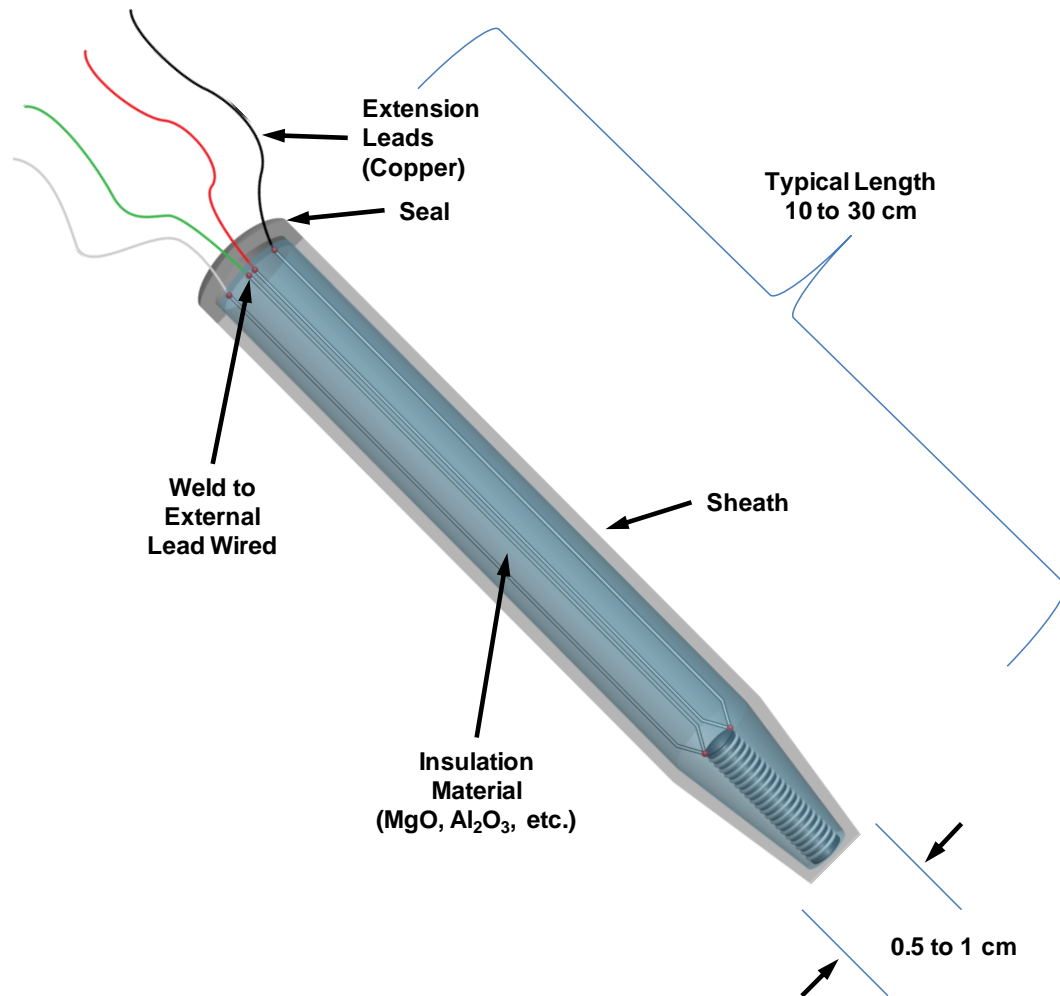


Figure 2-2 Typical RTD Assembly



**Table 2-1 Typical Characteristics of RTDs in Nuclear Power Plants<sup>[10]</sup>**

Average Length	30 to 60 cm well-type 12 to 18 cm wet-type
Average Diameter	0.6 to 1.0 cm RTD 1.0 to 2.0 cm thermowell
Immersion Depth in Process Fluid	5 to 10 cm in 1 meter ID pipe
Average Weight	100 to 250 grams RTD 300 to 3000 grams thermowell
Sheath Material	Stainless steel or Inconel
Sensing Element	Fully annealed platinum wire
Ice Point Resistance ( $R_0$ )	100 or 200 $^{\circ}\Omega$
Temperature Coefficient ( $\alpha$ )	0.003850 $\Omega/\Omega/^{\circ}\text{C}$ regular grade 0.003902 $\Omega/\Omega/^{\circ}\text{C}$ premium grade
R vs. T Curvature ( $\delta$ )	1.5 ( $^{\circ}\text{C}$ )
Temperature Range	0 to 400 $^{\circ}\text{C}$
Insulation Resistance (IR)	Greater than 100 megohm at room temperature, measured with 100 VDC
Response Time (1 m/sec water)	0.3 to 3 sec wet-type 4 to 8 sec well-type
Self-heating Index (1 m/sec water)	2 to 10 $\Omega/\text{W}$

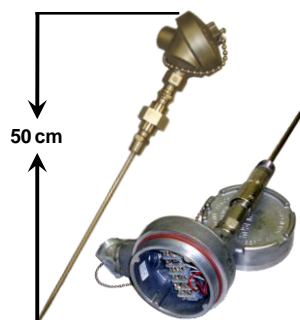
cm = centimeter

 $\Omega$  = ohm

W = watt

m/sec = meter per

second



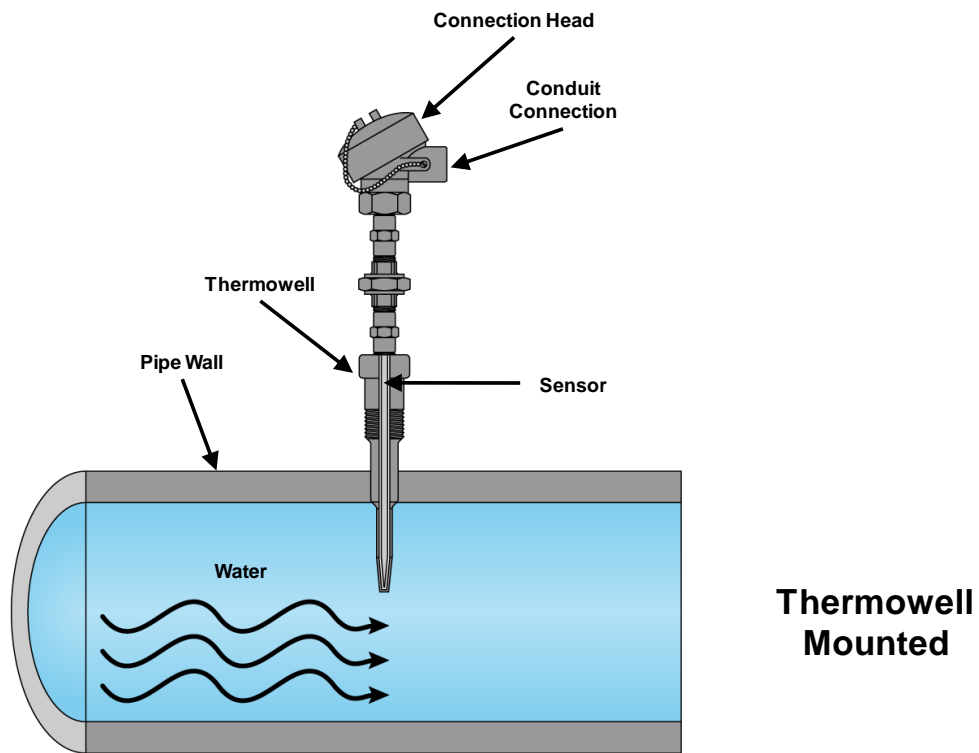
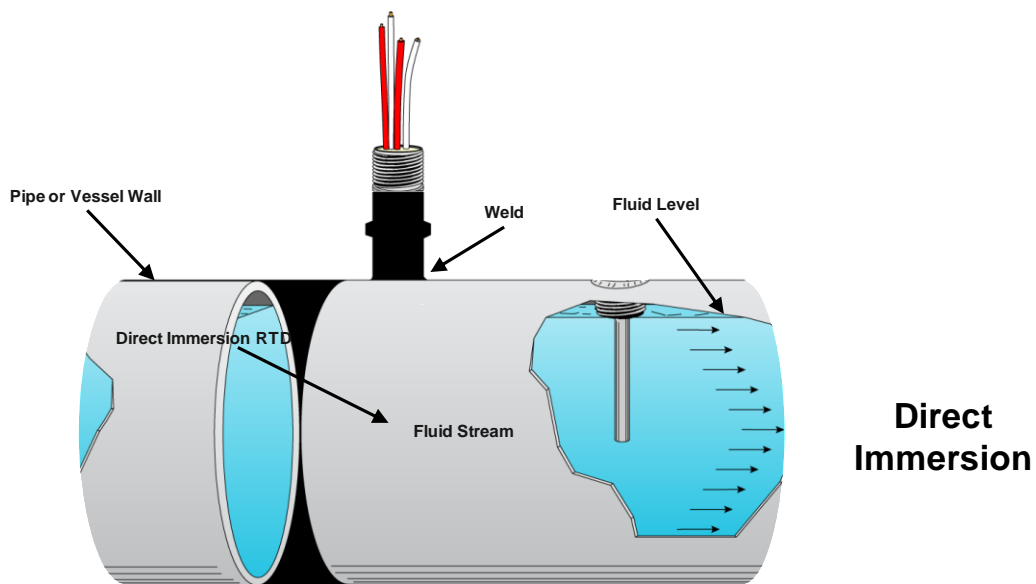


**Figure 2-3 Installation of Direct-Immersion and Thermowell-Mounted RTDs**

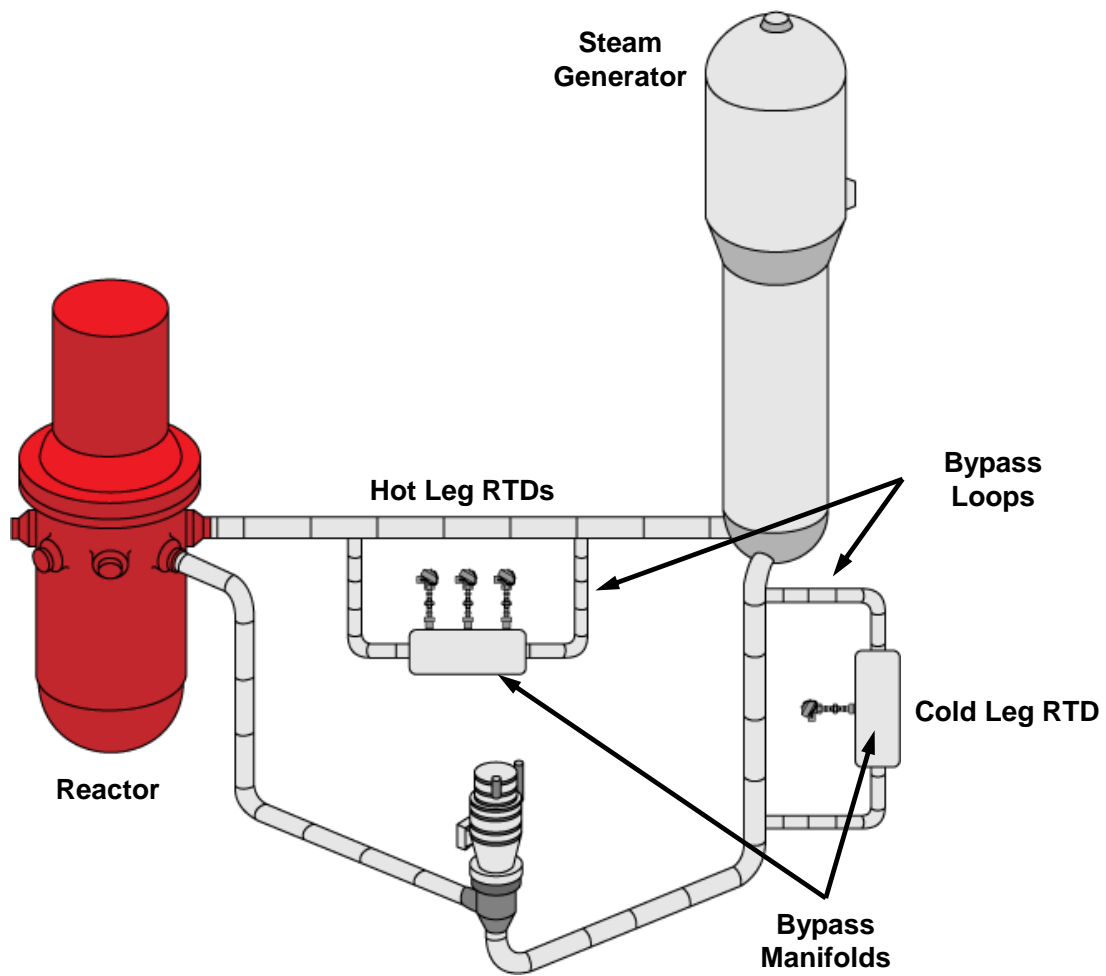


**Figure 2-4** Direct-Immersion RTDs in Bypass Loops of a PWR Plant

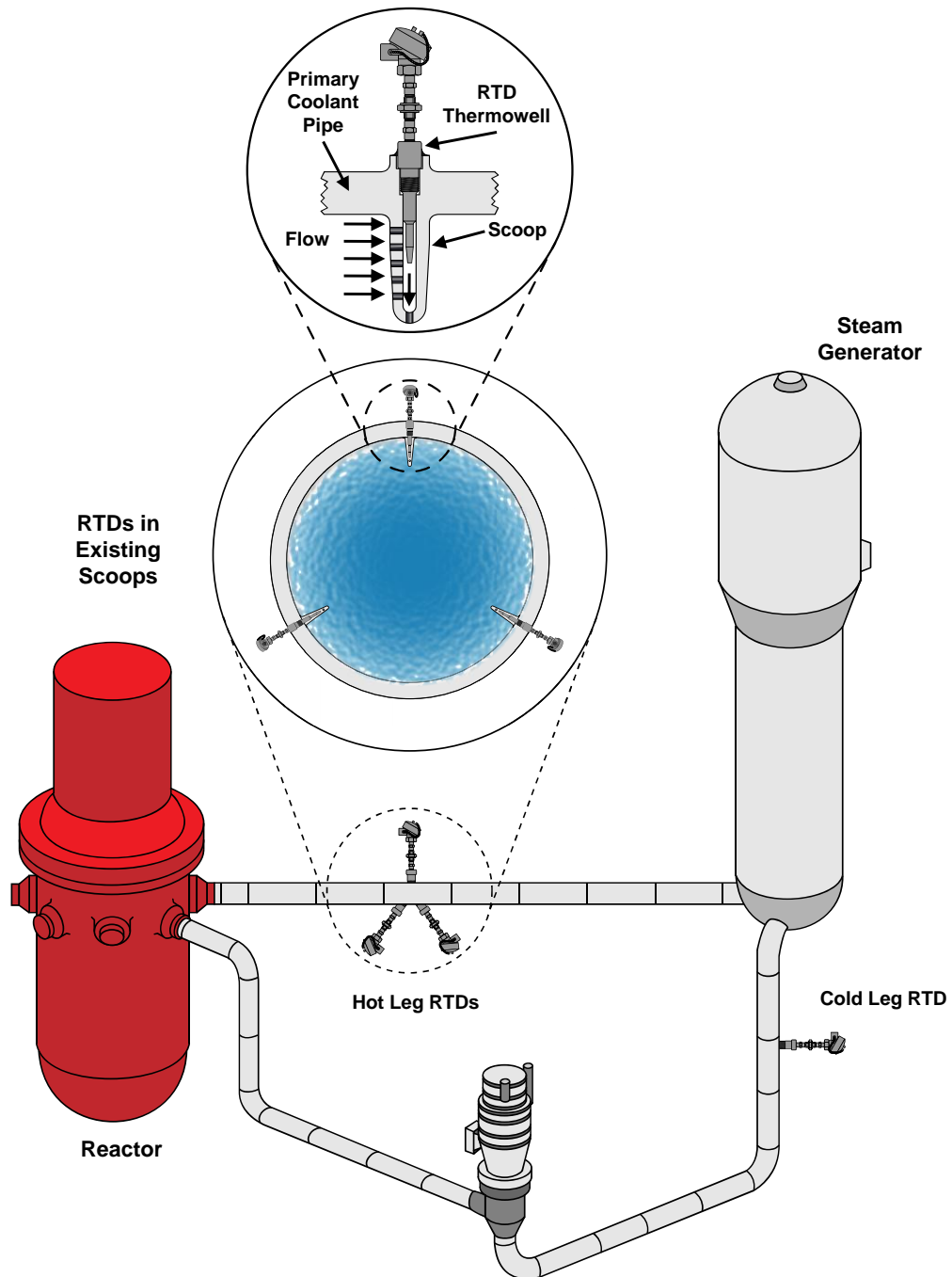


**Figure 2-5 Thermowell-Mounted RTDs Installed Directly in the Primary Coolant Loops of a PWR Plant**

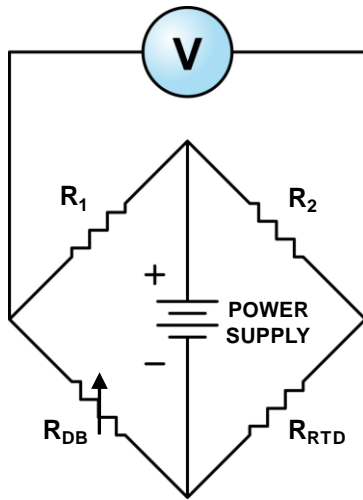
To accurately measure the resistance of an RTD and convert it into the corresponding temperature, one of the two types of Wheatstone bridge is normally used (see Figure 2-6). A simple form, called the two-wire bridge, consists of two fixed resistors, a variable resistor or a decade box (DB) and a DC power supply. If the RTD is used to monitor temperature in applications where high accuracy is not required, a two-wire bridge is sufficient. That is, no compensation for the resistance of the extension leads is normally required. However, if accuracy is important, a three-wire bridge must be used. The three-wire bridge automatically compensates for the lead wire resistances, as long as the resistance of the two RTD leads at the two sides of the bridge have equal values.

Figure 2-7 shows typical configurations of RTD extension wires for use with two- and three-wire bridges. As for four-wire RTDs, two wires are used rather than a bridge to apply a measuring current ( $I$ ) to the RTD. The other two wires are used to measure the voltage drop ( $V$ ) across the RTD element while using Ohm's law to identify the resistance ( $R = V/I$ ). This arrangement is shown in Figure 2-8.

## 2.2 Pressure Transmitters

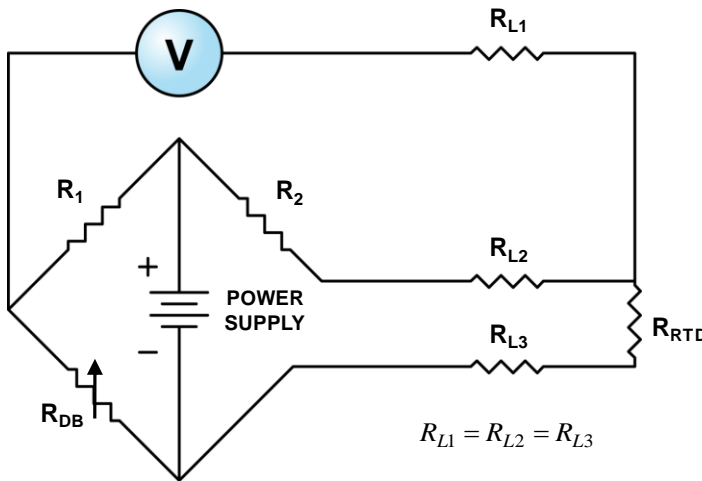
A pressure transmitter may be viewed as a combination of a mechanical system and an electronic system. The mechanical system contains an elastic sensing element (diaphragm, bellows, Bourdon tube, etc.) that flexes in response to the applied pressure. The movement of this sensing element is detected using a displacement sensor and converted into an electrical signal that is proportional to the pressure.

Typically, *motion-balance* or *force-balance* pressure transmitters are used in most nuclear power plants for safety-related pressure measurements. In motion-balance transmitters, the displacement of the sensing element is measured with a displacement sensor (e.g., a strain gauge or a capacitive detector) and converted into an electrical signal (e.g., 4 mA - 20 mA DC current) that is proportional to the pressure. In force-balance transmitters, the applied pressure forces a sensing rod in the transmitter to



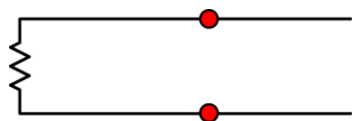
**Two Wire  
Bridge**

$$\frac{R_1}{R_2} = \frac{R_{DB}}{R_{RTD}} \quad R_1 = R_2 \quad R_{RTD} = R_{DB}$$

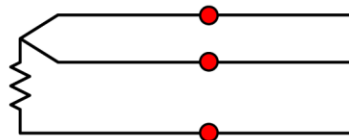


**Three Wire  
Bridge**

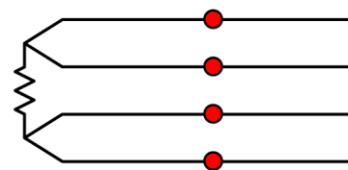
**Figure 2-6 Wheatstone Bridge Configurations for Measuring RTD Resistance**



Two-Wire



Three-Wire



Four-Wire

Figure 2-7 RTD Wire Configurations

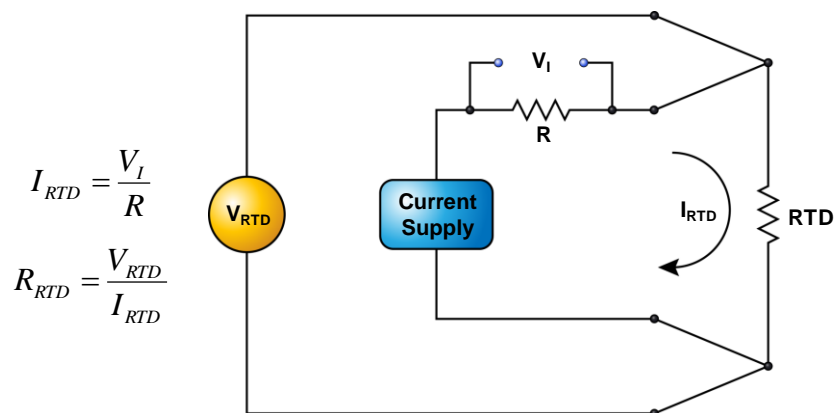


Figure 2-8 A Four-Wire RTD Measurement Circuit

deflect. This deflection is opposed by an electromechanical feedback system in the transmitter, which uses a motor to keep the sensing rod at an equilibrium position. The amount of electrical current supplied to the force motor is proportional to the applied pressure exposed by the sensing rod.

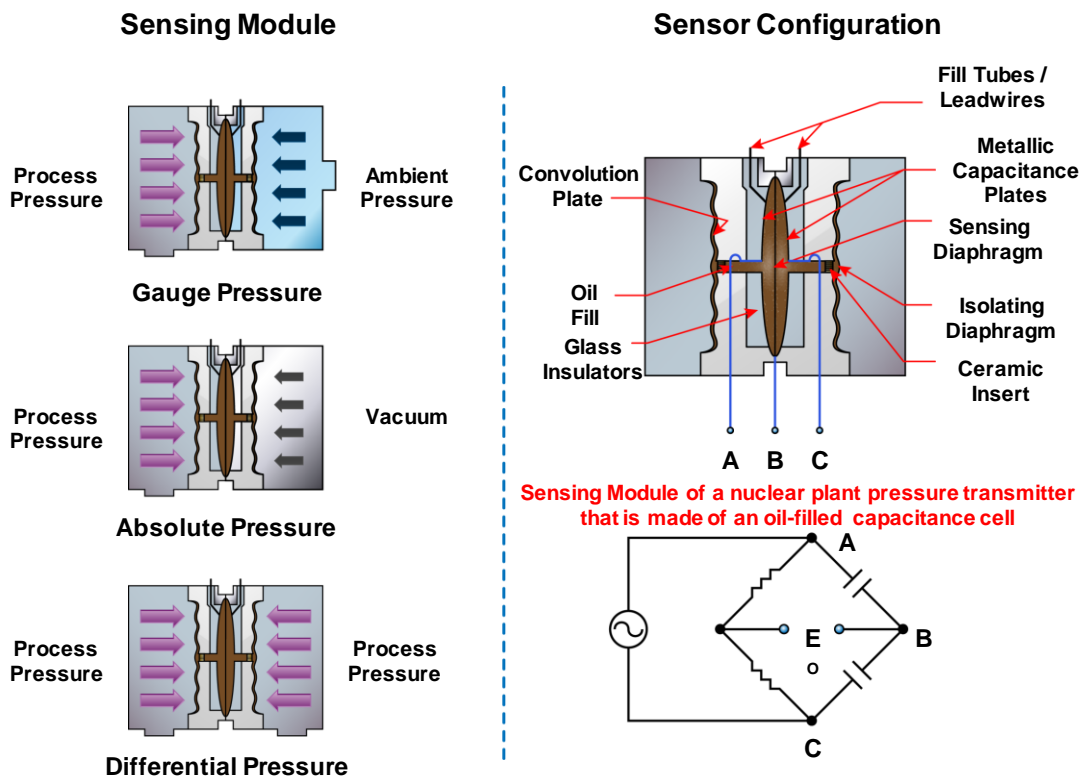
The transmitter's electronic system consists of active and passive components and circuitry that perform signal conditioning, temperature compensation, and linearity adjustments on the output signal. Typically, the transmitter electronics for low- and high-pressure applications are the same, while the sensing elements are different. For example, one manufacturer uses three different elastic elements to accommodate several pressure ranges, from 0 to a maximum of about 200 bars (about 3000 psi), but using the same transmitter housing design.<sup>[11]</sup>

A nuclear power plant generally contains between about 1,000 and 2,000 pressure and differential pressure transmitters, depending on the type and design of the plant. For example, the number of transmitters used in PWRs depends on the number of reactor coolant loops. Figure 2-9 shows the principle behind absolute, gauge, and differential pressure measurements. Figure 2-9 also illustrates a capacitance cell, which is used in a certain class of nuclear-grade pressure transmitters.

For measuring the absolute pressure, one side of the sensing element (called the *high side*) is opened to the process pressure, and the other side is evacuated. For gauge pressure measurements, one side (the *high side*) is opened to the process pressure, and the other side is left at the ambient pressure. In differential pressure measurements, however, both sides of the sensing element are connected to the process pressure, with one side arbitrarily marked high and the other side marked low. Any differential pressure transmitter can be configured to measure gauge pressure by connecting one side to the process line and opening the other side to the atmosphere.

The movement of the sensing element in nuclear plant pressure transmitters is normally converted into a DC current and transmitted in a two-wire circuit. This circuit consists





**Photograph of Nuclear and Commercial Grade Pressure Transmitters**  
(Photograph, taken by author, of two Rosemount Transmitters used to conduct work described in this thesis)

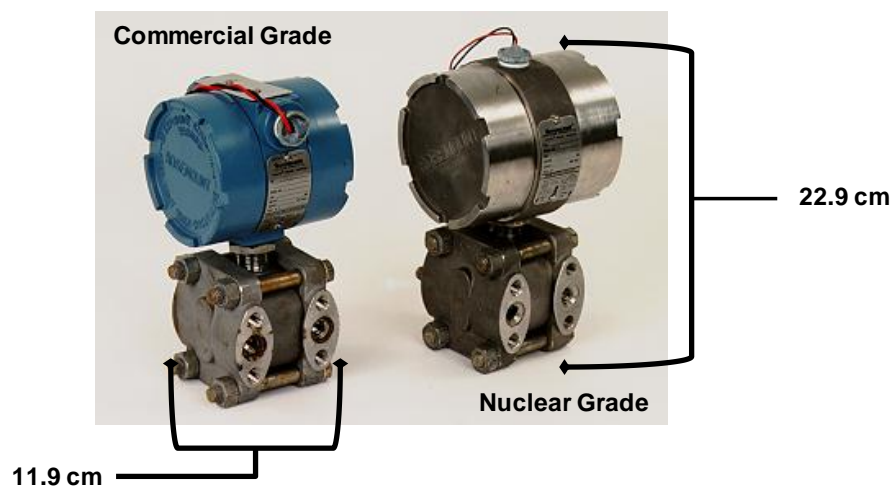


**Figure 2-9 Typical Transmitter Configurations and Sensing Element Varieties to Measure Gauge, Absolute, and Differential Pressures**

of the transmitter in the field and its power supply, which is usually located remotely from the transmitter in an instrument cabinet in the control room area. The same two wires that are used to supply power to the transmitter electronics also serve to provide the current loop on which load resistors are placed in series, as shown in Figure 2-10. The voltage drops across the resistors are used to measure or monitor pressure or differential pressure. Using a current loop allows the pressure information to be transmitted over a long distance without loss of signal strength and with reduced electrical noise and interferences. Table 2-2 summarizes the typical characteristics of nuclear plant pressure transmitters.

### **2.3 Sensing Lines**

Sensing lines are used to locate pressure transmitters away from the process so as to reduce the effect of ambient temperature on the transmitter's operability and qualified life. High ambient temperatures can affect both the transmitter's mechanical components and also shorten the life of its solid-state electronics. Other reasons for locating a transmitter away from the process are to reduce the adverse effects of vibration and to facilitate access to the transmitter for replacement or maintenance.

Figure 2-11 illustrates two possible sensing line configurations. Both liquid-filled and gas-filled sensing lines are used in nuclear power plants. Liquid sensing lines typically contain the process liquid or oil, depending on the sensing line's design and application. Gas sensing lines typically contain steam, air, nitrogen, or other gases. Some gas sensing lines use a diaphragm, bellows, or condensate pot to transition from one gas to another medium such as oil or water.

Sensing lines are typically made of small-diameter (on the order of 1.5 cm to 2 cm) stainless steel, carbon steel, or copper tubing in thicknesses of about 2 millimeters. Tubing is preferred over piping because it may be installed in one piece, reducing the chance of potential leaks. Sensing lines can be as short as a few meters or as long as

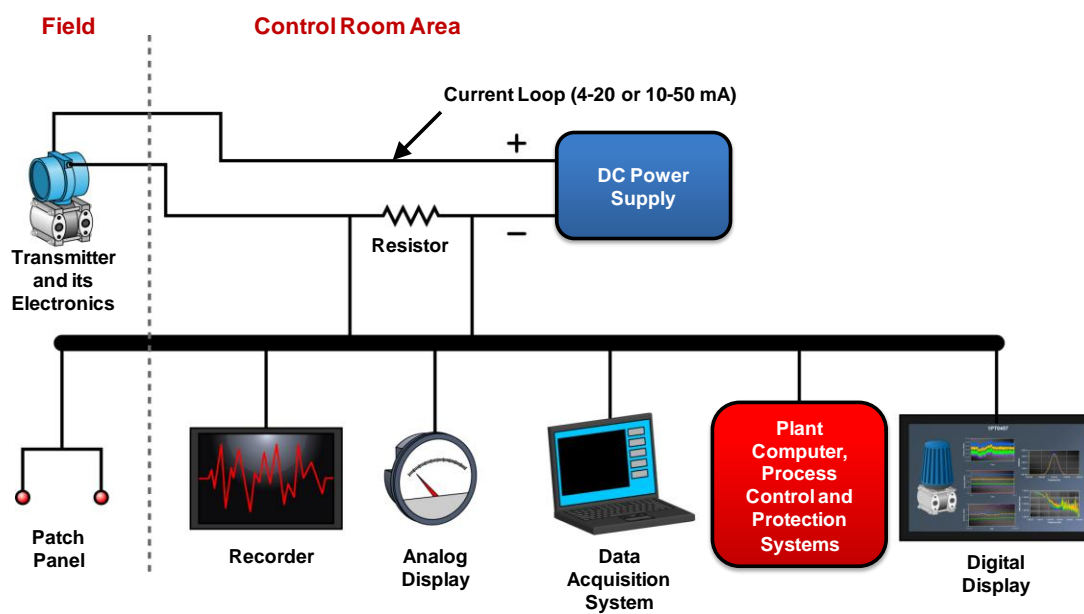


**Figure 2-10** Various Ways to Display the Output of a Pressure Transmitter

**Table 2-2 Typical Characteristics of Nuclear Plant Pressure Transmitters<sup>[12]</sup>**

<b>Type of Measurement</b>	Absolute Pressure Gauge Pressure Differential Pressure
<b>Typical Length</b>	Manufacturer 1: 30.5 cm Manufacturer 2: 22.9 cm Manufacturer 3: 15.2 cm
<b>Typical Cross-Section</b>	Manufacturer 1: 15.2 cm Manufacturer 2: 11.4 cm Manufacturer 3: 19.1 cm
<b>Typical Weight</b>	Manufacturer 1: 16 – 24 kg Manufacturer 2: 5.4 – 7.3 kg Manufacturer 3: 8.6 kg
<b>Materials</b>	Stainless Steel, Carbon Steel, Cast Iron
<b>Classifications</b>	Safety or Safety-Related Non-Safety
<b>Sensing Element</b>	Manufacturer 1: Bourdon, Bellows, Diaphragm Manufacturer 2: Capacitance Cell Manufacturer 3: Bourdon, Bellows, Strain Gauge
<b>Sensor Output</b>	Typical Range: 4 – 20mA or 10 – 50 mA
<b>External Power</b>	Typical Range: 12 – 45 Vdc or 30 – 85 Vdc
<b>Overpressure</b>	Typical Limits: 13.8 MPa or 31.0 MPa
<b>Operating Temperature</b>	Typical Limits: -28.9 to 100 <sup>0</sup> C
<b>Response Time</b>	Manufacturer 1: 0.3 seconds or better (typical) Manufacturer 2: 0.2 seconds or better (typical) Manufacturer 3: 0.2 seconds or better (typical)
<b>Accuracy</b>	Manufacturer 1: 0.50% to 1.25% of span Manufacturer 2: 0.25% (nuclear qualified) Manufacturer 3: ±0.25% or ±0.50%



**Pressure Transmitters Used in the Research  
Described in This Dissertation**

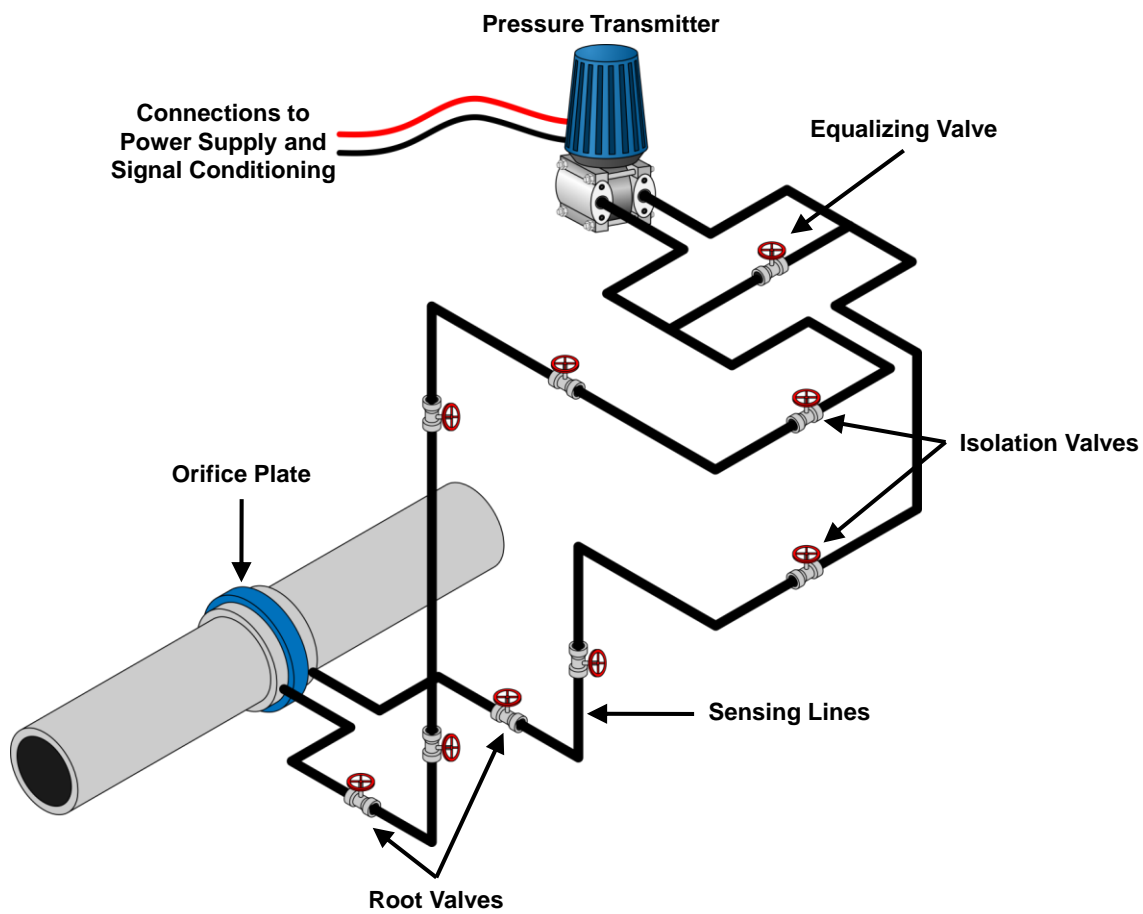


**Figure 2-11** Example of Pressure Transmitter and Sensing Line Installation

200 or 300 meters. Their average length is 10 to 50 meters. Since the length of sensing lines affects the overall response time of a pressure sensing system, attempts are often made to make the sensing lines as short as possible.

Voids, blockages, and freezing in sensing lines can cause errors in pressure measurements and affect the dynamic response of the pressure sensing system. The causes and effects of these problems, which though designed against do still occur in nuclear power plants, are as follows:

- **Voids:** Air or gas trapped in liquid-sensing lines can cause false pressure readings, sluggish response, and extraneous noise resulting from acoustic resonances. For example, in differential-pressure measurements, an air pocket in the low pressure side can cause the pressure indication to be higher than the actual pressure. It can also delay the transmission of the pressure information. Though one would expect air pockets in lines to dissolve in the liquid under the high pressures common in industrial pressure measurements, voids are difficult to purge and remain a persistent problem.
- **Blockages:** Blockages occur in sensing lines when the chemicals used to treat the water and sludge solidify or when other contaminants accumulate. It also occurs when isolation and equalizing valves are improperly aligned or seated or where sensing lines become crimped, creating obstructions. A partial blockage is detrimental only to the dynamic response time of the pressure sensing system and does not normally affect the static output of the transmitter. When the blockage completely restricts the line, however, the pressure information can be totally unreliable.
- **Freezing:** In cold weather, freezing can occur in fluid sensing lines if the sensing line's heat tracing, which is used to prevent the fluid from freezing, is ineffective due to ageing or damage. This problem can go undetected if the freezing causes a normal operating pressure to be locked into the system.

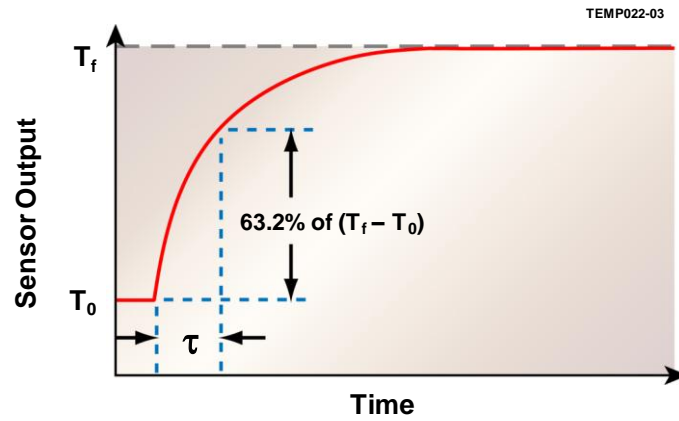
The work in this dissertation has focused on liquid-filled sensing lines as these are the most prevalent type of installation for safety-related pressure transmitters in nuclear power plants.

#### **2.4 Science of Sensor Response Time Testing**

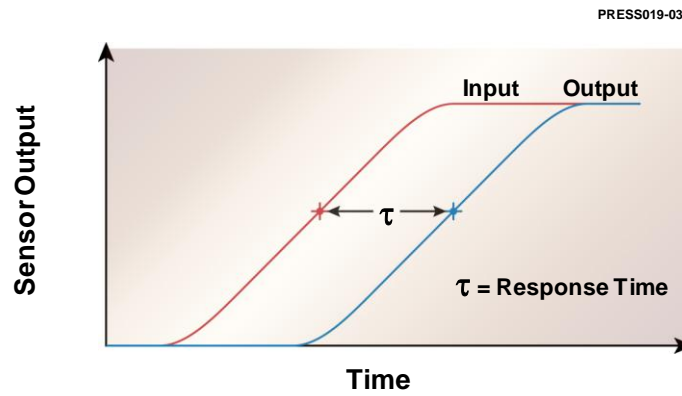
The dynamic response of a sensor may be identified theoretically or experimentally. The theoretical approach usually requires a thorough knowledge of the sensor's design and construction details, such as the properties of the sensor's internal components, their geometries, and the characteristics of the medium that surrounds the sensor. Since these properties are usually not known accurately, or may change under process operating or aging conditions, the theoretical approach by itself can only provide an estimate of dynamic response behavior. Therefore, theory is typically verified or complemented with experimental data to identify the response time. In fact, the data from the experiment is analyzed using formulas derived from the theory that relate the input and output of the sensor. These formulas are sometimes referred to as analytical, theoretical, or mathematical model, or just *the model*.

Identifying a sensor's response time involves exposing it to a change in an external input signal, such as a step change; measuring its output response; and matching the output response with the model. Once this process, referred to as *fitting*, is completed, the parameters of the model are identified and used to determine the sensor's dynamic response for any input from which the response time is to be deduced. If the sensor can be represented by a first-order model, it is not necessary to fit the data to a model, and the response time can be determined directly from the output of the sensor. Figure 2-12 shows the step (a), ramp (b), and frequency response (c) curves of a sensor that has first-order dynamics. Each graph in Figure 2-12 also shows how the response time ( $\tau$ ) is calculated directly from the recorded data.

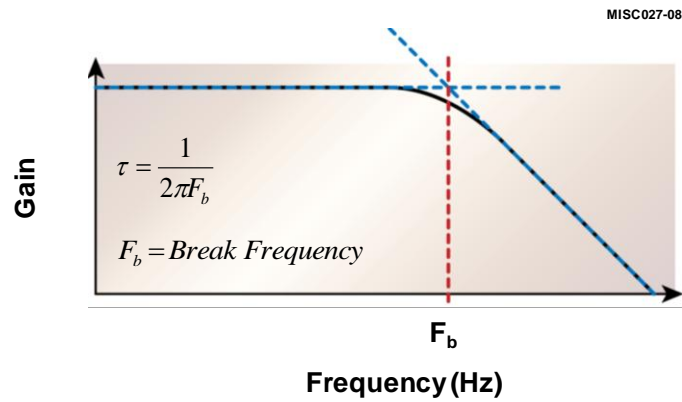
First-order approximation is, of course, the most common as well as the classical way to characterize the dynamic response of a sensor. In reality, however, sensor dynamics are



(a) Step Response



(b) Ramp Response



(c) Frequency Response

**Figure 2-12 Step, Ramp, and Frequency Response for a First-Order Dynamic Model**



not necessarily first order. For example, the overall response time ( $\tau$ ) of an RTD for a step change in temperature has been shown to relate to its modal time constants ( $\tau_1, \tau_2, \tau_3, \dots$ ) by the following formula:

$$\tau = \tau_1 \left[ 1 - \text{Ln}\left(1 - \frac{\tau_2}{\tau_1}\right) - \text{Ln}\left(1 - \frac{\tau_3}{\tau_1}\right) - \dots - \text{Ln}\left(\frac{\tau_n}{\tau_1}\right) \right] \quad (2.1)$$

$\tau$  = overall time constant

$\tau_i$  =  $i^{\text{th}}$  modal time constant

$\text{Ln}$  = natural logarithm operator

Similarly, for pressure transmitters, the overall response for a ramp input signal is referred to as the “ramp time delay” and is given by the summation of the modal time constants as follows:

$$\text{Ramp Time Delay} = \tau_1 + \tau_2 + \dots + \tau_n \quad (2.2)$$

The derivations of Equations 2.1 and 2.2 are shown in Appendix A together with the assumptions that must be satisfied for these equations to provide valid results. In Chapters 5 and 6 these equations are used to determine the response time of RTDs and pressure transmitters using the LCSR and noise analysis techniques whose application and refinement are the subject of this research. In Figure 2-13, a flow chart illustrates the steps used for measuring sensor response time. Note that the penultimate step in this flow chart is the application of a correction factor (explained in Chapter 5).

## 2.5 Sensing Line Effects on Dynamics of Pressure Transmitters

Adding sensing lines to pressure transmitters increases the complexity of the dynamics of the resulting system. Appendix B contains mathematical derivations to show that the dynamic response of a pressure sensor may be modeled using a second-order linear differential equation, which can be solved for a step or ramp pressure input signal to yield:

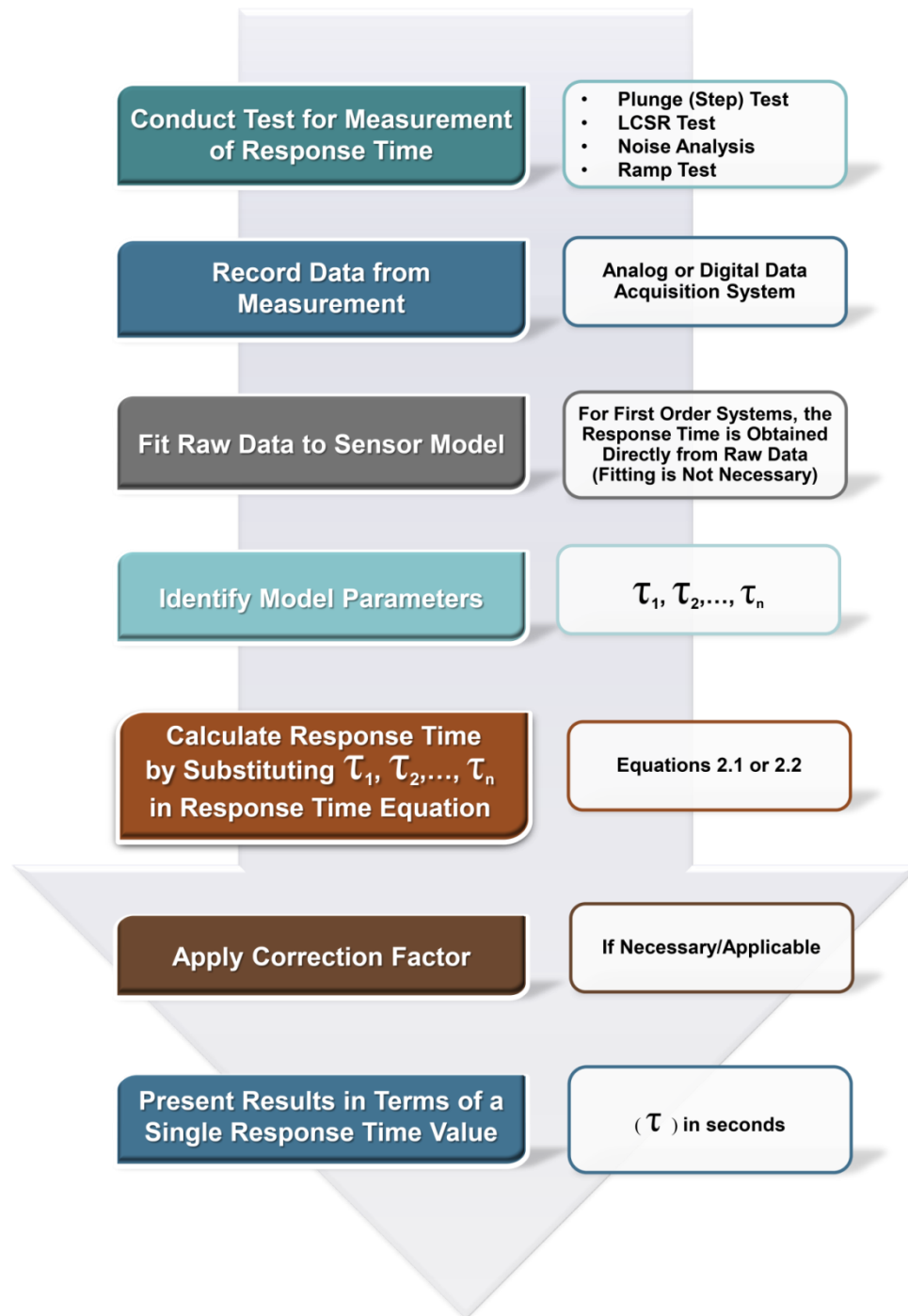


**Figure 2-13** Steps in Testing Response Time of a Temperature or Pressure Sensor

### Step Response

$$x(t) = K \left[ 1 - \frac{\omega_n}{\omega_d} e^{-\alpha t} \sin \left( \omega_d t + \arctan \left( \frac{\omega_d}{\alpha} \right) \right) \right] \quad (2.3)$$

### Ramp Response

$$x(t) = Kr \left[ t - \frac{2\alpha}{\omega_n^2} + \frac{1}{\omega_d} e^{-\alpha t} \sin \left( \omega_d t + 2 \arctan \left( \frac{\omega_d}{\alpha} \right) \right) \right] \quad (2.4)$$

$x(t)$  = signal amplitude

$\omega_n$  = transmitter natural frequency, *rad/sec*

$\omega_d$  = damped natural frequency of system, *rad/sec*

$\alpha$  = damping coefficient, *N/s·m*

The parameters in these equations are defined in Appendix B and are also included in the list of mathematical symbols at the beginning of this dissertation. These equations represent the underdamped responses of a pressure sensing system, ignoring the effect of such components as the transmitter's electronics, any mechanical linkages beyond the sensing element, and so on.

Equations 2.3 and 2.4 were used to calculate the effect of sensing line length, diameter, and void on the response time of three commonly used pressure transmitters in the nuclear power industry (i.e., Rosemount, Barton, and Foxboro). In doing so, these transmitters were represented by their compliance values, obtained from their manufacturers (Table 2-3). A parameter that is unique to each sensor, compliance, is calculated by measuring the change in volume of the sensing chamber per unit change

**Table 2-3 Compliance Values of Pressure Transmitters Used in This Study**

<u>Manufacturer</u>	<u>Model</u>	<u>Compliance (cm<sup>3</sup>/bar)</u>
Barton <sup>(1)</sup>	764	9.51
Rosemount	1153R67	0.01
Foxboro <sup>(2)</sup>	E13DM	0.12

(1) Barton transmitters are now supplied by Cameron Products Company.

(2) Foxboro transmitters are now supplied by Weed Instrument Company.

in input pressure. Therefore, transmitters such as Barton, whose sensing element consists of a bellows, have a larger compliance value than Rosemount transmitters, which have capacitance cells.

The results of calculating the effects of sensing line length, diameter, and void are shown in Tables 2-4 through 2-6 as described below:

- (1) Table 2-4 shows results from the study of the effect of length on the response time. In this study, two different sensing lines were used: one with an ID of 6.25 mm and another with an ID of 9.53 mm. The length was varied from 15 to 150 meters. As expected, the results demonstrate that the response time of the transmitters increases as the length of the sensing line increases, depending on sensor type (i.e., compliance value) and the sensing line's diameter.
- (2) Table 2-5 shows the response time results in relation to the varying inside diameter of a sensing line that is 15 meters in length. Again, the results demonstrate that the response time values increase as the sensing line diameter decreases, with the amount of increase depending on the compliance value.
- (3) Table 2-6 shows the effect of a void on transmitter response time at two different pressures (0.25 Bar and 15 Bar). It is evident that this effect is more significant at low pressures.

The results shown in Tables 2-4 through 2-6 were calculated from the step response of the sensors as shown in Figure 2-14. That is, the response time of the oscillatory output (Figure 2-14) was defined arbitrarily as the time to reach the first peak ( $\tau_p$ ) divided by 3.<sup>[13]</sup> This arbitrary definition was adopted from reference 13 to provide a basis for comparison of response time results from an oscillatory output. There is no analytical basis for this definition.

Using Equations 2.3 and 2.4, the frequency response of a Barton, Foxboro, and Rosemount transmitter was plotted for four different situations shown in Figure 2-15. As in Tables 2-4 through 2-6, the results in Figure 2-15 illustrate that the dynamics of a pressure sensing system is affected by its compliance value (Figure 2-15a), the length of the sensing line (Figure 2-15b), the sensing line's diameter (Figure 2-15c), and the presence of voids (Figure 2-15d). To arrive at these PSDs, the natural frequency and

**Table 2-4 Theoretical Effect of Sensing Line Length on Response Time**

<u>Length (meters)</u>	<u>Response Time (seconds)</u>		
	<u>Barton</u>	<u>Foxboro</u>	<u>Rosemount</u>
<b>Sensing Line Inside Diameter = 6.35 mm</b>			
15	0.22	0.03	0.11
30	0.31	0.04	0.15
60	0.44	0.06	0.22
90	0.54	0.07	0.27
120	0.63	0.09	0.31
150	0.71	0.11	0.35
<b>Sensing Line Inside Diameter = 9.53 mm</b>			
15	0.14	0.02	0.07
30	0.20	0.03	0.10
60	0.29	0.04	0.15
90	0.35	0.06	0.18
120	0.41	0.07	0.21
150	0.46	0.09	0.24

**Table 2-5 Theoretical Effect of Diameter (Simulating Blockage) on Transmitter Response Time**

<u>I.D. (mm)</u>	<u>Response Time (seconds)</u>		
	<u>Barton</u>	<u>Foxboro</u>	<u>Rosemount</u>
16	0.086	0.012	0.044
13	0.108	0.014	0.054
10	0.143	0.018	0.072
5	0.216	0.026	0.108
3	0.637	0.050	0.232

---



---

The length of sensing line for these results was 15 meters.

**Table 2-6 Theoretical Effect of Void on Response Time**

<u>Manufacturer</u>	<u>Response Time (sec)</u>		
	<u>No Void</u>	<u>15 cm Void</u>	<u>150 cm Void</u>
<b><u>Pressure = 0.25 Bar</u></b>			
Barton	0.143	0.307	0.880
Foxboro	0.018	0.272	0.868
Rosemount	0.008	0.271	0.868
<b><u>Pressure = 15 Bar</u></b>			
Barton	0.143	0.148	0.184
Foxboro	0.018	0.040	0.116
Rosemount	0.008	0.037	0.115



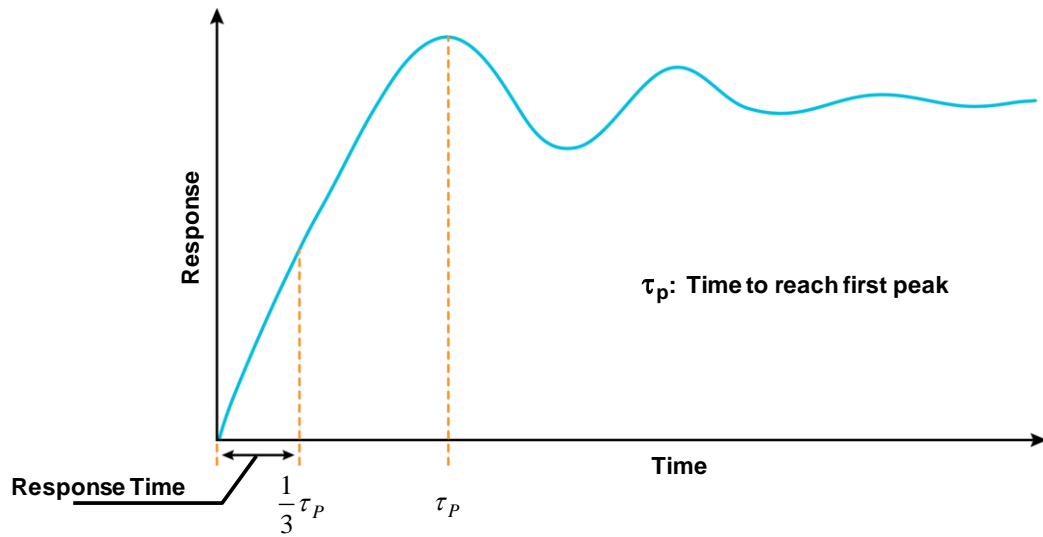


**Figure 2-14 Output of an Underdamped System for a Step Input and Calculation of Sensor Response Time**

(Note: for definition of response time in cases like this, one could also use “rise time”; as the time to go from 10% to 90% of the steady state value).

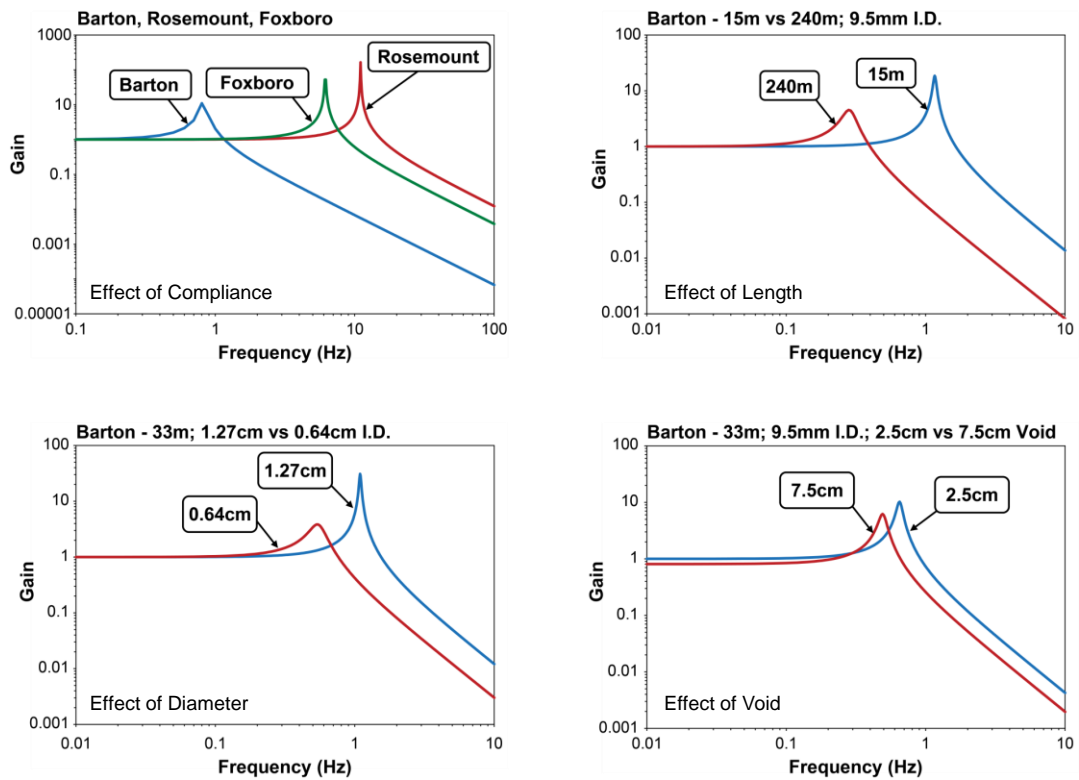


**Figure 2-15** Frequency Responses of Representative Pressure Transmitters from Four Sensing Line Configurations

damping ratio were calculated for each sensor and used in Equations 2.3 and 2.4, and the data were then converted to equivalent PSD plots.

# 3

## BACKGROUND AND LITERATURE REVIEW

---

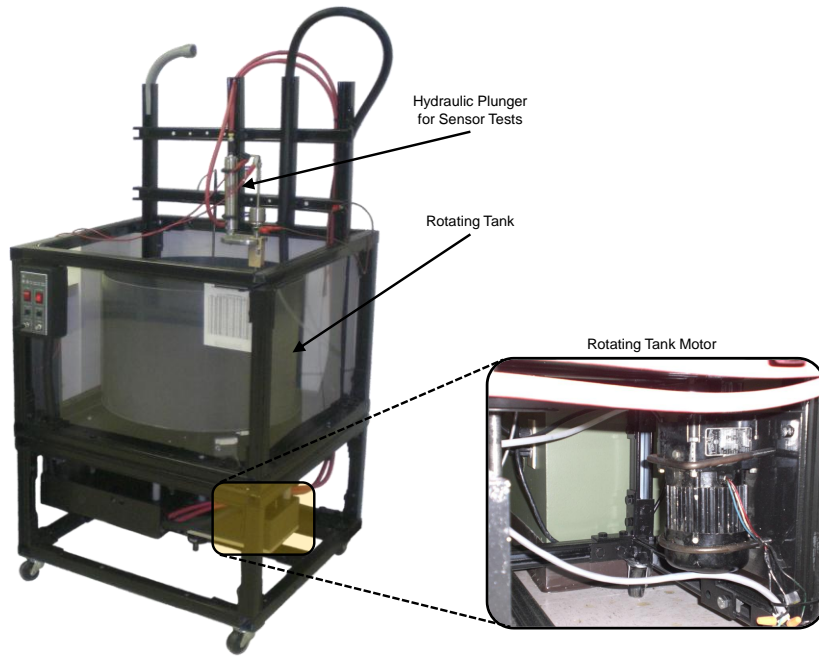
This chapter describes the conventional methods for testing the response time of temperature and pressure sensors. It includes the results of laboratory measurements to produce baseline data that will be used to validate the new response time measurements methods described in Chapter 5. This chapter also includes a review of prior work and the literature on sensor response time testing in the nuclear power industry and a brief history of related developments.

### 3.1 Conventional Method for Testing RTD Response Time

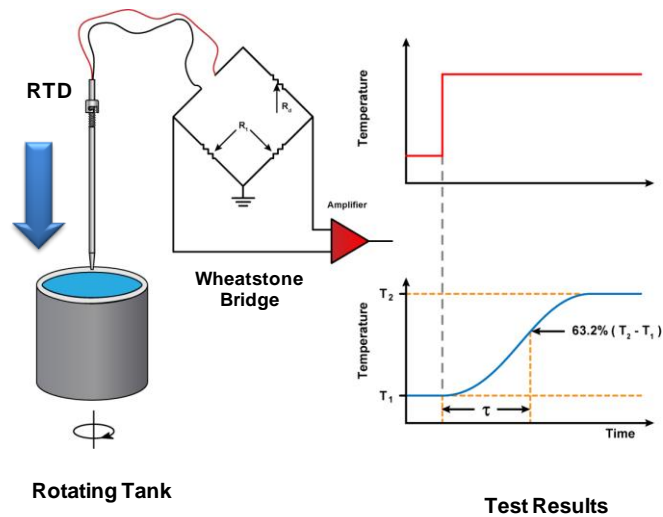
Historically, the response time of RTDs has been characterized by a single variable called the *plunge time constant*. This is defined as the time required for the sensor output to achieve 63.2 percent of its final value after a step change in temperature is impressed on its surface. This step change is typically achieved by suddenly immersing the sensor in a rotating tank of water that is flowing at 1 meter per second (m/s). The water must be at either a higher or lower temperature than that of the RTD.

Measuring response time in this way is referred to as *plunge testing*. The procedure is illustrated in Figure 3-1, which includes photographs of a laboratory setup used to produce the experimental results presented in this dissertation. Because the plunge test results depend on process conditions (e.g., fluid flow rate and temperature), a number of standards have been written to ensure that RTD response time measurements produce comparable results. Four examples of these standards are:

1. ASTM Standard E644-09, “Standard Test Methods for Testing Industrial Resistance Thermometers,” American Society for Testing and Material (2009).
2. ISA Standard 67.06, “Performance Monitoring for Nuclear Safety-Related Instrument Channels in Nuclear Power Plants.” International Society of Automation (May 2002).



(a) Rotating Tank for Plunge Testing of RTDs



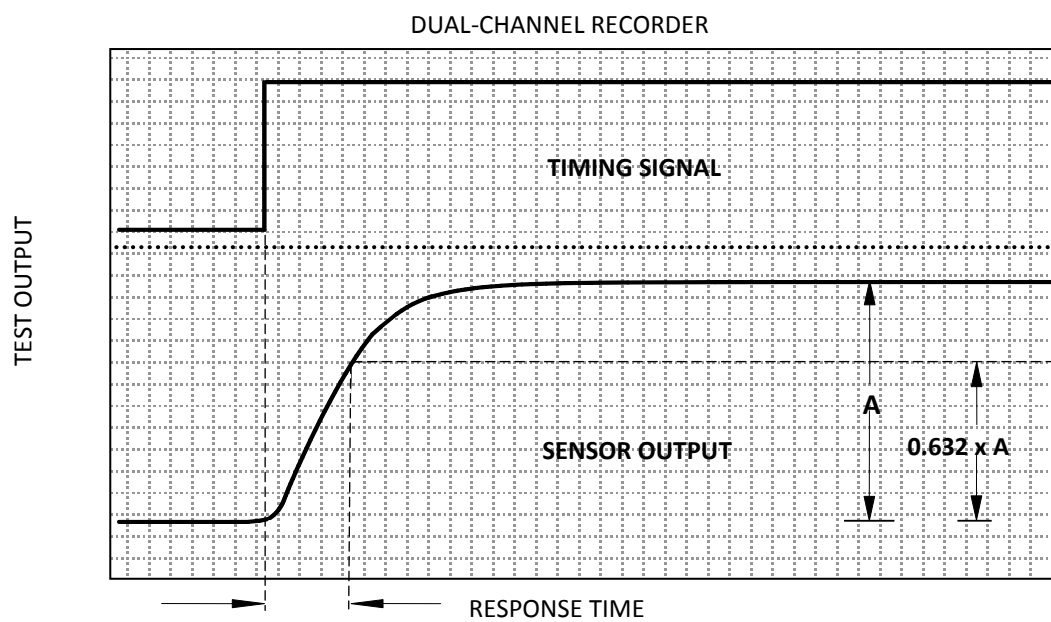
(b) Illustration of Plunge Test Procedure

Figure 3-1 Plunge Test Procedure

3. IEC Standard 60751, “Industrial Platinum Resistance Thermometers and Platinum Temperature Sensors,” International Electrotechnical Commission (2007).
4. IEC Standard 62385, “Nuclear Power Plants – Instrumentation and Control Important to Safety – Methods for Assessing the Performance of Safety System Instrument Channels,” International Electrotechnical Commission (2007).

These standards describe the plunge test setup used in the research conducted for this dissertation. They require that the test be performed in a flow rate of 1 m/s and at a temperature that does not shock the sensor or cause changes in the heat transfer properties of its material. The user of the response time data is responsible for verifying that the measurement was performed according to an acceptable standard, specifying any deviation from the standard method, and describing the consequences of that deviation. In particular, RTD response time results must be accompanied by either a statement of the fluid flow rate and temperature in which the test was performed, and/or a description of the standard or procedure that was used to perform the response time measurement.

A Wheatstone bridge is typically used to produce the output from a plunge test. With the RTD connected to one arm of the bridge, the bridge is balanced with 1 to 2 mA of DC current running through the circuit, and the bridge output is then recorded. As soon as the RTD is plunged into the rotating tank of water, the resistance of the sensing element gradually changes, producing an exponential transient at the output of the bridge (referred to as the plunge test transient). This data is then used to identify the RTD’s response time by measuring the time constant of the output response. Figure 3-2 shows an actual plunge test transient for an RTD and the calculation of its response time. In this test, a strip chart recorder was used to record the data. Often, an analog-to-digital (A/D) converter samples the data from the output of the bridge, and a computer then calculates the response time from the data. Today, almost all sensor manufacturers use an automated setup to sample the plunge test data and produce RTD response time results. The data in this dissertation were produced partly from strip chart recorder traces and partly from computer-aided testing. Table 3-1 presents



**Figure 3-2 Plunge Test Transient for an RTD and Calculation of Response Time**

**Table 3-1 Plunge Test Results for Representative RTDs Used in this Research**

<u>RTD Identification</u>	<u>RTD Tip Configuration</u>	<u>Installation</u>	<u>Dimension in O.D. (mm)</u>		<u>Response Time (sec)</u>
			<u>Sheath</u>	<u>Thermowell</u>	
<b><u>MANUFACTURER A</u></b>					
A-1-0	Flat	Wet type	9.5	N/A	0.4
A-2-1	Tapered	Well type	3.2	6.4	7.1
A-2-2	Tapered	Bare	3.2	N/A	3.1
A-3-1	Tapered	Well type	3.2	6.4	5.3
A-3-2	Tapered	Bare	3.2	N/A	2.3
<b><u>MANUFACTURER B</u></b>					
B-1-1	Tapered	Well type	6.4	9.5	2.9
B-1-2	Tapered	Bare	6.4	N/A	1.6
B-2-1	Flat	Wet type	9.5	N/A	2.9
B-3-0	Tapered	Well type	6.4	9.5	4.1
<b><u>MANUFACTURER C</u></b>					
C-1-0	Flat	Wet type	9.5	N/A	2.0
C-2-1	Flat	Well type	6.4	9.5	4.9
C-2-2	Flat	Bare	6.4	N/A	0.9
C-3-1	Flat	Well type	6.4	9.5	5.1
C-3-2	Flat	Bare	6.4	N/A	1.8

- Wet type: Direct-immersion RTD
- Well type: Thermowell-mounted RTD
- “Bare” means without thermowell
- Dimensional information is given in approximate, rounded numbers
- O.D.: outside diameter
- mm: millimeter
- Measurements were made at a laboratory in a rotating tank of room temperature water flowing at 1 meter per second



representative results of these measurements for fourteen nuclear-grade RTDs from three different manufacturers (identified in the table as manufacturers A, B, and C). Table 3-1 shows results for both direct-immersion (wet-type) and thermowell-mounted (well-type) RTDs (see Section 2.1 in Chapter 2 for a description and the physical configuration of direct-immersion and thermowell-mounted RTDs). For the thermowell-mounted RTDs, response times with and without thermowell are listed. The outside diameter (O.D.) of the bare RTDs (those without a thermowell) and the corresponding thermowells are also shown in Table 3-1.

A logical assumption is that the response time of an RTD depends very much on its O.D. However, the results in Table 3-1 do not sustain this conclusion. The response time results for the bare RTDs identified in Table 3-1 as A-2-2, B-1-2, and C-2-2 are not correlated with their O.D. The same is true for direct-immersion (wet-type) RTDs, identified in the table as A-1-0, B-2-1, and C-1-0. In actuality, the internal and external design of an RTD, such as the type of insulation material used, also plays a role in its response time. Note as well from Table 3-1 that the response time results for identical RTD/thermowell sets from the same manufacturers can be different because of the dimensional tolerances between the RTDs and thermowells. In particular, the tolerances of sheath O.D. and thermowell inside diameter (I.D.) can typically account for the differences between the response times of identical RTD/thermowell sets.

The response time of an RTD depends greatly on the air gap in the thermowell at the sensing tip of the sensor. For example, if an RTD is tested in a thermowell in a laboratory but installed in a different thermowell in the plant, the response time result can differ significantly. To obtain the in-service response time of a thermowell-mounted RTD, the test must therefore be performed as the RTD is installed in the plant thermowell. Though this is not the case for direct-immersion RTDs, which lack a thermowell, the “in-service” response time of direct-immersion RTDs must also be measured in situ to account for the effect of process conditions on response time.

### 3.2 Conventional Method for Testing Response Time of Pressure Transmitters

The response time of nuclear plant pressure transmitters is measured using the ramp test method. This method involves applying a pressure ramp signal simultaneously to both the transmitter being tested and an ultrafast reference transmitter (Figure 3-3). The asymptotic delay between the output of the two transmitters is then measured. This delay is referred to by the synonymous terms of transmitter *response time*, *ramp time delay*, or *asymptotic ramp time delay*.

The ramp test can be performed in a laboratory, on a bench, or in the field on a transmitter as installed in the plant. Figure 3-4 shows how a ramp test may be performed on a sensor as installed in a plant. (The figure also shows that response time can be measured by sampling the sensor output and using the noise analysis technique to produce the sensor transfer function from which the transmitter response time can be deduced, details of which are presented in Chapters 5 and 6). Today, nuclear plant personnel carry a ramp generator to perform ramp tests on sensors in the field. Since the pressure transmitters' response time is not influenced by process conditions, this procedure results in accurate response time measurements, albeit without accounting for the effect of sensing lines.

In performing a ramp test, it is critical to ensure that no air is present in the pressure signal lines that run from the ramp test equipment to the sensor or in the sensor itself. Such air can cause oscillation in the ramp test data as shown in Figure 3-5, complicating the response time measurement.

In lieu of measuring the asymptotic ramp time delay, the response time of a transmitter may be measured against a pressure setpoint. Figure 3-6 shows actual ramp transients from laboratory testing of a pressure transmitter using both increasing and decreasing ramp input signals. The response times from the two transients, which was calculated based on a setpoint of 3.0 volts, are 0.120 seconds for the increasing ramp and 0.122 seconds for the decreasing ramp. Although the two results would ideally be the same, in practice normal variation between experimental test results creates a small difference.

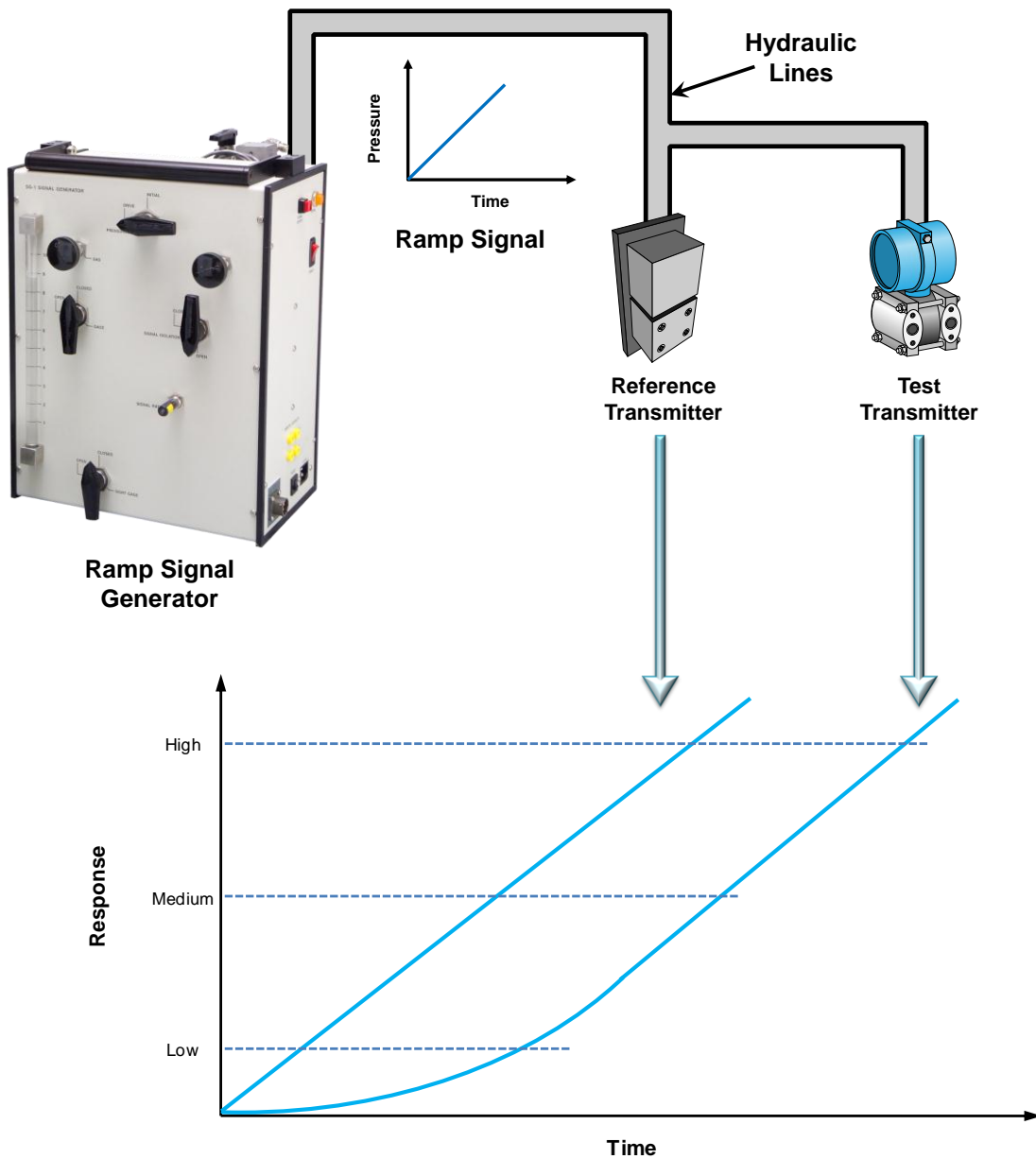


**Figure 3-3 Hydraulic Ramp Generator and Test Results from Laboratory/Bench Testing of Response Time of a Pressure Transmitter**

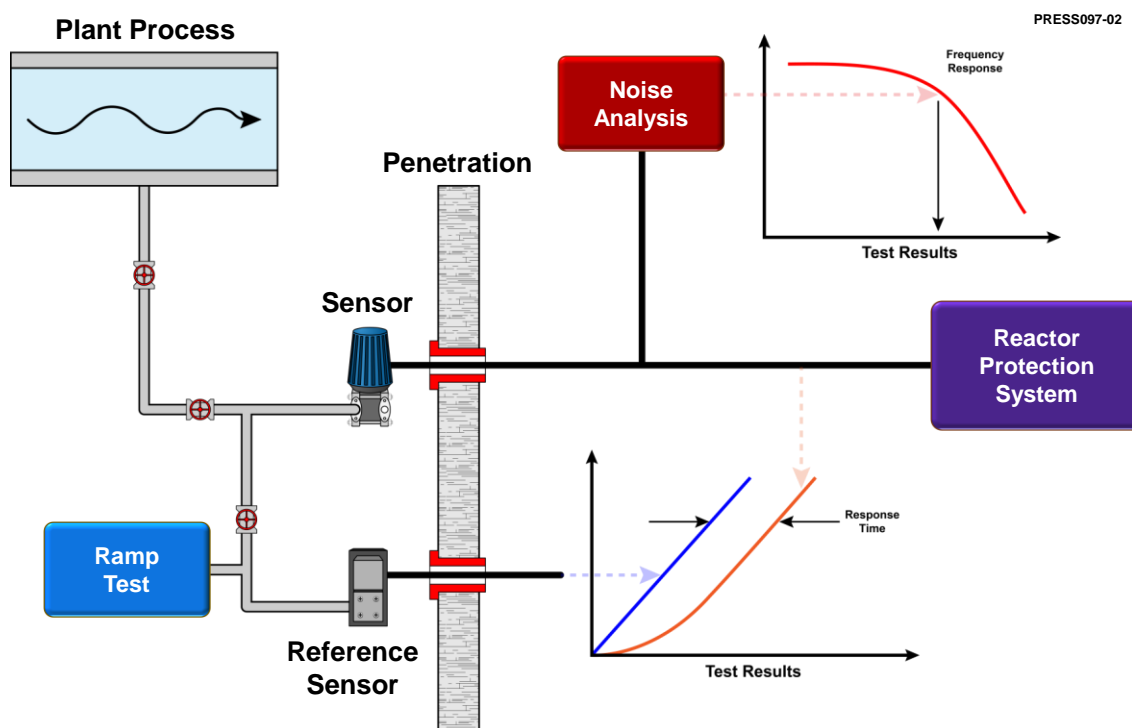


**Figure 3-4 Response Time Testing of an Installed Transmitter Using the Ramp or Noise Methods**

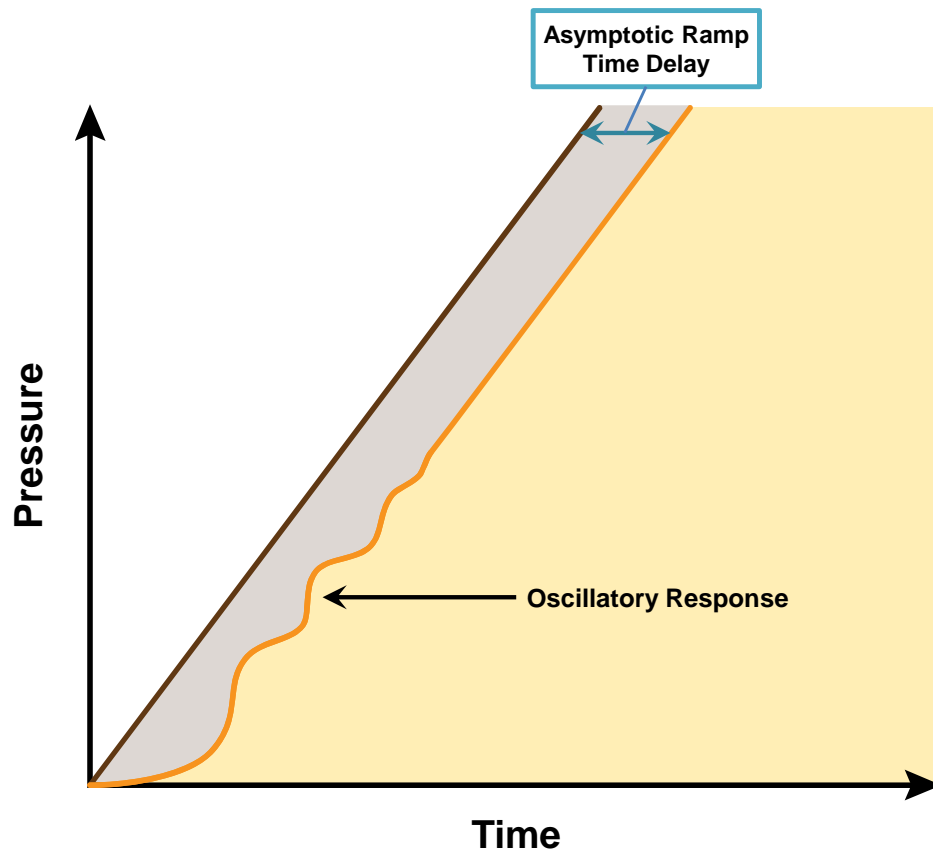


**Figure 3-5 Oscillatory Output of a Pressure Transmitter During a Ramp Test**

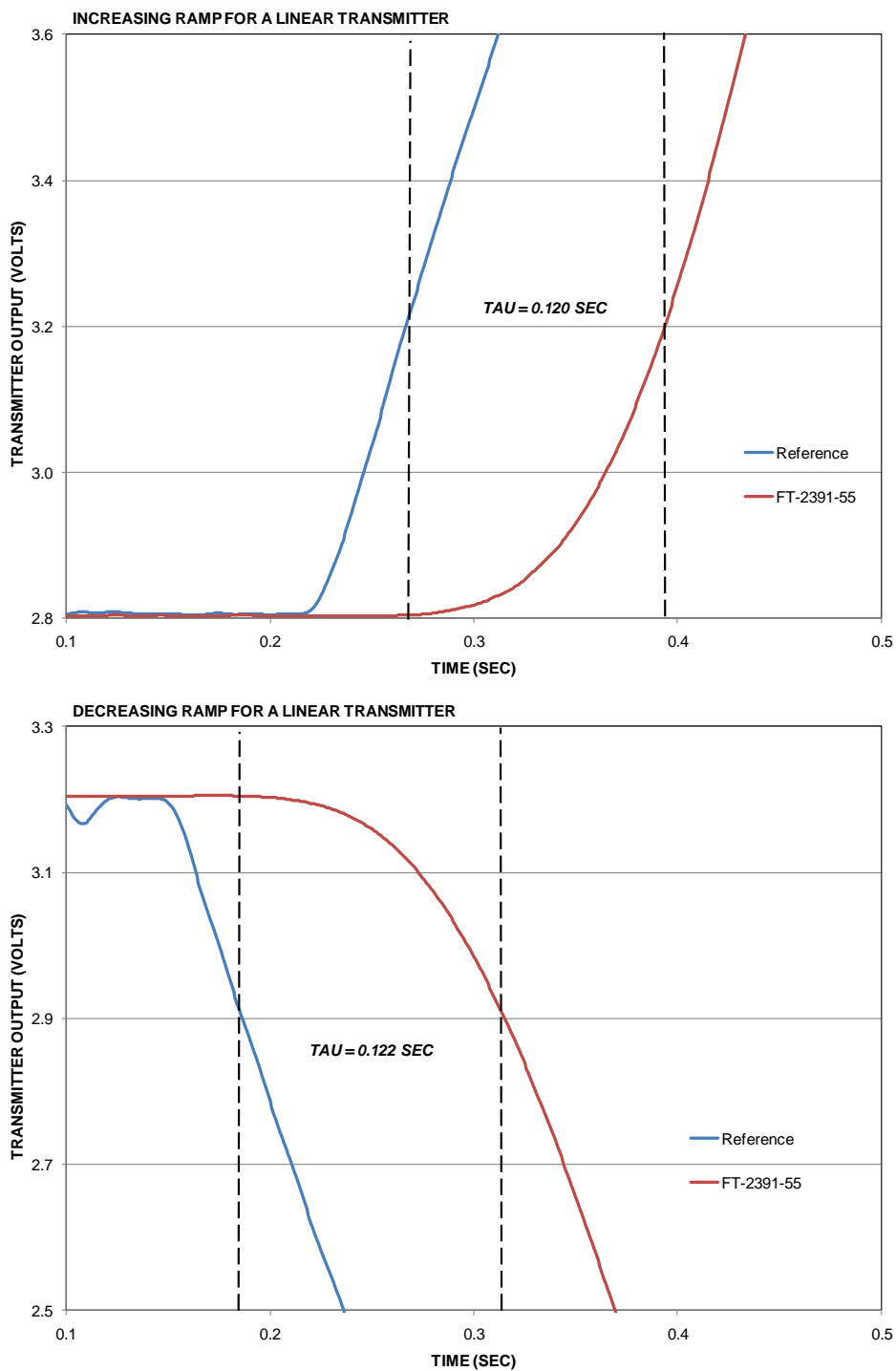


**Figure 3-6 Example of Ramp Test Results Produced During this Research**

Table 3-2 (and Figure 3-7) shows results of laboratory response time testing for 56 pressure transmitters of the types used for measuring pressure, level, or flow in nuclear power plants. These results indicate that the response time of pressure transmitters is an order of magnitude faster than those of the RTDs shown in Table 3-1. Generally, RTD response time in nuclear power plants is in the range of 1 to 8 seconds, while pressure transmitter response time is typically in the range of 0.1 to 0.5 seconds. However, the response time for a pressure sensing system (transmitter plus sensing lines) can be dominated by the response time of its sensing lines. This is especially the case with pressure transmitters that have a large compliance.

Linearity is another key factor that influences the response time of a pressure transmitter. Typically, pressure transmitters are designed to be highly linear throughout their operating range or at least for the span of the measurement for which they are used. This can be verified by performing ramp tests on the transmitter.

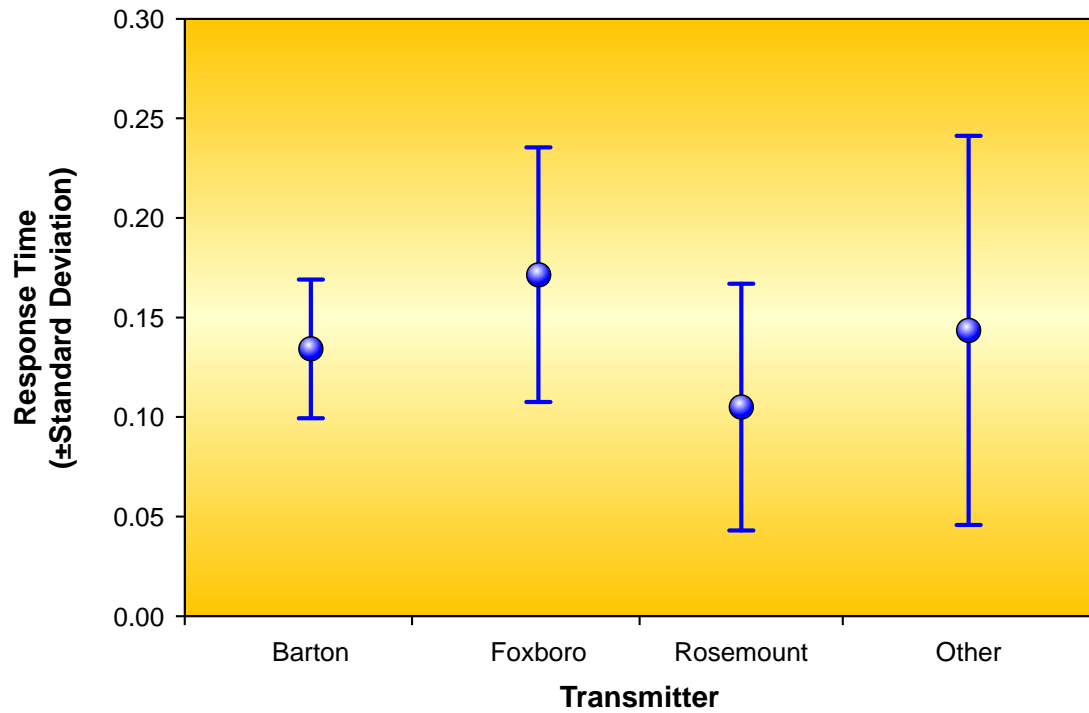
Table 3-3 presents results for a linear and nonlinear differential pressure transmitter. The ramp tests were performed for three different setpoints along the ramp test output with both increasing and decreasing ramp input signals. Note that the response time results are essentially the same for the linear transmitter whether it is tested with an increasing or a decreasing ramp input signal. In contrast, for the nonlinear transmitter the results of the decreasing ramp are substantially different from those with an increasing ramp. The sensing module consists of a diaphragm in the center and two oil-filled chambers on the diaphragm's two sides (see Chapter 2). While the high side chamber in the nonlinear transmitter was normal, the left side chamber had lost its fill fluid.<sup>[14]</sup> The resulting nonlinearity correlates with the results shown in Table 3-3 where an increasing ramp provides normal results because the normal chamber is in play, but the results for decreasing ramp are sporadic because the other chamber is in play and its fill fluid has leaked out.

Figure 3-8 shows the ramp test results for a transmitter that has less severe nonlinearity. Note that the result from the increasing ramp at 3.0 volt setpoints is 0.174 seconds

**Table 3-2 Results of Laboratory Testing of Response Time of Representative Nuclear-Grade Pressure Transmitters**

<u>Number</u>	<u>Response Time (sec)</u>	<u>Number</u>	<u>Response Time (sec)</u>
<b>Barton</b>		<b>Foxboro</b>	
1	0.05	1	0.13
2	0.17	2	0.21
3	0.17	3	0.16
4	0.12	4	0.09
5	0.12	5	0.29
6	0.11	6	0.25
7	0.12	7	0.28
8	0.15	8	0.10
9	0.11	9	0.13
10	0.15	10	0.10
11	0.19	11	0.14
12	0.17	12	0.15
13	0.11	13	0.16
14	0.14	14	0.21
<b>Rosemount</b>		<b>Other</b>	
1	0.05	1	0.15
2	0.32	2	0.21
3	0.07	3	0.02
4	0.10	4	0.03
5	0.11	5	0.08
6	0.09	6	0.15
7	0.09	7	0.33
8	0.10	8	0.11
9	0.12	9	0.15
10	0.09	10	0.13
11	0.09	11	0.19
12	0.08	12	0.04
13	0.09	13	0.07
14	0.07	14	0.35





**Figure 3-7 Summary of Results of Baseline Response Time Measurements Performed in This Study**

**Table 3-3 Ramp Test Results to Demonstrate Transmitter Linearity**

<u>Setpoint</u>	<u>Response Time (sec)</u>	
	<u>Increasing Ramp</u>	<u>Decreasing Ramp</u>
<u>Linear Transmitter</u>		
Low	0.12	0.13
Medium	0.12	0.13
High	0.15	0.13
<u>Nonlinear Transmitter</u>		
Low	0.23	171.0
Medium	0.25	19.0
High	0.25	1.1

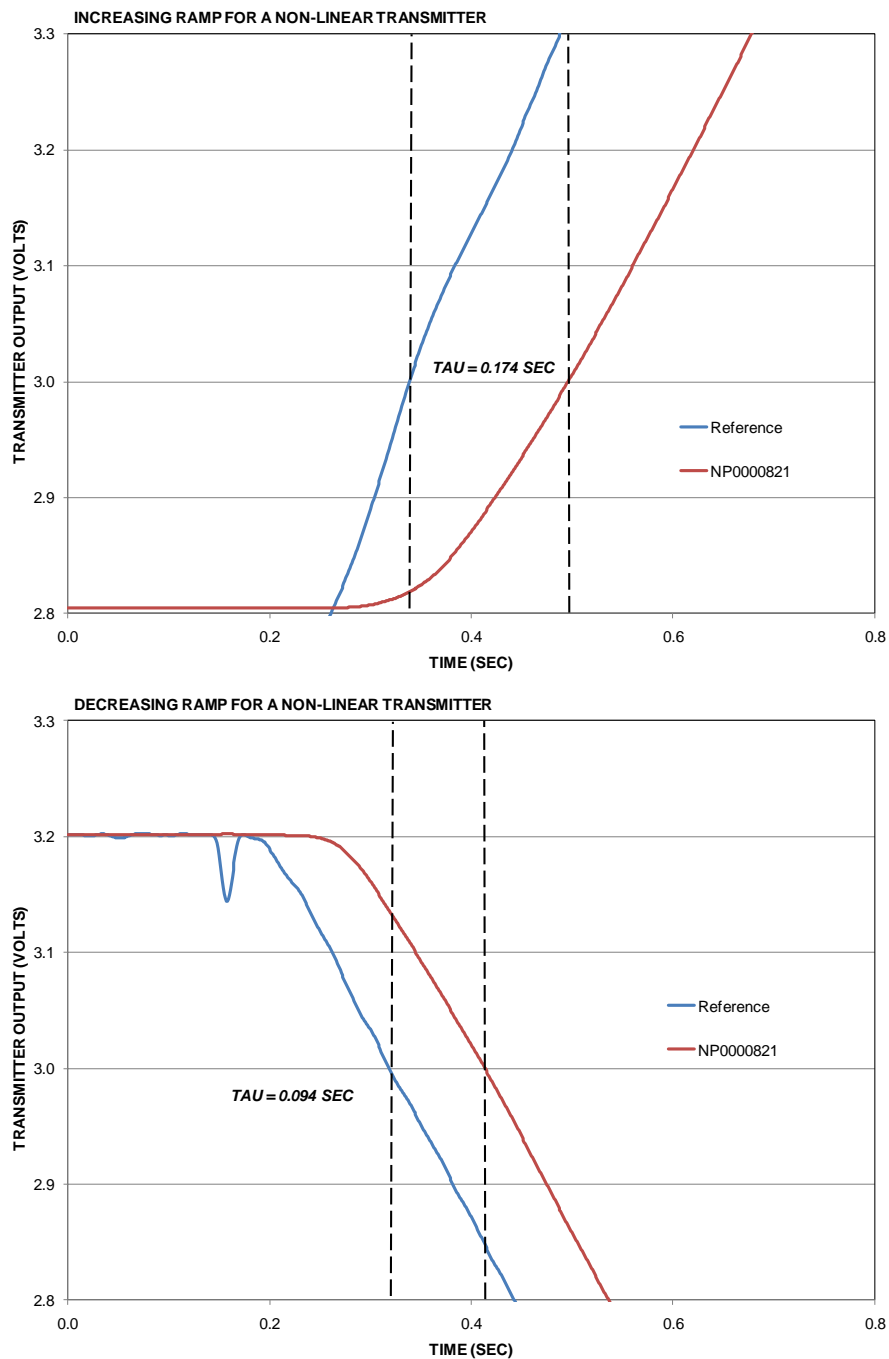


Figure 3-8 Ramp Test Results for a Transmitter with Minor Nonlinearity

compared to 0.094 seconds for the decreasing ramp. This indicates that the nonlinearity of this transmitter is not as severe as for the nonlinear transmitter in Table 3-3.

### 3.3 Prior Work

The work conducted in this dissertation builds on an existing body of work that extends back almost a half century. The development of in-situ methods for testing the response time testing of sensors to improve the accuracy of dynamic process measurements dates to the mid-1960s. In particular, the National Aeronautics Space Administration (NASA) first conceived the LCSR idea to improve the measurement of transient temperatures in aerospace vehicles.<sup>[15]</sup> In the 1970s, the Oak Ridge National Laboratory (ORNL) further developed NASA's work to apply the LCSR technique to the measurement of in-service response time for thermocouples in liquid metal fast breeder reactors (LMFBRs).<sup>[16]</sup>

This ORNL work was funded by the U.S. government to support the Clinch River Breeder Reactors (CRBR) project, a plutonium-fueled LMFBR that used liquid sodium as its primary coolant. In this reactor, thermocouples were to be used to measure the temperature of the liquid sodium. In LMFBRs, the speed of response of primary coolant temperature sensors is critical to plant safety and must therefore be verified.<sup>[17]</sup> This work was performed by R.L. Shepard and R.M. Carroll of ORNL and T.W. Kerlin of the University of Tennessee.<sup>[18]</sup> In particular, R.L. Shepard and R.M. Carroll performed much of the experimental work that developed the LCSR method for this application, while T.W. Kerlin developed the analytical basis for obtaining the response time of temperature sensors from the LCSR test and formulated the effects of process conditions on sensor response time.

The author was also involved in these developments as a graduate student of Professor Kerlin working on his master's degree in nuclear engineering at the University of Tennessee.<sup>[19]</sup> After about five years of R&D and feasibility studies performed on the CRBR project, the U.S. Congress cancelled the CRBR in the early 1980s, and the work of ORNL on the LCSR method came to a halt. More recently, LMFBR reactors have

returned as the “next generation” of reactors; the LCSR technique can serve these plants when they become operational.

The author’s work on LCSR technology did not come to a halt when CRBR was cancelled. Since then, the author has continued to evolve LCSR as a method and to test and adapt it in multiple practical applications – especially during the last four years in which the research that is the focus of this dissertation was conducted. Specifically, the experimental data presented in this dissertation confirms the validity of the LCSR method for RTD response time testing in nuclear power plants. Moreover, the author’s research for this dissertation has both validated the noise analysis technique for testing the response time of pressure transmitters and quantified the contribution of sensing lines to overall response time.

The work on the noise analysis technique for dynamic testing of nuclear power plants’ I&C systems also dates back to the late 1960s and 1970s.<sup>[20-21]</sup> Most of the development in this era is due to Dr. Joe Thie, who is regarded as the father of the noise analysis technique for nuclear power plants.<sup>[22]</sup> Dr. Thie’s research work continued until the late 1980s, after which he joined with the author to apply the noise analysis technique for equipment performance monitoring, sensor response time testing, and diagnostics in nuclear power plants. In fact, some of the foundational material in this dissertation originates from the author’s work implementing the noise analysis technique for sensor response time testing in nuclear power plants. In particular, the author demonstrated the effect of sensing line blockages and voids on response time, verified that the noise analysis technique can identify these effects, and performed laboratory and field measurements to validate the noise analysis technique for sensor response time testing in nuclear power plants.

Since the 1990s, the interest in using noise analysis techniques for equipment and process diagnostics and prognostics has accelerated. In particular, Professor B. R. Upadhyaya at the University of Tennessee has applied the concept to numerous applications over a wide spectrum of industries including nuclear reactors, manufacturing facilities, and fossil power plants, among others.<sup>[23]</sup> In fact, Dr.

Upadhyaya was a pioneer in applying and evolving the noise analysis technique in the 1990s for equipment and process condition monitoring and has demonstrated the benefits of this technique for a variety of industrial applications. The noise analysis technique has also found applications in medicine and health care for heart monitoring, detecting clogged arteries, and distinguishing the pulses of a pregnant woman's heart from her baby's.<sup>[24]</sup> Similarly, at the University of Arizona in Tempe, Professor Keith Holbert and his research team have been working extensively on the pressure sensing line questions treated in this dissertation as well as on the potential application of noise analysis techniques for diagnostics of sensing line problems.<sup>[25]</sup>

And recently, the Electric Power Research Institute (EPRI) has become interested in resurrecting an old noise analysis concept called "zero crossing" in order to develop a hand-held system (capable even of operating on an iPhone) to perform sensor health monitoring.<sup>[26]</sup>

Research work on the LCSR and noise analysis techniques is not limited to the United States. Others in Europe, Asia, and Canada have also been active in this area. For example, France's Commissariat à l'énergie atomique et aux énergies alternatives (CEA) and Électricité de France (EdF) were early pioneers in evaluating the LCSR and noise analysis techniques for sensor response time testing.<sup>[27]</sup> Furthermore, CEA and EdF contributed to the development of an International Electrotechnical Commission (IEC) standard governing the use of the LCSR and noise analysis techniques in nuclear power plants.<sup>[28]</sup> Also, at the University of Western Ontario in Canada, a graduate student is applying the LCSR concept to support the development of a sensor with self-diagnostic capability.<sup>[29]</sup>

Canada and Sweden have also been active in developing and implementing the noise analysis technique for testing the response time of pressure transmitters in nuclear power plants.<sup>[30-33]</sup> Furthermore, a number of researchers in Spain remain active in exploring noise analysis applications to nuclear power plant sensors and have published extensively in this area for over two decades.<sup>[34, 35]</sup>

The nuclear industry is not unique in its interest in dynamic process measurements. In fact, in 1963, the U.S. National Bureau of Standards (NBS) published a document (Monograph 67) titled “Methods for the Dynamic Calibration of Pressure Transducers.” This comprehensive publication covering both theoretical and practical aspects of dynamic pressure measurements was written to support the design and development of modern rocket engines for missiles and space vehicles. The U.S. Bureau of Naval Weapons, Aeronautical Systems Division; U.S. Air Force; White Sands Missile Range; U.S. Army; and NASA were among the U.S. government entities sponsoring this seminal publication.

This brief literature review shows that the LCSR and noise analysis techniques have been evolving for decades. Much research has already been done to establish their theoretical basis and to apply them in industrial processes, especially nuclear power plants. The author has contributed to these developments first through his work on the in-situ response time testing of RTDs (for his master’s degree) and more recently through his work toward this Ph.D. on validating the noise analysis technique for pressure transmitters and refining the application of LCSR for use in nuclear power plants. More specifically, in this dissertation the author identifies the effect of compliance on the total response time of a pressure sensing system and quantifies this effect through laboratory measurements using a variety of pressure transmitters. In using pressure transmitters of the type used in nuclear power plants, he shows that the response time of a pressure sensing system can be dominated by the sensing line to an extent governed by the transmitter’s compliance value. He also demonstrates that the noise analysis technique can yield the response time of a pressure sensor and its sensing line in a single test.

### **3.4 History of Sensor Response Time Testing in Nuclear Power Plants**

When commercial nuclear power plants were designed and built in the 1960s and 1970s, a manufacturer’s specifications for sensor response time were typically regarded as fact. No questions were raised as to the effect of process conditions, installation, and aging on sensor performance. As experience accumulated over the initial years of

nuclear plant operation, it became apparent that manufacturers' specifications have little bearing on the "in-service" response time of process sensors. Furthermore, it was determined that degradation can occur, leading to sluggish dynamic response and other performance issues. As a result, regulations, standards, and guidelines were written in the 1980s to mandate periodic response time testing of safety system sensors in nuclear power plants. For many years, sensors were removed from service and tested for response time in a laboratory or on a bench to satisfy the regulators or meet the plant's technical specification requirements. This was done during plant refueling outages using conventional test procedures. However, during these *ex situ* tests, the nuclear industry recognized that the conventional test procedures do not account for the influence of process conditions and installation on response time. A major gap in the industry's ability to meet an important safety requirement was exposed. This gap can be filled using the *in-situ* response time testing techniques presented in this dissertation.

Over the years, national regulators, international nuclear energy organizations, utilities, vendors, and others have worked together to establish objective requirements for testing sensor response times in nuclear power plants. The following documents testify to some of these efforts:

1. Regulatory Guide 1.118 (April 1995), "Periodic Testing of Electric Power and Protection Systems," U.S. Nuclear Regulatory Commission, Revision 3.
2. NUREG-0809 – Safety Evaluation Report (1981), "Review of Resistance Temperature Detector Time Response Characteristics," U.S. Nuclear Regulatory Commission.
3. IEEE Standard 323 (1987), "Criteria for the Periodic Surveillance Testing of Nuclear Power Generation Safety Systems," Institute of Electrical and Electronics Engineers.
4. ANSI Guide B88.1 (1987), "A Guide for the Dynamic Calibration of Pressure Transducers," American National Standards Institute.



5. ISA 67.06 – Performance Monitoring for Nuclear Safety-Related Instrument Channels in Nuclear Power Plants. The Instrumentation, Systems, and Automation Society (ISA) (May 2002).
6. IEC 62385 – Nuclear Power Plants – Instrumentation and control important to safety – Methods for Assessing the Performance of Safety System Instrument Channels. International Electrotechnical Commission (IEC) (June 2007).
7. IEC 62342 – Nuclear Power Plants – Instrumentation and control systems important to safety – Management of Aging. International Electrotechnical Commission (IEC) (August 2007).
8. IEC 62397 – Nuclear Power Plants – Instrumentation and control important to safety – Resistance Temperature Detectors. International Electrotechnical Commission (IEC) (May 2007).

# 4

## FACTORS INFLUENCING SENSOR PERFORMANCE

---

This chapter describes experimental results conducted for this dissertation to demonstrate the influence of installation, process conditions, and aging on sensor response time. This empirical foundation will set the stage for the discussion in Chapter 5 of in-situ response time testing techniques that can account for these effects.

### 4.1 Effects on RTDs

Figure 4-1 shows experimental data on the effect of installation on the response time of an RTD that was installed properly so it reached the bottom of its thermowell, resulting in an optimum response time of 3.3 seconds. The RTD was then gradually moved out of its thermowell so as to demonstrate how the response time degrades as an air gap is created at its sensing tip. A feeler gauge was used to measure the displacement, as shown in Figure 4-1. Note that the response time results increase by a factor of more than two, from 3.3 seconds to 7.5 seconds, as the RTD is withdrawn 1 mm from the thermowell to simulate the effect of installation. Considering that the length of this particular RTD is about 30 cm, a 1 mm air gap is relatively small. Yet the difference in response time it causes is significant. Debris, dirt, and metal shavings entering the thermowell during installation are only some of the factors that can cause an extra millimeter of air gap that prevents the RTD from reaching the very bottom of its thermowell. Dimensional differences; RTD movement in the thermowell due to vibration, thermal, or mechanical shock; and other effects can cause the RTD's sensing tip to displace away from the bottom of the thermowell. There is, of course, a trade-off between response time and the size of the air gap at the RTD/thermowell tip. If there is no air gap, the RTD and thermowell will be in metal-to-metal contact.

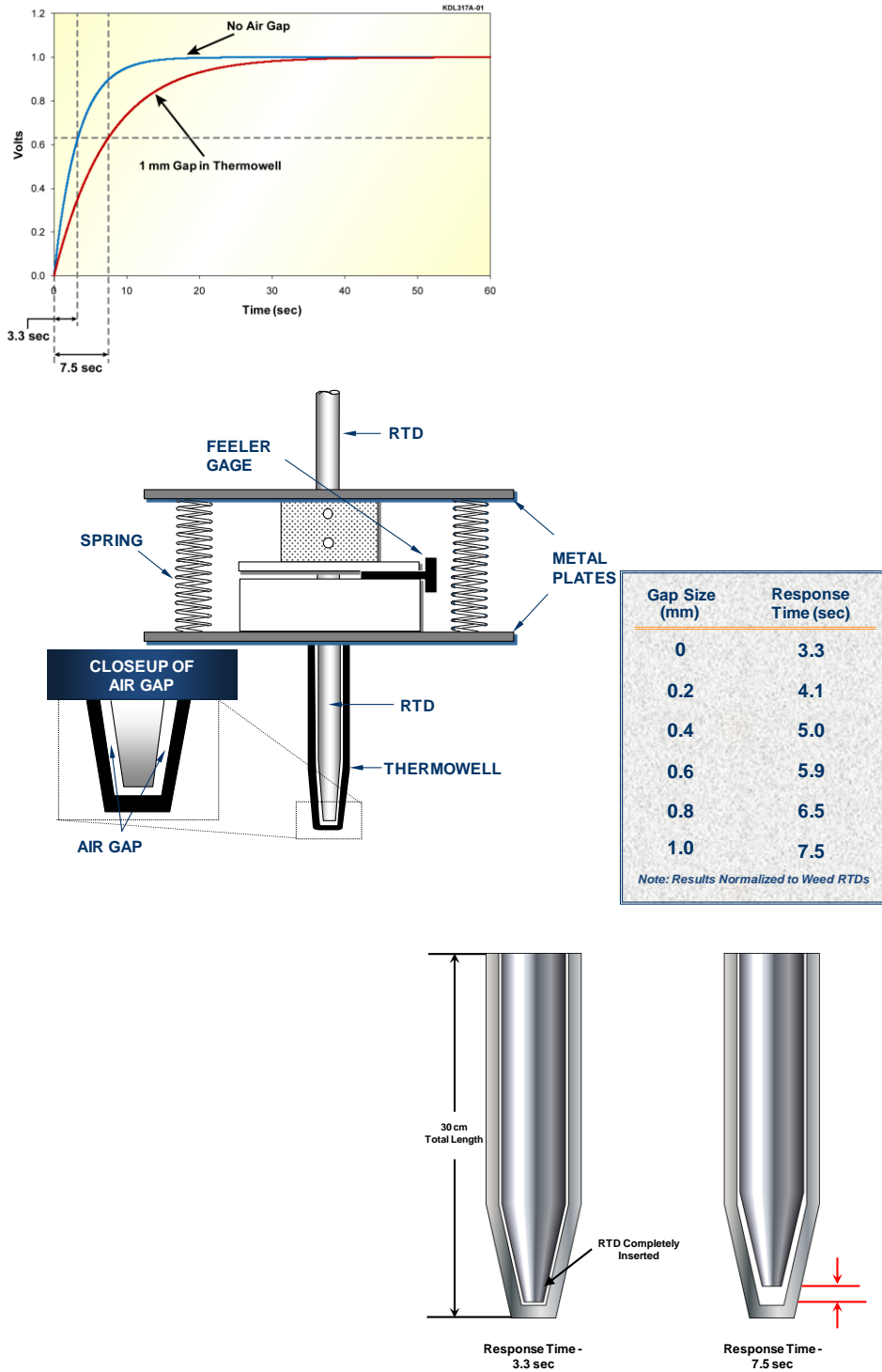


**Figure 4-1 Laboratory Research to Study the Effect of Installation on an RTD Response Time**

This complete absence of air gap may degrade the RTD in that thermal expansion of the thermowell can stress the RTD and weaken the platinum element inside its sensor. On the other hand, any air gap increases the sensor's response time.

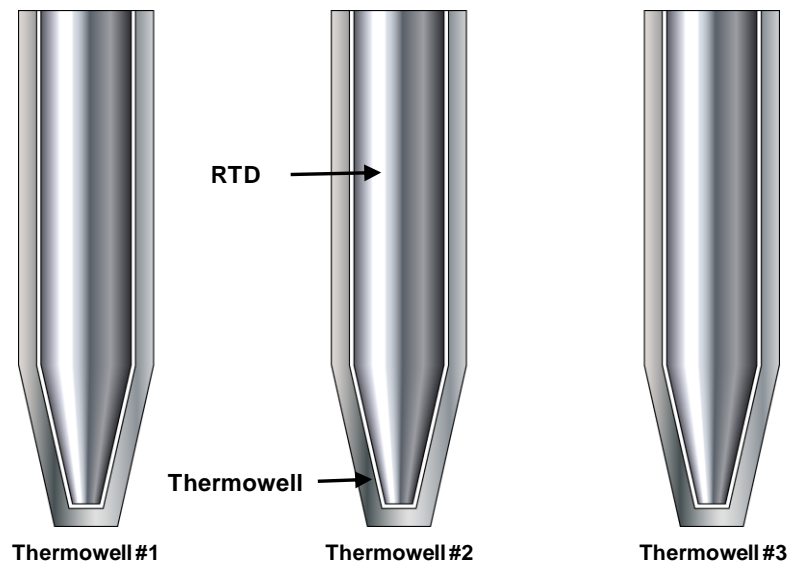
To obtain the optimum response time, an RTD should be matched to a thermowell before the two are installed in the plant. Table 4-1 shows laboratory response time results on RTD/thermowell interchangeability. The data derives from plunge testing of three identical RTDs tested in three identical thermowells; all from the same manufacturer. It is evident from the table that the same RTD can experience different response times in different thermowells of identical designs and dimensions. This provides empirical support for the best practice of performing laboratory plunge testing prior to installation so as to match each RTD to a thermowell that yields the best response time. In fact, the nuclear industry is using this procedure to produce the fastest possible response times for every set of new RTDs and thermowells, matched before they are installed in a plant.

To show the effect of process conditions on response time, over 50 plunge tests were performed in water and in air for three different RTDs labeled A, B, and C. The results in Table 4-2 reveal significant differences between the response time measured in water and in air. These results demonstrate that RTD response time can be affected dramatically by the medium in which the sensor is used. The effect of process conditions on an RTD's dynamic response time was reinforced by a second laboratory experiment, the results of which are shown in Figure 4-2. This figure presents transient responses for an RTD tested under three different conditions: in flowing water (at 1 meter per second), stagnant water (no flow), and flowing air (at 15 meters per second). This experiment provides further evidence of process effect on RTD response time.

The heat transfer properties of the fluid around an RTD relate to the effect of process conditions on response time. These properties are typically expressed in terms of a numerical quantity referred to as the *convection heat transfer coefficient* ( $h$ ), which is a function of fluid type and its temperature, pressure, flow rate, and other variables. For

**Table 4-1 Research Results on Study of Dimensional Tolerances on RTD Response Time**

<u>RTD Type</u>	<u>Response Time (sec)</u>		
	<u>Thermowell #1</u>	<u>Thermowell #2</u>	<u>Thermowell #3</u>
A	4.8	5.2	6.0
B	3.6	4.1	4.6
C	4.4	4.9	5.9



Notes:

- 1) The RTDs and thermowells used in this experiment are identical. Response time differences in the table are the result of dimensional tolerances at the sensing tip of the RTD and thermowell.
- 2) Response time results in this table are derived from plunge testing in room temperature water flowing at 1 meter per second.

**Table 4-2 Laboratory Data on Influence of Process Media on RTD Response Time**

<u>RTD</u>	<u>Response Time (sec)</u>	
	<u>Water</u>	<u>Air</u>
A	4.8	14.4
B	3.6	22.0
C	4.4	24.0

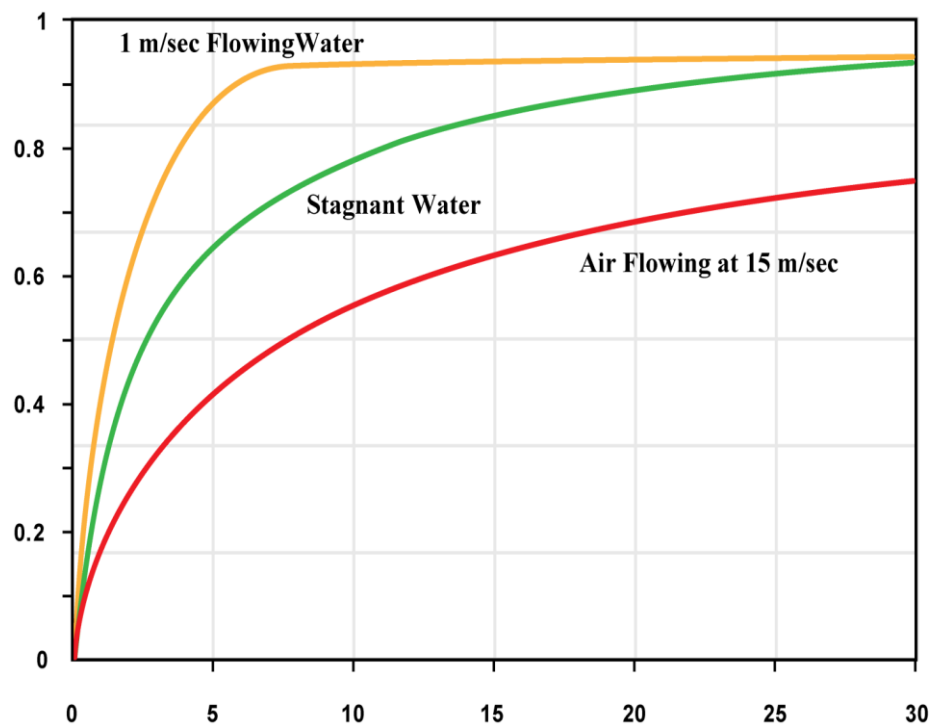


**Figure 4-2** Results of Laboratory Testing to Demonstrate the Effect of Process Media on Dynamic Response of an RTD (from LCSR Test)

example, the heat transfer coefficient increases as fluid flow rate is increased, and the corresponding response time decreases in accordance with the following equation for a first-order thermal system:

$$\tau = \frac{mc}{hA} \quad (4.1)$$

$\tau$  = response time, sec

$m$  = mass of the part of the sensor that is in the fluid, kg

$c$  = sensor specific heat, J/kg·K (K: Kelvin)

$A$  = area that is in contact with the fluid in which the sensor is installed, m<sup>2</sup>

## 4.2 Effects on Pressure Transmitters

Although process conditions have little or no effect on the response time of pressure transmitters, the length of the transmitter's sensing line can have a significant effect, varying in accordance with the compliance of the transmitter at the end of the sensing line.

In Chapter 2 it was shown that calculations derived from theory support the assumption that, for transmitters with high compliance values, the length of sensing line and any blockages or voids can produce significant response time differences. In this chapter, we will demonstrate this experimentally. Also, if and when applicable, we will calculate and add the effect of sonic delays on the measured response times. The sonic delay is also called the *acoustic delay* and corresponds to the time that it takes for the pressure signal to travel through a completely filled and vented sensing line from the process to the transmitter at the speed of sound. It is usually neglected because it is small relative to the overall sensing system response time. Furthermore, the sonic delay is independent of transmitter type, transmitter design, or sensing line diameter; however, it is dependent on the bulk modulus of the water, the density of the water, and the length of the sensing line.

The sonic delay is calculated based on Hooke's law:



$$\text{Sonic delay (SD) (sec)} = L / \sqrt{K / \rho}$$

$L$  = length of the sensing line, m

$K$  = bulk modulus of fluid, Pa

$\rho$  = fluid density, kg/m<sup>3</sup>

For water, the values of  $K$  is  $2.15 \times 10^9$  Pa, and  $\rho$  is  $999.8$  kg/m<sup>3</sup>. With this information, we arrived at 0.002 seconds as the sonic delay of a short sensing line (1m) and 0.024 seconds as the sonic delay of a long sensing line (35m). This information is used in Chapter 6 (section 6.3) in presenting in-plant test results on the validation of the noise analysis technique to measure sensing line effects.

Table 4-3 shows the results of ramp testing performed on three different transmitters (Rosemount, Foxboro, and Barton) with short and long sensing lines and an induced blockage. The short sensing line was ~1 meter, the long sensing line was 35 meters, and the blockage was induced using a snubber. These results show that length and blockage affect the response time in proportion to the transmitter compliance. Confirming the theoretical results from Chapter 2, Table 4-4 shows the good agreement between the theoretical results and the laboratory measurements for the three transmitters used to arrive at these results. Table 4-5 presents additional experimental results from laboratory measurements on the effect of line length on response time (both of the transmitters and the sensing lines) for four types of nuclear plant pressure transmitters.

In another laboratory experiment, a Barton transmitter was ramp tested with a short and long sensing line and a huge snubber. The results, shown in Table 4-6, reveal how significantly the response time of the Barton transmitter is affected by the length of its sensing line and the snubber. The Barton transmitter was selected for this demonstration because it has the largest compliance of all pressure transmitters available for this research project.

Table 4-7 shows laboratory test results for a Foxboro transmitter that was ramp tested with varying amounts of air in the lines between the test equipment and the transmitter.

**Table 4-3 Experimental Research Data on the Effect of Length and Blockage on Response Time**

Transmitter Manufacturer	Compliance (cm <sup>3</sup> /bar)	Response Time (sec)		
		Short Line	Long Line	Blockage
Rosemount	0.01	0.06	0.12	0.26
Foxboro	0.12	0.24	0.34	2.12
Barton	9.51	0.14	0.43	4.35

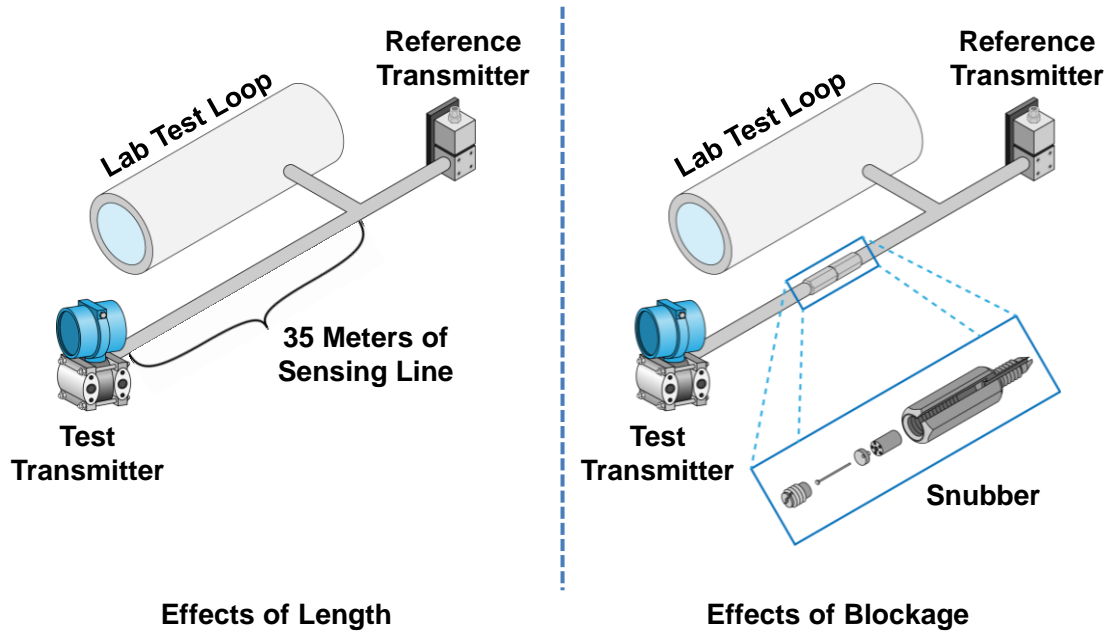


**Table 4-4 Theoretical and Experimental Estimations of Response Time of Sensing Line Alone\***

<u>Length (meters)</u>	<u>Response Time (sec)</u>	
	<u>Theoretical</u>	<u>Experimental</u>
	<b><u>Barton</u></b>	
30	0.15	0.07
60	0.22	0.15
120	0.31	0.29
	<b><u>Foxboro</u></b>	
30	0.02	0.02
60	0.04	0.05
120	0.07	0.10
	<b><u>Rosemount</u></b>	
30	0.02	0.02
60	0.03	0.02
120	0.06	0.06

\* The experimental results in this table were obtained by performing the following two series of measurements and subtracting the results: 1) laboratory measurement of response time with sensing line lengths from 30 to 120 meters; and 2) laboratory measurement of response times of the same transmitters with short (negligible) sensing line lengths. That is, these results represent the response time of the sensing line alone: (Sensor + Sensing Line) – Sensor = Sensing Line.

**Table 4-5 Experimental Results on the Effect of Sensing Line Length on Transmitter Response Time**

<b>Length (meter)</b>	<b>Response Time (sec)</b>			
	<b><u>Rosemount</u></b>	<b><u>Foxboro</u></b>	<b><u>Barton</u></b>	<b><u>Tobar</u></b>
1	0.06	0.24	0.14	0.28
30	0.08	0.26	0.21	0.33
60	0.08	0.29	0.29	0.38
120	0.12	0.34	0.43	0.42

Notes:

1. Results are for sensing lines made of copper tubing with I.D. of 1.27 cm.
2. The above response times were obtained by laboratory testing of the pressure transmitter using a hydraulic ramp generator.



**Table 4-7      Response Time of a Foxboro Transmitter as a Function of Air  
in Sensing Line**

<u>Length of Bubble(m)</u>	<u>Response Time (sec)</u>
0	0.12
0.2	0.13
0.5	0.13
0.8	0.19
1.5	0.39

---

The above tests were performed with a 10-meter, 0.5-cm nylon tube connecting the test unit and the transmitter under test. The bubble lengths given above are approximate values.

Although the compliance of the Foxboro transmitter is small (nearly two orders of magnitude less than that of Barton transmitters), its response time is affected by the volume of air in the sensing line.

Conventionally, nuclear plants have measured the response time of pressure transmitters by excluding the sensing line. The data produced by the research for this dissertation demonstrates that response time measurements made without the sensing lines are meaningless insofar as the effect of length, blockages, and void can dominate the response time. The noise analysis technique presented in Chapter 5 mitigates this critical measurement discrepancy by providing a means for including the sensing lines in the measurement of a transmitter's response time.

### **4.3 Aging Effects**

Process sensors are subject to both external stressors from the environment surrounding them in the plant, such as, temperature, humidity, radiation, and vibration, and internal stressors, which arise from the operation of the sensors, such as internal heating, physical stresses, or the wearing of electrical or mechanical parts during operation.

Over the years, the nuclear industry has gained insight into the degradation modes of nuclear plant RTDs and pressure transmitters. Tables 4-8 and 4-9 show examples of anomalies that RTDs and pressure transmitters may experience as they are used in nuclear power plants and the potential consequences of these anomalies on the calibration or response time of these sensors. It is because of these potential consequences that the nuclear industry is required by regulators and/or plant technical specification provisions to perform periodic calibration and response time testing on its safety-related temperature and pressure instrumentation.

#### **4.3.1 Aging of RTDs**

Aging can cause degradation in RTDs in a number of ways. For example, the sensing element's resistance normally increases under tensile stress and decreases with compression stress. These effects can result in calibration shift, response-time degradation, reduced insulation resistance, erratic output, wiring problems, and the like.

**Table 4-8 Examples of Potential Causes of RTD Degradation**

Degradation	Potential Cause	Affected Performance	
		Calibration	Response Time
Failure of Sensing Element	<ul style="list-style-type: none"> <li>- Vibration</li> <li>- Thermal or mechanical shock</li> <li>- Impurities</li> <li>- Chemical interaction with insulation material</li> <li>- Installation deficiency</li> <li>- Design or fabrication flaws</li> </ul>	✓	✓
Deterioration of Accuracy	<ul style="list-style-type: none"> <li>- Inaccurate factory calibration</li> <li>- Mishandling during storage or installation</li> <li>- Damage during removal or maintenance</li> <li>- Dimensional changes in sensing element</li> <li>- Moisture intrusion reducing insulation resistance</li> </ul>	✓	
Response Time Changes	<ul style="list-style-type: none"> <li>- Improper installation of RTD in thermowell</li> <li>- Changes in air gap between the sensing tip of the RTD and its thermowell caused by vibration and/or mechanical shock</li> <li>- Changes in RTD insulation properties</li> <li>- Expansion or contraction of air gaps in RTD insulation material</li> </ul>		✓
Failure of Insulation Resistance	<ul style="list-style-type: none"> <li>- Failure of seals</li> <li>- Manufacturing flaws</li> <li>- Moisture intrusion through sheath</li> </ul>	✓	✓



**Table 4-9 Examples of Potential Causes of Performance Degradation in Nuclear Plant Pressure Transmitters**

Degradation	Potential Cause	Affected Performance	
		Calibration	Response Time
Partial or Total Loss of Fill Fluid	<ul style="list-style-type: none"> <li>- Manufacturing flaws</li> <li>- High pressure</li> </ul>	✓	✓
Viscosity Change of Fill Fluid	<ul style="list-style-type: none"> <li>- Radiation and heat</li> </ul>		✓
Wear, Friction, and Sticking of Mechanical Linkages (Especially in Force Balance Transmitters)	<ul style="list-style-type: none"> <li>- Pressure fluctuations and surges</li> <li>- Corrosion and oxidation</li> </ul>		✓
Failure of Seals Allowing Moisture into Transmitter Electronics	<ul style="list-style-type: none"> <li>- Embrittlement and cracking of seals due to radiation and heat</li> </ul>	✓	
Leakage of Process Fluid into Cell Fluid Resulting in Temperature Changes in Sensor, Viscosity Changes in Fill Fluid, etc.	<ul style="list-style-type: none"> <li>- Failure of seals</li> <li>- Manufacturing flaws</li> <li>- Rupture of sensing elements</li> </ul>	✓	✓
Changes in Characteristic Values of Electronic Components	<ul style="list-style-type: none"> <li>- Heat, radiation, humidity</li> <li>- Changes in power supply voltages</li> <li>- Maintenance</li> </ul>	✓	
Changes in Spring Constants of Bellows and Diaphragms	<ul style="list-style-type: none"> <li>- Mechanical fatigue</li> <li>- Pressure cycling</li> </ul>	✓	✓

Among these, sensor calibration and response time are the most important functionalities affected by aging. As such, they must be verified periodically to justify continued operation, meet regulatory requirements, or comply with the plant's technical specification provisions.

Table 4-10 shows the results of response time measurements for three direct-immersion and three thermowell-mounted RTDs in a nuclear power plant tested two years apart. These results show that both direct-immersion and thermowell-mounted RTDs are affected by aging. Figure 4-3 shows the distribution of results gained from tracking the response times of a group of RTDs over three years. The base period shows a mean response time of 4.4 seconds, which increased by about 10 percent to 4.8 over three years. The standard deviations of these two mean values were 0.77 and 0.72 seconds, respectively.

Although some plants have experienced significant RTD response time increases over shorter periods of time, this is not typical. Table 4-11 shows response time data for 20 RTDs measured in 2008, 2009, and 2010. Most of the RTDs in this plant experienced some increase in response time, and four exceeded the plant's limit for response time and had to be replaced, as noted in the table.

#### **4.3.2 Aging of Pressure Transmitters**

As with RTDs, the qualified life of most nuclear plant pressure transmitters is typically 20 years, although most pressure transmitters last longer if they are properly maintained. Typical aging mechanisms for nuclear plant pressure transmitters include thermal, mechanical, or electrical fatigue; wear; corrosion; erosion; embrittlement; diffusion; chemical reaction; cracking or fracture; and surface contamination. These degradations may result from exposure to any combination of the following stressors: heat, humidity, vibration, radiation, mechanical shock, thermal shock, temperature cycling, pressure cycling, testing, and electromagnetic interferences.

Figure 4-4 shows response time trending results from approximately 1,000 tests of nuclear plant pressure transmitters performed over twelve years. Results are shown for four services: (a) feedwater flow, (b) steam generator level, (c) steam flow, and (d)

**Table 4-10 Examples of RTD Response Time Degradation in Nuclear Power Plants**

<u>Item</u>	<u>Response Time (Sec)</u>		
	<u>Reference Results</u>	<u>Two Years Later</u>	<u>Change</u>
<u>Thermowell-Mounted RTDs</u>			
1	2.7	3.7	37%
2	4.0	5.9	48%
3	2.4	3.3	38%
<u>Direct-Immersion RTDs</u>			
4	1.9	2.5	32%
5	2.8	3.9	39%
6	2.0	2.5	25%

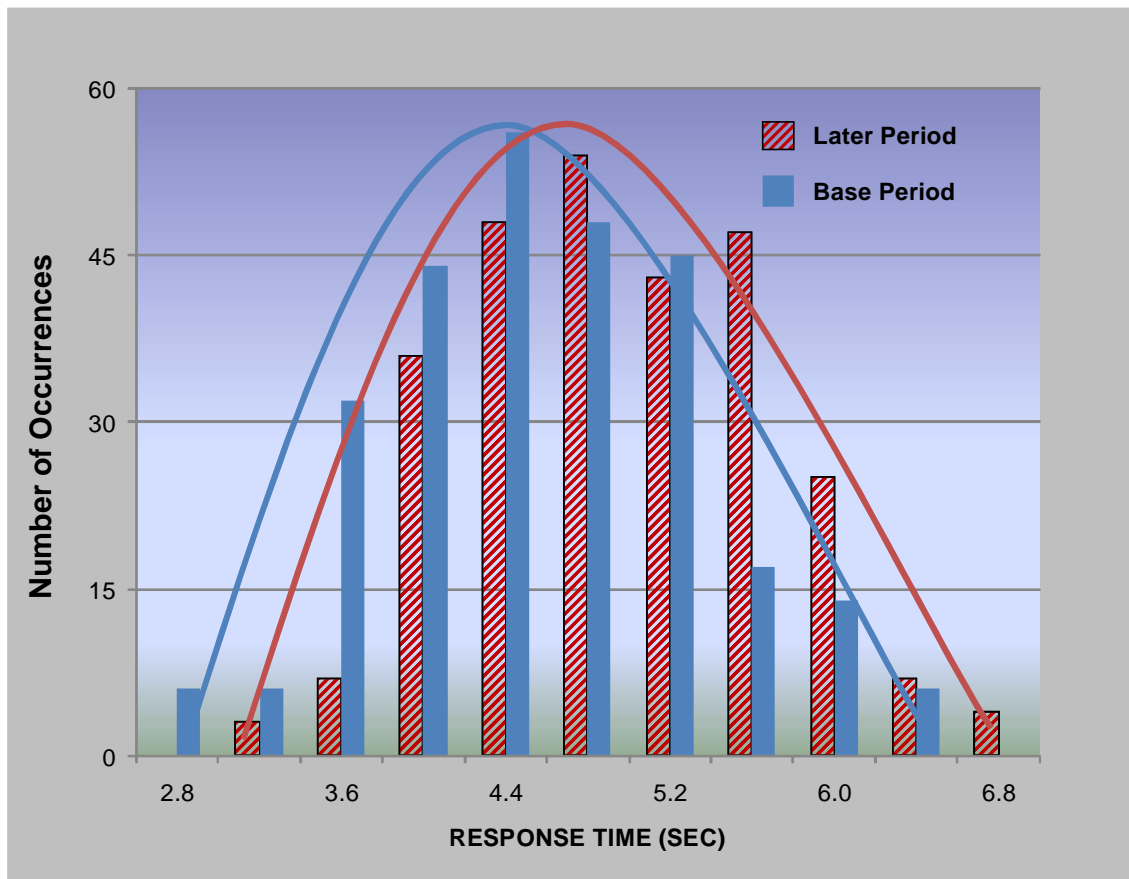
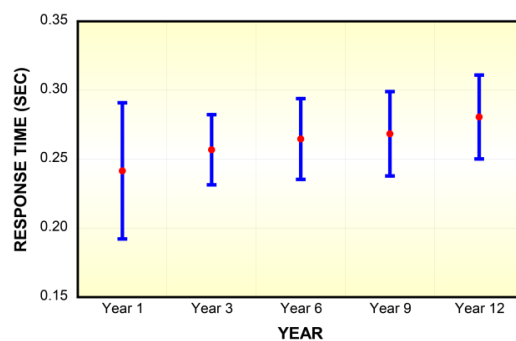


**Figure 4-3** Distribution of Response Time Results, Indicating an Increase over the Period of Observation

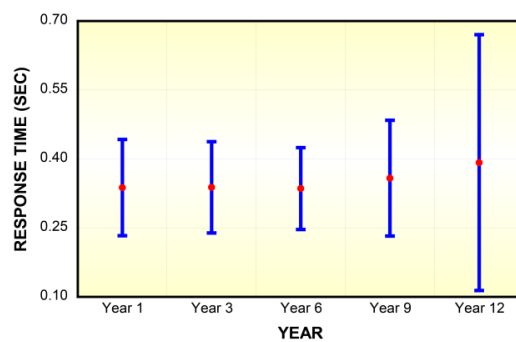
**Table 4-11 Aging Effects on RTD Response Time**

<u>RTD</u>	<u>2008</u>	<u>2009</u>	<u>2010</u>
1	3.3	3.3	4.2
2	3.9	4.3	4.9
3	4.4	4.0	4.5
4	4.5	4.0	4.1
5	4.5	4.2	5.2
6	4.7	5.2	5.6
7	4.7	5.4	5.4
8	4.7	5.2	5.1
9	4.8	4.8	4.6
10	4.8	5.4	5.8
11	4.9	5.6	5.7
12	5.0	5.0	4.9
13	5.3	5.9	6.3
14	5.4	5.5	5.6
15	5.5	5.8	6.2
16	5.7	5.7	5.7
17	5.4	6.3	Replaced*
18	5.4	6.1	Replaced*
19	5.7	6.3	Replaced*
20	5.8	6.3	Replaced*
<b>Average</b>	<b>4.9</b>	<b>5.2</b>	<b>5.2</b>

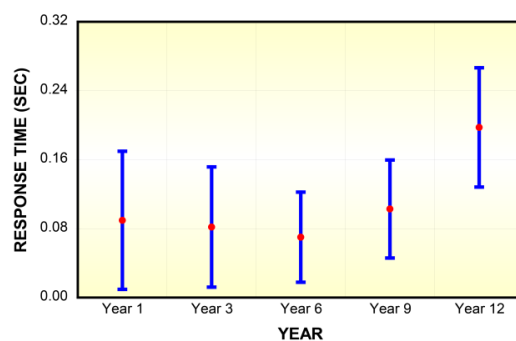
\*RTD failed response time test so it was replaced.



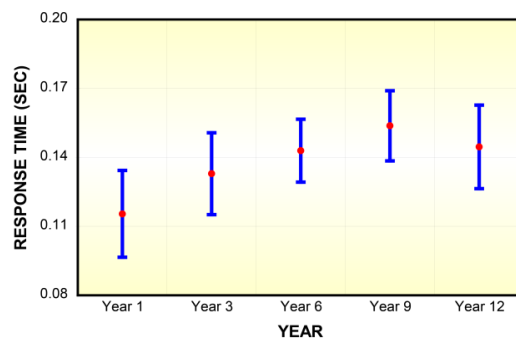
(a) FEEDWATER FLOW



(b) STEAM GENERATOR LEVEL



(c) STEAM PRESSURE



(d) STEAM FLOW

**Figure 4-4 Response Time Trends from In-plant Testing of Pressure Transmitters in Four Different Services in a PWR plant**

steam pressure. For each service that is included in these figures, the average and standard deviation of the results are shown together with a least-square-line fit to establish the trend. This data indicates an upward trend in response time. Fortunately, the response time increases are small, revealing that response time measurements performed in nuclear power plants once a cycle (i.e., every 18 to 24 months) are adequate for detecting any transmitter that may exceed acceptable limits.

# 5

## SOLUTIONS DEVELOPED FROM THIS RESEARCH

---

This chapter describes the two techniques—LCSR and noise analysis—developed to address the inadequacies of the conventional methods for measuring response time. Table 5-1 summarizes both the problems with the conventional method for testing sensor response time in RTDs and the solutions to the problems offered by the LCSR method. Table 5-2 summarizes both the problems posed by the conventional method for testing the response time of pressure transmitters and the solutions that noise analysis offers.

### 5.1 LCSR Test Principle

During this research, the author advanced, refined, and implemented the LCSR method to test the in-situ response time of installed RTDs in nuclear power plants. The principle behind the LCSR method is to heat the sensing element of the RTD with an electric current (30 to 60 mA). The method will only work for RTDs whose design ensures that the heat transfer to and from the RTD sensing element follows the same path whether the RTD experiences a step change in temperature from the outside or in the inside. Figure 5-1 shows two identical experimental setups involving an RTD in a tank of room-temperature water. In the LCSR test, heat is generated inside the RTD and dissipates to the outside, passing through the RTD material, namely, the insulation, sheath, the air gap in the thermowell, the wall of thermowell, and the heat transfer resistance on the RTD surface. This heat transfer process results in a transient that is referred to as the *LCSR data*.

In the traditional plunge test, the heating begins at the sensor surface and diffuses through the sensor material to reach the sensing element, resulting in a transient that we refer to as the *plunge data*. Figure 5-2 shows the test setup and the shape of the



**Table 5-1 Summary of Problems with Conventional Plunge Test Method for RTD Response Time Testing and Solutions Offered by the LCSR Technique**

<u>Conventional Method</u>	<u>Problems with Conventional Method</u>	<u>Solutions (LCSR Technique)</u>
<p><u>Plunge Test:</u> Performed in a laboratory environment according to a conventional procedure described in the American Society for Testing and Material (ASTM) Standard E-644, International Electrotechnical Commission (IEC) Standards 60751 and 62385, and International Society of Automation (ISA) Standard 67.06. This method is useful for comparing different sensor designs from a response time standpoint. However, its results do not yield the response time for a temperature sensor after it is installed in a process.</p> <p>The test involves a rotating tank of room-temperature water that provides a flow rate of 1 m/s. The RTD is heated or cooled in the air and suddenly immersed in the water while its output is converted into an electrical signal and recorded to provide the raw data for measuring response time.</p>	<ul style="list-style-type: none"> <li>• Does not account for process influence</li> <li>• Does not account for installation effects</li> <li>• Requires that sensors be removed from plant for testing</li> <li>• Involves radiation exposure to plant personnel</li> <li>• Increases the duration of plant outages</li> <li>• Susceptible to human error and may damage sensors and other plant equipment</li> <li>• Cannot be performed while the plant is operating</li> <li>• Does not meet the intent of regulatory regulations and technical specifications for RTD response time</li> <li>• Does not provide the “in-service” response time of RTDs</li> </ul>	<ul style="list-style-type: none"> <li>• Accounts for the effect of temperature, pressure, and flow on response time</li> <li>• Accounts for installation effects (e.g., air gap in thermowell)</li> <li>• Can be performed remotely on installed sensors (in-situ)</li> <li>• Does not involve radiation exposure to plant personnel (sensor does not have to be accessed to conduct the test)</li> <li>• Does not increase the duration of plant outages</li> <li>• Is immune from human error and potential damage to sensors and other plant equipment</li> <li>• Test is performed during plant operation (online testing)</li> <li>• Meets regulatory objectives and plant technical specification requirements</li> <li>• Provides the “in-service” response time of RTDs</li> </ul>

**Table 5-2 Summary of Problems with Conventional Ramp Test Method for Response Time Testing of Pressure Transmitters and Solutions Offered by the Noise Analysis Technique**

<u>Conventional Method</u>	<u>Problems with Conventional Method</u>	<u>Solutions (Noise Analysis Technique)</u>
<p><u>Ramp Test:</u>            Performed in a laboratory environment or on a bench using a hydraulic ramp signal generator according to Standard 67.06 of the International Society for Automation (ISA) and Standard 62385 of the International Electrotechnical Commission (IEC).            A ramp pressure signal is used to test response time of pressure transmitters because design-based accidents in nuclear power plants are assumed to result in a ramp in pressure (in contrast, for RTDs such design basis events can result in a step change in temperature).            In a ramp test, the transmitter is isolated from the process. Therefore, this method does not account for the contribution of sensing lines to the overall response time of a pressure sensing system.</p>	<ul style="list-style-type: none"> <li>• Does not account for effect of sensing line length, blockages, or voids</li> <li>• Requires physical access to transmitters</li> <li>• Involves radiation exposure to plant personnel</li> <li>• Susceptible to human error</li> <li>• Increases plant outage duration</li> <li>• Can damage transmitters, sensing lines, isolation valves, equalizing valves, and other plant equipment</li> <li>• Only one transmitter can be tested at a time</li> </ul>	<ul style="list-style-type: none"> <li>• Accounts for the effect of sensing line length, blockages, and voids</li> <li>• Provides remote, passive, and in-situ testing capability</li> <li>• Does not involve radiation exposure to plant personnel</li> <li>• Immune from human error</li> <li>• Does not increase outage time</li> <li>• Causes no damage to transmitters, sensing lines, or other plant equipment.</li> <li>• Multiple transmitters can be tested at a time</li> </ul>

---

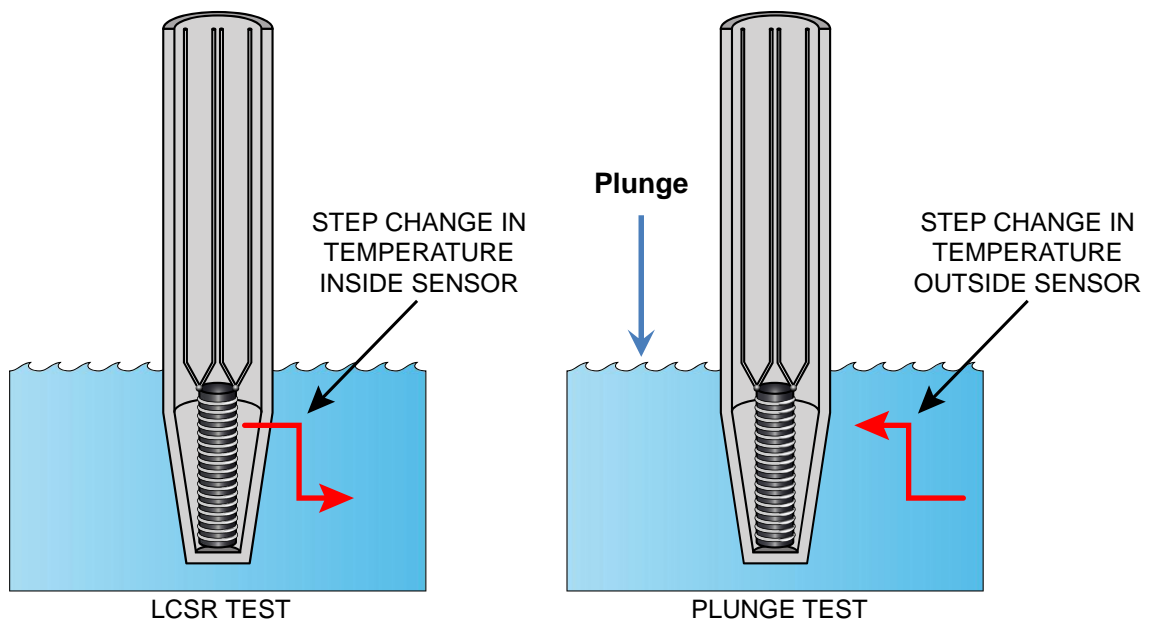


**Figure 5-1 Heat Transfer Process in Plunge and LCSR Methods**

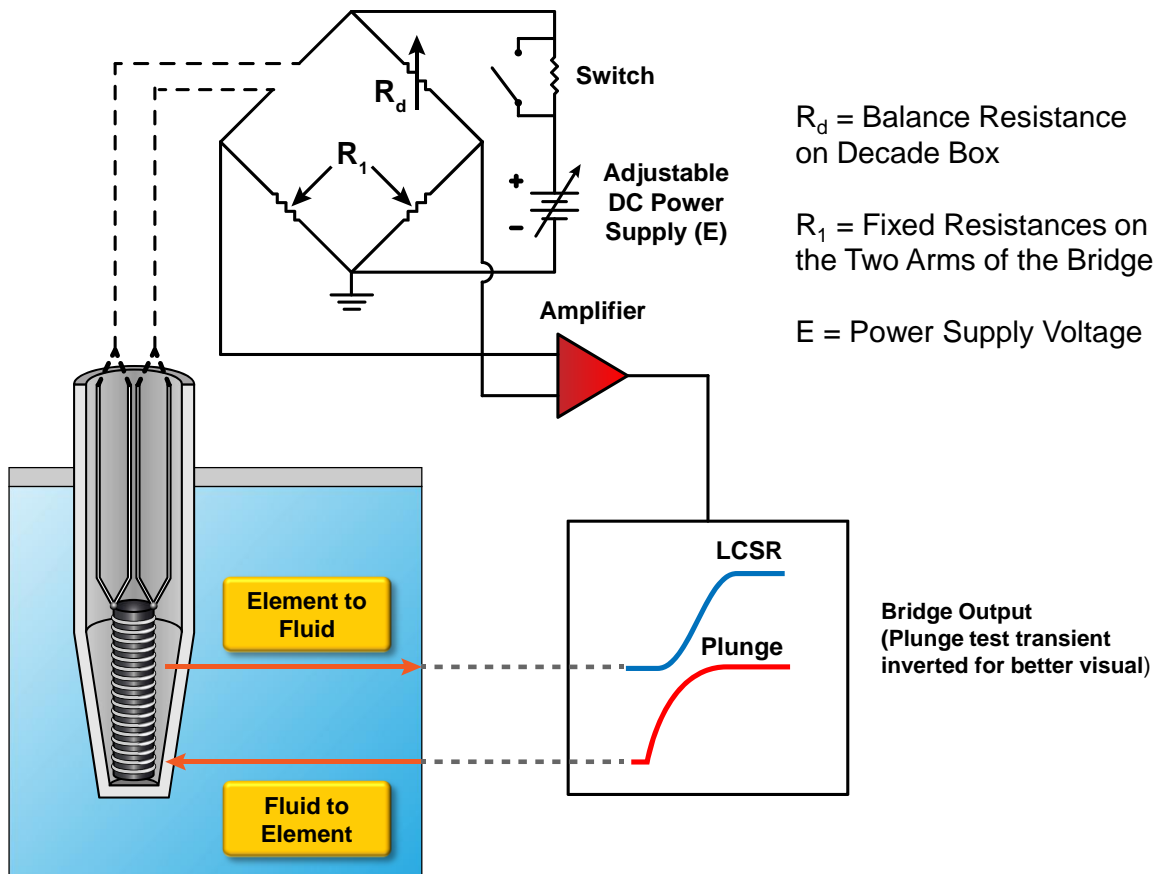


Figure 5-2 LCSR and Plunge Test Transients

transients that result from the plunge and LCSR tests. If there is no axial heat transfer, the heat path in the LCSR and plunge test will be identical, a condition that must be satisfied if the LCSR method is to succeed (Figure 5-3). In particular, the following assumptions must be satisfied for the LCSR test to provide valid results:

1. The sensing element must be centrally located in the RTD assembly, or no heat sink must be present between the sensing element and the centerline of the RTD (Figure 5-4).
2. The heat that is generated in the sensing element in the LCSR test must dissipate radially (Figure 5-5).
3. The RTD must be able to withstand repeated application of the DC current (30 to 60 mA) that is required to perform the LCSR test, and the process temperature must be relatively stable and exhibit little or no drift.

In the execution of the LCSR test, a Wheatstone bridge is used, as illustrated in Figure 5-2. First the bridge is balanced with 1 to 2 mA of DC current running through the RTD. Then, the current is switched “high” to about 30 to 60 mA depending on the RTD, its resistance value, plant temperature stability during the tests, and the desired amplitude of the test output. This causes the RTD sensing element to heat up gradually and settle at a few degrees above the ambient temperature. As noted, the result is an exponential transient that is referred to as the “LCSR data” (Figure 5-6). This transient is then analyzed (as described later in this chapter) to yield the response time of the RTD. The amount by which the temperature rises in the RTD depends both on the magnitude of the heating current and on the rate of heat transfer between the RTD and its surrounding medium. Typically, the RTD heats up by about 5°C to 10°C during the LCSR test, depending on the self-heating index of the sensor (see Appendix D for a description of the self-heating index, how it is calculated for an RTD, and its relationship to the RTD response time).

During the LCSR test, the Wheatstone bridge’s output voltage (V) changes almost linearly with changes in RTD resistance ( $\delta R$ ). The following derivation bears this out.

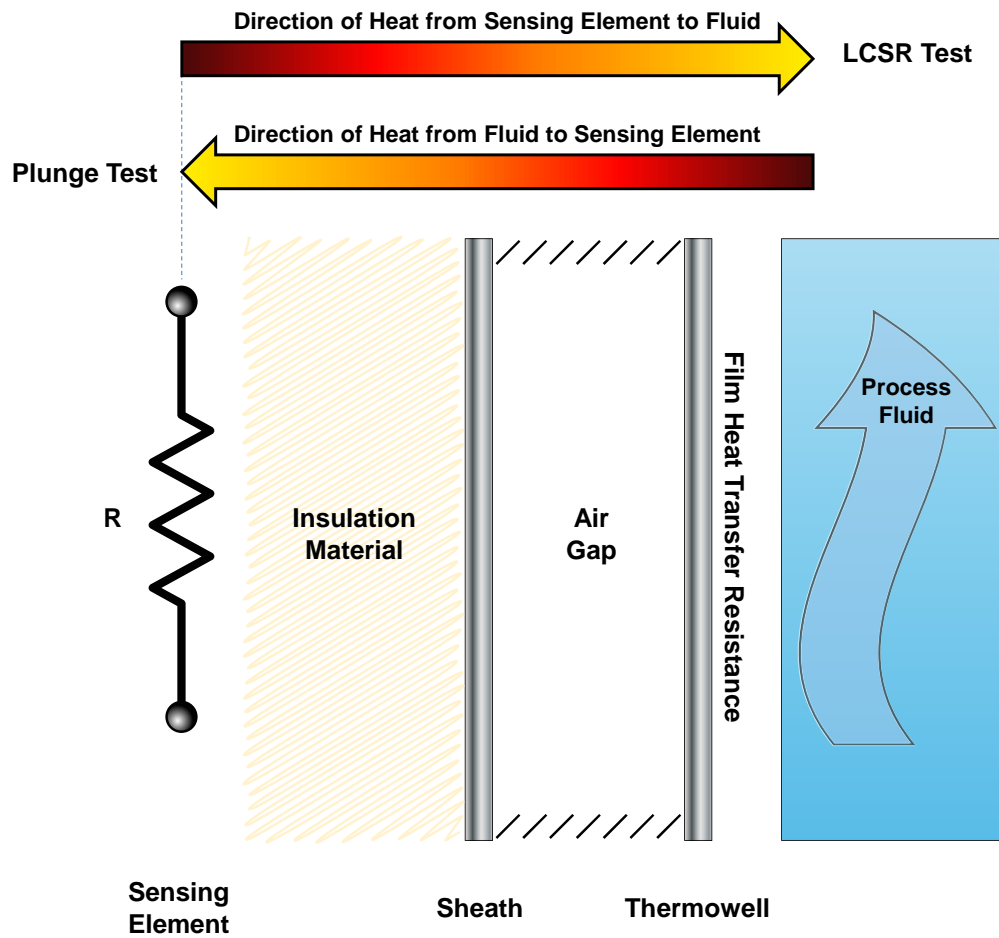
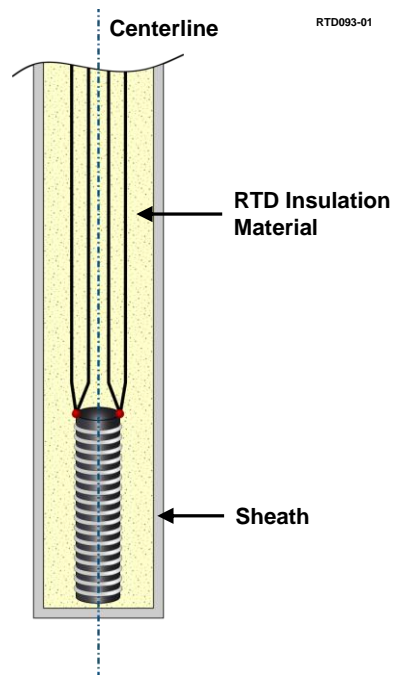
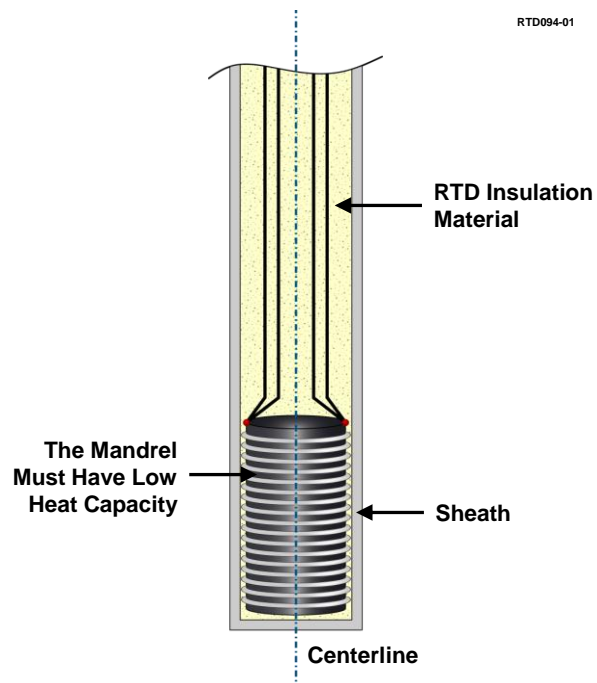


**Figure 5-3** Direction of Heat/Cooling through the RTD Material during an LCSR or a Plunge Test



(a) Sensing element wound around a mandrel located at the center of the sensor



(b) Sensing element attached to the sheath

**Figure 5-4 RTD Designs Which Satisfy LCSR Assumptions**

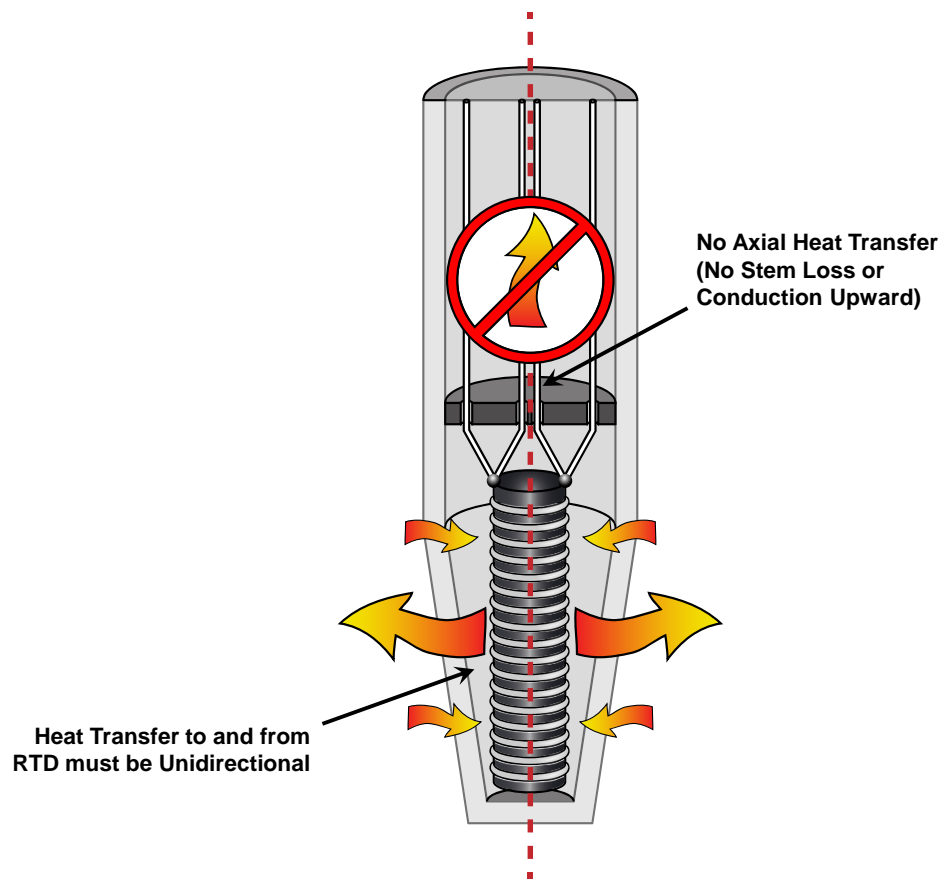


**Figure 5-5 Radial Heat Transfer to and from an RTD**



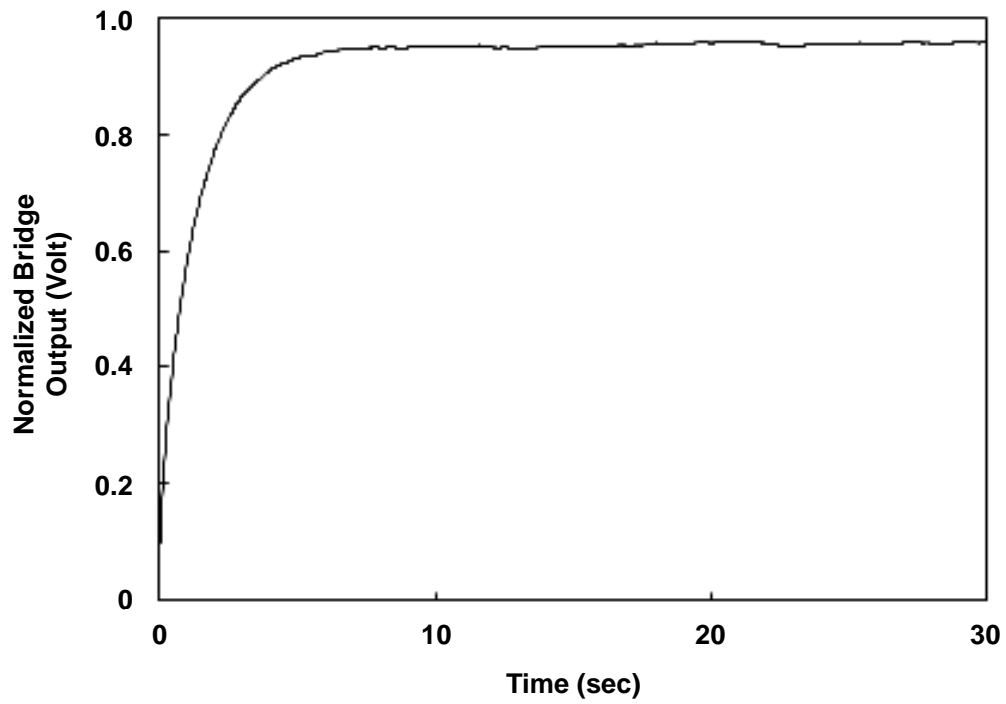


**Figure 5-6 LCSR Transient from Laboratory Testing of an RTD (in Room-Temperature Water Flowing at 1m/sec)**

We begin with a simple circuit analysis to arrive at the bridge output (see Figure 5-2 for the terms in this equation):

$$V = \frac{R_I (R_{RTD} - R_d)}{(R_I + R_d)(R_I + R_{RTD})} E \quad (5.1)$$

$V$  = Bridge output voltage, V

$E$  = Bridge power supply voltage, V

$R_I$  = Fixed bridge arm resistances,  $\Omega$

$R_d$  = Decade box resistance,  $\Omega$

$R_{RTD}$  = RTD resistance,  $\Omega$

When the bridge is balanced in preparation for LCSR testing,  $R_{RTD} = R_d$  and  $V = 0$ . As soon as the current is stepped up to begin the LCSR test, the bridge output rises exponentially, while the RTD resistance increases to  $R_{RTD} + \delta R$ . The bridge output eventually settles at a steady-state value. Bearing these points in mind, the bridge output voltage can be written as:

$$V = \left( \frac{R_I}{R_I + R_d} \right) \left( \frac{\delta R}{R_I + R_d + \delta R} \right) E \quad (5.2)$$

Assuming that  $R_I + R_d$  is much greater than  $\delta R$ , we can write:

$$\boxed{V = C \delta R E} \quad (5.3)$$

where  $C$  is a constant. Equation 5.3 shows that the bridge output changes linearly with  $\delta R$  as long as  $R_I + R_d$  is much greater than  $\delta R$ . Typically,  $\delta R$  is less than 10 ohms, and  $R_I + R_d$  is in the range of 300 to 600 ohm, depending on the RTD and the temperature to which it is exposed. Therefore, the assumption that  $V$  changes linearly with  $\delta R$  is easily

met. If necessary,  $R_1$  can be increased to satisfy the linearity assumption. Normally, a value of 100 to 200 ohms for  $R_1$  is adequate.

## 5.2 LCSR Test Theory

The heat transfer between the sensing element and the medium (fluid) that surrounds the sensor can be represented by a lumped variable network, such as the one shown in Figure 5-7, in terms of nodal temperatures ( $T_i$ ). For this network, the transient heat-transfer equation for node  $i$  can be written in terms of the mass ( $m$ ) and specific heat capacity ( $c$ ) of material in the node and the conductive heat-transfer resistances  $R_1$  and  $R_2$  (assuming that each node has an internal heat generation rate or a heat input,  $Q_i$ ):

$$mc \frac{dT_i}{dt} = \frac{1}{R_1} (T_{i-1} - T_i) - \frac{1}{R_2} (T_i - T_{i+1}) + Q_i \quad (5.4)$$

$$\frac{dT_i}{dt} = a_{i,i-1} T_{i-1} - a_{i,i} T_i + a_{i,i+1} T_{i+1} + b Q_i \quad (5.5)$$

where:

$T_i$  = temperature at node  $i$

$m$  = mass of material in node  $i$

$c$  = specific heat capacity of material in node  $i$

$R_i$  = conductive heat transfer resistance at node  $i$

and:

$$\begin{aligned} a_{i,i-1} &= \frac{1}{mcR_1} \\ a_{i,i} &= \frac{1}{mc} \left( \frac{1}{R_1} + \frac{1}{R_2} \right) \\ a_{i,i+1} &= \frac{1}{mcR_2} \\ b &= \frac{1}{mc} \end{aligned} \quad (5.6)$$

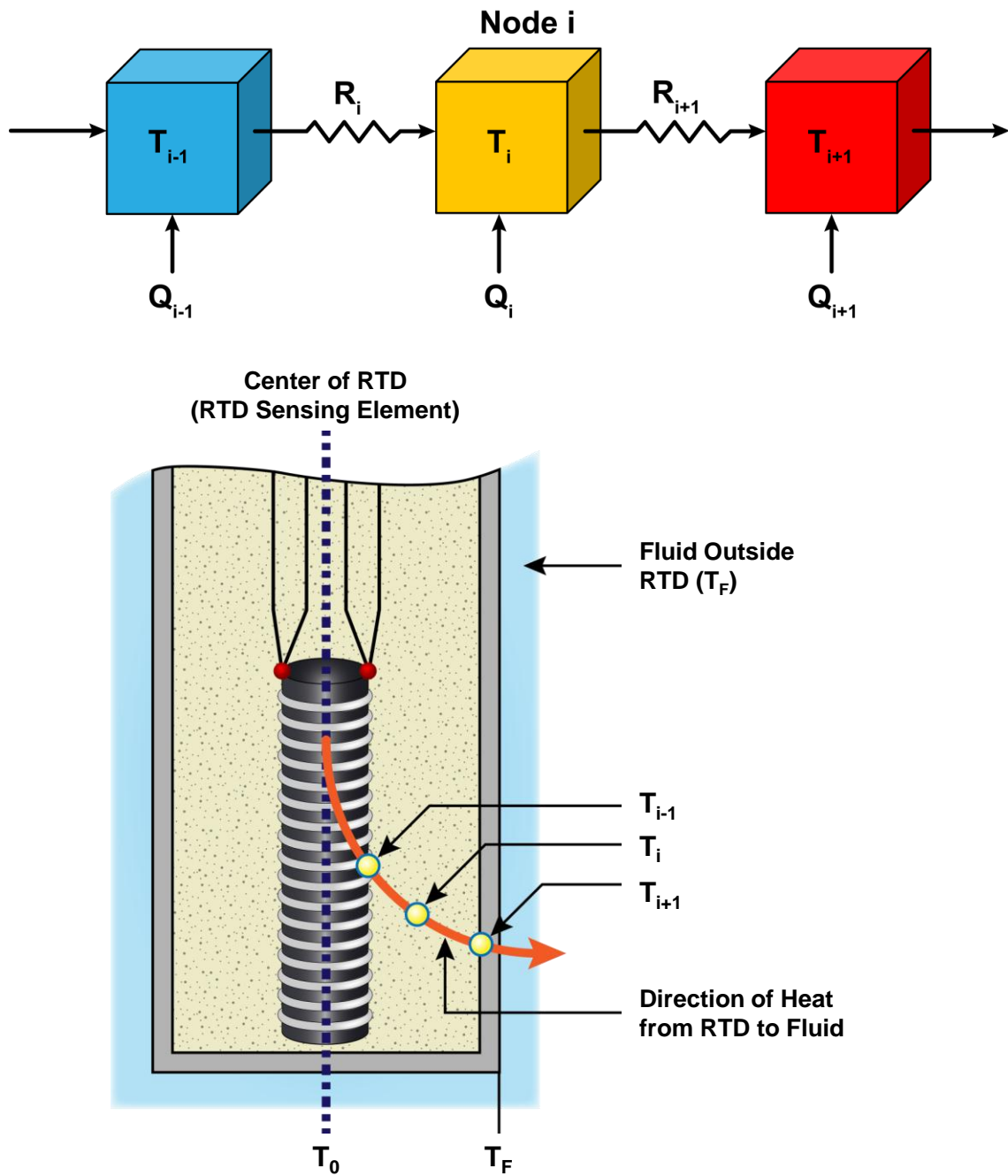


Figure 5-7 Lump Variable Representations for LCSR Analysis

The nodal equations can be applied to a series of nodes, starting with the node that is closest to the center ( $i = 1$ ) and ending with the node closest to the surface ( $i = n$ ):

$$\begin{aligned}
 \frac{dT_1}{dt} &= -a_{11}T_1 + a_{12}T_2 + bQ_1 \\
 \frac{dT_2}{dt} &= a_{21}T_1 - a_{22}T_2 + a_{23}T_3 + bQ_2 \\
 \frac{dT_3}{dt} &= a_{32}T_2 - a_{33}T_3 + a_{34}T_4 + bQ_3 \\
 &\cdot \\
 &\cdot \\
 &\cdot \\
 \frac{dT_n}{dt} &= a_{n,n-1}T_{n-1} - a_{n,n}T_n + a_{nF}T_F
 \end{aligned} \tag{5.7}$$

where:

$T_i$  = temperature of the  $i$ th node (measured relative to the initial fluid temperature)

$T_F$  = fluid temperature from its initial value

These equations can be written in matrix state-space equations as follows:

$$\frac{d\underline{x}}{dt} = A\underline{x} + \underline{c}T_F + b\underline{Q} \tag{5.8}$$

where:

$$\underline{x} = \begin{bmatrix} T_1 \\ T_2 \\ T_3 \\ \cdot \\ \cdot \\ T_n \end{bmatrix}; A = \begin{bmatrix} -a_{11} & a_{12} & 0 & 0 & 0 & 0 \\ a_{21} & -a_{22} & a_{23} & 0 & 0 & 0 \\ 0 & a_{32} & -a_{33} & a_{34} & 0 & 0 \\ 0 & \cdot & \cdot & \cdot & \cdot & \cdot \\ 0 & \cdot & \cdot & \cdot & \cdot & \cdot \\ 0 & \cdot & \cdot & \cdot & a_{n,n-1} & -a_{n,n} \end{bmatrix}; \underline{c} = \begin{bmatrix} 0 \\ 0 \\ 0 \\ \cdot \\ \cdot \\ a_{nF} \end{bmatrix}; \underline{Q} = \begin{bmatrix} Q_1 \\ Q_2 \\ Q_3 \\ \cdot \\ \cdot \\ Q_n \end{bmatrix} \tag{5.9}$$

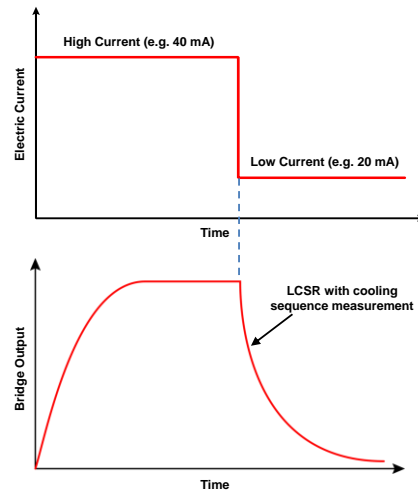
(Note: Here, we are switching from  $T$  to  $x$  as the variable of interest to comply with the convention in treating this issue). A Laplace transformation of Equation 5.8 yields:

$$[sI - A]\underline{x}(s) = \underline{x}(0) + \underline{c}T_F(s) + b\underline{Q}(s) \quad (5.10)$$

We will now proceed to solve Equation 5.10 for three different cases; two for LCSR test and one for plunge test. The LCSR test is normally performed by monitoring the output of the Wheatstone bridge while the RTD is heating up (see Section 5.1). It can also be performed by monitoring the bridge output after the current is stopped and while the RTD is cooling down. The latter corresponds to Case 1 below and the former corresponds to Case 2. The LCSR equations corresponding to these two cases are derived below followed by the derivation of the equation for the plunge test (Case 3).

### **Case 1: LCSR Cooling Transient**

This is the case where the LCSR test is performed by heating the sensor with an electric current and monitoring its output after the current is cut off and while the RTD is cooling down to the temperature of the surrounding fluid. (Note: This case corresponds to the way that thermocouples are LCSR tested; nevertheless, it is included here for completeness and also because it is the simplest case with which to begin the derivations.)



### LCSR Analysis Based on Cooling Curve

In this case,  $T_F$  is not a perturbation, but a constant. Assuming that all  $Q_i(s)$  values are zero; Equation 5.10 becomes:

$$(sI - A)\underline{x}(s) = \underline{c} \begin{bmatrix} T_1(0) \\ T_2(0) \\ \cdot \\ \cdot \\ T_n(0) + a_{nF}T_F(0) \end{bmatrix} \begin{array}{l} \text{Initial Condition Response} \\ \\ \\ \\ \leftarrow \text{This can be assumed to be zero} \end{array} \quad (5.11)$$

Cramer's Rule, in the form of Equation 5.12 below, can be used to solve for  $T_i(s)$ :

$$T_1(s) = \frac{|B(s)|}{|sI - A|} \quad (5.12)$$

where:

$$B(s) = \begin{bmatrix} T_1(0) & -a_{12} & 0 & \cdot & \cdot & 0 \\ T_2(0) & (s+a_{22}) & -a_{23} & \cdot & \cdot & 0 \\ \cdot & -a_{32} & (s+a_{33}) & -a_{34} & \cdot & \cdot \\ \cdot & \cdot & \cdot & \cdot & \cdot & \cdot \\ \cdot & \cdot & \cdot & \cdot & \cdot & \cdot \\ T_n(0) + a_{nF}T_F(0) & 0 & 0 & 0 & -a_{n,n-1} & (s+a_{nn}) \end{bmatrix} \quad (5.13)$$

Equation 5.12 is a ratio of the determinates of  $B$  and  $(sI-A)$ . Performing these determinates will yield a ratio of following general form:

$$T_1 = \frac{C_{1,1}s^{n-1} + C_{1,2}s^{n-2} + \dots + C_{1,n-1}s + C_{1,n}}{C_{2,1}s^n + C_{2,2}s^{n-1} + \dots + C_{2,n}s + C_{2,n+1}}$$

An inspection of the above equation shows that  $T_1$  may be written as the ratio of a polynomial of order  $n-1$  to a polynomial of order  $n$  multiplied by a constant  $K$ . The numerator is a direct result of the determinate of  $B$  just as the denominator is a direct result of the determinate of  $(sI-A)$ . Algebraically, these two polynomials can be factored into a more familiar form as follows:

$$T_1(s) = K \frac{(s-z_1)(s-z_2)\dots(s-z_{n-1})}{(s-p_1)(s-p_2)\dots(s-p_n)} \quad (5.14)$$

where

$K$  = constant (gain)

$z_i$  = zero; a number which causes  $T_1(s)$  to equal zero

$p_i$  = pole; a number which causes  $T_1(s)$  to equal infinity

Now, the inverse Laplace transform of Equation 5.14 yields:

$$T_1(t) [\text{LCSR cooling transient}] = A_1 e^{p_1 t} + A_2 e^{p_2 t} + \dots + A_n e^{p_n t} \quad (5.15)$$



where:

$$A_1 = \frac{(p_1 - z_1)(p_1 - z_2) \cdots (p_1 - z_{n-1})}{(p_1 - p_2)(p_1 - p_3) \cdots (p_1 - p_n)}$$

$$A_2 = \frac{(p_2 - z_1)(p_2 - z_2) \cdots (p_2 - z_{n-1})}{(p_2 - p_1)(p_2 - p_3) \cdots (p_2 - p_n)}$$

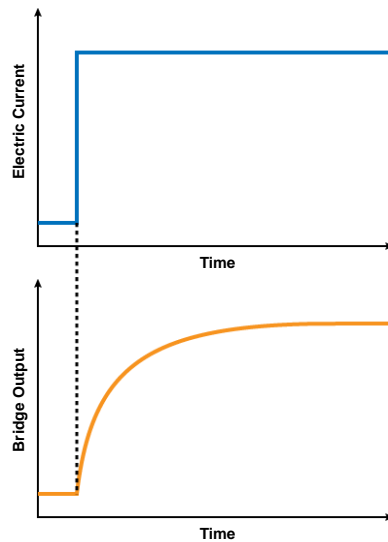
⋮  
⋮  
⋮  
⋮

$$A_n = \frac{(p_n - z_1)(p_n - z_2) \cdots (p_n - z_{n-1})}{(p_n - p_1)(p_n - p_2) \cdots (p_n - p_{n-1})}$$

$$p_i = -\frac{1}{\tau_i}; \tau_i \text{ is the modal time constant in second}$$

### **Case 2: LCSR Heating Transient**

In this case, the LCSR data results from monitoring the Wheatstone bridge output while the LCSR heating current is running through the RTD. That is, the LCSR data correspond to heating in node 1 (i.e., the term  $Q_1(s)$  is the step input), and all other elements in  $\underline{Q}$  are zero. Furthermore, all initial conditions are zero with the test starting at equilibrium conditions and changes in temperature are with respect to this initial state ( $T(t=0)$ ). With these points in mind, Equation 5.10 becomes:



**LCSR Analysis Based on Heating Curve**

$$(sI - A)\underline{x}(s) = b\underline{Q}(s) \quad (5.16)$$

where

$$Q = \begin{bmatrix} Q_1 \\ 0 \\ 0 \\ \cdot \\ \cdot \\ \cdot \\ 0 \end{bmatrix}$$

Again, Cramer's Rule given below can be used to solve for  $T_1(s)$ :

$$T_1(s) = \frac{|B(s)|}{|(sI - A)|} \quad (5.17)$$

where:

$$B(s) = \begin{bmatrix} Q_1(s) & -a_{12} & 0 & \cdot & \cdot & 0 \\ 0 & (s + a_{22}) & -a_{23} & \cdot & \cdot & 0 \\ 0 & -a_{32} & (s + a_{33}) & -a_{34} & \cdot & \cdot \\ \cdot & \cdot & \cdot & \cdot & \cdot & \cdot \\ \cdot & \cdot & \cdot & \cdot & \cdot & \cdot \\ 0 & 0 & 0 & 0 & -a_{n,n-1} & (s + a_m) \end{bmatrix} \quad (5.18)$$

Evaluating the determinants  $|B(s)|$  and  $|sI - A|$  in Equation 5.17 yields the following solution for this case:

$$T_1(s) = Q_1(s) K \frac{(s - z_1)(s - z_2) \cdots (s - z_n)}{(s - p_1)(s - p_2) \cdots (s - p_n)} \quad (5.19)$$

The internal heating term  $Q_1(t)$  is a step input for the LCSR test. The inverse Laplace transform of Equation 5.19 provides the solution as follows:

$$T_1(t) = [\text{LCSR Heating Transient}] = A_0 + A_1 e^{p_1 t} + A_2 e^{p_2 t} + \dots + A_n e^{p_n t} \quad (5.20)$$

where:

$$A_0 = \frac{(-z_1)(-z_2)\cdots(-z_{n-1})}{(-p_1)(-p_2)\cdots(-p_n)}$$

$$A_1 = \frac{(p_1 - z_1)(p_1 - z_2)\cdots(p_1 - z_{n-1})}{(p_1 - p_2)(p_1 - p_3)\cdots(p_1 - p_n)}$$

$$A_2 = \frac{(p_2 - z_1)(p_2 - z_2)\cdots(p_2 - z_{n-1})}{(p_2 - p_1)(p_2 - p_3)\cdots(p_2 - p_n)}$$

$$\vdots$$

$$\vdots$$

$$\vdots$$

$$\vdots$$

$$A_n = \frac{(p_n - z_1)(p_n - z_2)\cdots(p_n - z_{n-1})}{(p_n - p_1)(p_n - p_2)\cdots(p_n - p_{n-1})}$$

$$p_i = -\frac{1}{\tau_i}; \tau_i \text{ is the modal time constant in second}$$

### **Case 3: Plunge Test**

In this case, again all the initial conditions are zero, and the perturbation is a step change in the fluid temperature  $T_F(t)$ . Also, all the  $Q_i(t)$  terms are zero. Therefore, Equation 5.10 becomes:

$$(sI - A)\underline{x}(s) = \underline{c}T_F(s) = \begin{bmatrix} 0 \\ 0 \\ \vdots \\ \vdots \\ \vdots \\ \vdots \\ a_{nF} \end{bmatrix} T_F(s) \quad (5.21)$$

and Cramer's Rule remains in the form:

$$T_1(s) = \frac{|B(s)|}{|(sI - A)|}$$

where:

$$B(s) = \begin{bmatrix} 0 & -a_{12} & 0 & \cdot & \cdot & 0 \\ 0 & (s + a_{22}) & -a_{23} & \cdot & \cdot & 0 \\ 0 & -a_{32} & (s + a_{33}) & -a_{34} & \cdot & \cdot \\ \cdot & \cdot & \cdot & \cdot & \cdot & \cdot \\ \cdot & \cdot & \cdot & \cdot & \cdot & \cdot \\ a_{nF}T_F(s) & 0 & 0 & 0 & -a_{n,n-1} & (s + a_{nn}) \end{bmatrix} \quad (5.22)$$

The resulting  $T_1(s)$  has the form:

$$T_1(s) = \frac{K T_F(s)}{(s - p_1)(s - p_2) \cdots (s - p_n)} \quad (5.23)$$

Where all the poles in the denominator are the same as in the LCSR test Equation (5.20). Solving Equation 5.23 by inverse Laplace transformation; we obtain:

$$T_1(t)[plunge\ test] = B_0 + B_1 e^{p_1 t} + B_2 e^{p_2 t} + \cdots + B_n e^{p_n t} \quad (5.24)$$

where:

$$\begin{aligned} B_0 &= \frac{1}{(-p_1)(-p_2) \cdots (-p_n)} \\ B_1 &= \frac{1}{p_1(p_1 - p_2)(p_1 - p_3) \cdots (p_1 - p_n)} \\ B_2 &= \frac{1}{p_2(p_2 - p_1)(p_2 - p_3) \cdots (p_2 - p_n)} \\ &\cdot \\ &\cdot \\ &\cdot \\ &\cdot \end{aligned}$$

$$B_n = \frac{1}{p_n(p_n - p_1)(p_n - p_3) \cdots (p_n - p_{n-1})}$$

$$p_i = -\frac{1}{\tau_i}; \tau_i \text{ is the modal time constant in second}$$

Note that the LCSR heating equation (5.20) corresponds exactly with the plunge test equation (5.24) except for the coefficients. That is, the coefficients in the plunge test Equation (5.24) are functions of poles and not zeros. That is, if we identify the poles by fitting the LCSR data to Equation 5.20, we can then generate the plunge test transient using Equation 5.24 from which the sensor response time can in turn be identified.

### 5.3 LCSR Test Procedure

From the derivations in section 5.2 above, we can draw the following conclusions:

1. The exponential terms ( $p_1, p_2, \dots, p_n$ ) in Equation 5.24 for the plunge test are the same as those of the LCSR Equation (5.20). This is expected since the exponents depend only on the heat-transfer resistances and the heat capacities between the fluid surrounding the sensor and the centerline of the sensor. These heat transfer resistances and heat capacities are the same in the LCSR and plunge tests.
2. The coefficients ( $B_0, B_1, B_2, \dots, B_n$ ) in Equation 5.24 are determined by the values of only the poles (i.e., the zeros are not needed to construct the plunge test transient). Therefore, a knowledge of the poles alone is sufficient to determine the coefficients of Equation 5.24 and use them to arrive at the plunge test transient from which the RTD response time can be deduced.

We then employ these conclusions to establish the five-part LCSR test procedure as follows and arrive at the RTD response time. In particular, the following five steps are used to convert the LCSR transient into an equivalent plunge test transient, from which the RTD response time is obtained:

1. Disconnect the RTD from its plant instrumentation and connect it to the LCSR test equipment (the Wheatstone bridge). This step must be performed using a formal plant procedure by qualified plant personnel. All RTD leads must be disconnected from the plant instrumentation, and two of the leads from the two sides of the sensing element must be connected to the Wheatstone bridge. Of course, the RTD channel has to be removed from service or placed in “test” for the duration of the LCSR measurement.

The LCSR test can be performed in either the hot standby conditions or during normal power operation as long as the process is at normal operating temperature, pressure, and flow. The number of RTDs that can be tested at any one time depends on the number of channels in the LCSR test equipment. Usually up to four RTDs can be tested at a time (typically, plant instrumentation cabinets in nuclear power plants contain only four RTDs in each cabinet).

2. Execute the LCSR test by switching the bridge current from “low” to “high,” and then sample the data using a digital data acquisition system. For typical RTDs, the data is sampled at a rate of 50 to 500 samples per seconds for 5 to 50 seconds, depending on the expected response time of the RTD. If it is anticipated that the RTD has a fast response time ( $< 1$  second), then 5 to 10 seconds of data and 500 samples per second is adequate. If, on the other hand, the RTD is slow (e.g., 4 to 8 seconds), then 40 to 80 seconds of data sampled at a rate of 50 samples per second is often necessary.
3. Fit the LCSR data to Equation 5.20 and estimate the poles ( $p_i$ 's). A least-square fitting procedure may be used in this step.
4. Substitute the  $p_i$ 's (estimated in Step 3) in Equation 5.24 to produce the plunge test transient.
5. Use the plunge test transient to obtain the RTD response time.

The execution of this five-part procedure will convert the LCSR data to equivalent plunge test data, as shown in Figure 5-8. Instead of steps 4 and 5, to arrive at the RTD's response time we can use the following equation from Chapter 2 (and Appendix B):

$$\tau = \tau_1 \left[ 1 - \text{Ln} \left( 1 - \frac{\tau_2}{\tau_1} \right) - \text{Ln} \left( 1 - \frac{\tau_3}{\tau_1} \right) - \dots \right] \quad (5.25)$$

where:

$\tau$  = Overall response time of the RTD

$\tau_1, \tau_2, \dots$  = modal time constants

$\text{Ln}$  = natural logarithm operator

Although more than two modal time constants are shown in Equation 5.25, it is often difficult to resolve more than two modal time constants ( $\tau_1$  and  $\tau_2$ ) from the LCSR

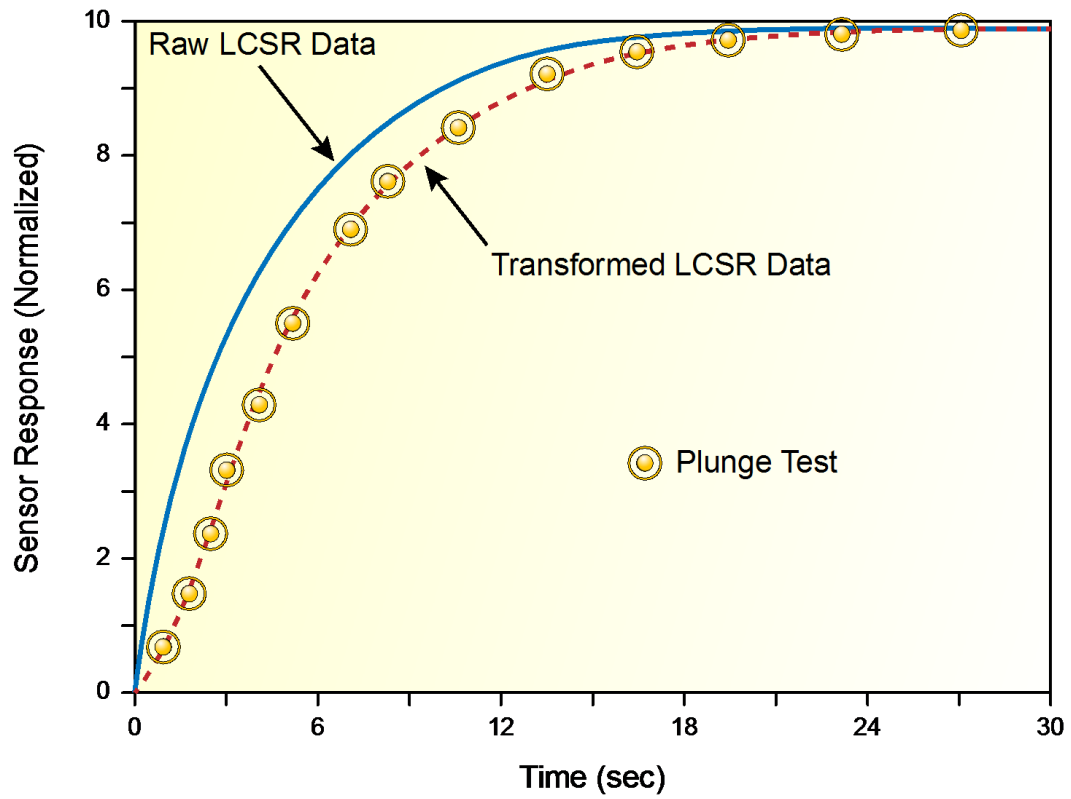


**Figure 5-8 Conversion of LCSR Data to Equivalent Plunge Test Data**

data. This was recognized in the 1980s when the LCSR transformation was first developed at the University of Tennessee.<sup>[36]</sup> As a result, Equation 5.25 was abbreviated to become:

$$\tau = \tau_1 \left[ 1 - \text{Ln} \left( 1 - \frac{\tau_2}{\tau_1} \right) \right] \quad (5.26)$$

To account for the effect of higher modes, Poore<sup>[37]</sup> developed a correction factor (CF) that uses the ratio of the first two modal time constants,  $\tau_2 / \tau_1$ , to account for the effect of the higher modes ( $\tau_3, \tau_4, \dots$ ) omitted in using Equation 5.26. The correction factor is shown graphically in Figure 5-9 and is given by the following formula:

$$CF = 1.0043 + 0.05578 \left( \frac{\tau_2}{\tau_1} \right) + 19.59 \left( \frac{\tau_2}{\tau_1} \right)^2 - 238.38 \left( \frac{\tau_2}{\tau_1} \right)^3 + 1352.2 \left( \frac{\tau_2}{\tau_1} \right)^4 - 2622.9 \left( \frac{\tau_2}{\tau_1} \right)^5 \quad (5.27)$$

Using this CF (Equation 5.27), an RTD response time can be determined from the LCSR test using the following formula:

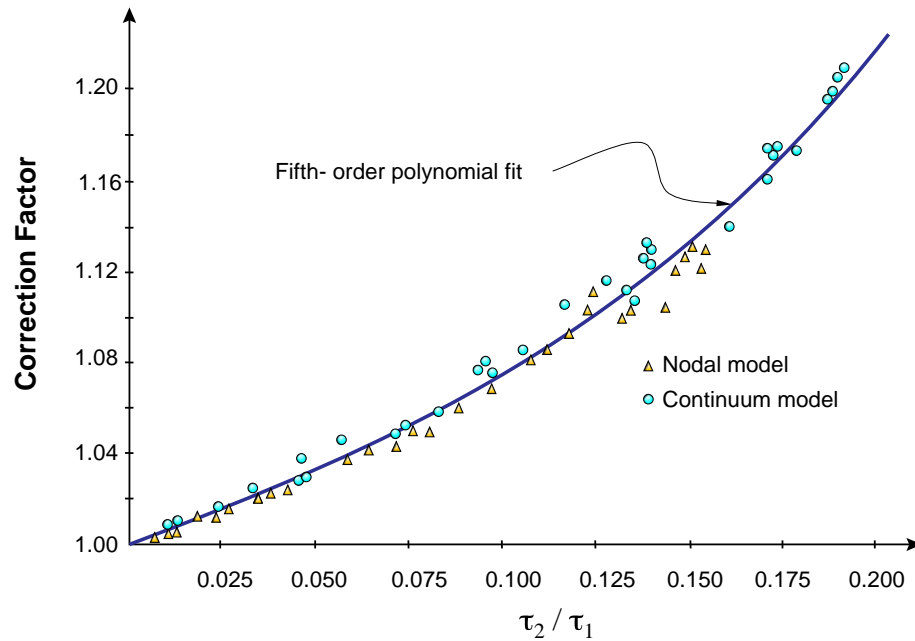
$$\tau = \tau_1 \left[ 1 - \text{Ln} \left( 1 - \frac{\tau_2}{\tau_1} \right) \right] \cdot CF \quad (5.28)$$

Figure 5-10 illustrates the steps involved in executing the LCSR test, including the application of the correction factor, to arrive at the final response time. This procedure has been implemented in nuclear power plants and provides the results that are shown in Chapter 6.

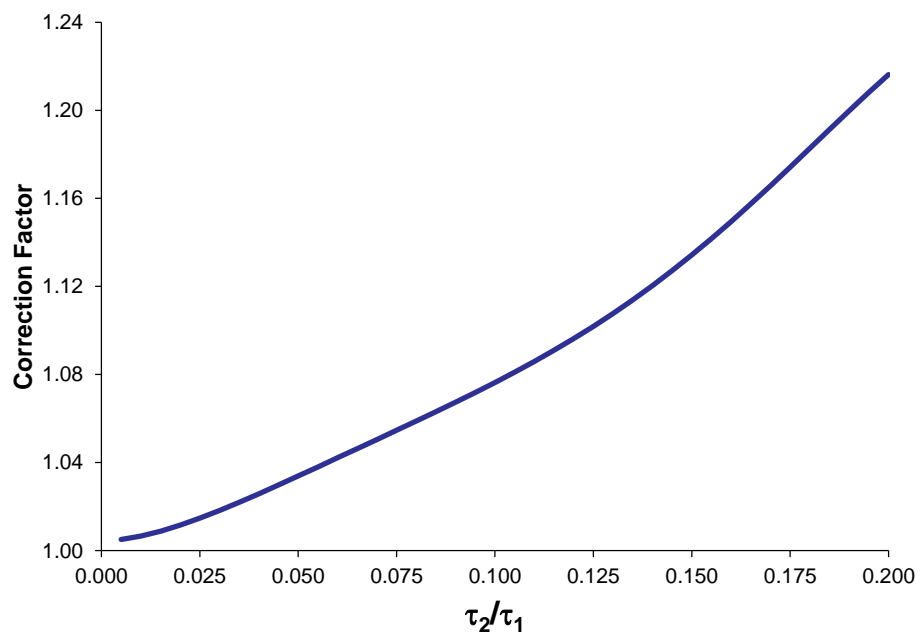
#### 5.4 Noise Analysis Technique

Like the LCSR technique, the author advanced, refined, and implemented the noise analysis technique to develop a robust and reliable method that improves upon a traditional response-time testing method for nuclear plant pressure transmitters. The





(a) Correction Factor Data From Two Analytical Models of RTDs (Courtesy: W.P. Poore, M.S. Thesis – University of Tennessee 1980)



(b) Plot of Correction Factor Equation

**Figure 5-9 LCSR Correction Factor**

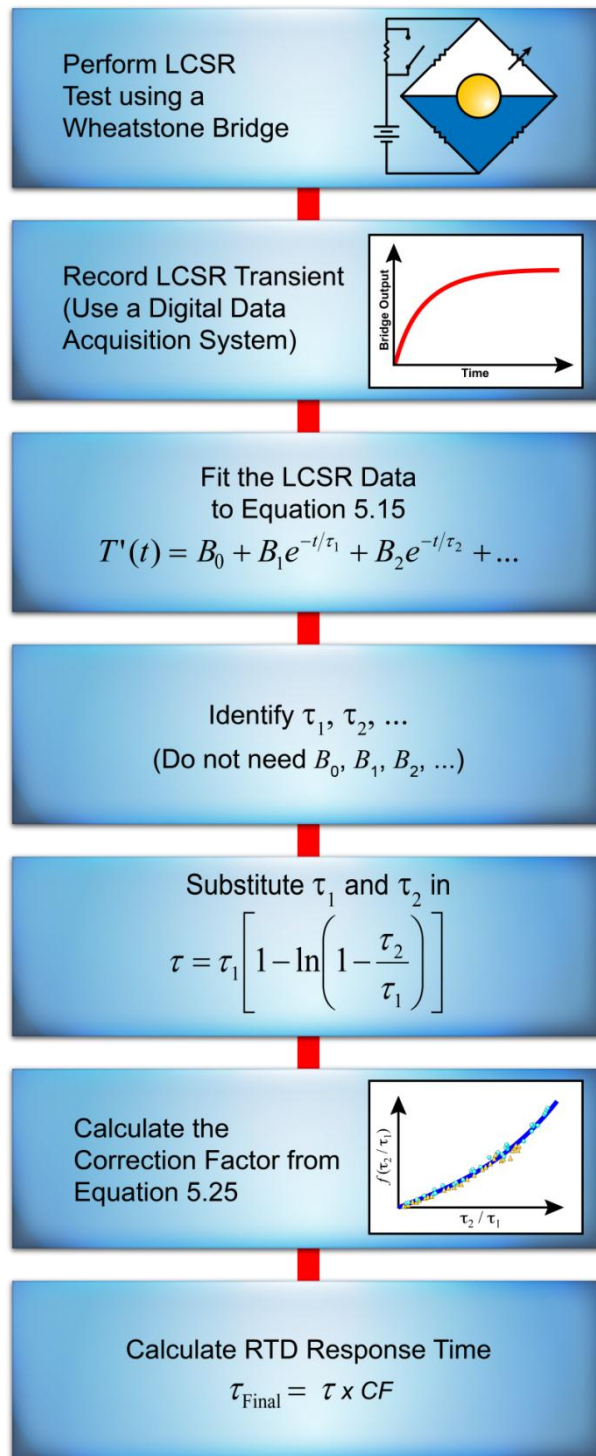


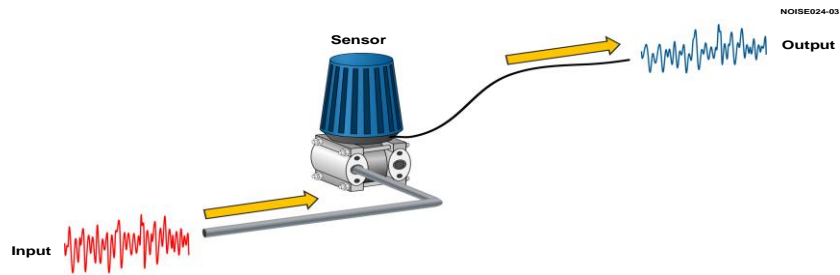
**Figure 5-10 LCSR Test and Analysis Procedure**

noise analysis technique, the second core technique focused on in this research, is a passive method for testing the response time of pressure sensors and associated sensing lines in situ. It is based on monitoring the natural process fluctuations that are superimposed on the output of a sensor while the process is operating. These fluctuations arise randomly in nuclear power plants as a result of random flux, random heat transfer, turbulent flow, vibration, process control action, and so on. In principle, the response time of any sensor can be measured using the noise analysis technique as long as the sensor is linear and is installed in a process that generates: (1) suitable fluctuations with respect to amplitude and bandwidth, and (2) proper statistical characteristics. However, when a more exact method such as the LCSR test is available, the noise analysis technique may still be used as a supplement or as a second option. As will be seen in Chapters 6 and 8, the author has validated the noise analysis technique not only for pressure transmitters, but also for RTDs, although the noise analysis technique has been developed primarily for pressure transmitters.

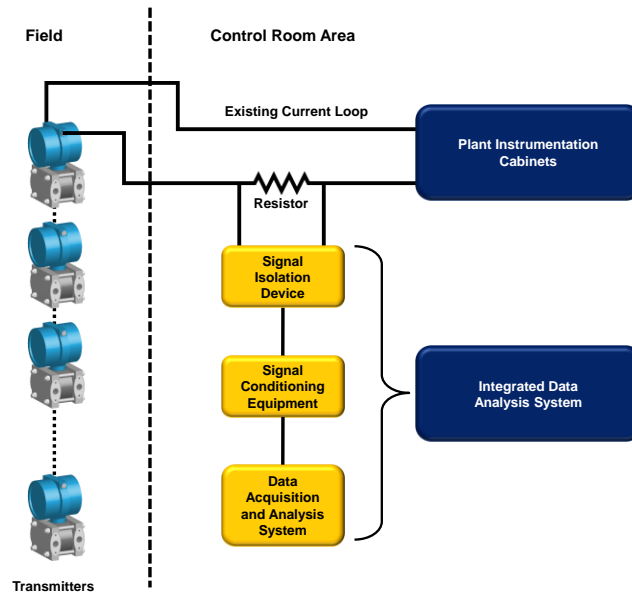
#### **5.4.1 Noise Data Acquisition**

In performing response time measurements using the noise analysis technique, the normal output of pressure transmitters of interest are recorded using a fast data acquisition system (e.g., at a sampling rate of 1kHz). The DC component of the output is subtracted out by signal conditioning hardware or by software. The remaining signal is amplified, filtered, digitized, and analyzed to yield the response time of the transmitter. Figure 5-11 illustrates the principle of the noise analysis test in terms of the following three displays: (a) shows how process noise enters and exits the sensor, (b) shows how the data is recorded from a plant in the current loop between the transmitter in the field and its power supply or instrumentation circuits in the control room, and (c) shows a 5-second record of noise data from a nuclear power plant pressure transmitter. Normally, one hour of such noise data is recorded and analyzed to obtain the response time of a transmitter.

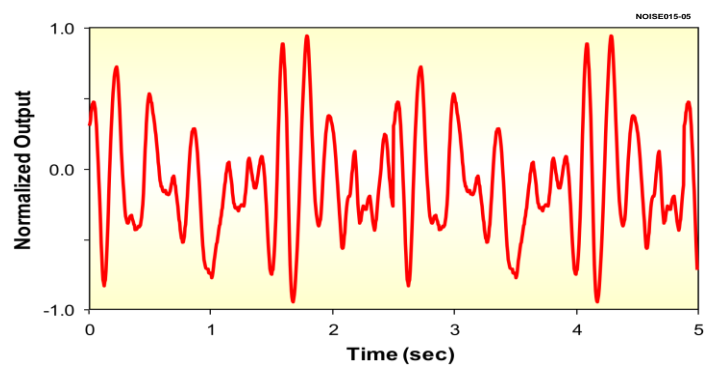
Although Figure 5-11 shows only one transmitter under test, multiple transmitters can be tested simultaneously if a multichannel data acquisition system with isolation



(a)



(b)



(c)

**Figure 5-11 Principle of Noise Analysis Technique (a, b) and Actual Noise Record from a Nuclear Plant Pressure Transmitter (c)**

modules is deployed. The isolation modules play a critical role in accessing live signals from an operating nuclear power plant. The modules must have a high input impedance ( $>1\text{M}\Omega$ ) and must continue to provide isolation even when AC power to the isolator is lost.

### **5.4.2 Test Assumptions**

The five assumptions listed below must be satisfied in order for the noise analysis technique to provide valid response-time results:

1. The process fluctuations must be wideband, meaning that their spectrum is nearly flat or at least they have a larger bandwidth than that of the sensor under test.
2. The sensor must be predominantly linear. This assumption is normally met because pressure transmitters are designed to be as linear as possible.
3. The process fluctuations that drive the sensor must have sufficient strength (in amplitude or RMS value) to excite the sensor so it exhibits a measurable fluctuating output.
4. The process noise and the resulting sensor output should have a Gaussian (Normal) distribution. (Note: Gaussian or Normal distribution is not mandatory for the success of noise analysis technique but desirable.)
5. No significant resonances can be present in the process that might draw the sensor output beyond its frequency response.

If these assumptions are met, then the noise analysis technique can provide results comparable to those of the conventional ramp test method. If they cannot, then the noise analysis technique may not produce accurate response time results, although it may still be useful for qualitatively evaluating sensor performance, identifying gross changes in response time, or separating process effects from sensor issues.

### **5.4.3 Data Processing for Response Time Measurements**

The results of the noise analysis test are typically provided in terms of spectrum of the noise data, which is essentially the variance (mean squared value) of the data in a narrow frequency band as a function of frequency plotted versus frequency on a semi-log or log-log graph. This graph is referred to as the power spectral density (PSD) plot and is typically obtained by a fast Fourier transform (FFT) of the noise signal. There

are in fact commercial FFT analyzers that can sample the noise data, process them, and plot the PSD graph automatically. Figure 5-12 shows four redundant transmitters in a nuclear power plant connected to an FFT analyzer that processes the noise data and produces PSDs. These PSDs are then used to arrive at the transmitter response time. If the transmitter can be approximated as a first-order system, then the roll-off frequency of the PSD will provide the sensor response time directly through the formula  $\tau = 1/2\pi F$ , where  $\tau$  is the response time and  $F$  is the roll-off frequency of the PSD in Hz. If the transmitter cannot be assumed to be a first-order system, then the PSD must be fit to a mathematical model for the transmitter dynamics to yield its response time. Typically, a linear second-order and underdamped model is used for this purpose to account for the dynamics of a transmitter and its sensing line combined. Figure 5-13 shows how response time is obtained from the PSD of a first-order system (5-13a) and also when the measurement is made by fitting a mathematical model to the PSD from which the model parameters are extracted and used to arrive at the response time (5-13b).

#### **5.4.4 Effect of Process Bandwidth on Noise Analysis Results**

Figure 5-14 shows potential shapes of frequency spectrum for an input noise signal, the sensor, and the sensor output, illustrating the impact of various bandwidths on the relative accuracy of the response time results obtained from the noise analysis method. The purpose of this illustration is to show that the noise analysis technique can produce accurate results when the process noise input to the sensor is “white” (has a flat spectrum) or when the process noise has a bandwidth that is sufficiently larger than that of the transmitter under test (e.g., larger by about a decade). If the spectrum of the input noise signal is not flat or not sufficiently wideband, the noise analysis results will correspond to the dynamics of the process rather than sensor. In this case, the noise analysis technique will not provide the exact response time of a sensor, but it can provide assurance that a sensor has not degraded beyond a limit. That limit is set by the bandwidth of the process noise. If the process noise is not broadband (i.e., its bandwidth is smaller than that of the sensor), then the response time obtained from the noise analysis technique will be larger than the response time of the sensor but often lower than the plant requirement for response time. This uncertainty is not ideal, but it

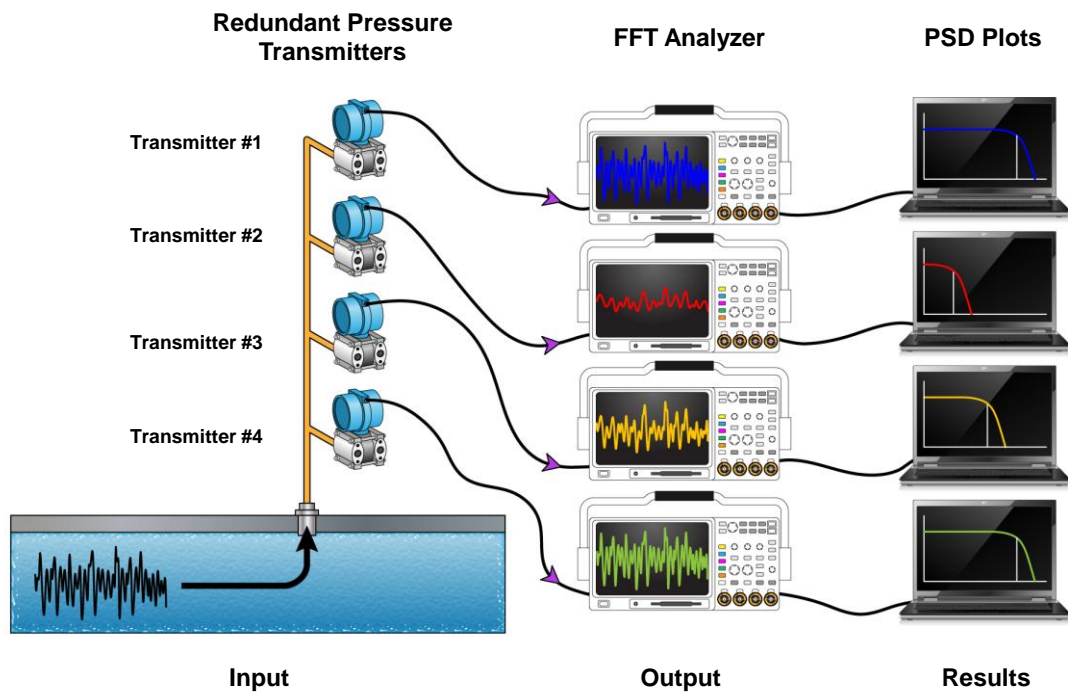
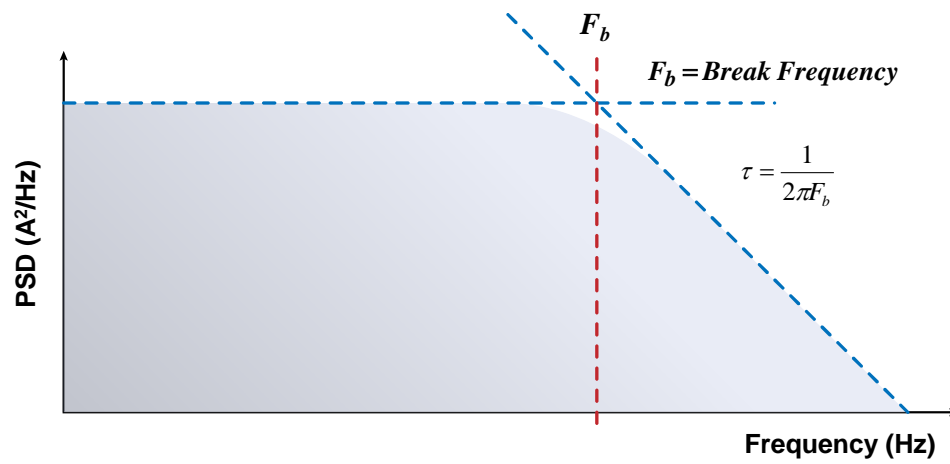
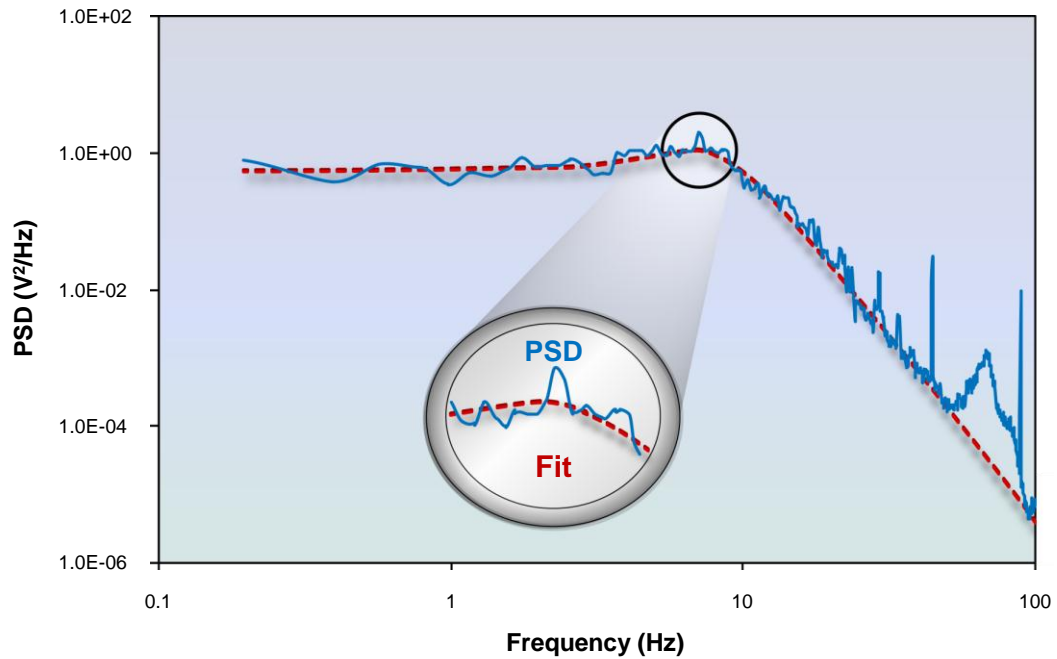


**Figure 5-12 Response of Four Different Pressure Transmitters to the Same Input**



(a) Response Time Calculation From Break Frequency  
(Note: Break Frequency is Also Called Corner Frequency)



(b) Response Time Calculation From Fit to PSD

**Figure 5-13 Pressure Transmitter PSD and Determination of Response Time**



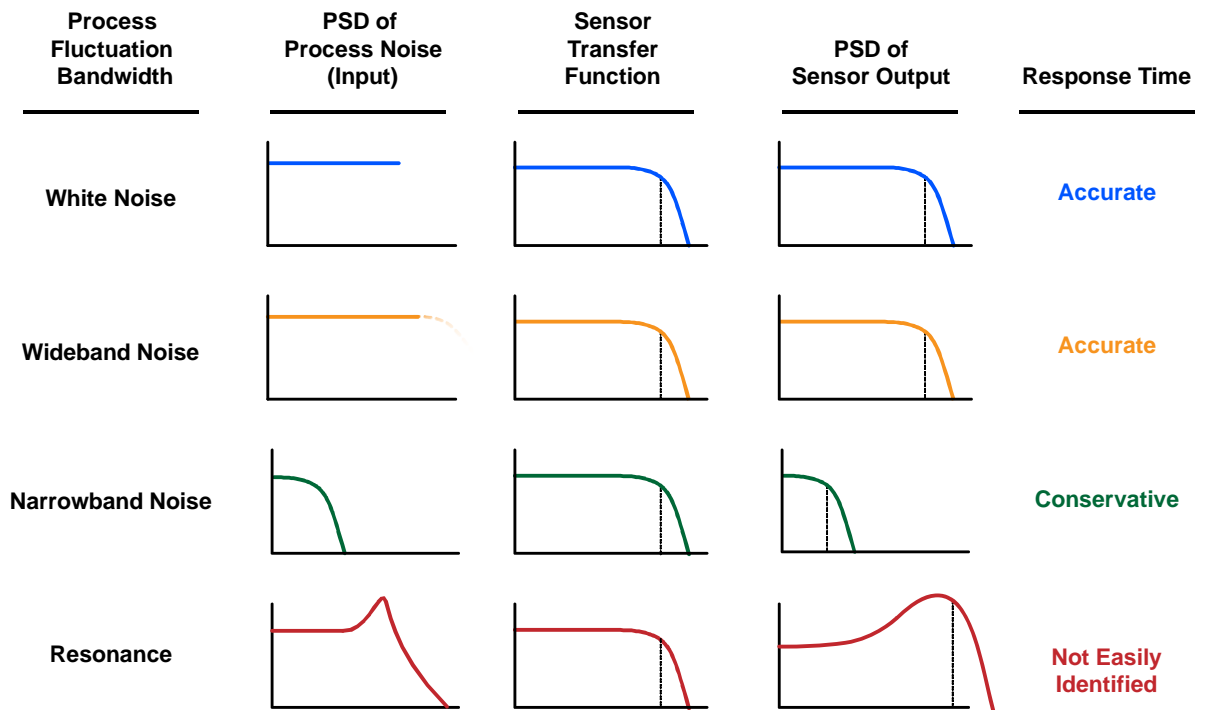


**Figure 5-14 Potential Results of Noise Analysis in Relation to the Bandwidth of the Input Noise**

is reasonable. A practical axiom in the nuclear industry is that “if a method cannot produce exact results, it is still acceptable if it can be shown that it produces conservative results.” “Conservative” here means that the estimated response time is larger than the actual value. As long as the measured response time is faster than the plant requirement, it does not matter that the measured response time is slower than the actual response time. Since pressure transmitters are normally fast (i.e., their response time is less than 1 second) and response time requirements for pressure transmitters in nuclear power plants are not very tight (i.e., response time requirements are greater than 1 second), sufficient margin is often available for conservative results.

As shown in the last column of Figure 5-14, if there is a significant resonance in the process that affects the spectrum of the output in the region where the response time results is to be resolved, then the noise analysis technique may produce results which may not easily yield the response time of the transmitter.

#### 5.4.5 Theory of Noise Analysis Technique

Figure 5-15 illustrates a transmitter that exhibits a time-varying output,  $\delta Y$ , for a time-varying input,  $\delta X$ . These are related to one another through a transfer function ( $G$ ) as follows (assuming that the dynamics of the transmitter is linear and time invariant):

$$G = \frac{\delta y(s)}{\delta x(s)} \quad \text{or} \quad \delta y = G\delta x \quad (5.29)$$

Equation 5.29 can also be expressed in terms of the PSDs of the input and output signals:

$$(PSD)_y = |G|^2 (PSD)_x \quad (5.30)$$

If the noise from the process pressure fluctuation is stationary and broadband, it can be approximated by a *white noise signal* whose PSD is constant. That is:

$$(PSD)_y = (\text{Constant})|G|^2 \quad (5.31)$$

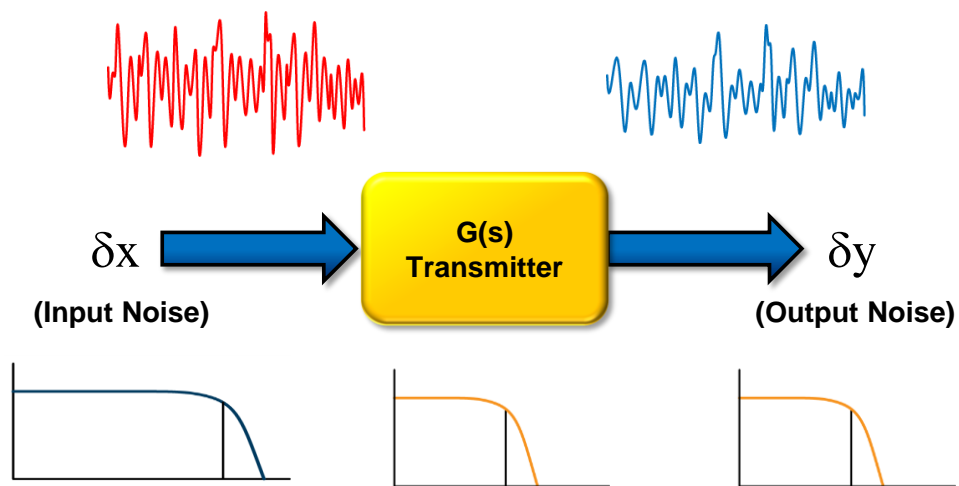
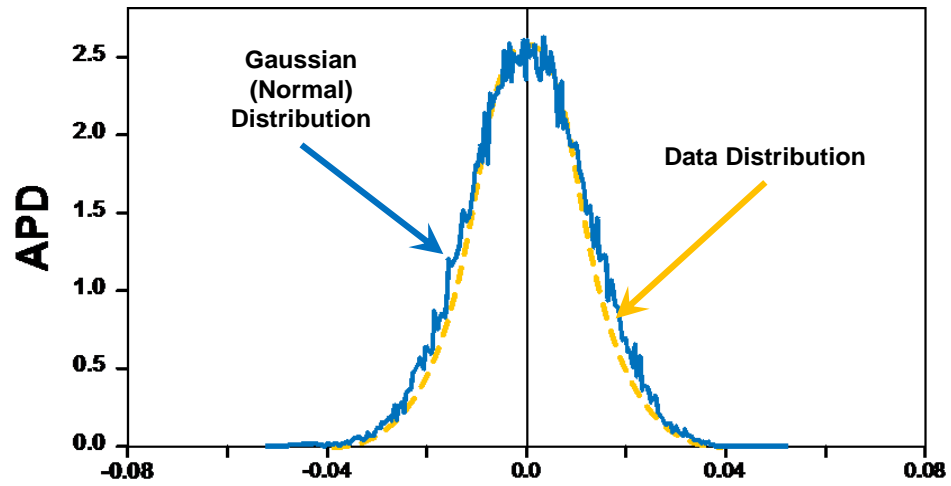


**Figure 5-15** Input and Output Noise through a Sensor

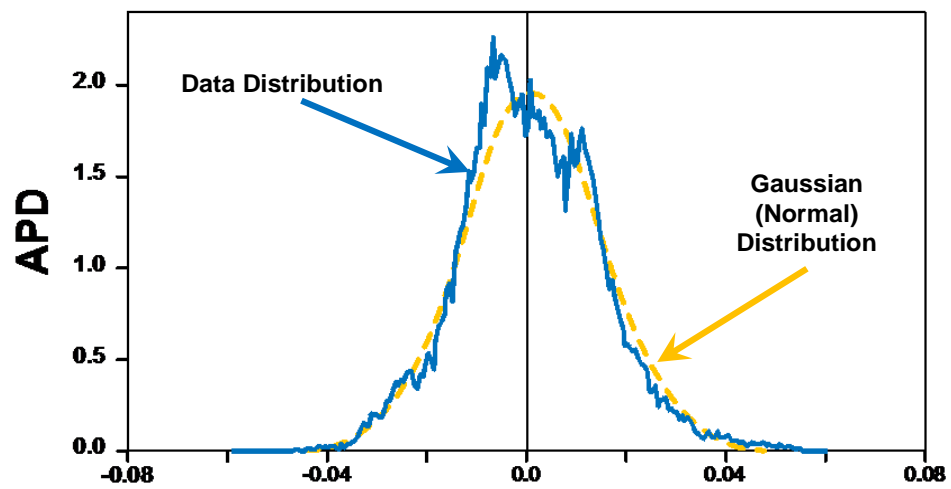
Equation 5.31 shows that the PSD of the transmitter's output fluctuations is proportional to the sensor's transfer function. From this, the sensor's response time can be obtained using the following five-step procedure:

1. Acquire the noise data remotely from the output of the transmitter(s) while the plant is operating. An isolated multichannel data acquisition system should be employed in this step so multiple transmitters can be tested.
2. Plot the amplitude probability density (APD) of the noise data, and verify that it is normal. Figure 5-16 shows two APDs for nuclear plant pressure transmitters, one that has a normal distribution and another that has a skewed APD.
3. Perform FFT and generate the PSD of the noise data. Autoregressive (AR) modeling may be used instead of or in addition to FFT to yield the PSD of the noise signal. (In this dissertation, however, the FFT approach is used to arrive at the PSD.)
4. Fit the PSD to the dynamic model of the pressure transmitter (represented by the transfer function  $G$ ). A second-order, underdamped model is normally suitable for nuclear plant pressure transmitters and sensing lines. (However, if the transmitter can be assumed to be first order, its response time can simply be deduced from the roll-off frequency of the PSD.)
5. Use the model variables from the fit in step 4 to identify the response time of the transmitter.

Figure 5-17 illustrates this five-step procedure. This procedure has been used in PWR and BWR plants to test the response time of transmitters in the services shown in Table 5-3.



(a) Gaussian



(b) Skewed

Figure 5-16 Two APDs for a Nuclear Plant Pressure Transmitter

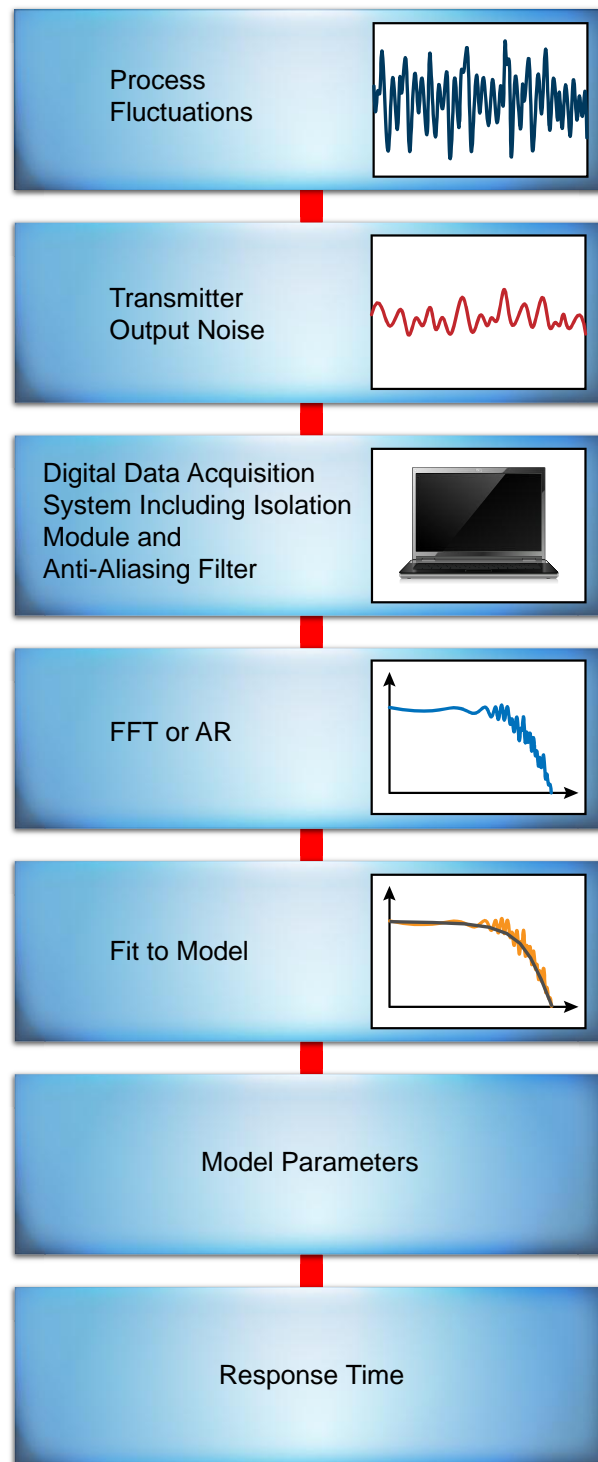


**Figure 5-17** Noise Analysis Procedure to Measure the In-Situ Response Time of a Pressure Transmitter

**Table 5-3 Typical Services for Which Transmitter Response Time Testing Is Performed in Nuclear Power Plants**

<u>PWRs</u>	<u>BWRs</u>
<ul style="list-style-type: none"> <li>• Pressurizer level</li> <li>• Pressurizer pressure</li> <li>• Reactor coolant system pressure</li> <li>• Reactor coolant flow</li> <li>• RWST level</li> <li>• Steam flow</li> <li>• Steam generator level</li> <li>• Steam pressure</li> <li>• Turbine impulse pressure</li> <li>• Containment pressure</li> <li>• Feedwater flow</li> <li>• Seal injection flow</li> <li>• Seal leak-off flow</li> <li>• First stage turbine pressure</li> <li>• Let-down flow</li> <li>• Let-down pressure</li> <li>• Safety injection flow</li> <li>• Turbine oil pressure</li> </ul>	<ul style="list-style-type: none"> <li>• Containment pressure</li> <li>• Drywell pressure</li> <li>• HPCI steam flow</li> <li>• Isolation condensers steam flow</li> <li>• Main steam flow</li> <li>• RCIC flow</li> <li>• Reactor vessel pressure</li> <li>• Reactor vessel water level – WR, NR</li> <li>• RWCU flow</li> <li>• Scram discharge level</li> <li>• LPCI pressure</li> <li>• LPCI flow</li> <li>• Core scram</li> <li>• HPCI differential press</li> <li>• HPCI differential flow</li> <li>• Isolation condenser condensate flow</li> <li>• Feedwater flow</li> <li>• Containment vacuum differential pressure</li> <li>• Core spray flow</li> <li>• Safety injection flow</li> <li>• Steam dome pressure</li> </ul>

---

RCIC: Reactor core isolation cooling  
 HPCI: High pressure coolant injection  
 LPCI: Low pressure coolant injection  
 RWCU: Reactor water cleanup flow  
 RWST: Reactor water storage tank  
 WR: Wide range  
 NR: Narrow range

# 6

## VALIDATION OF RESEARCH TECHNIQUES

---

This chapter presents the results of the validation research the author performed to ascertain the equivalence and reliability of the LCSR and noise analysis techniques as substitutes for conventional response-time testing methods. The validation procedure consisted of rigorously comparing the results of response-time measurements obtained from both the conventional methods (plunge and ramp tests) and those advanced during this research (LCSR, noise analysis). The purpose of this validation stage is to demonstrate that the proposed methods can provide the same response time values that are obtained using the conventional methods (but with the additional in-situ benefits provided by these methods, as described earlier in this dissertation). The assumption of this validation stage is that if the conventional and research methods agree in laboratory tests, they will also generally agree if performed on sensors as installed in a plant. Of course, this agreement is approximate due to the differences in test assumptions, measurement uncertainties, and data analysis algorithms described earlier in this dissertation. For the purposes of validation, therefore, we contend that if the results of the conventional and research methods agree within  $\pm 20$  percent, the two methods are assumed to be comparable.

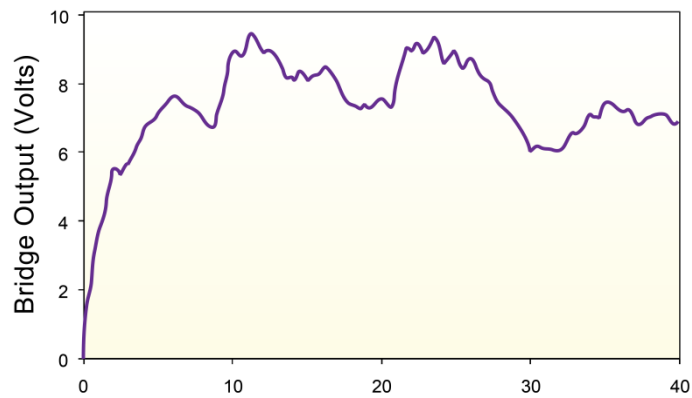
### 6.1 Validation of the LCSR Technique

The validity of the LCSR method depends on: (1) how well the RTD design satisfies the assumptions of the LCSR test, (2) the quality of the obtained LCSR data in terms of signal-to-noise ratio, (3) the application of proper sampling parameters for the data acquisition of LCSR, and (4) the suitability of the algorithms and fitting processes used in the data analysis stage of LCSR.

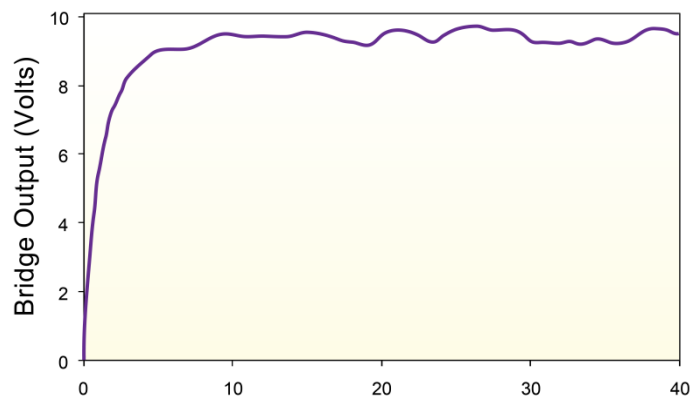


Figure 6-1 shows typical LCSR curves for an RTD whose sensor data was sampled at a frequency of 50 Hz using a 12-bit analog-to-digital (A/D) converter. LCSR data is typically shown in terms of the output of the Wheatstone bridge (in volts) versus time (in seconds) or equivalent A/D counts versus time. The top frame (a) in Figure 6-1 is a single LCSR test, and the lower two frames (b, c) are the averages of 20 and 40 LCSR transients, respectively. Note that the single LCSR data shows significant fluctuations. These fluctuations can interfere both with the analysis of the LCSR data and with the accuracy of its results and must therefore be minimized. Since the frequency of these fluctuations is low, they cannot be filtered out electronically. Therefore, they must be minimized by repeating the LCSR test on the same RTD and applying ensemble or aggregate averaging of the multiple LCSR traces. Figure 6-2 shows the output of a software program written to automatically read and average multiple LCSR transients and plot the results in terms of the individual traces and their ensemble average. The averaged transient is then analyzed, as described in Chapter 5, to produce the RTD response time.

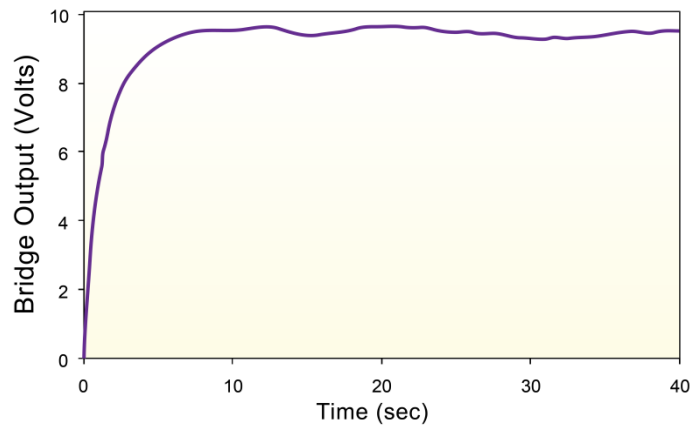
Figure 6-3 shows average results of over 100 laboratory plunge and LCSR tests performed under the same conditions during this research to establish the validity of the LCSR method. The results are for RTDs manufactured by Weed Instrument Company, which currently manufactures most of the nuclear plant RTDs used in the United States and elsewhere. For each Weed RTD or RTD/thermowell assembly, a plunge test was performed in room-temperature water flowing at 1 meter per second. Subsequently, the RTD was left in the water and tested under the same conditions using the LCSR method to determine if the LCSR method provides the same results as the plunge test. The median value (and standard deviation) of the plunge time constants for all the RTDs used in this experiment was 3.67 ( $\pm 0.60$ ) seconds. The corresponding LCSR results were 3.86 ( $\pm 0.67$ ) seconds, as shown in Figure 6-3. This shows excellent agreement between the median values of the response time derived from the two methods. Based on these experimental results, it can be concluded that the LCSR method produces the response time of an RTD with an acceptable accuracy and is therefore a valid technique,



(a) Single LCSR Transient



(b) Average of 20 LCSR Transients



(c) Average of 40 LCSR Transients

**Figure 6-1 Single (a) and Average (b, c) LCSR Transients Obtained by Testing an RTD in an Operating Nuclear Power Plant**

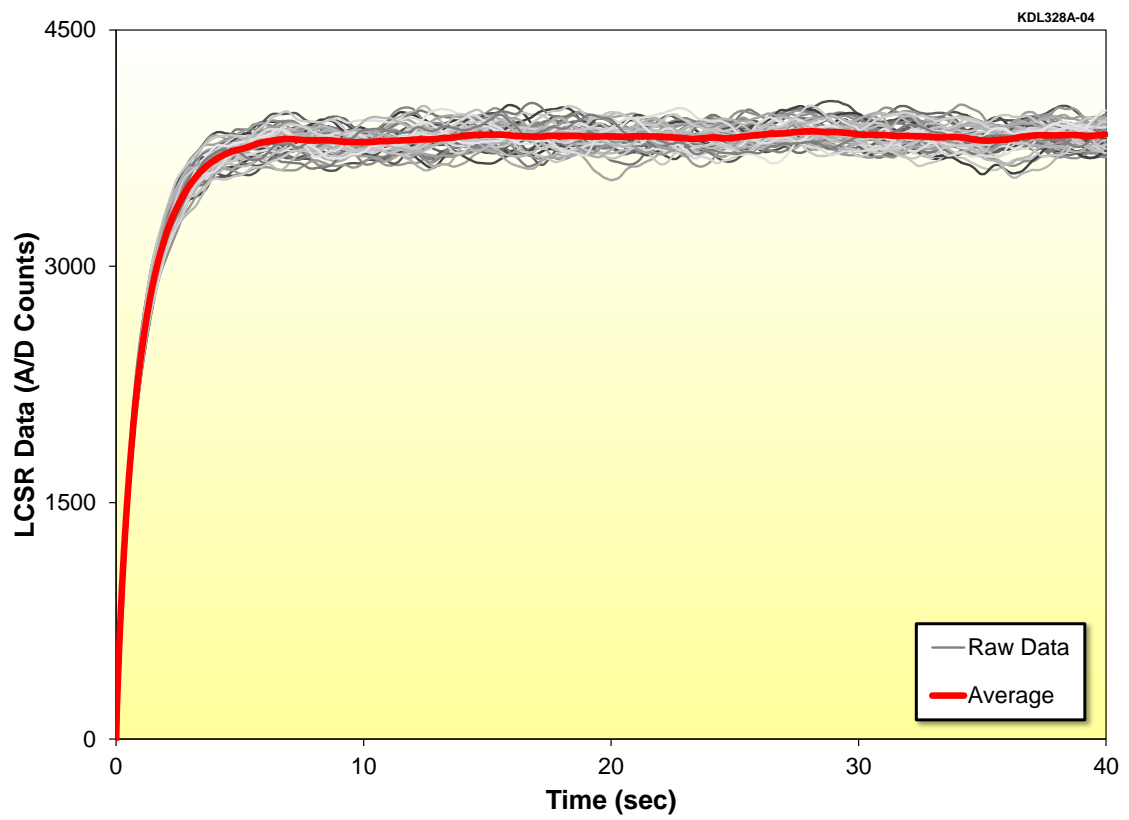


**Figure 6-2** Output of Software Program That Automatically Reads and Averages Multiple LCSR Transients

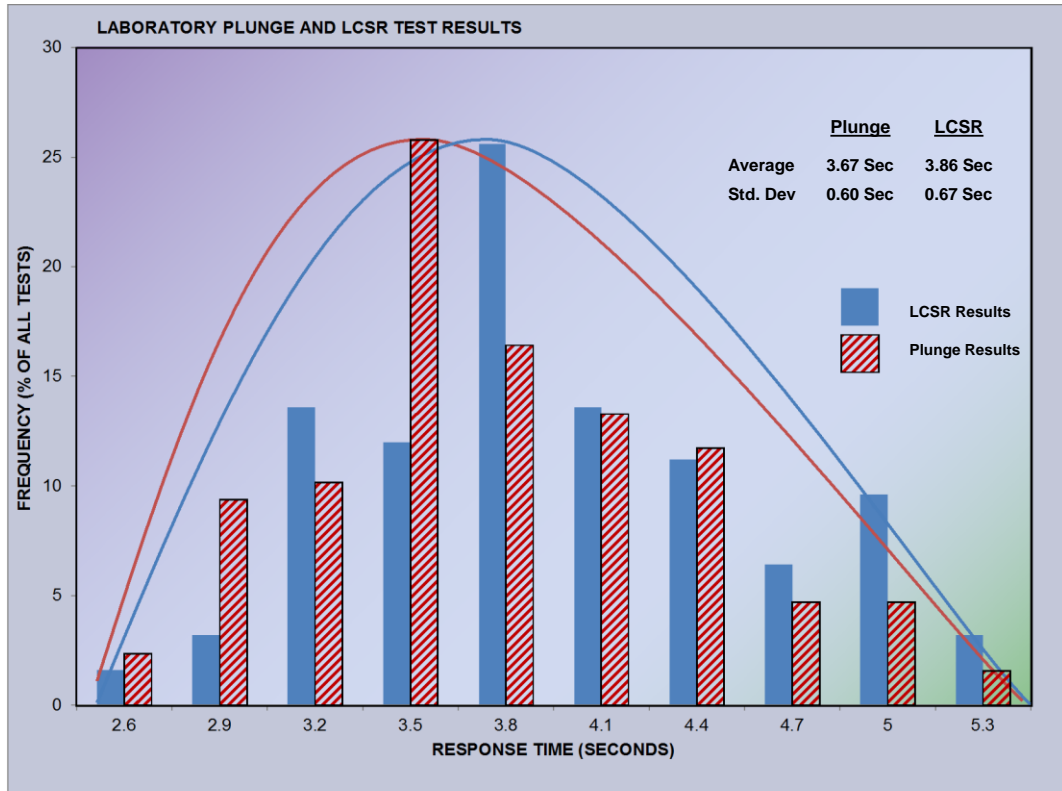


**Figure 6-3 Results of Laboratory Tests of One Population of RTDs Involved in this Research**

for RTD response time measurement. This statement is further confirmed by the results shown in Figure 6-4, which shows over 100 data points from laboratory plunge and LCSR testing. To confirm that the plunge and LCSR methods provide the same results, all data points should ideally fall on the 45° line. In practice, however, the data points display some distribution around the 45°. Significantly, however, almost all of the plunge and LCSR results fall within  $\pm 10$  percent of one another.

To quantify the accuracy of the LCSR method, Figure 6-5 shows a bar chart illustrating the percentage difference between plunge and LCSR results for over 100 RTDs from four manufacturers of nuclear plant RTDs. Note that almost all LCSR results fall within  $\pm 10$  percent of the plunge test. Consolidating the validation data presented in Figures 6-3 through 6-5 justifies the claim that the LCSR method and plunge test method both provide results within  $\pm 10$  percent of each other.

Although we have established that laboratory measurements show that the plunge test and LCSR test are practically equivalent methods, one significant additional benefit that the LCSR method offers over the plunge test method is its ability to verify that RTDs are properly installed in a plant so as to provide optimum response time results. We will demonstrate this in the remainder of this section.

If a safety-system RTD fails to provide sufficiently rapid response time while installed in a nuclear power plant, the plant must be shut down to replace the RTD, at substantial operational and personnel cost. To avoid this problem, the LCSR method may be used during cold shutdown conditions to verify that RTDs are properly installed and to minimize the possibility of a response time failure when the plant resumes power operation. An LCSR test during cold shutdown will not provide the correct response time, but it can reveal if an RTD is installed improperly, does not fit the thermowell, or is too slow to measure a transient temperature. Table 6-1 shows LCSR results from tests in nuclear power plants performed to verify RTD installation. Two columns of results are included in this table: one to show the values when the tests were performed (as-found), and the other to show the values after the installation problem was corrected

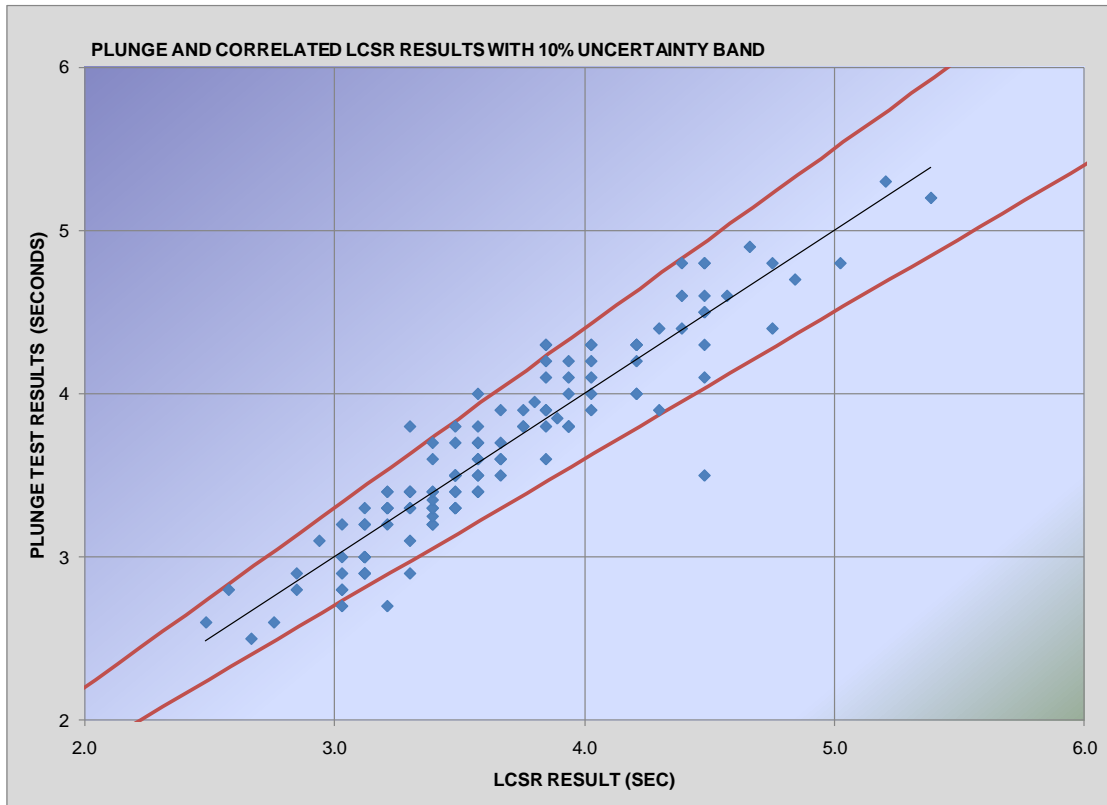


**Figure 6-4 Summary of Research Results on LCSR Validation**

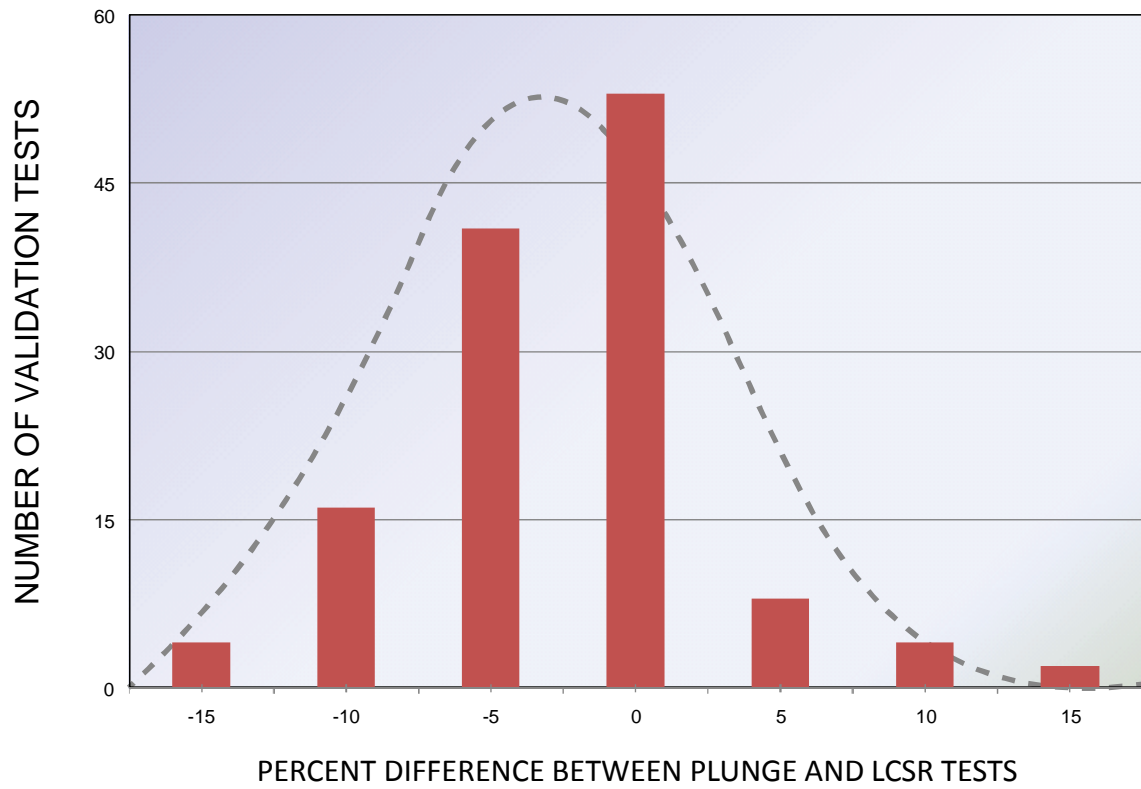


**Figure 6-5** Summary of Research Results to Quantify the Accuracy of LCSR Method

**Table 6-1 LCSR Results for RTD Installation Tests**

<b>LCSR Results (Seconds)</b>		
<b><u>As Found</u></b>	<b><u>As Left</u></b>	<b><u>Corrective Action</u></b>
11.6	4.7	Cleaned Thermowell
22.5	7.5	Cleaned Thermowell
14.7	5.9	Cleaned Thermowell
37.4	13.0	Cleaned Thermowell
9.0	5.0	Reseated RTD
18.0	14.0	Reseated RTD
19.2	9.5	Reseated RTD
14.5	5.4	Installed New RTD
24.0	7.8	Installed New RTD
24.0	17.0	Debris Removed
27.9	5.8	Replaced Thermowell



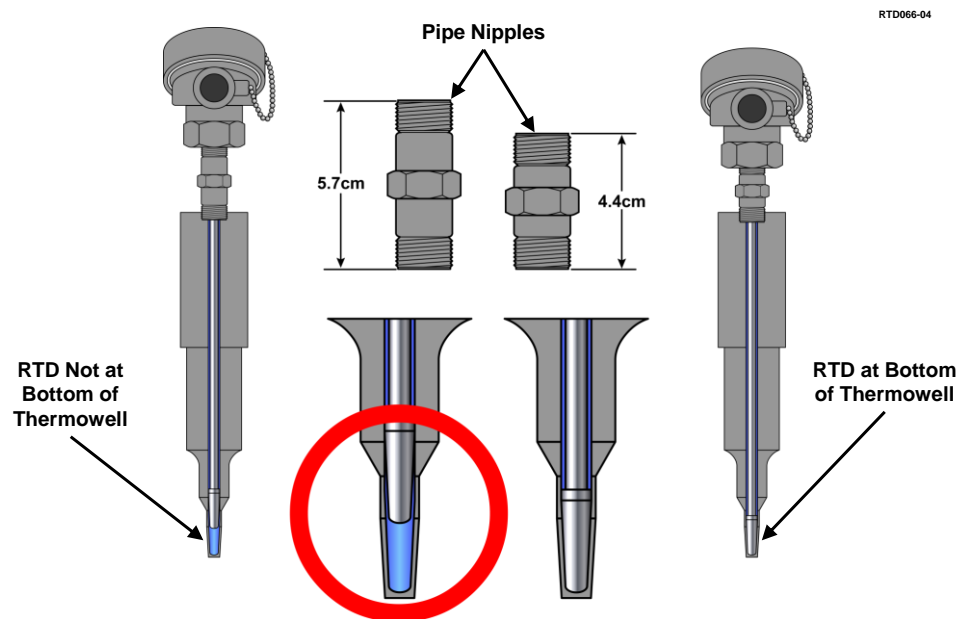
(as-left). Note that the LCSR results in Table 6-1 do not correspond to the actual response times of the RTDs because actual response times must be measured at process operating conditions. Rather, these numbers are useful for verifying that a sensor has not bottomed out in its thermowell or that dirt, obstruction, or other issue is not interfering with the RTD's optimum performance. Table 6-1 also states the corrective action that the plant personnel implemented to resolve the problem.

Recently, LCSR tests were performed on a set of 24 RTDs in a nuclear power plant during cold shutdown. During these tests, an RTD was found to have inadequate insertion in its thermowell due to use of a wrong pipe nipple, as shown in Figure 6-6(a). This caused the RTD to seat approximately 1.2 cm away from the tip of the thermowell, resulting in a significantly sluggish response, as shown by the LCSR transients in Figure 6-6(b). Fortunately, using the LCSR data shown in this figure, the problem was identified during cold shutdown and resolved before the plant resumed power operation. Without this intervention, this RTD would have been too slow to initiate safety system actuation in the event of an undesirable temperature transient in the reactor. In other in-plant tests, the LCSR method has identified RTDs that had significantly slower response times than others in the plant, as shown in Figure 6-7. Because this problem was discovered during cold shutdown, the plant's personnel were able to correct the problem before startup.

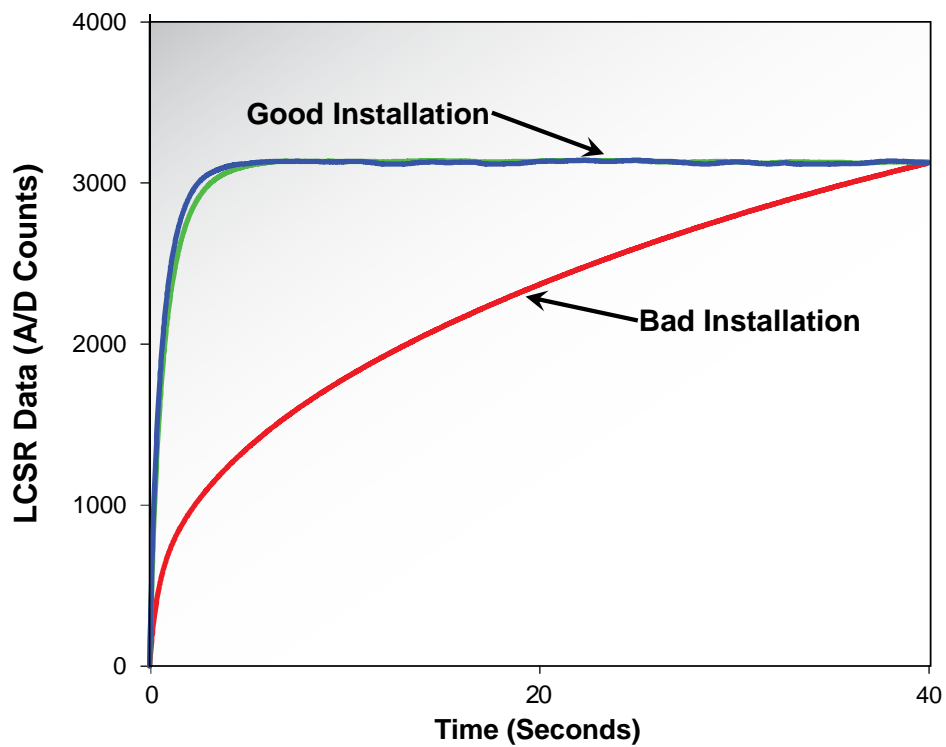
The empirical data provided in this section serves to further demonstrate the validity of the LCSR method for measuring RTD response times and for identifying installation problems that can result in sluggish RTD performance.

## **6.2 Validation of Noise Analysis Technique**

The noise analysis technique was validated using laboratory experiments involving nearly fifty nuclear-grade pressure transmitters from four manufacturers of sensors commonly used in nuclear power plants. Figure 6-8 summarizes the results in terms of differences between the average results of the ramp test (the conventional test for pressure transmitter response time) and the noise analysis tests. It is clear from the

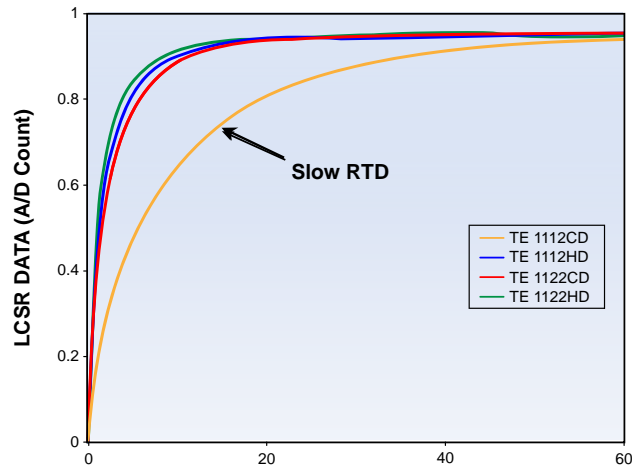


(a) RTD and Thermowell Installation

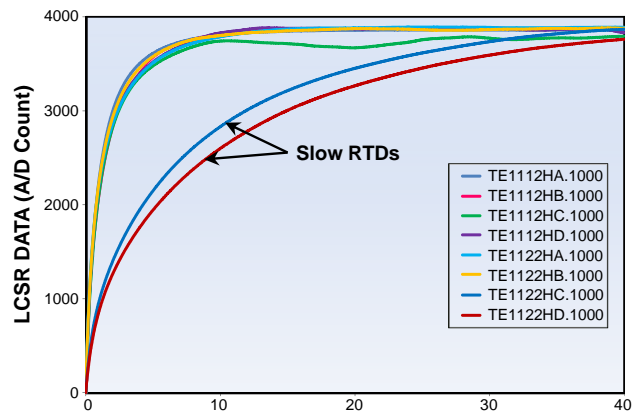


(b) LCSR Transients

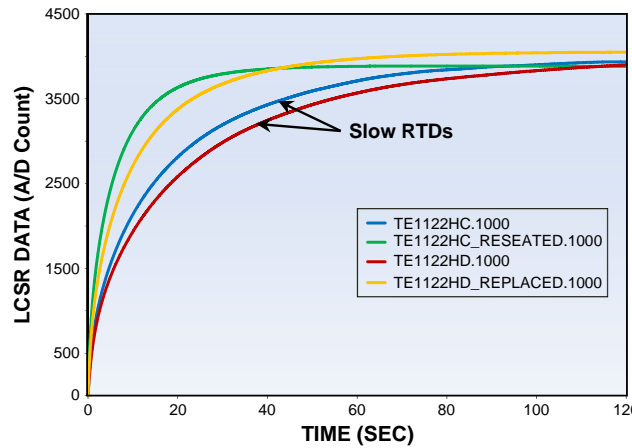
**Figure 6-6 Example of an RTD Installation Mishap in a Nuclear Power Plant (a) and Resulting LCSR Data (b)**



(a)



(b)



(c)

**Figure 6-7 Raw LCSR Data from Redundant RTDs Tested at Cold Shutdown to Identify Installation Problems**

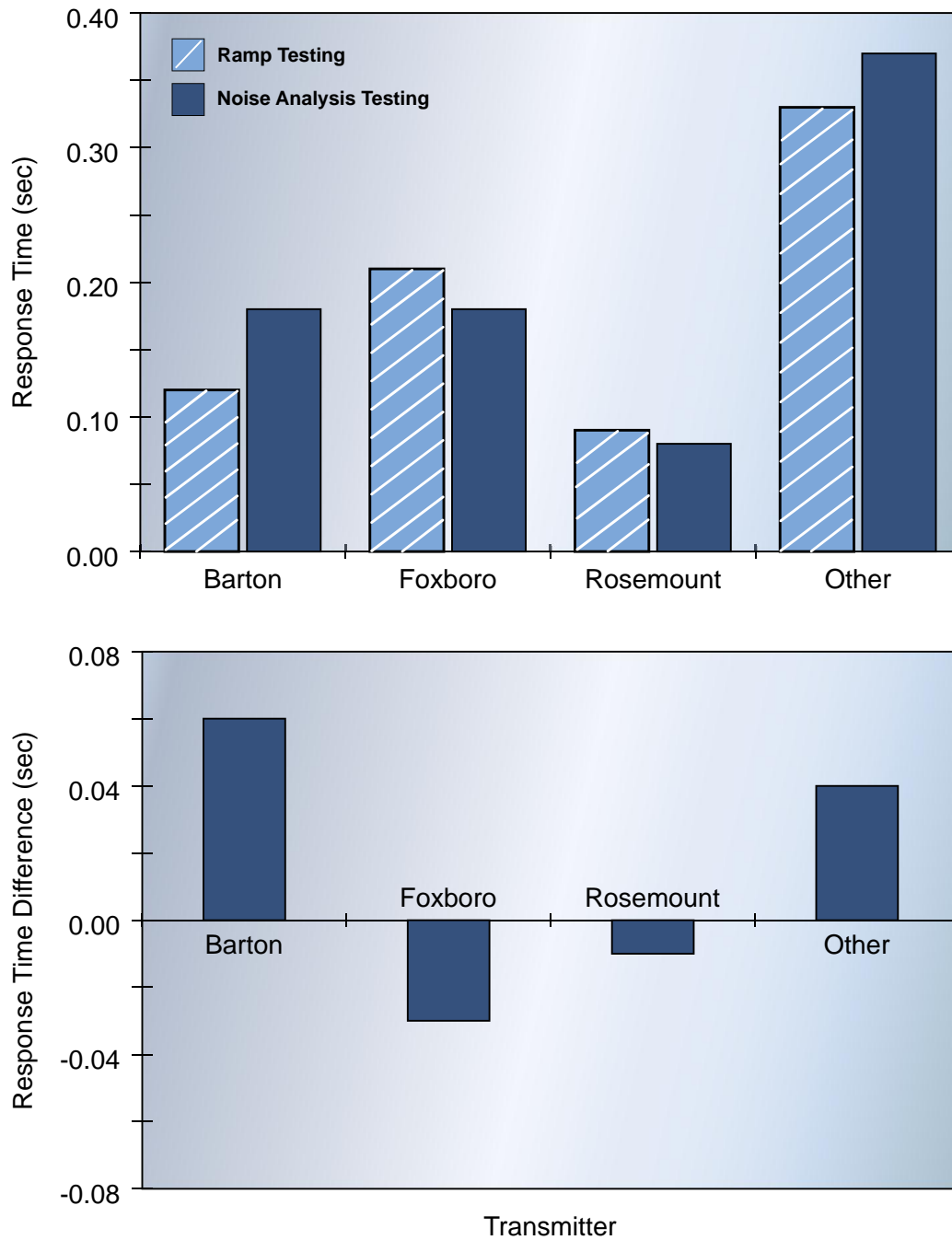


**Figure 6-8 Summary of Research Results on Validation of Noise Analysis Technique**

results in Figure 6-8 that the noise analysis technique provides response-time results that compare well with the ramp test method.

To quantify the accuracy of the noise analysis technique, the results of additional laboratory measurements were analyzed. The results indicated that the response times obtained for 80 percent of the transmitters agree with the corresponding ramp-test results to better than 0.05 seconds, as shown in the test data in Figure 6-9. Furthermore, the author researched a comprehensive database of nearly 5,000 response-time results for pressure transmitters in nuclear power plants (Figure 6-10). These results indicated that the median response-time value of nuclear plant pressure transmitters is about 0.25 seconds. Thus, a difference of less than 0.05 seconds amounts to an accuracy of better than 20 percent for the noise analysis technique. In examining the database of response-time results for nuclear plant pressure transmitters, the author also tabulated the results in terms of the services in the plant, the type of transmitter, and the minimum, maximum, and average values of response time for eight different services (Table 6.2).

### **6.3 Validation of the Noise Analysis Technique to Account for Sensing Lines**

To demonstrate that the noise analysis technique can identify the effect of sensing lines on response time (which the ramp test cannot do), the author conducted laboratory experiments involving simulated blockages and short and long sensing lines. For each experiment, both ramp tests and noise tests were performed, and the response time of the transmitters and sensing lines (including any blockages) were measured under controlled laboratory conditions. Representative results for one of the experiments are given in Table 6-3, together with a photograph of the test setup and corresponding drawings.

Figure 6-11 summarizes the results of a collection of laboratory tests designed to validate the noise analysis technique for detecting the contribution of the sensing line to the response time of pressure transmitters. These confirm that the noise analysis technique can produce the response time of a pressure sensing system while specifically accounting for the effect of sensing line length and any blockages.

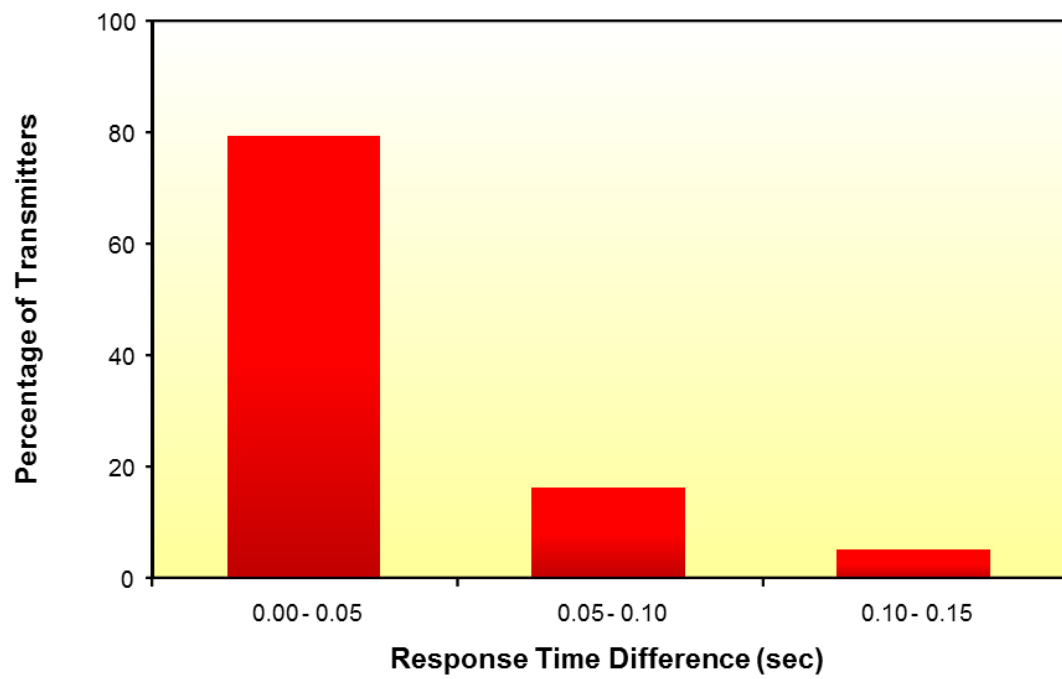


**Figure 6-9** Summary of Research Results to Quantify the Accuracy of Noise Analysis Technique

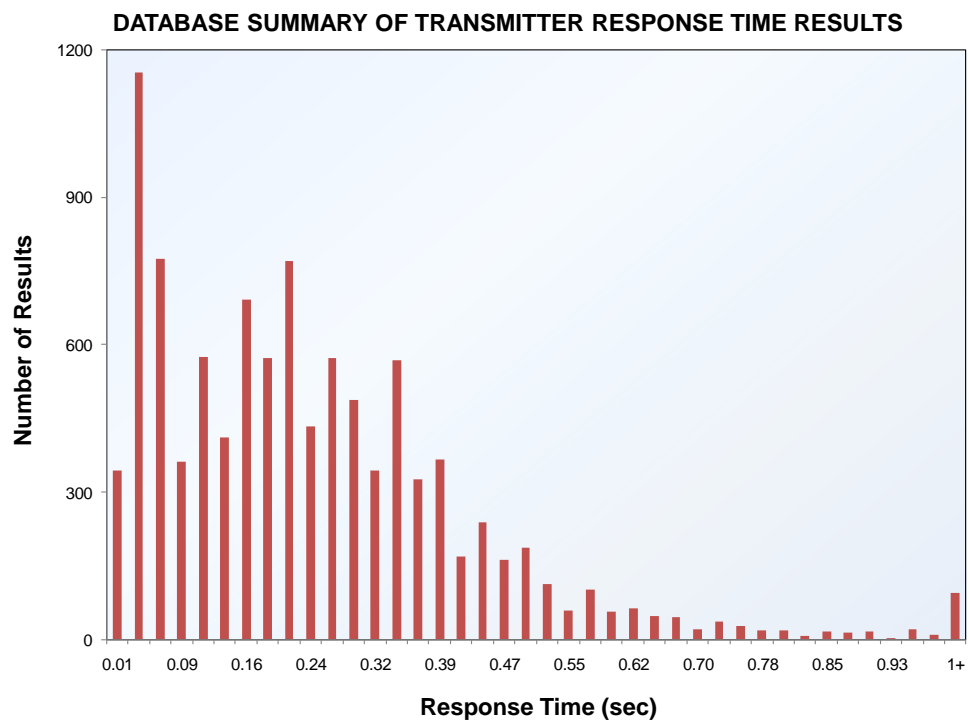


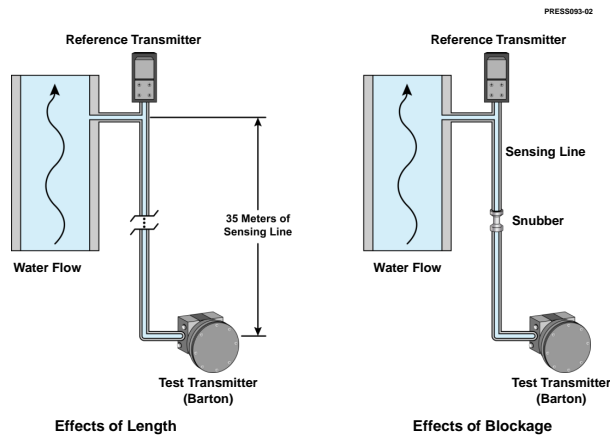
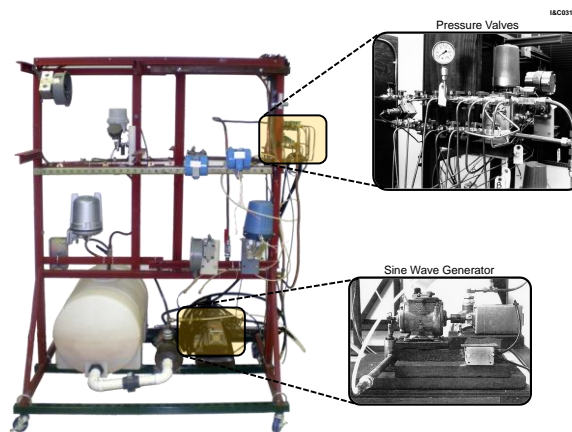
**Table 6-2 Summary from Transmitter Database**

<u>Item</u>	<u>Service</u>	<u>Manufacturer</u>	<u>Model</u>	<u>Type</u>	<u>Range</u>	<u>Response Time</u>		
						<u>Min</u>	<u>Avg</u>	<u>Max</u>
1.	Containment Pressure	Rosemount	1152	Gauge	5	0.14	0.16	0.20
		Rosemount	1153	Gauge	5	0.12	0.15	0.19
2.	Feedwater Flow	Rosemount	1151	DP	6	0.20	0.22	0.27
3.	Reactor Pressure	Rosemount	1153	Gauge	NA	0.02	0.05	0.12
4.	Recirculation Flow	Rosemount	1151	DP	4	0.05	0.06	0.07
		Rosemount	1153	DP	4	0.07	0.30	0.56
5.	Reactor Level	Rosemount	1153	DP	5	0.07	0.23	0.44
		Rosemount	1153	DP	NA	0.05	0.11	0.27
6.	Scram Discharge Level	Statham	NA	DP	32	0.27	0.45	0.63
7.	Steam Flow	Rosemount	1152	DP	7	0.19	0.24	0.30
		Rosemount	1153	DP	7	0.01	0.03	0.06
8.	Steam Pressure	Rosemount	1153	Gauge	9	0.01	0.03	0.63



**Table 6-3 Laboratory Test to Demonstrate Effectiveness of Noise Analysis Method in Identifying Sensing Line Effects**

<u>Test Configuration</u>	<u>Response Time (sec)</u>	
	<u>Ramp Testing</u>	<u>Noise Analysis Testing</u>
Transmitter tested alone (Negligible sensing line length)	0.12	0.17
Transmitter tested with 30 meters of sensing line tubing	0.27	0.28
Transmitter tested with a snubber on the sensing line	3.00	2.94



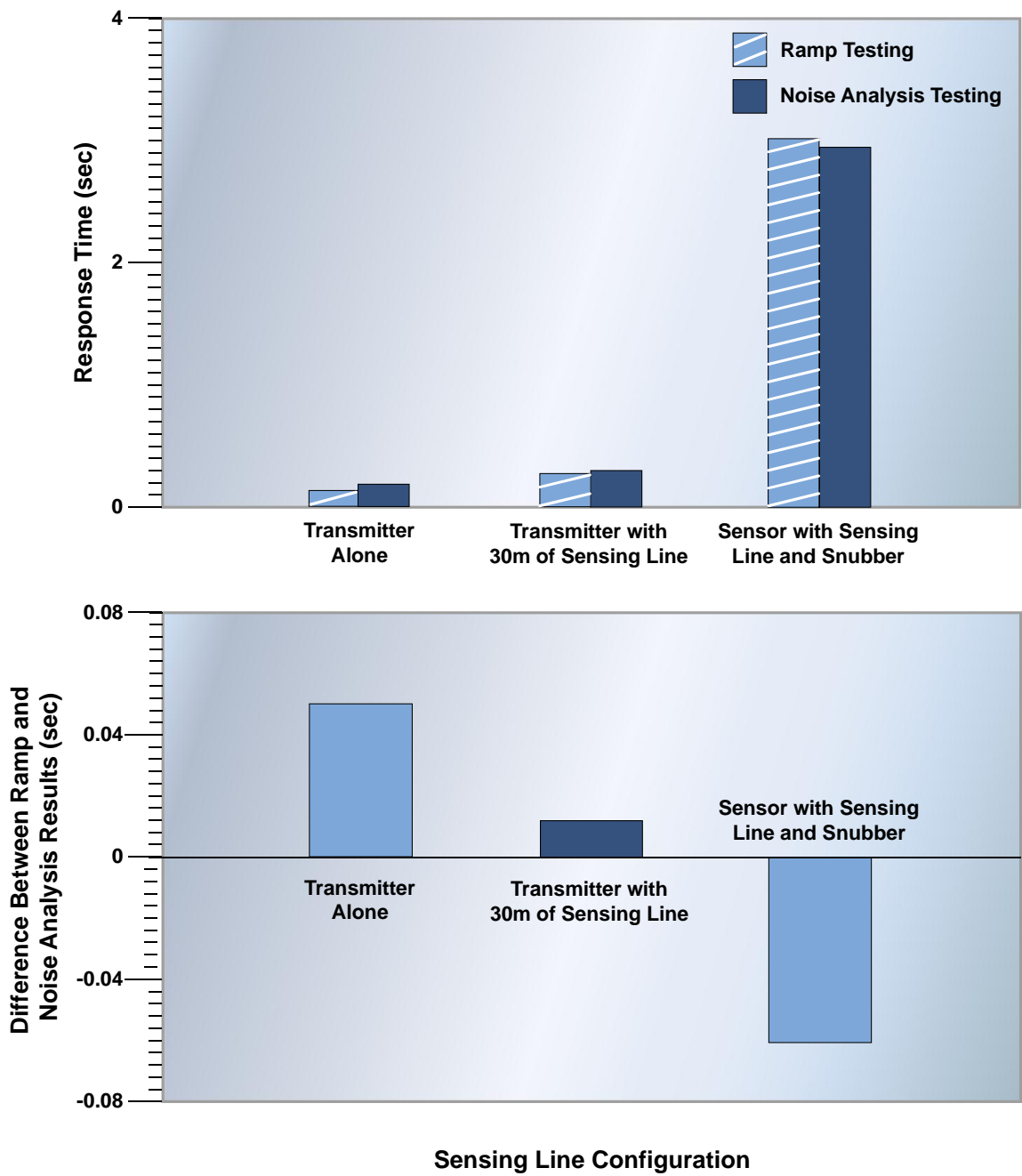


**Figure 6-11 Summary of Research Results on Validation of Noise Analysis Technique for Detecting Sensing Line Effects**

#### **6.4 In-Plant Experience with Detection of Sensing Line Problems**

The author and his organization have successfully used the noise analysis method in nuclear power plants to consistently identify and resolve sensing line problems where they would previously have gone undiscovered. Figure 6-12 shows representative results of in-plant testing that revealed blocked sensing lines. The data consists of PSD plots from noise tests performed before and after the sensing lines were flushed to remove blockages. From another in-plant test, Figure 6-13 shows online monitoring data plots from the output of four redundant transmitters under similar plant transient conditions. One transmitter is significantly slower than the other, evidence that sluggish transmitters are indeed an issue for nuclear power plants and that in situ response time measurements made using the method the author has advanced can effectively identify the affected transmitters.

Sensing line problems in nuclear power plants can also be detected by examining the APD of the noise signal from the affected transmitter, as shown in Figure 6-14(a) (which also shows the corresponding PSDs [b]). Note that transmitter 374A shows sluggish behavior in both the APD and PSD plots. Figure 6-15 contains additional PSD plots that track the dynamics of a nuclear plant pressure transmitter. Interestingly, the transmitter appears to have degraded over a relatively short time--between October 2010 and November 2010. This degradation also appears in the low-frequency plant computer data shown in Figure 6-16, which was sampled every 10 seconds from the plant computer. Figures 6-15 and 6-16 both show a degradation of the mean and standard deviation of transmitter 374A output signal between October and November 2010. Subsequently, the sensing line of this transmitter was flushed, and both the mean and standard deviations returned to normal.

#### **6.5 In-Plant Experience with Response Time Testing Using Noise Analysis**

Table 6-4 shows representative results of in-plant tests conducted during the preparation of this dissertation of nuclear plant pressure transmitters in which the noise analysis

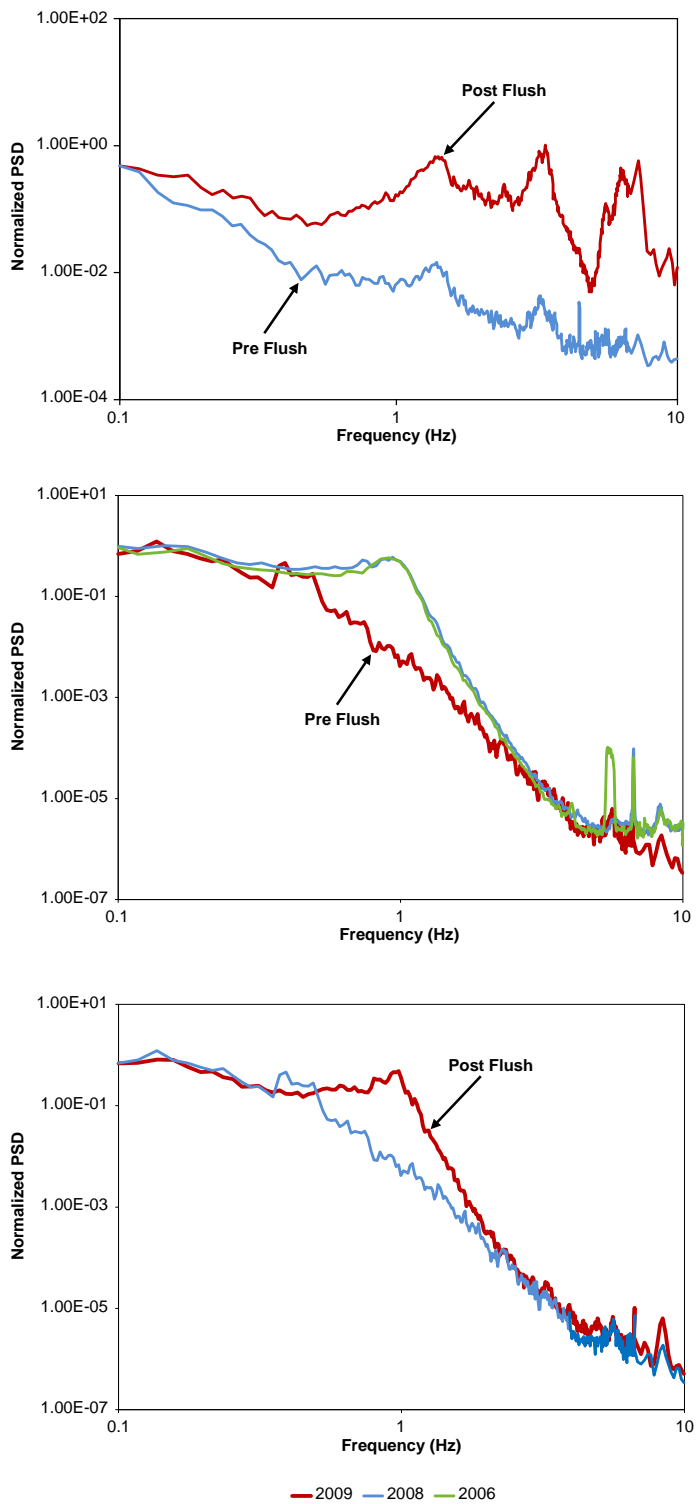


**Figure 6-12 Results of Noise Analysis Test of Pressure Transmitters Before and After Flushing the Sensing Line to Clear Blockages**

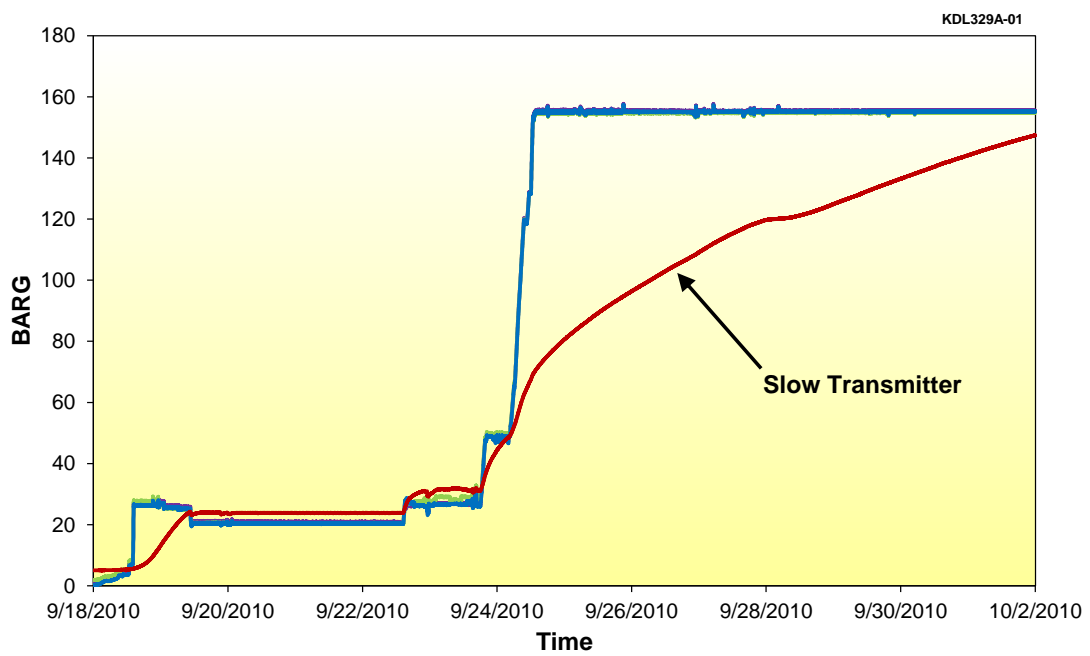
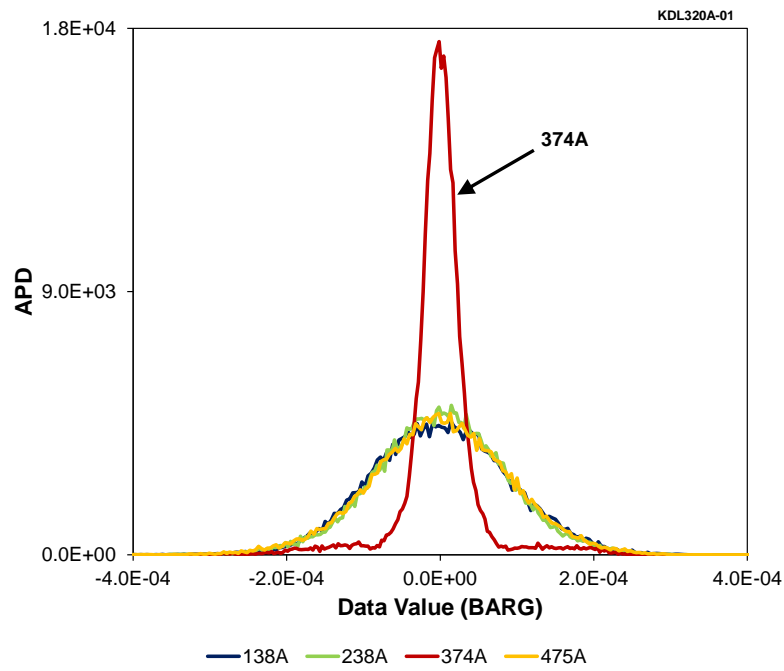
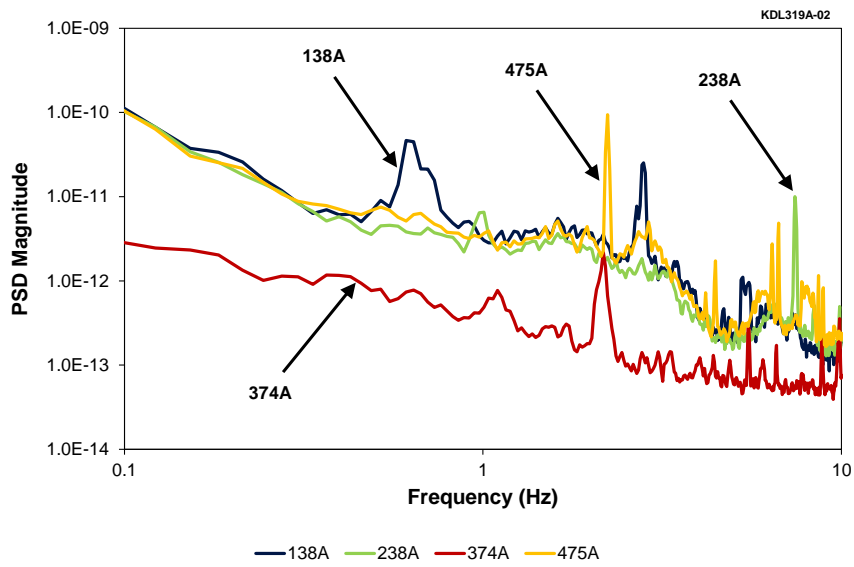


**Figure 6-13** Online Monitoring Data for Four Transmitters during a Plant Transient



(a) APD



(b) PSD

**Figure 6-14** APD (a) and PSD (b) Results from In-Plant Test of Four Pressure Transmitters

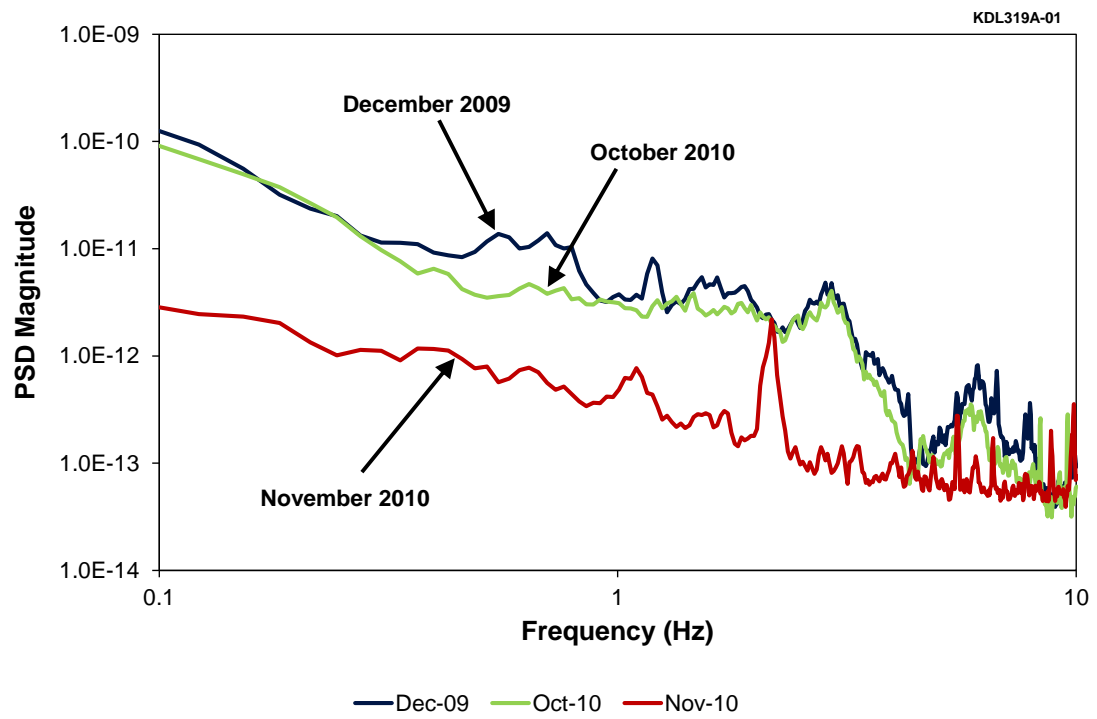
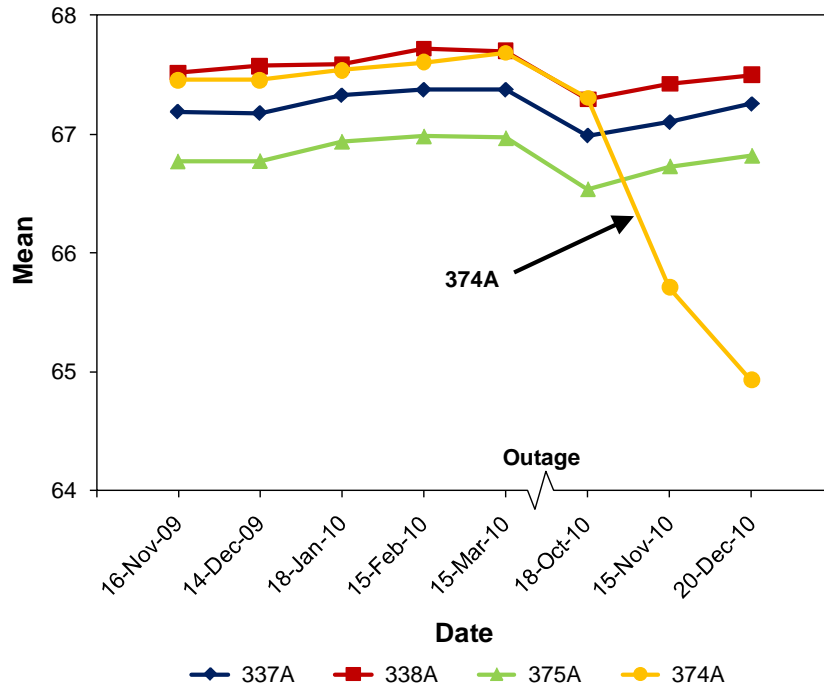
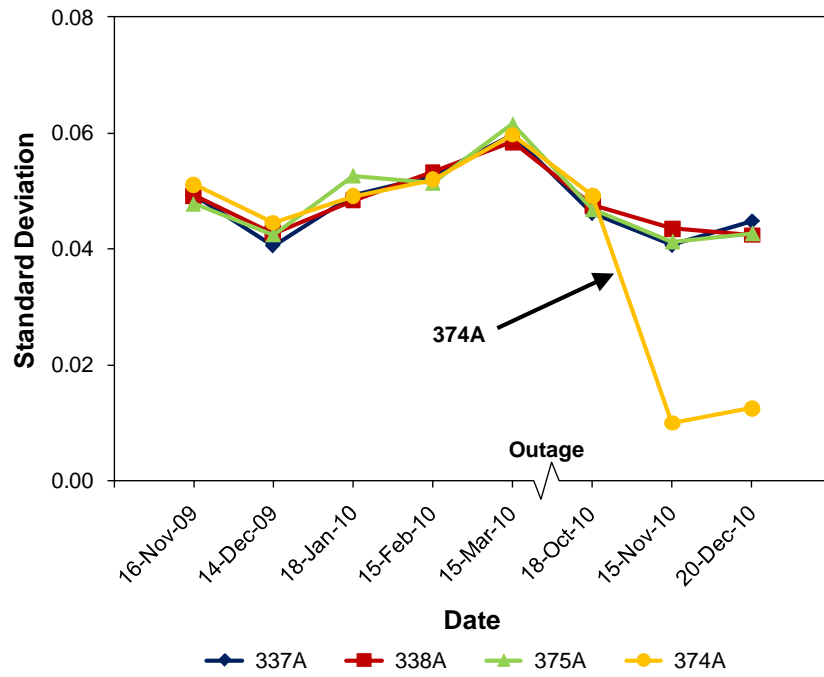


**Figure 6-15** Tracking PSDs of a Nuclear Plant Pressure Transmitter



(a)



(b)

**Figure 6-16 Plant Computer Data for the Transmitter Degradation Observed in November 2010**



**Table 6-4 Response Time Problems Detected by Noise Analysis Method**

<b><u>Nuclear Plant #1 (PWR)</u></b>					
<b><u>Item</u></b>	<b><u>Transmitter Identification</u></b>	<b><u>Test 1</u></b>	<b><u>Test 2</u></b>	<b><u>Test 3</u></b>	<b><u>Problem Identified</u></b>
1	RC-FT-434	0.17	0.16	0.30	Failed Isolation Valve
2	RC-FT-435	0.14	0.14	0.13	None
3	RC-FT-436	0.13	0.13	0.10	None
<b><u>Nuclear Plant #2 (PWR)</u></b>					
4	CFLT-5550	0.37	0.39	0.37	None
5	CFLT-5551	0.37	0.58	0.38	Blocked Sensing Line
6	CFLT-5560	0.43	0.49	0.45	None
7	CFLT-5570	0.40	0.43	0.40	None
<b><u>Nuclear Plant #3 (PWR)</u></b>					
8	AB-PT-437A	0.10	0.11	0.10	None
9	AB-PT-438A	0.10	0.48	0.10	Faulty Steam Manifold
10	AB-PT-474A	0.11	0.11	0.10	None
11	AB-PT-475A	0.09	0.11	0.11	None
<b><u>Nuclear Plant #4 (BWR)</u></b>					
12	FT-2391-52	0.52	No previous data		Inadvertent Damping
13	FT-2391-53	0.53	No previous data		Inadvertent Damping
14	FT-2391-54	0.17	No previous data		None
15	FT-2391-55	0.17	No previous data		None

technique revealed problems. The measurements were performed in three consecutive series of in-plant tests about one year apart in four different nuclear power plants (three PWRs and one BWR). Again, the noise analysis technique demonstrated its ability to identify response-time problems in situ, thereby potentially mitigating significant maintenance and operational costs.

In implementing the noise analysis technique in nuclear power plants, the author was given opportunities to perform ramp tests and noise tests on the same pressure transmitters under the same conditions. This allowed the author to compare the results of the two methods to demonstrate that the ramp and noise analysis methods produce comparable results when the test assumptions are satisfied. Figure 6-17 shows representative results of these tests, including corrections that were made in the ramp test results to account for the sonic and hydraulic delays due to sensing lines. That is, we simply added 0.05 seconds to ramp-test results to account for 0.02 seconds of sonic delays and 0.03 seconds of hydraulic delays. These values were estimated based on the theoretical analysis of sensing line contributions to the response time as discussed in Chapter 4 and on information about the average length and diameter of sensing lines in nuclear power plants as well as the effect of static pressure.

Figure 6-18 presents another view of data on the in-plant validation of the noise analysis technique. In this figure, response time results from the noise analysis technique are plotted against corresponding ramp test results. Again, the ramp test data were corrected by 0.05 seconds to account for the effect of sonic and hydraulic delays in the sensing lines. It is evident from the data presented in Figure 6-17 and 6-18 that the ramp and noise methods produce comparable response time results for nuclear plant pressure transmitters. In Figure 6-18, a band of  $\pm 0.10$  seconds is drawn about the 45° line to demonstrate that the majority of results fall within  $\pm 0.10$  seconds of one another.

## **6.6 When the Methods Fail**

Part of the research conducted for this dissertation has concerned itself with delineating the practical limits of the LCSR and noise analysis techniques. The author has

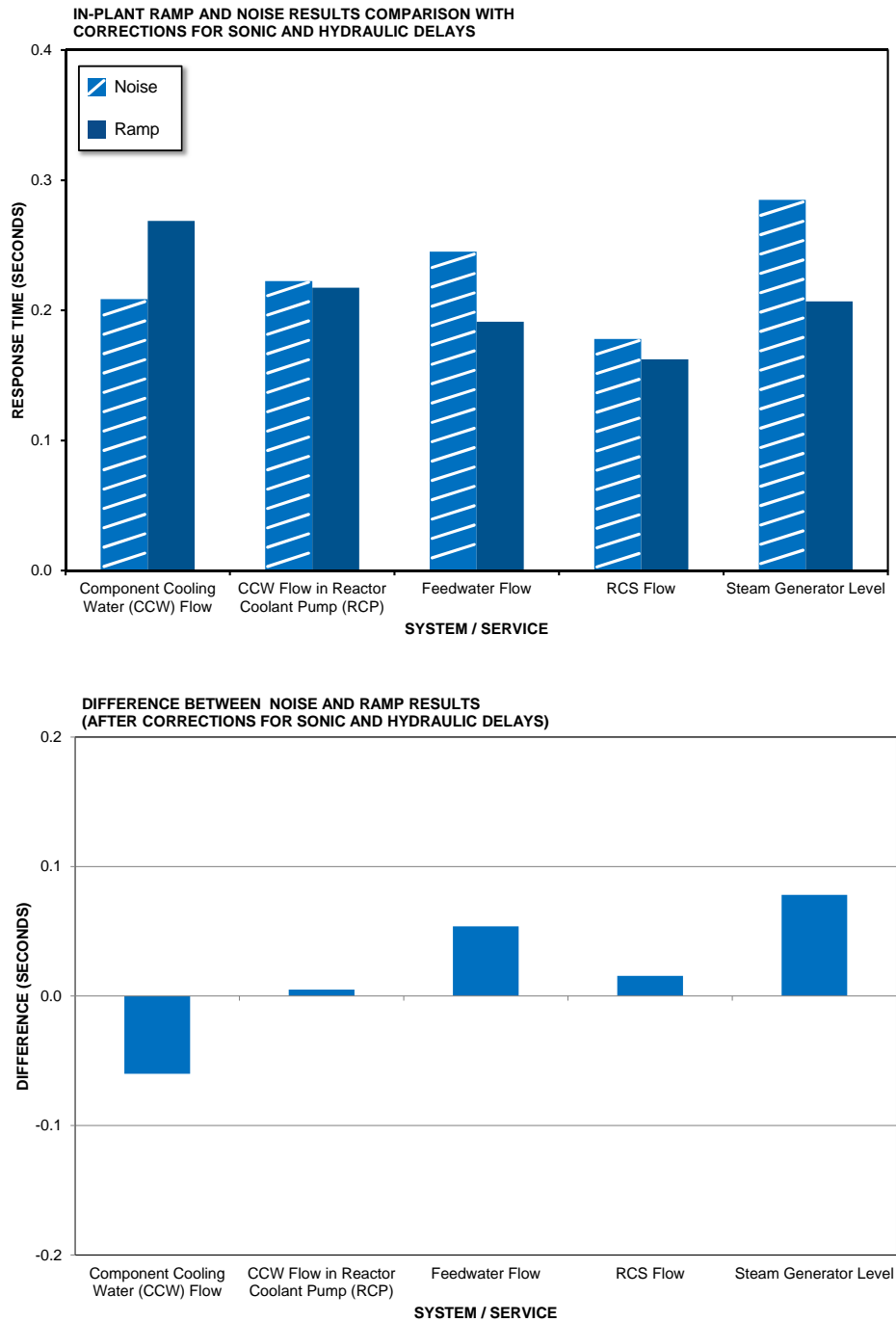


**Figure 6-17 Results of In-Plant Validation of Noise Analysis Technique with Correction of Ramp Results for Sonic and Hydraulic Delays**

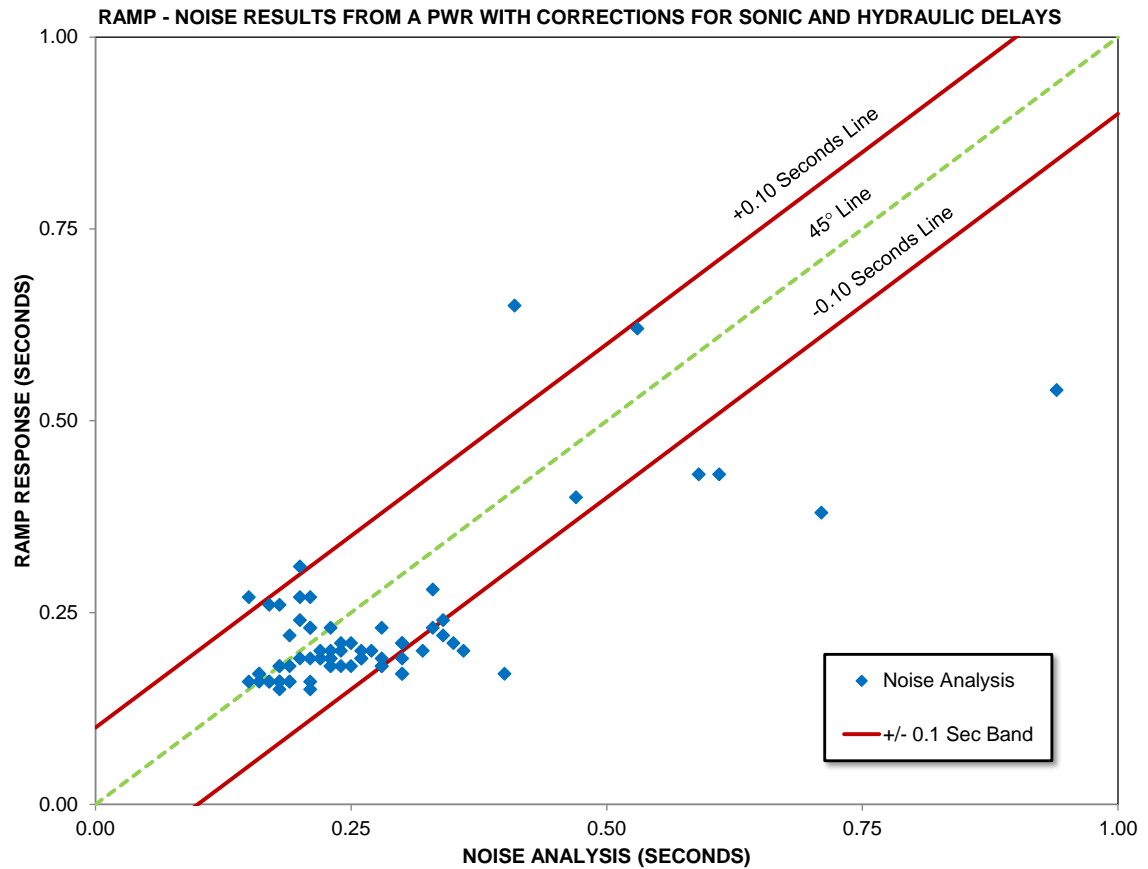


**Figure 6-18 Spread of Response Time Data from Ramp and Noise Tests**

(Data from in-plant measurement to validate the noise analysis technique)

determined that both methods can indeed fail if the assumptions on which their validity rests are not met or if the process conditions they are used in are not appropriate to them. Table 6-5 shows laboratory LCSR and plunge test results for two RTDs and two thermowells from the Sizewell nuclear power plant in the United Kingdom. These RTDs do not satisfy the LCSR validation assumptions when they are installed in the thermowell. As a result, the LCSR method underestimates the response time of the RTD-in-thermowell assembly by as much as 71 percent. While the LCSR method seems to be valid for the bare RTD (without thermowell), its results become unacceptable when the RTD is used in its thermowell. Apparently, the LCSR assumption of one-directional heat transfer is violated when the thermowell is added to the RTD. Fortunately, when the in-service response time for an RTD cannot be measured with the LCSR method, *the noise analysis technique may be used as an alternative*. Indeed, for the Sizewell RTDs, the author has successfully used the noise analysis technique to measure RTD response time (see Table 8-1 in Chapter 8.) However, in a recent set of in-plant measurements using the noise analysis technique, a group of eight RTDs were found to exceed their historical response time values by a factor of two or more as shown in Table 6-6. This is rather unexpected because RTDs do not normally degrade so much as a group over a single fuel cycle (in this case 18 months). Therefore, an investigation into the cause of the failure of these RTDs was launched. This effort revealed that, due to other changes made in the plant, the characteristics of temperature noise affecting these RTDs in the plant had changed (i.e., slowed). This change in process noise characteristics had in turn reduced the bandwidth of the input noise, causing slower RTD response time results. This demonstrates once again that if the process noise has inadequate bandwidth, the noise analysis method fails to produce accurate results.

The noise analysis technique can also fail if the sensor under test is nonlinear or the noise signal does not have a Gaussian distribution. Figure 6-19 shows the results of ramp and noise tests for three redundant pressure transmitters, including plots of their APDs. The transmitters were tested as installed in a nuclear power plant. The ramp tests were performed in the plant after the noise analysis tests to investigate the cause of

**Table 6-5 Results of Laboratory Testing of Sizewell RTDs**

<b>Sensor Identification</b>		<b>Installation</b>	<b>Response Time (seconds)</b>		<b>Percent Difference</b>
<b>RTD</b>	<b>Thermowell</b>		<b>Plunge</b>	<b>LCSR</b>	
1	None	Bare RTD	0.6	0.6	0
2	None	Bare RTD	0.6	0.6	0
1	1	RTD in Thermowell	2.4	1.4	-71
1	2	RTD in Thermowell	2.5	1.4	-71
2	1	RTD in Thermowell	2.5	1.6	-56
2	2	RTD in Thermowell	2.9	1.8	-61

Above results involved two spare RTDs and two thermowells tested in a laboratory in room-temperature water flowing at 1 m/s.

**Table 6-6 Noise Analysis Results for Sizewell RTDs**

<b><u>Item Number</u></b>	<b><u>RTD Identification</u></b>	<b>Response Time (seconds)</b>	
		<b><u>Recent Test</u></b>	<b><u>Historical Average</u></b>
1	480	3.8	2.5
2	483	2.4	1.4
3	643	3.3	1.4
4	644	2.4	1.8
5	648	3.2	1.2
6	450	3.8	2.4
7	615	2.3	1.5
8	617	3.1	1.7
	Average	3.0	1.7

Transmitter Tag Number	Response Time (sec)			Amplitude Probability Density Plot
	Ramp	Noise	Difference	
PT-524	0.13	0.16	0.03	
PT-526	0.12	0.18	0.06	
PT-505	0.16	0.78	0.62	

**Figure 6-19 Response Time and APD Results for Three Pressure Transmitters**



the apparent failure of PT-505. Comparing the response time results and the APDs, the author has concluded that the noise analysis technique failed on PT-505 due to transmitter nonlinearity. Non-Gaussian noise can also cause the method to fail, but this cannot be the case here because the other two redundant transmitters display Gaussian APDs.

In some nuclear power plants, redundant transmitters can sometimes share sensing lines, as shown in Figure 6-20. In this case, the response time that is measured for the transmitters that share a sensing line will be dominated by the response time of the slowest transmitter. Shared sensing lines could also be a concern when transmitters with different compliances are installed on the same lines. In such situations, each transmitter's response time is dominated by the transmitter that has the highest compliance. This effect was observed while testing the response times of four Rosemount transmitters used to measure steam generator level in a PWR plant. Figure 6-21 and 6-22 illustrate the situation. In Figure 6-21, four Rosemount transmitters (tag numbers 518, 528, 538, and 548) are shown sharing a sensing line with a wide-range Barton transmitter. In Figure 6-22, the four PSDs of these transmitters are shown. The PSDs on the left-hand side are from noise testing of the Rosemount transmitter, but their shapes correspond to that of Barton transmitters. This is because the Barton transmitters have larger compliances than the Rosemount transmitters. They therefore act as snubbers and dominate the noise output of the Rosemount transmitters.

The Rosemount transmitters were tested two years later and found to have the same PSDs, with the exception of 528. More specifically, transmitter 528 had a PSD that resembled that of a Rosemount transmitter. An investigation into this observation revealed that during the time between the two tests, the Barton transmitter sharing a sensing line with 528 was replaced with a Rosemount transmitter. Of course, if the ramp method is used instead of the noise analysis technique, the resulting response time will be correct for each transmitter whether or not the transmitter is sharing a sensing line with another transmitter. The noise analysis failed in this particular situation, but the good news is that the failure is safe because it resulted in conservative response times for the affected transmitter(s).

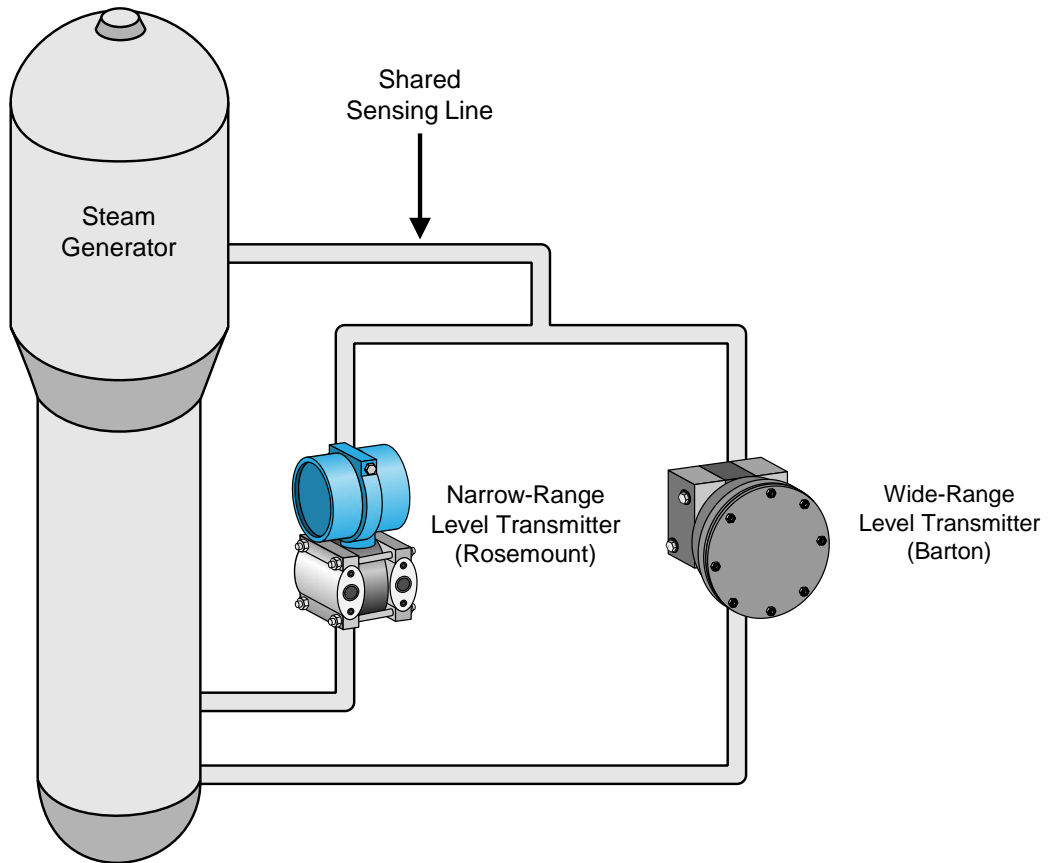


**Figure 6-20 Shared Sensing Line in a Nuclear Power Plant**

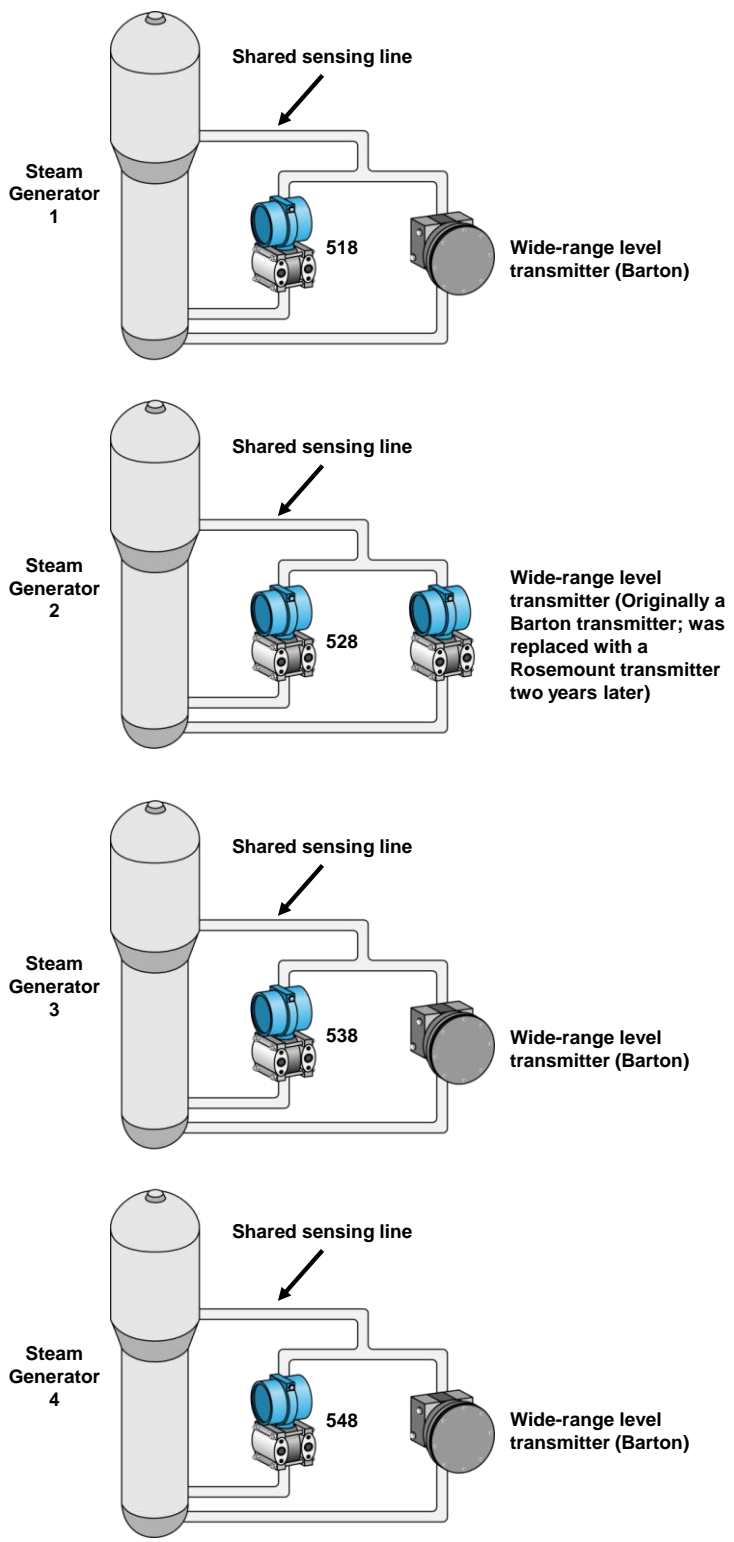


**Figure 6-21 Example of Shared Sensing Line Arrangement in a Nuclear Power Plant**

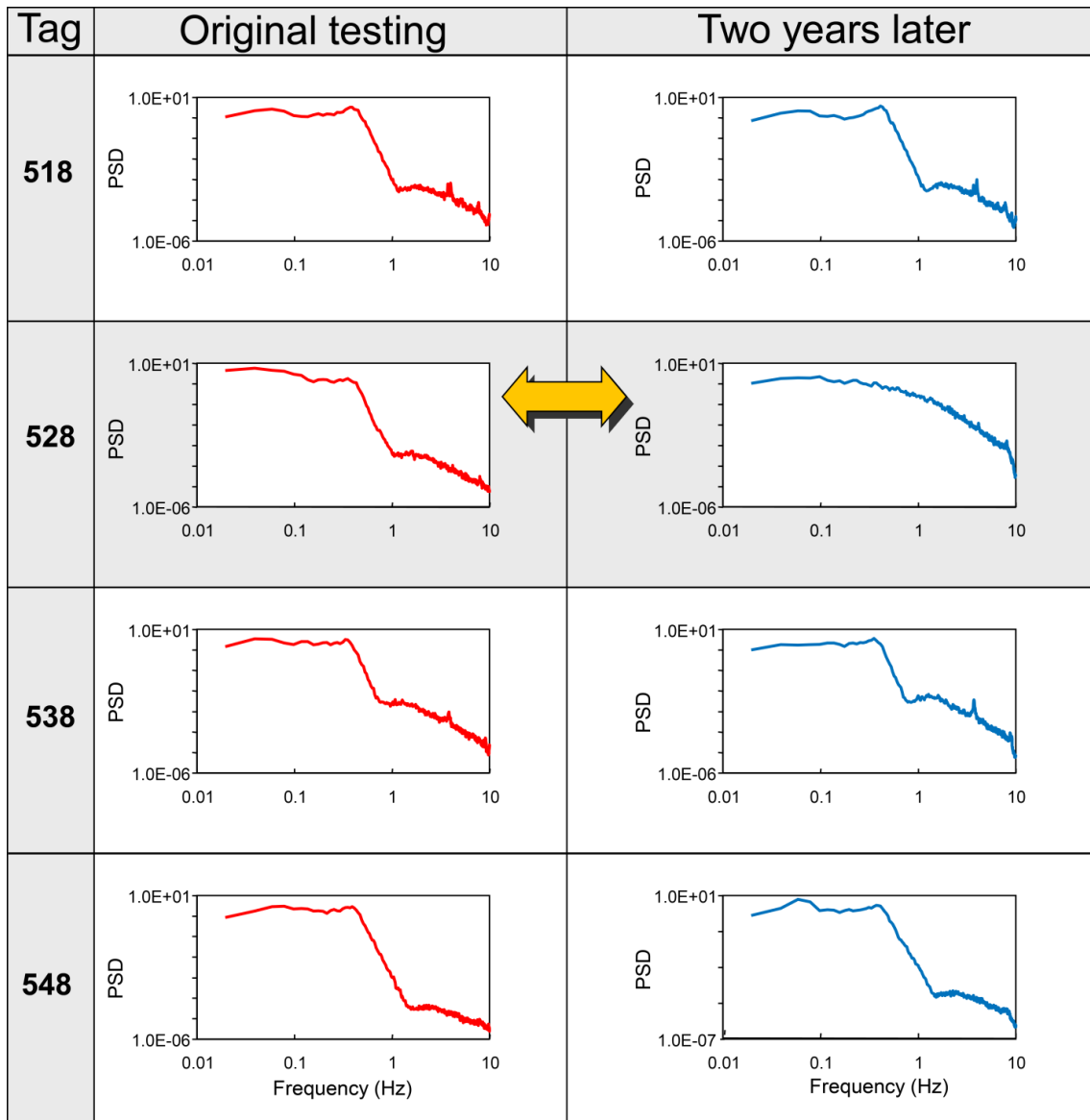


**Figure 6-22 PSDs of Four Steam Generator Level Transmitters with Shared Sensing Lines**

# 7

## APPLICATIONS OF RESEARCHED TECHNIQUES IN AND BEYOND THE NUCLEAR INDUSTRY

---

The focus of this research has been the in-situ testing of the response time of RTDs and pressure, level, and flow transmitters used in the safety systems of PWRs. Although PWRs are the most popular type of nuclear plant, the two testing methods developed for this research—LCSR and noise analysis—are also fully applicable to other reactor types, including BWRs, heavy water reactors such as the Canadian deuterium uranium (CANDU) plants, liquid metal fast breeder reactors (LMFBRs), Russian PWRs or VVERs, gas-cooled reactors including the current generation of advanced gas reactors (AGRs), and the Gen IV reactors that are slated to be deployed circa 2030.

Specifically, CANDU reactors have hundreds of RTDs and pressure transmitters that can benefit from the two in-situ testing techniques advanced in this research. Today, some current-generation CANDU reactors use a cumbersome procedure to measure the dynamic response of their safety-related pressure transmitters: electromechanical hardware made of isolation valves and solenoid devices injects a step pressure signal into the transmitter under test as well as into a reference transmitter. The output of the transmitter is then compared with that of the reference transmitter to determine if the transmitter response time is acceptable. The noise analysis technique described in this dissertation can obtain these same results but passively and automatically. In fact, the next generation of CANDU plants as well as other advanced and new-generation reactors will be designed from the start to fully exploit the automated performance monitoring of instrumentation systems that LCSR and noise analysis methods make possible.

In fact, the potential contribution of the techniques presented in this dissertation extends far beyond nuclear power to the process, power, aerospace, manufacturing, and other

industries. These techniques can find application in essentially all industries that depend on transient temperature or pressure measurements for control or safety applications. Figure 7-1, for example, shows data produced by Dr. Robert J. Moffat, Professor Emeritus of Mechanical Engineering at Stanford University, illustrating the importance of response time in the testing of jet engines. The data was recorded by thermocouples installed in the burner outlet and turbine inlet of a jet engine during a startup test. The two temperatures are essentially the same, and so the two curves should overlay, but they do not. This is partly because of the differences in installation details and in the response times of the two thermocouples. In this test, the jet engine caught fire because temperatures rose to over 30 percent beyond the highest temperature indicated by the thermocouples. Figure 7-2 shows the true temperature of the engine during the startup test. This data was constructed by correcting the measured temperature data for the response time of the thermocouples. (For illustration purposes, we altered the actual temperature data in minor ways to underscore the point that the measurement of true transient temperatures is strongly affected by the response time of the sensors used to make the measurements.)

This is only one example of the many potential applications of advanced in-situ methods for measuring response time both for operational efficiency and human safety.

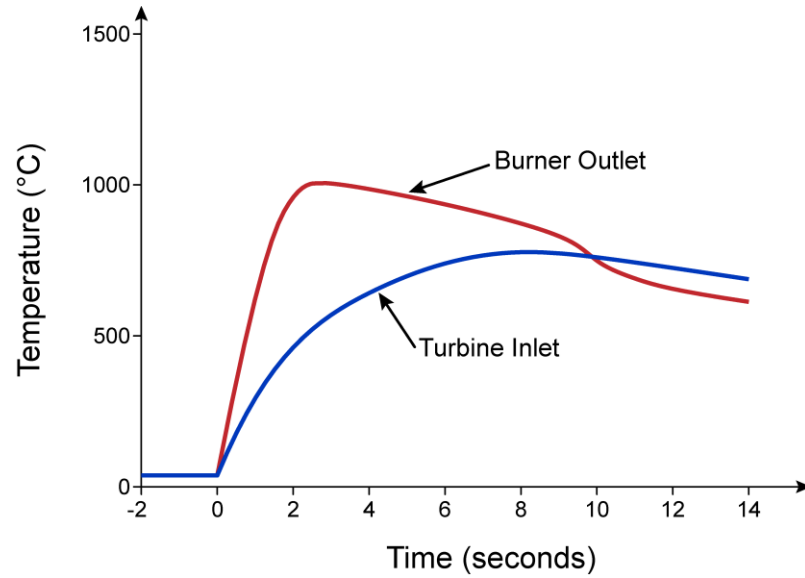


**Figure 7-1 Temperature Data from Jet Engine under Test Firing**

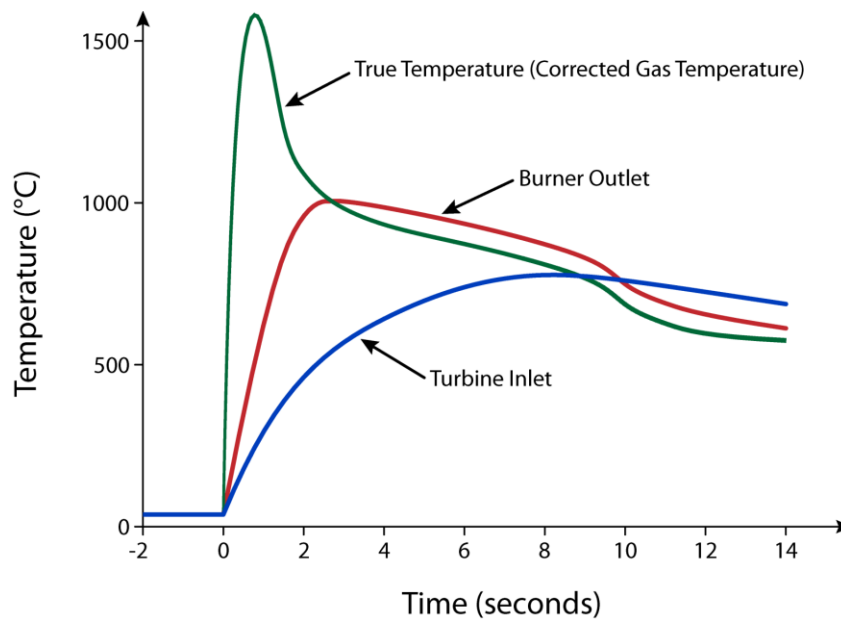


**Figure 7-2 True Temperature Curve Constructed by Correcting the Output of Thermocouple for Response Time**

# 8

## CONCLUSIONS

---

### 8.1 Conclusions From This Research

The conclusions that may be derived from the research conducted for this dissertation can be summarized as follows:

1. The LCSR method is a valid technique for measuring the in-service response time of RTDs as installed in operating nuclear power plants. It accounts for all installation and process condition effects on response time and provides results with an average accuracy of better than  $\pm 10$  percent for RTDs that meet the validation assumptions of LCSR. The LCSR assumptions must be satisfied by the design of the RTD to ensure that heat transfer to and from the sensing element follows the same path, whether the heat source is in the fluid surrounding the RTD or stems from the internal heating of the sensing element in the LCSR test. The author determined during the research for this dissertation that most RTD designs currently used in nuclear power plants meet the LCSR test assumptions and can thereby employ the method to yield their response times.

It is somewhat amazing that an RTD can be heated in the inside and the resulting heating transient used to establish the response time if the RTD were heated from the outside. But that is the case.

2. The noise analysis technique can provide valid results for the response time of pressure, level, and flow transmitters and associated sensing lines. The term *noise* normally refers to an extraneous effect or high-frequency interference rather than a useful driving force for sensor response time testing, but however inaptly named, the noise analysis technique has proved its effectiveness.

For the noise analysis technique to succeed, the process fluctuations must have certain characteristics. Ideally, they must have an unlimited bandwidth (white noise) to yield accurate response-time results. In practice, however, white noise does not exist in a process nor is it always necessary. The noise analysis technique will succeed as long as the bandwidth of the process noise is greater

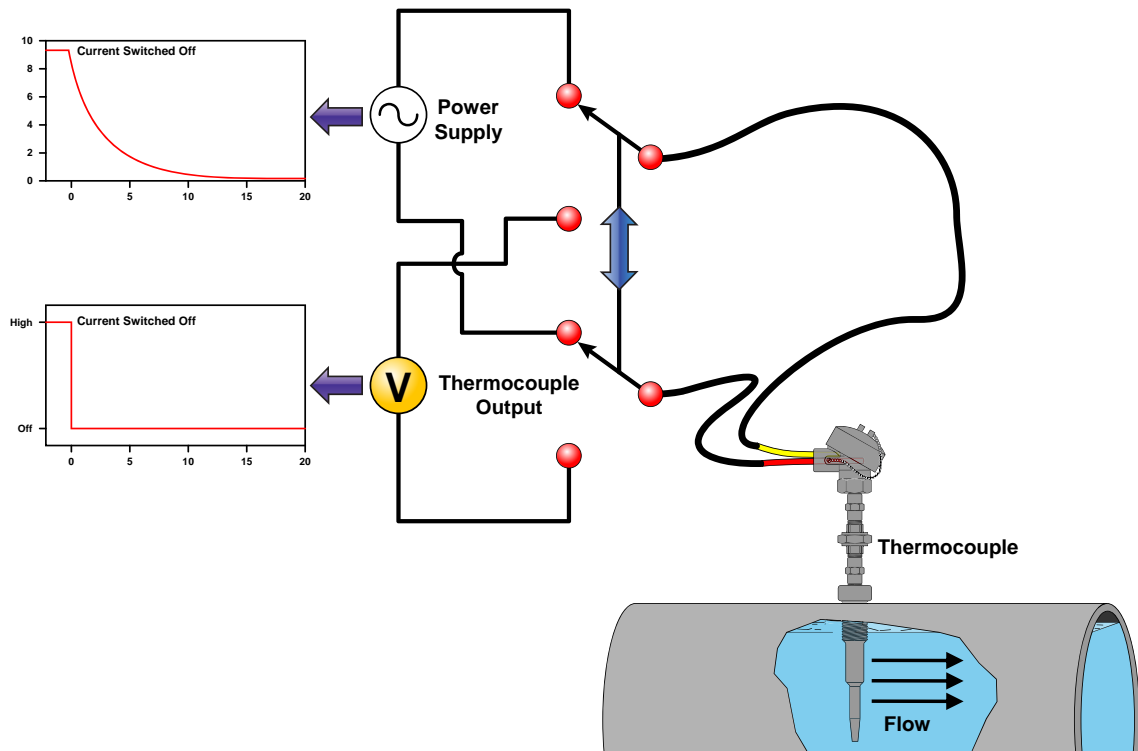


than the frequency response of the sensor under test. If this assumption is met, the sensor is linear, and the sensor noise output has a Gaussian (normal) distribution, the noise analysis technique will provide the response time of a pressure transmitter and its sensing line with an accuracy of better than  $\pm 20$  percent.

3. The response time of RTDs depends heavily on the air gap between the tip of the RTD and inside wall of the thermowell. It is also affected by the flow rate and temperature of the fluid in which the RTD is used. The effect of flow rate on response time is predictable and can be quantified theoretically. However, the effect of temperature is not predictable and cannot be quantified. The response time may increase or decrease depending on how temperature affects the thermal conductivity of the material inside the RTD. It is because of this effect that the in-service response time of an RTD can only be identified by in-situ testing at plant operating conditions.
4. The response time of a pressure transmitter is affected by the length of its sensing lines and any blockages or voids that may exist in these lines. The response time increases with length or as a result of blockages or voids, depending on the compliance of the transmitter. If the compliance is large, then these effects will significantly affect response time. If they are not, sensing line effects will be small. Fortunately, the noise analysis technique can provide the response time of a pressure transmitter and its sensing line during the same test. It can account for the effect of compliance, thereby including the contributions of length, blockages, and voids in the overall response time of the pressure transmitter.

## **8.2 Recommendations for Future Research**

Although the in-situ response-time testing methods described in this dissertation have focused on nuclear plant RTDs and pressure transmitters, they apply equally to other nuclear plant sensors such as thermocouples (Figure 8-1) and neutron detectors. However, using the LCSR method to test the response time of thermocouples is much more challenging than for RTDs.<sup>[38]</sup> This is because the electrical current required for LCSR testing of thermocouples heats the entire thermocouple circuit, whereas for RTDs the heating occurs only at the tip of the RTD. In an RTD circuit, the circuit's resistance is dominated by the resistance of the sensing element, which is located at the tip of the RTD. In contrast, the resistance of a thermocouple circuit is distributed along the entire circuit. The LCSR current therefore heats not only the thermocouple but also its



The LCSR testing of thermocouples is performed by heating the thermocouple with an AC or DC current (500 to 1,000 ma) and measuring the thermocouple output after the current is suddenly switched off and while the thermocouple cools to the ambient temperature.

**Figure 8-1 Principle of LCSR Test for Thermocouples**

extension leads and connectors. As a result, while LCSR testing of thermocouples requires currents of 500 to 1000 mA, RTDs can be LCSR tested with as little as 30 mA.

Because of these application-specific factors, a substantial research and development (R&D) effort is needed to establish the validity of the LCSR method for in-situ response time testing of thermocouples. This R&D should build on the foundational work performed by many in the academy and in industry, including the author, but especially on a decade of research conducted at the Oak Ridge National Laboratory (ORNL) in the late 1970s and early 1980s on the application of the LCSR method for in-situ response time testing of thermocouples. In recent years, researchers at the Mechanical and Aerospace Engineering Department of the University of Tennessee have used the LCSR method to develop new technology for heat flux measurements using thermocouples.<sup>[39]</sup> As a result, some of the shortcomings of the LCSR method for thermocouples are being addressed by the University of Tennessee researchers.

Although thermocouples are simple devices, the challenges of adapting the LCSR test to these sensors are many. First, as noted, it must be determined if thermocouples can tolerate the high electrical current (about 1 amp) required for the LCSR test. Because of the electrical resistance distributed along the thermocouple and its extension wires, 1 amp of current may heat the sensor and its wires significantly (e.g., 100°C). The wires may tolerate this, but the thermocouple seal and insulation material will not. Furthermore, if the thermocouple is LCSR tested using a DC current, its measuring junction may heat or cool due to the “Peltier Effect.”<sup>[40]</sup> Whether the junction heats or cools, and by how much, depends on the direction and magnitude of the applied DC current. The Peltier Effect may therefore dictate that LCSR testing of thermocouples employ AC current.

It is suggested that the R&D work to be performed determine the extent of the Peltier Effect on the LCSR results and verify that the problem (if any) can be resolved using AC current. The author believes that the Peltier Effect may in fact be helpful in LCSR testing of thermocouples if the direction of the DC current is selected to heat the

measuring junction in addition to the joule heating that is induced by the LCSR test. This, of course, must be researched experimentally in a laboratory setting.

Another recommended focus of R&D is determining if, during an LCSR test, heat conduction along the thermocouple circuit can cause a drift in LCSR signals, thereby complicating the analysis of the test data. Recall that the LCSR test requires that heat transfer to and from the sensing junction be unidirectional and radial. If any significant axial heat transfer is present, the LCSR's validation assumption may not be satisfied.<sup>[39]</sup>

The noise analysis technique was validated in the research leading to and during this dissertation to test the response time of pressure, level, and flow transmitters. This method can also be used to test the response time of neutron detectors in nuclear power plants. However, as is the case with extending LCSR methods to thermocouples, extending the noise analysis technique to neutron detectors could pose significant research challenges, including the kind of intensive validation tests performed for pressure transmitters during the research for this dissertation. For example, neutron detectors are normally very fast (e.g., their response time is on the order of a few milliseconds), and the process fluctuations (neutron noise) may not be sufficiently wide-band to yield an accurate response time value for the neutron detector. Although this question merits investigation, the author is relatively certain that process fluctuations input to neutron detectors in nuclear power plants are too slow to drive the detectors beyond their frequency response. Nevertheless, the noise analysis technique should be useful in tracking the dynamic characteristics of neutron detectors so as to isolate evidence of gross dynamic degradation. This may be accomplished by tracking the PSD of the neutron noise signal to detect changes in dynamic behavior resulting either from the process or the detector. Furthermore, the noise analysis technique can be helpful in distinguishing between problems in the detector and those in its cables and connectors. Such discrimination is critical to the effective troubleshooting of anomalous signals from neutron instrumentation systems in nuclear power plants. The noise analysis technique offers this potential to isolate problem sources. Indeed, the noise analysis technique may be used together with cable testing techniques (such as the time domain reflectometry [TDR] test) and impedance measurements (including

insulation resistance [IR] tests as well as inductance [L], capacitance [C], and resistance [R] measurements or LCR tests) to identify the root cause of neutron detector problems.<sup>[41]</sup>

If this suggested R&D established the feasibility of the noise analysis technique for the testing of neutron detectors or for the health monitoring and troubleshooting of its cables and connectors, then its application could reap substantial benefits for the nuclear industry. These benefits will come in the form of life extension of neutron detectors, the establishment of reliable replacement schedules for these sensors, and the effective isolation of cable and connector problems from detector problems. Similar benefits will result for thermocouples if the LCSR method proves capable of yielding objective data on the dynamic health of thermocouples and/or helping to separate problems in thermocouples from issues in their extension wires or connectors.

Some nuclear power plants have replaced neutron detectors, thermocouples, or other sensors at a cost of up to US\$2 million per sensor and then discovered the problem was not in the sensor but in the cables or connectors. The R&D efforts suggested here should help resolve these issues and provide the nuclear industry with new tools for distinguishing problems in cables and connectors from problems in the device at the end of the cable, such as a sensor, a detector, or a motor.

Two other areas for further research warrant mentioning here:

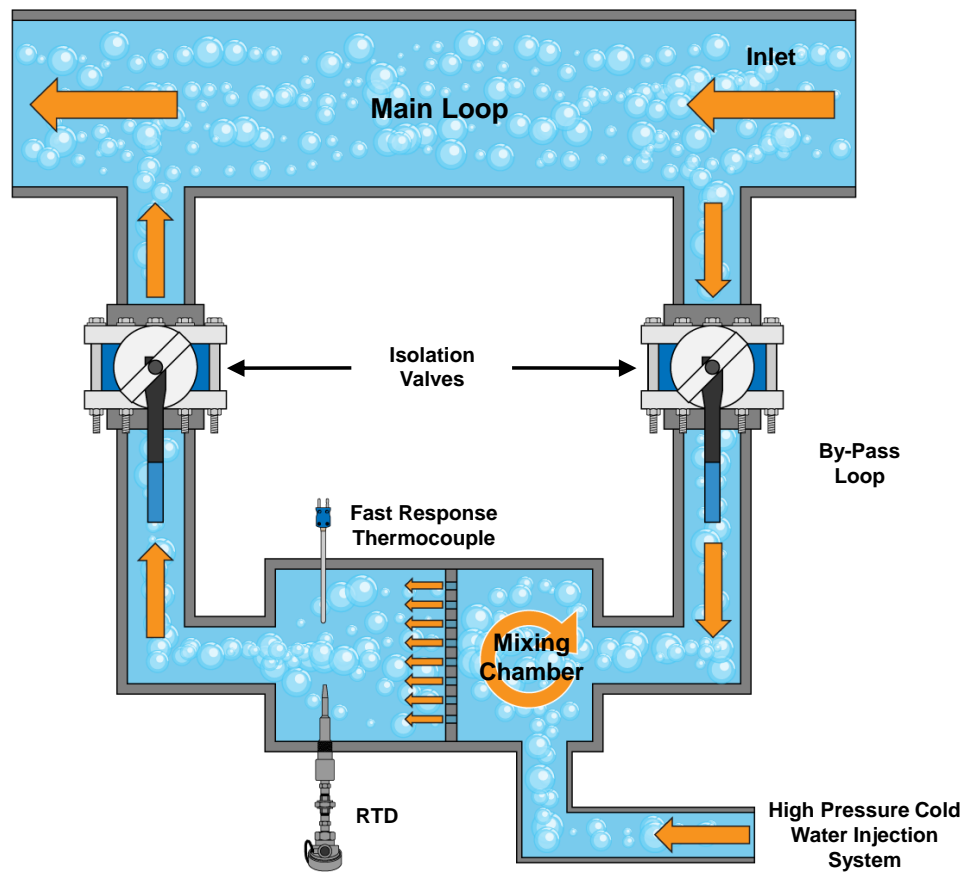
1. The LCSR method provides accurate response time results for RTDs that satisfy the validation assumptions of LCSR. If an RTD does not meet these assumptions, then its response time may be tested using the noise analysis technique, provided that: (1) a very accurate response time result is not required (as when the purpose of the testing is to trend response time only so as to detect gross degradation), and (2) sufficient margin exists between the response time requirement for the RTD and the results that can be obtained from the noise analysis technique.

Table 8-1 shows the results of a limited set of laboratory tests conducted to validate the noise analysis technique for the response time testing of RTDs. Additional research must be performed to better establish the validity of the noise analysis technique for the response time testing of RTDs and to quantify the accuracy of the noise analysis results.

**Table 8-1 Results of Validation of Noise Analysis Technique for In-Situ Response Time Testing of RTDs**

<u>RTD ID</u>	<u>Conventional Method</u>	<u>Noise Analysis</u>	<u>% Diff</u>
1	0.9	0.9	0.0
2	0.8	0.9	12.5
3	3.9	3.7	-5.4
4	4.5	4.4	-2.2
5	3.4	3.0	-13.3
6	4.6	4.4	-4.5
7	4.6	4.4	-4.5
8	5.0	5.0	0.0
9	4.3	3.6	-19.4
10	0.2	0.2	0.0
11	0.2	0.2	0.0
12	0.2	0.2	0.0
13	0.2	0.2	0.0
14	0.2	0.2	0.0
15	0.2	0.2	0.0
16	0.2	0.2	0.0
17	0.2	0.2	0.0
18	0.2	0.2	0.0
19	0.2	0.2	0.0
20	0.2	0.2	0.0
21	0.2	0.2	0.0
22	0.2	0.2	0.0
23	2.9	2.7	-7.4
24	3.2	2.9	-10.3
25	3.5	3.4	-2.9
26	4.4	3.9	-12.8
27	3.8	3.8	0.0
28	3.4	3.0	-13.3
29	3.3	2.7	-22.2
30	3.7	3.4	-8.1
31	4.0	4.4	10.0
32	2.9	3.3	13.8
<b>Average</b>	<b>2.11</b>	<b>2.00</b>	<b>-2.81</b>

2. As described in this dissertation, the validation of the LCSR and noise analysis techniques for sensor response time testing was primarily performed using laboratory data. An area of future research could be to perform the validation work under the operating conditions of nuclear power plants. Substantial investment would be required to build a test loop for this work that could deliver high temperature, pressure, and flow. The author performed limited research in this area in the late 1970s in cooperation with the Electricité de France (EdF) in an EdF laboratory near Paris. This work involved four Rosemount RTDs, which at that time were the most commonly used temperature sensors for safety-related applications in nuclear power plants. The loop operated at PWR operating conditions (temperature near 300°C, pressure near 150 bar, and flow between 5 to 10 meters per second).
3. The test loop and the RTD response time results are shown in Figure 8-2. Each RTD was first tested in the loop by injecting cold water (direct test) and then measuring the response time using a fast thermocouple to provide the timing signal. Subsequently, the RTD was tested as installed in the loop under the same conditions using the LCSR method. The results shown in Figure 8-2 indicate good agreement between the two tests.



**Schematic of EdF Test Loop**

<u>RTDs</u>	<u>Response Time (sec)</u>		
	<u>Direct Test</u>	<u>LCSR Test</u>	<u>Difference</u>
Rosemount Model 104AFC	6.2	6.5	+5%
Rosemount Model 104 NS	4.1	4.1	0%
Rosemount Model 177HW	8.8	9.2	+5%
Rosemount Model 176KF	0.14	0.14	0%

**Figure 8-2 LCSR Validation Performed at EdF Test Loop**



# 9

## REFERENCES

---

The following publications were cited in this dissertation by the numbers indicated.

1. Arkansas Nuclear One Unit 2, Internal Correspondence and Letter to Nuclear Regulatory Commission on “*Power Margin and RTD Response Time*,” (1986).
2. IAEA Nuclear Energy Series, No. NP-T-3.9, “*Power Uprate in Nuclear Power Plants: Guidelines and Experience*,” International Atomic Energy Agency, Vienna, Austria (January 2011).
3. IAEA Nuclear Energy Series, Nos. NP-T-1.1 and NP-T-1.2, “*On-Line Monitoring for Improved Performance of Nuclear Power Plants*,” International Atomic Energy Agency, Vienna, Austria (September 2008).
4. NUREG-0800, “*Standard Review Plan for the Review of Safety Analysis Reports for Nuclear Power Plants: LWR Edition*.” U.S. Nuclear Regulatory Commission (Revision 6, March 2007).
5. ANSI/ISA Standard 67.06 – “*Performance Monitoring for Nuclear Safety-Related Instrument Channels in Nuclear Power Plants*.” The International Society of Automation (ISA) (May 2002).
6. IEC 62342 – *Nuclear Power Plants – Instrumentation and control systems important to safety – Management of Aging*. International Electrotechnical Commission (IEC) (August 2007).
7. American Society For Testing And Materials, “*Test Methods for Testing Industrial Resistance Thermometers*,” ASTM Standard E-644 (2002).
8. Lillis, David, “*Online Monitoring to Support Condition Based Maintenance of Safety Category Sensors at Sizewell ‘B’ Nuclear Power Plant*.” Proceedings of 7<sup>th</sup> International Topical Meeting on Nuclear Plant Instrumentation and Control and Human Machine Interface Technology (NPIC&HMIT), American Nuclear Society 2010 Winter Meeting, Las Vegas, NV (November 2010).
9. Glöckler, O., “*Reactor noise analysis applications in NPP I&C systems*,” Proceedings of 5<sup>th</sup> ANS Nuclear Plant Instrumentation, Control and Human Machine Interface Technology (NPIC & HMIT), American Nuclear Society 2006 Winter Meeting, Albuquerque, NM (November 2006).

10. Hashemian, H.M., and Jiang, J., "Nuclear Plant Temperature Instrumentation." Nuclear Engineering and Design, 239, pages 3132-3141 (2009).
11. U.S. Nuclear Regulatory Commission, "Effect of Aging on Response Time of Nuclear Plant Pressure Sensors." NUREG/CR-5383 (June 1989).
12. U.S. Nuclear Regulatory Commission, "Long Term Performance and Aging Characteristics of Nuclear Plant Pressure Transmitters." NUREG/CR-5851 (March 1993).
13. Schohl, Gerald A., Brackett, C. Ann, Duncan, Michael L., "Laboratory Tests of Air Entrapment in Slightly Sloped Sensing Lines and the Consequent Pressure Transmission Error," Tennessee Valley Authority Office of Natural Resources and Economic Development, RN WR 28-1-85-124, Rev. 1 (June 1987).
14. Nuclear Regulatory Commission Bulletin No. 90-01, Supplement 1, "Loss of Fill-Oil in Transmitters Manufactured by Rosemount," Washington, D.C. (December 1992).
15. Warshawsky, I., "Heat Conduction Errors and Time Lag in Cryogenic Thermometer Installations," ISA Trans. – Vol. 13, No. 4, pp. 335-346 (1974).
16. Carroll, R.M., Shepard, R.L., and Kerlin, T.W., "In-Situ Measurements of the Response Time of Sheathed Thermocouple," Trans. Amer. Nucl. Soc., Vol. 21, p. 427 (June 1975).
17. Carroll, R.M., Shepard, R. L., "Measurement of Transient Response of Thermocouples and Resistance Thermometers Using an In-Situ Method," Oak Ridge National Laboratory, Report Number ORNL/TM-4573, Oak Ridge, Tennessee (June 1977).
18. Kerlin, T.W., "Analytical Methods for Interpreting In-Situ Measurements of Response Times in Thermocouples and Resistance Thermometers," Oak Ridge National Laboratory Report, ORNL/TM-4912 (March 1976).
19. Kerlin, T.W., et al., "In-Situ Response Time Testing of Platinum Resistance Thermometers." Electric Power Research Institute, EPRI Report Number NP-834, Vol. 1 (July 1978).
20. Thie, Joseph A., *Reactor Noise*, Rowman and Littlefield, NY (1963).
21. Uhrig, Robert E., *Random Noise Techniques in Nuclear Reactor Systems*, Wiley, John & Sons Incorporated (June 1970).
22. Thie, Joseph A., *Power Reactor Noise*, American Nuclear Society, LaGrange, IL (1981).
23. Baofu, L., Upadhyaya, B., and Perez, R., "Structural Integrity Monitoring of Steam Generator Tubing Using Transient Acoustic Signal Analysis," IEEE Transactions on Nuclear Science, Vol. 52, No. 1 (February 2005).

24. Wong, C., Noujaim, D., Fu, H., Huang, W. Cheng, C., Thie, J., Dalal, I., Chang, C., Nagle, C., “*Time Sensitivity: A Parameter Reflecting Tumor Metabolic Kinetics by Variable Dual-Time F-18 FDG PET Imaging,*” *Molecular Imaging and Biology* (2009).
25. Lin, K., Holbert, K.E., “*Blockage diagnostics for nuclear power plant pressure transmitter sensing lines.*” *Nuclear Engineering and Design* 239, 365-372 (2009).
26. McCollough, Norman, D., “*Private Discussions*” Electric Power Research Institute (EPRI), Power Optimization Center, Knoxville, TN (2011).
27. Meuwisse, C. and Puyal, C., “*Surveillance of neutron and thermodynamic sensors in EDF nuclear power plants,*” paper presented at the CORECH Meeting, Chatou, France (1987).
28. International Electrotechnical Commission, “*Nuclear reactors – Response time in resistance temperature detectors (RTD) – In situ measurements,*” IEC Std. 1224 (1993).
29. Ma, J. and Jiang, J., “*Applications of Fault Detection and Diagnosis Methods in Nuclear Power Plants: A Review.*” *Progress in Nuclear Energy* 53 (3): 255-266 (April 2011).
30. Glöckler, O., “*Estimating the response time of pressure/flow transmitters and RTDs via in-situ noise measurements*”, 21<sup>st</sup> Annual Conference of the Canadian Nuclear Society, Toronto, Ontario (June 11-14, 2000).
31. Bergdahl B.G., Morén M., and Oguma R., “*Experience from sensor tests and evaluation of sensor performance,*” *Progress in Nuclear Energy*, Volume 43, Issues 1-4 (2003).
32. Glöckler, O., “*Reactor Noise Measurements in the Safety and Regulating Systems of CANDU Stations*”, 8<sup>th</sup> Symposium on Nuclear Reactor Surveillance and Diagnostics, Göteborg, Sweden (May 2002).
33. Glöckler, O., “*Measurement-based estimation of response time parameters used in safety analysis of CANDU reactors*”, paper presented at Nuclear Mathematical and Computational Sciences Conf., Gatlinburg, TN (2003).
34. García-Berrocal, A., Chicharroa, J.M., Blásquez, J., Balbása, M., “*Non-linear noise analysis from a capacitive pressure transmitter.*” *Mechanical Systems and Signal Processing* 18 (1), 187-197 (January 2004).
35. Barbero, J., Blásquez, J., Oscar, V., 1. “*Bubbles in the sensing line of nuclear power plant pressure transmitters: the shift of spectrum resonances.*” *Nuclear Engineering and Design* 199 (3), 327-334 (July 2000).
36. Kerlin, T.W., et al., “*Temperature Sensor Response Characterization,*” Electric Power Research Institute, EPRI Report No. NP-1486 (August 1980).

37. Kerlin, T.W., et al., "*Response of Installed Temperature Sensors.*" *Temperature its Measurement and Control in Science and Industry*, Volume 5, pp. 1357-1366, American Institute of Physics (1982).
38. National Aeronautics and Space Administration (NASA) report entitled "*New Instrumentation Technologies for Testing the Bonding of Sensors to Solid Materials.*" Marshall Space Flight Center, NASA/CR-4744 (May 1996).
39. Elkins, B., Keyhani, M., Frankel, J.I., "*Global Time Method for Inverse Heat Conduction Problem,*" 2011 International Conference on Inverse Problems in Engineering (May 4-6, 2011).
40. Kerlin, T.W., Shepard, R.L., "*Industrial Temperature Measurement,*" Instructional Resource Package of the International Society of Automation, Research Triangle Park (1982).
41. Hashemian, H.M., Shumaker, B.D., Sexton, C.D., Beverly, D.D., Morton, G.W., Riggsbee, E.T., "*Neutron Detector Life Extension Through Predictive Maintenance.*" 17<sup>th</sup> Annual Joint ISA POWID/EPRI Controls and Instrumentation Conference, Pittsburgh, PA, USA (June 2007).

The following additional publications were consulted, reviewed, or studied in the writing of this dissertation although they were not specifically cited in the body:

42. Korsah, K., et al., "*Instrumentation and Control in Nuclear Power Plants: An Emerging Technology Update,*" NUREG/CR-6992, U.S. Nuclear Regulatory Commission (October 2009).
43. Kerlin, T.W., et al., "*Time Response of Temperature Sensors,*" Paper C.I. 80-674, The Instrumentation, Systems, and Automation Society (ISA), International Conference and Exhibit, Houston, Texas (October 1980).
44. U.S. Air Force, "*New Technology for Remote Testing of Response Time of Installed Thermocouples,*" Arnold Engineering Development Center, Report No. AEDC-TR-91-26, Volume 1 (January 1992).
45. Doebelin, Ernest O., "*Measurement Systems: Application and Design,*" McGraw-Hill Book Co., Inc. (1966).
46. Anderson, R.C., Englund, Jr., D.R., "*Liquid-Filled Transient Pressure Measuring Systems: A Method for Determining Frequency Response,*" NASA TN D-6603 (December 1971).
47. Kerlin, Thomas W., "*Frequency Response Testing in Nuclear Reactors,*" New York, Academic Press (1974).
48. Poujol A., Papin B., Bernard P., Evrard J.M., and Thomas J.B., *Advanced techniques for nuclear plants malfunctions detection, diagnosis, and mitigation.* SMORN VI, 1.01-1.12 (1991).

49. Andersson T., Demazière C., Nagy A., Sandberg U., Garis N.S., and Pázsit I., *Development and application of core diagnostics and monitoring for the Ringhals PWRs*. Progress in Nuclear Energy, Vol. 43, No. 1-4, pp. 35-41 (2003).
50. Kitamura M., Kobayashi J., Takahashi M. and Suglyama K., *Combined use of model-based and symptom-based techniques for diagnosis and prognosis of BWR dynamic characteristics*. SMORN VI, 11.01-11.12 (1991).
51. Wach D., "On-line monitoring and dynamic feature trending as a means to improve in-service inspection, maintenance, and long-term assessment of systems and components." Nuclear Plant Instrumentation, Control, and Human-Machine Interface Technologies (NPIC & HMIT), Nuclear Technology, Vol. 141, No. 1 (2003).
52. J. Runkel, D. Stegemann, "Experience with noise analysis in German PWRs and BWRs." Invited paper, 1996 American Nuclear Society International Topical Meeting in Nuclear Power Plant Instrumentation, Control, and Human Interface Technologies, Pennsylvania State University, USA (1996).
53. International Atomic Energy Agency, "Management of Ageing of I&C Equipment in Nuclear Power Plants." IAEA Publication TECDOC-1147, Vienna, Austria (2000).
54. Electric Power Research Institute (EPRI), "On-line monitoring of instrument channel performance." EPRI technical report number TR-104965-RI NRC SER. Palo Alto, California (September 2000).
55. Hines, J.W., et al., "Technical Review of On-line Monitoring Techniques for Performance Assessment. State of the Art. Vol. 1," US Nuclear Regulatory Commission, NUREG/CR-6895 (2006).
56. Hines, J.W., et al., "Technical Review of On-line Monitoring Techniques for Performance Assessment. Theoretical Issues. Vol. 2," US Nuclear Regulatory Commission, NUREG/CR-6895 (2008).
57. TECDOC-1402, "Management of Life Cycle and Aging at Nuclear Power Plants," International Atomic Energy Agency, Vienna, Austria (August 2004).
58. Bergdahl B.G., et al., "Experiences from Sensor Tests and the Evaluation of Long-term Sensor Performance Using SensBase™," NPIC & HMIT, Washington, DC (2000).
59. Czibók, T., Kiss, G., Kiss, S., Krinizs, K., Végh, J., "Regular neutron noise diagnostics measurements at the Hungarian Paks NPP," Prog. Nucl. Energy 43, 67 (2003).
60. Roverso, D., "Dynamic empirical modeling techniques for equipment and process diagnostics in nuclear power plants," Proc. Conf. on On-Line Condition

Monitoring of Equipment and Processes in Nuclear Power Plants Using Advanced Diagnostic Systems, Knoxville, TN (2005).

61. Glöckler, O., "Testing the dynamics of shutdown systems instrumentation in reactor trip measurements," *Progress in Nuclear Energy*, vol. 43, nos. 1-4, pp. 91-96 (2003).
62. International Atomic Energy Agency, "Implementation Strategies and Tools for Condition Based Maintenance at Nuclear Power Plants," IAEA-TECDOC-1551. Vienna, Austria: IAEA (May 2007).
63. Barutcu, B., Seker, S., Ayaz, E., and Turkcan, E., "Real time reactor noise diagnostics for the Borssele (PWR) nuclear power plant." *Progress in Nuclear Energy*, Vol. 43, No. 1, pgs. 137-143 (2003).
64. Bergdahl, B.G., Morén, M., and Oguma, R., "Experiences from sensor tests and evaluation of sensor performance." *Progress in Nuclear Energy*, Volume 43, Issues 1-4, pgs. 343-348 (2003).
65. Demazière, C. and Pázsit, I., "Numerical tools applied to power reactor noise analysis." *Progress in Nuclear Energy*, Volume 51, Issue 1, 67-81 (2009).
66. Lindner, A. and Wach, D.H., "Experiences gained from independent assessment in licensing of advanced I&C systems in nuclear power plants." *Nuclear Plant Instrumentation, Control, and Human-Machine Interface Technologies*, Volume 143, Number 2, pgs. 197-207 (2003).
67. Mayo, C., "Pressurized water reactor neutron noise signal components." ANS NPIC-HMIT 2009 Topical Meeting – Nuclear Plant Instrumentation, Controls, and Human Machine Interface Technology (2009).
68. Jackson, T., Fredette, T., Kimberley Corp., and Ashcraft, J. – U.S. Nuclear Regulatory Commission, Rockville, MD, "Use of Design Acceptance Criteria for Instrumentation and Control Systems," presented at the NPIC-HMIT 2009 – Nuclear Plant Instrumentation, Control, and Human-Machine Interface Technologies Conference, Knoxville, TN (April 2009).
69. Korsah, K., Holcomb, D.E., Muhlheim, M., Mullens, J.A., Loebel, A., Bobrek, M., Howlader, M.K., Killough, S.M., Moore, M.R., Ewing, P.D. (1), Sharpe, M. (2), Shourbaji, A. A., Cetiner, S.M., Wilson, Jr., T.L. and Kisnera, R.A. (1) – (1) Oak Ridge National Laboratory, Oak Ridge, TN, (2) University of Tennessee, Knoxville, TN, "Emerging Technologies in Instrumentation and Controls and Their Potential Regulatory Implications for Nuclear Power Plants," presented at the NPIC-HMIT 2009 – Nuclear Plant Instrumentation, Control, and Human-Machine Interface Technologies Conference, Knoxville, TN (April 2009).

70. Holbert, K. and Lin, K. – Arizona State University, Tempe, AZ, “*Pressure Sensing Line Diagnostics with an Improved Equivalent PI Model*,” presented at the NPIC-HMIT 2009 – Nuclear Plant Instrumentation, Control, and Human-Machine Interface Technologies Conference, Knoxville, TN (April 2009).
71. Taft, C., Sorge, J., Willis, J., “*Thermocouple Response Time Study for Steam Temperature Control*,” presented at the 53<sup>rd</sup> ISA POWID Symposium, Volume 53, ISA Volume 483, Summerlin, NV (June 2010).

## CURRICULUM VITAE (CV)

---

### Work History

1985 – Present    **President**  
 Analysis and Measurement Services Corporation (AMS), USA

### Education

*Master of Science*; Nuclear Engineering (University of Tennessee, USA), 1977  
*Bachelor of Science*; Physics (National University of Iran, Tehran), 1974

### Professional Affiliations

Fellow: International Society of Automation (ISA)  
 Senior Member: Institute of Electrical and Electronics Engineers (IEEE)  
 Member: American Nuclear Society (ANS)  
 Member: European Nuclear Society (ENS)

### Publications and Patents

50 peer-reviewed journal and magazine articles, 200 conference papers, 2 books (translated into Chinese, Japanese, Korean and Russian), 10 book chapters, and 15 U.S. patents (10 awarded and 5 pending)

### Recent Publications (2009-2011)

#### Journal Articles

1. Hashemian, H.M., “*On-Line Monitoring Applications in Nuclear Power Plants.*” Progress in Nuclear Energy 53, Issue 2, pp. 167-181 (March 2011).
2. Hashemian, H.M., Kiger, C.J., Morton, G.W., and Shumaker, B.D., “*Wireless Sensor Applications in Nuclear Power Plants.*” Nuclear Technology, Volume 173, No. 1, pp. 8-16 (January 2011).
3. Hashemian, H.M., “*State-of-the-Art Predictive Maintenance Techniques.*” IEEE Transactions on Instrumentation and Measurement, pp.1-13 (2011).
4. Hashemian, H.M., “*Wireless Sensors for Predictive Maintenance of Rotating Equipment in Research Reactors.*” Annals of Nuclear Energy 38, pp. 665-680 (2011).
5. Hashemian, H.M., “*Accuracy in Temperature Sensor Response Time Estimation for New Nuclear Reactor Designs.*” Int. J. Nuclear Energy Science and Technology, Vol. 6, No. 1 (2011).



6. Hashemian, H.M., "Aging Management of Instrumentation & Control Sensors in Nuclear Power Plants." *Nuclear Engineering and Design*, Volume 240, Issue 11, pp. 3781-3790 (November 2010).
7. Hashemian, H.M., and Jiang, J., "Using the Noise Analysis Technique to Detect Response Time Problems in the Sensing Lines of Nuclear Plant Pressure Transmitters." *Progress in Nuclear Energy*, Volume 52, Issue 4, pp. 367-373 (May 2010).
8. Hashemian, H.M., and Jiang, J., "A Practical Review of Methods for Measuring the Dynamic Characteristics of Industrial Pressure Transmitters." *ISA Transactions*, Volume 49, Issue 1 (January 2010).
9. Hashemian, H.M., and Jiang, J., "Pressure Transmitter Accuracy." *ISA Transactions*, Volume 48, No. 4, pp. 383-388 (2009).
10. Hashemian, H.M., "The State of the Art in Nuclear Power Plant Instrumentation and Control." *Int. J. Nuclear Energy Science and Technology*, Volume 4, No. 4, pp. 330-354 (2009).
11. Hashemian, H.M., and Jiang, J., "Nuclear Plant Temperature Instrumentation." *Nuclear Engineering and Design*, 239, pp. 3132-3141 (2009).
12. Hashemian, H.M., "Regulations and Standards for the Measurement of Performance and Management of Ageing of I&C Systems of Nuclear Power Plants." *Int. J. Nuclear Law*, Volume 2, No. 4 (2009).

### **Magazine Articles**

1. Hashemian, H.M., "Ensuring Plant Safety & Reliability." *Nuclear Plant Journal*, Volume 29, No. 2, pp. 38-40 (March-April 2011).
2. Hashemian, H.M., "USA's First Fully Digital Station." *Nuclear Engineering International magazine*, pp. 12-16 (November 2010).
3. Hashemian, H.M., "The Temperature Tango: Temperature Instrumentation Problems and Solutions in Industrial Processes." *InTech Magazine* an ISA publication, pp. 44-47 (June 2010).
4. Hashemian, H.M. "Listening in Real Time." *Nuclear Engineering International Magazine*, pp. 13-20 (April 2010)
5. Hashemian, H.M., et. al., "Concerns About Electromagnetic Interference in Nuclear Plants Related to Digital Upgrades." *Power Magazine*, Vol. 154, No. 2 (February 2010).
6. Hashemian, H.M., and Jiang, J. "Pressure-Sensing Line Problems and Solutions." *Power Magazine* (September 2009).

7. Hashemian, H.M., et al., "*Nuclear Power Comeback Sure to Employ Wireless Tools.*" InTech Magazine; an ISA publication (January 2009).